The Biological Impact of High Throughput Continuous Bioprocessing

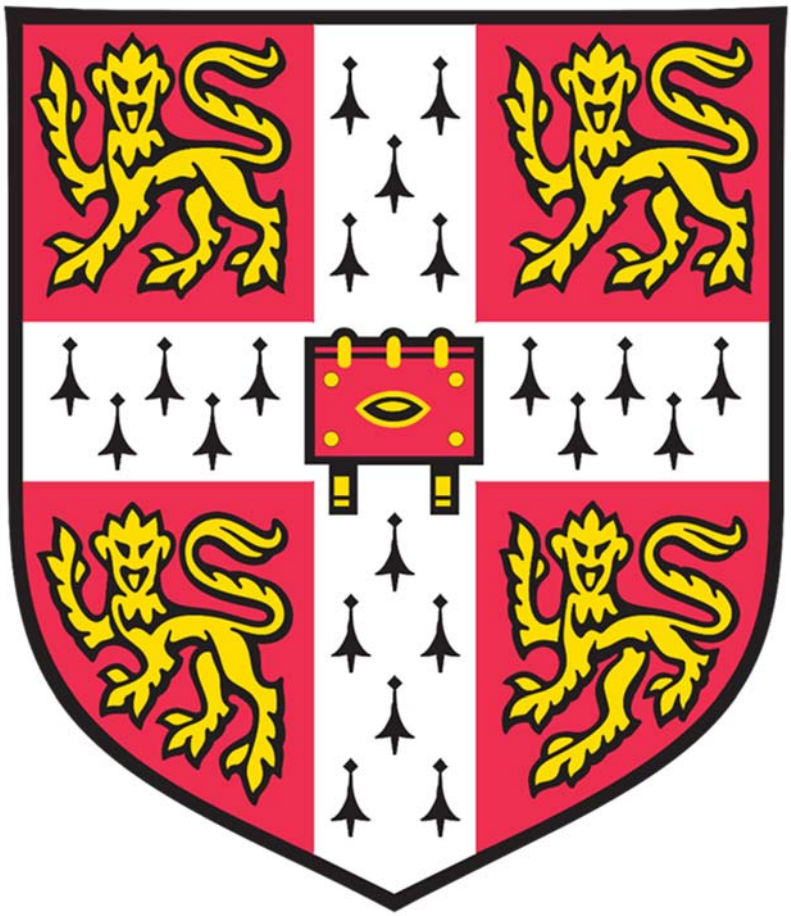

David John Sewell

Churchill College

Thesis submitted for the degree of Doctor of Philosophy

March 2020

Department of Chemical Engineering and Biotechnology

University of Cambridge

Preface

This thesis is the outcome of my own original research conducted from January 2016 through to March 2020 at the Department of Chemical Engineering and Biotechnology, University of Cambridge, UK. Any aspect that is performed in collaboration is identified in the text.

This dissertation is the result of my own work and includes nothing which is the outcome of work done in collaboration except as declared below and specified in the text. I further state that no substantial part of my dissertation has already been submitted, or, is being concurrently submitted for any such degree, diploma or other qualification at the University of Cambridge or any other University of similar institution except as declared below and specified in the text.

This thesis does not contain more than 65,000 words and 150 figures.

Acknowledgements

Supervision has been provided, with great thanks, by Professor Nigel Slater and Dr Duygu Dikicioglu. This work has been conducted as part of a wider collaboration with the Department of Biochemistry, University of Cambridge and industrial sponsor MedImmune, Cambridge. For their contribution to discussions and collaboration, I would like to thank Professor Stephen Oliver, Dr. Christopher Spencer, Dr. Ray Field, and Richard Turner.

Furthermore, I would like to acknowledge the employees of MedImmune, Cambridge for the welcoming lab environment for me to conduct my experiments.

To my family, thank you for your unwavering support.

I wish to dedicate this thesis to my wife Yvonne for her patience, faith and encouragement to the very end!

David John Sewell 2020

Abstract

The Biological Impact of High Throughput Continuous Bioprocessing

David John Sewell, Churchill College

Micro scale, high throughput perfusion technology is under-developed and not widely utilised in academic or industrial settings for the development of CHO based mAb bioprocesses. Work within this thesis highlights the design and characterisation of a sedimentation method of cell retention and its application in a fed batch designed ambr® micro scale bioreactor system.

The work identifies periods of up to one hour required to perform the necessary sedimentation and media exchanges. In comparison, bench scale equivalent culture reaches comparable cell densities as their microscale counterparts, highlighting suitability for screening development activities in this high throughput system that was previously unattainable with the high media demands of a perfusion process.

The comparison of scales highlighted a lag in growth between the two perfusion methods that was thought to be a combination of periods of uncontrolled parameters at microscale (while cells were undergoing sedimentation) and small but frequent removal of cells from the microscale cultures, as retention efficiency was below 100%.

In addition to this, the execution of the perfusion method highlighted CHO cell insensitivity to high levels of pH and DO variation that would normally elicit a severe decline in culture performance. Potential control strategies that focused on cellular sensitivity at inoculation were investigated and their application highlighted. Whilst applicable to fed batch cultures, it is in perfusion (or other continuous methods) where a significant benefit will be realised as they can attain high performance through tight control during inoculation and allowing flexibility during extended periods of cultivation.

Combining the functionality and capacity offered by the sedimentation method in the ambr® system with the highlighted potential control strategy for perfusion equips the bioprocessing industry to explore the benefits of perfusion culture to meet increasing global demand for mAbs.

Author publications

Enhancing the Functionality of a Microscale Bioreactor System as an Industrial Process Development Tool for Mammalian Perfusion Culture

David J Sewell[1], Richard Turner[2], Ray Field[2], William Holmes[2], Rahul Pradhan[2], Christopher Spencer[2], Stephen G Oliver[3,4], Nigel KH Slater[1], Duygu Dikicioglu[1,3]

[1]Department of Chemical Engineering and Biotechnology, University of Cambridge, CB3 0AS[2] BioPharmaceutical Development, MedImmune, Cambridge, UK, [3] Cambridge Systems Biology Centre, University of Cambridge, CB2 1GA, UK, [4] Department of Biochemistry, University of Cambridge, CB2 1GA, UK

Work published by the author unrelated to the work presented in this thesis:

A heuristic approach to handling missing data in biologics manufacturing databases

Jeanet Mante[1], Nishanthi Gangadharan[2], David J Sewell[2], Richard Turner[3], Ray Field[3], Stephen G Oliver[4,5], Nigel Slater[2], Duygu Dikicioglu[6,7].

[1]Pembroke College, Cambridge, UK. [2]Department of Chemical Engineering and Biotechnology, University of Cambridge. [3]Cell Sciences, Biopharmaceutical Development, MedImmune. [4]Cambridge Systems Biology Centre, University of Cambridge. [5]Department of Biochemistry, University of Cambridge. [6]Department of Chemical Engineering and Biotechnology, University of Cambridge, Cambridge, UK. [7]Cambridge Systems Biology Centre, University of Cambridge.

DNMT3A mutations occur early or late in patients with myeloproliferative neoplasms and mutation order influences phenotype

Jyoti Nangalia[1,2,3], Francesca L. Nice[1], David C. Wedge[3], Anna L Godfrey[1,2], Jacob Grinfeld[1,2,3], Clare Thakker[1], Charlie E. Massie[1], Joanna Baxter[2,4], David Sewell[2,4], Yvonne Silber[1], Peter J. Campbell[1,2,3] and Anthony R. Green[1,2]

[1]Department of Haematology, Cambridge Institute for Medical Research and Wellcome Trust/MRC Stem Cell Institute, University of Cambridge, Cambridge, UK [2]Department of Haematology, Addenbrooke's Hospital, Cambridge, UK [3]Wellcome Trust Sanger Institute, Hinxton, Cambridge, UK [4]Cambridge Blood and Stem Cell Bank, University of Cambridge, UK

Table of Contents

Abstract 5
Preface 3
Acknowledgements 3
Author publications 6
Table of Contents 7
Abbreviations 11
List of Tables and Figures 13
Tables 13
Figures 13
Appendix Figures 18
Motivation and Thesis Structure 19
Motivation 19
Thesis Structure 20
Chapter 1 Introduction 22
1.1 Antibodies 22
1.2 Therapeutic Application and Commercialisation of Antibodies (Abs) 23
1.3 Host Cell Lines, Expression Systems and Stable Cell Line Generation 24
1.4 Cell Line Response to Bioprocess Control, Development and Optimisation 26
1.4.1 Hydrodynamic Stress 26
1.4.2 pH Control 28
1.4.3 Temperature Control 28
1.4.4 Dissolved Oxygen and Carbon Dioxide Saturation 30
1.4.6 Nutrient Availability and Waste Accumulation 31
1.5 Modes of Operation 32
1.5.1 Batch 33

1.5.2 Fed-Batch....33
1.5.3 Continuous Culture – Non Cell Retention....37
1.5.4 Continuous Culture – Cell Retention....39
1.5.4.1 Cell Retention Devices....41
1.6 Scales of Operation....42
1.6.1 Commercial Manufacturing (Commercial Scale)....44
1.6.2 Clinical Supply (Pilot Scale)....45
1.6.3 Process Development (Bench Scale)....45
1.6.4 Process Development (Micro Scale)....46
1.6.5 Continuous Process Development Scales....48
1.7 Research Aims and Objectives....50
Chapter 2 Materials and Methods....51
2.1 Experimental numbering system....51
2.2 Cell line, Medium and Bioreactor systems....52
2.3 At-line and Offline Sample Analysis....53
2.4 Rate Calculations....55
Chapter 3 The Design, Execution, and Evaluation of a High-Throughput Continuous Microscale Environment....57
3.1 Introduction....57
3.2 Method Development....58
3.3 Experimental Design....62
3.3.1 Data Analysis....63
3.4 Results....64
3.4.1 Resuspension of the Culture and Recovery to the Set Points....64
3.4.2 Growth Performance....65
3.4.3 Cellular Content of the Perfusate....70
3.4.4 Controlled Process Parameters....72

3.4.5 Biochemical Analysis 74
3.4.6 Productivity and Product Quality 79
3.5 Discussion 81
Chapter 4 The Evaluation of Micro and Bench Scales Perfusion Cultures as Tools for Production Culture Inoculum Expansion 86
4.1 Introduction 86
4.2 Materials, Methods, and Experimental Design 88
4.2.1 Transition of Cultures From Perfusion to Production 89
4.2.1.1 Pooling Cultures – Production Phase Evaluation 89
4.3 Results 90
4.3.1 Experiment 4.1 The Cellular Characteristics of Micro and Bench Scale Perfusion Present in Production Cultures 90
4.3.1.1 Growth Performance and Biochemical Characteristics of Perfusion Cultures 90
4.3.1.2 Production Culture 96
4.3.2 Interim Discussion (Experiment 4.1) 122
4.3.3 Experiment 4.2 Culture Response to Reduced Dilution Rate 125
4.3.2.1 Perfusion Expansion 126
4.3.2.2 Production Phase 130
4.4 Discussion 139
Chapter 5 The Evaluation of Fed-Batch Culture Performance in Response to Targeted Parameter Deviation Before and After Controlled Inoculation 141
5.1 Introduction 141
5.2 Materials, Methods and Experimental Designs 142
5.2.1 Generation of Cell Banks 142
5.2.2 Experiment 5.1 142
5.2.3 Experiment 5.2 144
5.2.3.2 Equipment Failure (EF) 144
5.2.3.3 Operator Error 145

5.2.3.4 Data Analysis 146
5.3 Results 146
5.3.1 Preliminary Data, Cell Bank Generation 146
5.3.1 Experiment 5.1a - Cell Line Sensitivity to Cell Age and Enriched Media Exposure 149
5.3.2 Experiment 5.1b – Culture pH Sensitivity, Magnitude Verses Timing 159
5.3.2 Experiment 5.2 – Culture Robustness During Exponential Expansion 167
5.4 Discussion 176
Chapter 6 Overall Conclusions and Future Work 181
6.1 Overall Conclusions 181
6.2 Future Work 186
6.2.1 Refinement and Characterisation of Microscale Perfusion Methodology 186
6.2.2 Culture Phase Focused Bioprocess Development 187
6.2.1 Production Improvements Through Preconditioning 188
Appendix 190
References 191

Abbreviations

Abs	Antibodies
ambr®15	Advanced Microscale BioReactor
ANOVA	Analysis of Variance
ATF	Alternating tangential flow
CD40	Cluster of differentiation 40
CDRs	Complementarity determining regions
CHO	Chinese Hamster Ovary
COGs	Cost of goods
CPPs	Critical process parameters
CQAs	Critical Quality Attributes
CS	Culture station
DCB	Development cell bank
DHFR	dihydrofolate reductase
DLR	Dual Lifetime Referenced
DNA	Deoxyribonucleic acid
DO	Dissolved oxygen
DoE	Design of Experiments
DTE	difficult to express
E.coli	Escherichia coli
Fab	Antibody fragment
FB	Fed-batch
FBS	Fetal bovine serum
Fc	Constant
FDA	Food and drug administration
GS	Glutamine Synthase
HEK	Human embryonic kidney
HSPs	Heat shock proteins
ICH	International Council for Harmonisation
IgG	Immunoglobulin class G
IVCC	integral viable cell concentration
KPIs	Key performance indicators
mAbs	Monoclonal antibodies
MLV	murine leukaemia virus
mmHg	millimetre of mercury
mRNA	Messenger RNA
MTX	methotrexate
PI	proportional-integral

PQ	Product quality
QbD	Quality by design
SD	Standard deviation
SEC	Size exclusion chromatography
STR	Stir tank reactor
UPLC	Ultra-performance liquid chromatography
V	Variable
VCD	Viable cell density
VVD	Vessel volume per day

List of Tables and Figures

Tables

Table 1 Summary of experiments contained within this thesis. 51
Table 2 Monomer percentages of micro and bench scale cultures taken pre and post protein A purification 81
Table 3 Experimental outline for evaluations contained in Chapter 4 88
Table 4 Percentage monomer post Protein A purification of microscale cultures at 1x feed condition 104
Table 5 Percentage monomer post Protein A purification of microscale cultures at 2x feed condition 113
Table 6 Percentage monomer post Protein A purification of bench scale cultures at 1x and 2x feed conditions 122
Table 7 Percentage monomer post Protein A purification of production cultures at harvest, inoculated with cells from perfusion cultures of respective dilution rates (Experiment 4.2) 139
Table 8 Experimental conditions for vessels in Experiment 5.1 143
Table 9 Experiment 5.2 Conditions and the Classification of the Source of Variation 144
Table 10 Product quality (percentage monomer and aggregates) present for Experiment 5.1a cultures, at harvest, post product capture purification. 159
Table 11 Product quality (percentage monomer and aggregates) present for Experiment 5.1b cultures, at harvest, post product capture purification. 167
Table 12 Product quality (percentage monomer and aggregates) present for Experiment 5.2 cultures, at harvest, post product capture purification. 176

Figures

Figure 1 Diagrammatic representation of the constitutional components of an IgG class antibody 22
Figure 2 Example of batch culture operation setup 33
Figure 3 Example of fed batch culture operation setup 34
Figure 4 Example presentation of a typical growth profile over a batch or fed-batch bioprocess operation. 35
Figure 5 Example presentation of a log(Y) growth profile during bioprocess operation. 36
Figure 6 Example of chemostat culture operation setup 38
Figure 7 Example of a perfusion culture operation setup 40

Figure 8 Example volumes and dimensions for bioreactors at different scales.....43
Figure 9 Diagrammatic depiction of the ambr®15 vessel geometry and highlighted operational components 59
Figure 10 The relationship between, volume in vessel (mL) versus height of tip (mm).....60
Figure 11 Plotted histogram of cell removal from culture (%) at culture settling times (mins) 61
Figure 12 Sample traces of pH and dissolved oxygen in response to cell settling over a 1 day period 64
Figure 13 Sample traces of pH and DO from a single cell settling step.....65
Figure 14 Viable cell density of perfusion cultures over process duration in response to cell retention method. 66
Figure 15 Viability percentage of perfusion cultures over process duration in response to the cell retention method.....67
Figure 16 Position of the microscale vessels within their respective culture stations, and the actual settling times for each vessel observed prior to automated robotic liquid exchange 69
Figure 17 Cell retained per liquid exchange step (%) for microscale vessels. 70
Figure 18 Comparison of Average cell diameter (µm) plotted for microscale cultures and respective perfusate.....71
Figure 19 Culture response in online measured dissolved oxygen (%) plotted against process duration. 72
Figure 20 Culture response in online measured pH plotted against process duration. 73
Figure 21 Culture response in at-line measured glucose (g/L) plotted against process duration. 74
Figure 22 Culture cell specific glucose consumption rate (mg/cell/day) in response to scale over process duration (days). 75
Figure 23 Culture response in at-line measured lactate (g/L) plotted against process duration. 76
Figure 24 Glucose (g/L) presented with Amino Acid (mg/L) concentrations highlighting the metabolic shift in bench scale cultures plotted over process duration (days).....78
Figure 25 Titre (mg/L) of micro and bench scale cultures plotted across process duration (days) 79
Figure 26 Cell specific productivity (mg/cell/day) of micro and bench scale cultures plotted across process duration (days) 80
Figure 27 Diagrammatic representation of typical inoculum expansion.....86

Figure 28 Growth of perfusion vessels operated at micro and bench scale over process duration (days).....91
Figure 29 Measured glucose of perfusion vessels operated at micro and bench scale over process duration (days).....92
Figure 30 Measured lactate of perfusion vessels operated at micro and bench scale over process duration (days).....93
Figure 31 Dissolved oxygen (%) of perfusion vessels operated at micro and bench scale over process duration (days).....94
Figure 32 The pH of perfusion vessels operated at micro and bench scale over process duration (days).....95
Figure 33 Viability (%) of production phase micro scale vessels operated at incremental seeding densities at the 1x feed condition (Experiment 4.1a).....97
Figure 34 Viable cell density (cells/mL x 106) of production phase micro scale vessels operated at incremental seeding densities at the 1x feed condition (Experiment 4.1a).....98
Figure 35 Glucose concentration (g/L) of production phase micro scale vessels operated at incremental seeding densities at the 1x feed condition (Experiment 4.1a).....99
Figure 36 Lactate concentration (g/L) of production phase micro scale vessels operated at incremental seeding densities at the 1x feed condition (Experiment 4.1a).....100
Figure 37 Cell specific glucose consumption rate (g/cell/day) of production phase micro scale vessels operated at incremental seeding densities at the 1x feed condition (Experiment 4.1a) 101
Figure 38 Cell specific net lactate change (g/cell/day) of production phase micro scale vessels operated at incremental seeding densities at the 1x feed condition (Experiment 4.1a).....102
Figure 39 Titre (mg/L) representing the process performance of production phase micro scale vessels at 1x feed condition (Experiment 4.1a).....103
Figure 40 Cell specific productivity (g/cell/day) representing the process performance of production phase micro scale vessels at 1x feed condition (Experiment 4.1a).....104
Figure 41 Viability (%) representing the process performance of production phase micro scale vessels at 2x feed condition (Experiment 4.1a).....105
Figure 42 Viable cell density representing the process performance of production phase micro scale vessels at 2x feed condition (Experiment 4.1a).....106
Figure 43 Glucose concentration (g/L) representing the process performance of production phase micro scale vessels at 2x feed condition (Experiment 4.1a).....107

Figure 44 Lactate concentration (g/L) representing the process performance of production phase micro scale vessels at 2x feed condition (Experiment 4.1a)..... 108
Figure 45 Cell specific glucose consumption rate (g/cell/day)..... 109
Figure 46 Cell specific net lactate change (g/cell/day) representing the process performance of production phase micro scale vessels at 2x feed condition (Experiment 4.1a) 110
Figure 47 Dissolved oxygen (%) representing the process performance of production phase micro scale vessels at 2x feed condition (Experiment 4.1a)..... 111
Figure 48 Titre (mg/L) representing the process performance of production phase micro scale vessels at 2x feed condition (Experiment 4.1a) 112
Figure 49 Cell specific productivity (g/cell/day) representing the process performance of production phase micro scale vessels at 2x feed condition (Experiment 4.1a) 113
Figure 50 viability representing the process performance of production phase bench scale vessels at 1x and 2x feed condition (Experiment 4.1b) 114
Figure 51 Viable cell density representing the process performance of production phase bench scale vessels at 1x and 2x feed condition (Experiment 4.1b) 116
Figure 52 Glucose concentration (g/L) representing the process performance of production phase bench scale vessels at 1x and 2x feed condition (Experiment 4.1b)..... 117
Figure 53 Lactate representing the process performance of production phase bench scale vessels at 1x and 2x feed condition (Experiment 4.1b) 118
Figure 54 Online pH measurements representing the process performance of production phase bench scale vessels at 1x and 2x feed condition (Experiment 4.1b)..... 119
Figure 55 Titre representing the process performance of production phase bench scale vessels at 1x and 2x feed condition (Experiment 4.1b)..... 120
Figure 56 Specific productivity representing the process performance of production phase bench scale vessels at 1x and 2x feed condition (Experiment 4.1b)..... 121
Figure 57 Viable cell density (x10^6 cells/mL) representing the process performance of the n-1 phase vessels in Experiment 4.2 126
Figure 58 Glucose concentration (g/L) representing the process performance of the n-1 phase vessels in Experiment 4.2 128
Figure 59 Lactate concentration (g/L) representing the process performance of the n-1 phase vessels in Experiment 4.2 129
Figure 60 pH representing the process performance of the n-1 phase vessels in Experiment 4.2 130

Figure 61 Viable cell density (cells/mL) representing the process performance of the production phase vessels in Experiment 4.2 131
Figure 62 Viability (%) representing the process performance of the production phase vessels in Experiment 4.2 132
Figure 63 Glucose concentration (g/L) representing the process performance of the production phase vessels in Experiment 4.2 133
Figure 64 Lactate concentration (g/L) representing the process performance of the production phase vessels in Experiment 4.2 134
Figure 65 Dissolved oxygen (%) representing the process performance of the production phase vessels in Experiment 4.2 135
Figure 66 Cell specific glucose consumption rate (g/cell/day) representing the process performance of the production phase vessels in Experiment 4.2 136
Figure 67 Titre (g/L) representing the process performance of the production phase vessels in Experiment 4.2 137
Figure 68 Cell specific productivity (g/cell/day) representing the process performance of the production phase vessels in Experiment 4.2 138
Figure 69 Saw-Tooth plot of the expansion of DCB1 in the generation of DCB2 147
Figure 70 The expansion of DCB1 within a continuous bioprocessing environment, with exposure to enriched medium, in the generation of DCB3 148
Figure 71 Saw-Tooth plot of the expansion of DCB3 in the generation of DCB4 149
Figure 72 Viable cell density (VCD) of cultures within Experiment 5.1a plotted over duration (days) 150
Figure 73 Percentage viability of cultures within Experiment 5.1a plotted over duration (days) 152
Figure 74 Glucose Concentration of cultures within Experiment 5.1a plotted over duration (days) 153
Figure 75 Cell specific glucose consumption of cultures within Experiment 5.1a plotted over duration (days) 154
Figure 76 Lactate concentration of cultures within Experiment 5.1a plotted over duration (days) 155
Figure 77 pH of cultures within Experiment 5.1a plotted over duration (days) 157
Figure 78 Titre (mg/L) of cultures within Experiment 5.1a plotted over duration (days) 158
Figure 79 Viable cell density (VCD) of cultures within Experiment 5.1b plotted over duration (days) 159

Figure 80 Viability of cultures within Experiment 5.1b plotted over duration (days) 161
Figure 81 Glucose concentration (g/L) of cultures within Experiment 5.1b plotted over duration (days).....162
Figure 82 Lactate concentration (g/L) of cultures within Experiment 5.1b plotted over duration (days).....163
Figure 83 pH of cultures within Experiment 5.1b plotted over duration (days).....165
Figure 84 Titre (mg/L) of cultures within Experiment 5.1b plotted over duration (days).....166
Figure 85 Viable cell density (cells/mL x10^6) of cultures within Experiment 5.2, plotted over duration (days) 168
Figure 86 Viability (%) of cultures within Experiment 5.2, plotted over duration (days) 169
Figure 87 Dissolved oxygen (%) of cultures within Experiment 5.2, plotted over duration (days) 171
Figure 88 pH of cultures within Experiment 5.2, plotted over duration (days).....172
Figure 89 Lactate Concentration (g/L) of cultures within Experiment 5.2, plotted over duration (days).....173
Figure 90 Specific glucose consumption rate (g/cell/day) of cultures within Experiment 5.2, plotted over duration (days).....174
Figure 91 Titre (mg/L) of cultures within Experiment 5.2, plotted over duration (days).....175

Appendix Figures

Appendix Figure I Perfusate amino acid profiles for microscale and bench scale experiments (Chapter 3) 190

Motivation and Thesis Structure

Motivation

Continuous cell culture was popularised by the development of the chemostat in 1950 (Monod, 1950; Novick & Szilard, 1950). The chemostat method involves diluting a culture with fresh medium at a rate matched to the removal of cells and spent medium from the culture. The culture reaches a 'steady-state' cell concentration, that is representative of the limiting nutrient defined by the dilution rate, and physiochemical conditions applied (Pirt, 1975). Researchers have utilised continuous culturing to investigate the growth kinetics of a cell line through systematic interrogation of the physiochemical parameters (Hoskisson & Hobbs, 2005).

The reproducibility and robustness achieved by continuous cultures have allowed detailed systematic metabolic flux analysis to be conducted in both microbial and mammalian systems (Follstad, Balcarcel, Stephanopoulos, & Wang, 1999; Varma & Palsson, 1994). Additionally, complex multi-institution investigations that require extensive parallel quantitative analysis of a cell line is possible with an established continuous system. This is due to the system's ability to maintain an extended steady-state condition.(Canelas et al., 2010).

The operation of continuous cultures over batch, or fed-batch, provides advantages in the production of commercial products. Firstly, the low residence time possible in continuous culture has been shown to improve the product quality attributes of unstable molecules. This improved product quality sequentially results in an improved yield of the intact molecule (Lee et al., 2004; Rodriguez et al., 2010). Furthermore, the operational cost of goods (COGs) analysis for continuous systems has highlighted a reduction when compared to equivalent fed-batch production (Pollock, Ho, & Farid, 2013). This lower COGs is partially due to a reduction in required fermenter sizes at commercial scale, which in turn also simplifies the scale-up from development.

Despite these advantages, the commercial production of therapeutic proteins has relied heavily on the fed-batch mode of operation over the past 40 years. Contributing factors include the simplicity of operation, the ability to conduct analytical testing at the end of each fermentation, and the confirmation of cell line stability over shorter 'manufacturing windows'. The increased use of fed-batch has been combined with a preference for mAb production in mammalian systems (namely Chinese Hamster Ovary (CHO) cells). This is due to the ability of mammalian cell lines to process complex post-translational modifications (namely human

glycosylation patterns) to achieve desired product quality characteristics and avoid immunogenic responses (Birch & Racher, 2006).

The popularity of this method has promoted the invention of numerous high-throughput scale down technologies to enable optimisation campaigns in a low resource setting (Bareither & Pollard, 2011; Rameez, Mostafa, Miller, & Shukla, 2014). These systems provide the ability to satisfy the regulatory Quality by Design (QbD) directives (Guideline, 2009; Hakemeyer et al., 2016). As no equivalent systems exist for continuous commercial bioprocess development, there is an inherent lower utilisation of this advantageous method of production. This lower utilisation is coupled with lower prior knowledge and the ability to simplify the mode of operation.

The primary motivation for this thesis is to identify cellular and or, biochemical characteristics specific to continuous bioprocess systems. This identification will enable advance control strategies to be developed for commercial scale continuous bioprocess systems to add to prior knowledge on the continuous environment. This primary motivation is linked to a secondary motivation, to understand the scale dependent and independent variables of scale down continuous bioprocess technologies, present specifically in a high throughput setting.

Thesis Structure

Chapter 1 - Introduction

The first chapter provides a detailed context and comprehension for the investigations outlined in this thesis. Specifically, a review is offered on the topic of upstream bioprocessing, tools, and methods, enabling the production of monoclonal antibodies to meet growing global demand.

Chapter 2 - Materials and Methods

The second chapter details the organisation of experiments and the specific materials and methods utilised when conducting them.

Chapter 3 - The Design, Execution and Evaluation of a High-Throughput Continuous Microscale Environment

The third chapter presents the repurposing of an advance fed-batch microscale system to operate continuous cultivations, specifically as a perfusion system. This investigation entails the development of a cell retention methodology based on gravity cell settling.

Understanding the impact of the methodology on the continuous culture of mammalian cells highlights its suitability to identify cellular and or biochemical characteristics specific to continuous bioprocess systems. Comparison to bench scale perfusion system is offered by the parallel operation of a 7L STR vessel functionalised with an ATF perfusion setup.

Chapter 4 - The Evaluation of Micro and Bench Scales Perfusion Cultures as Tools for Production Culture Inoculum Expansion

The fourth chapter presents two key evaluations. Firstly, the characterisation of the microscale methodology from Chapter 3 is expanded to highlight the scale dependent differences in the cellular characteristics of the cultures. Secondly, the cellular impact of reducing the culture dilution rate is evaluated to decouple any inherent sensitivity of the cell line to scale and method related observations.

These evaluations are performed by progressing cells from the exponential growth phase of the respective perfusion cultures, into comparatively high physiochemical stress fed-batch cultures. By elucidating the differences in performance that may be attributed to the proceeding perfusion culture it is possible to evaluate scale and method dependent cellular characteristics of perfusion cultures.

Chapter 5 - The Evaluation of Fed-Batch Culture Performance in Response to Targeted Parameter Deviation Before and After Controlled Inoculation

The fifth chapter utilise fed batch operation to focus investigations on cell line sensitivity present in the exponential growth phase. Additionally, it highlights the need for contextual control strategies in the investigation of process limits. Understanding the culture characteristics during this phase will provide novel control strategies not previously investigated for continuous culture operation.

Chapter 6 - Conclusions and Future Work

The sixth chapter presents the overarching conclusions from the experimental. The logical next steps and directions for future work are presented.

Chapter 1 Introduction

1.1 Antibodies

As a function of the acquired immune response in mammals, antibodies (Abs) are produced by activated B-cells in response to antigen detection. The repeated exposure of the immune system to antigens generates clonal populations and the proliferation of activated B-cells. This results in an increase in the levels of Abs secreted as an immune response (Delves & Roitt, 2000).

Antibodies contain specialised structures that equip the molecules with the ability to simultaneously bind with antigens and recruit an immune response against the antigen. Utilising the IgG class of antibodies as an example, the basic Ab structure consists of two identical heavy chains combined with two light chains, with each chain consisting of variable and constant regions (Vidarsson, Dekkers, & Rispens, 2014) (Figure 1).

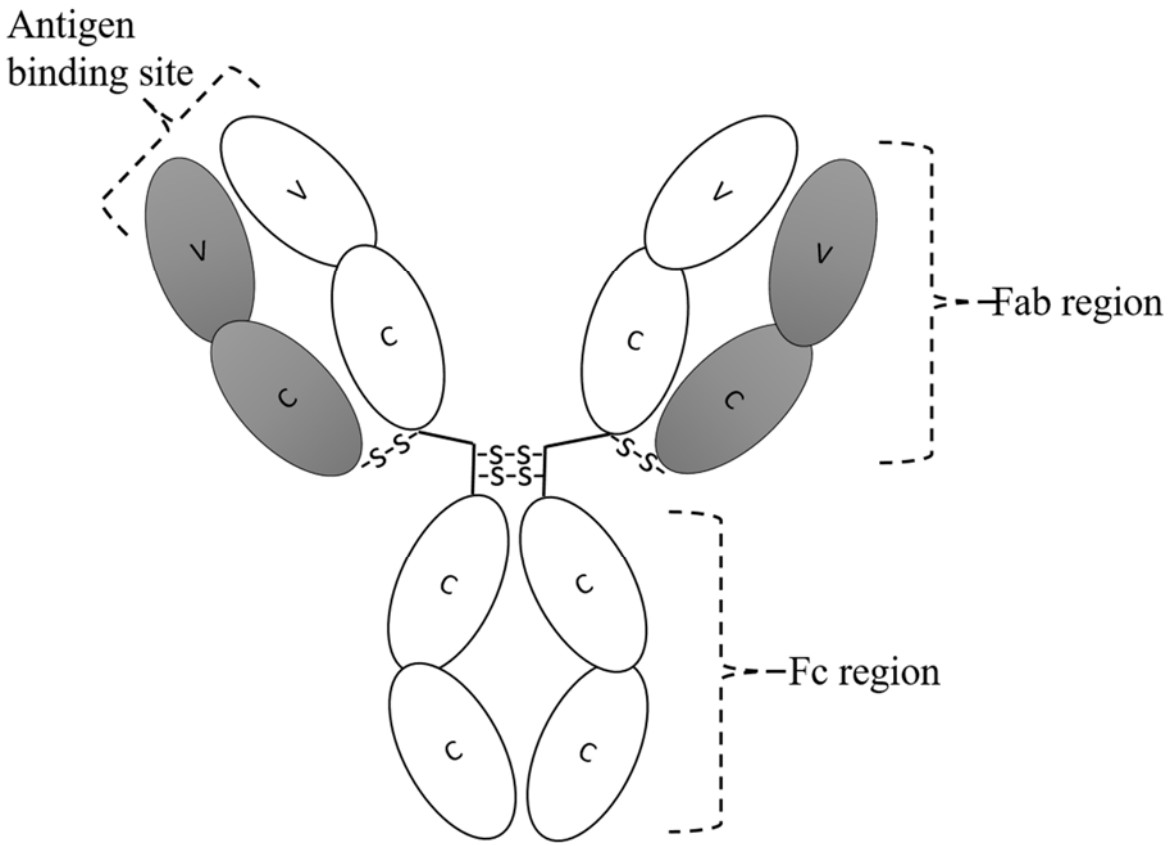

Figure 1 Diagrammatic representation of the constitutional components of an IgG class antibody
Highlighted by dashed braces are the functional structures within the antibody, antigen-binding site, Fab and Fc subdomains, respectively. Light (grey) and heavy (white) chains are represented with their constitutional variable (V) and constant (C) regions. Association of chains is performed by di-sulphide bonds (-s-s-).

Billions of combinations within the structures of the variable (V) domains of the heavy and light chains (Complementarity determining regions, or CDRs), enable comprehensive antigen recognition. The combination of these variable domains with constant domains forms the Fab

region of the Ab. Linkage of chains by di-sulphide bonds provides the Fab region with essential flexibility for interaction with the antigen-binding sites (Amzel & Poljak, 1979).

The continuation of the heavy chain constant regions beyond di-sulphide bonds forms the Fc region of the Ab. The Fc region provides the Ab with the ability to interact with the host system immune system (Unkeless, Scigliano, & Freedman, 1988).

Recent advancements in antibody design have focused on the therapeutic application of bi-specific antibodies. These molecules have the ability to recognise two unique antigens, and conceptually have an advantage in combating diseases that have evaded traditional bivalent antibodies (Labrijn, Janmaat, Reichert, & Parren, 2019). The manufacture of these molecules can be challenging. A popular approach, coined 'knob in hole', is used to promote heterodimerisation of two unique heavy chains. This involves engineering complementary mutations in the Fc region of the two desired heavy chains. This result in complementary binding, and the formation of an intact Ab (H. Liu, Saxena, Sidhu, & Wu, 2017; Ridgway, Presta, & Carter, 1996).

1.2 Therapeutic Application and Commercialisation of Antibodies (Abs)

Mature B cells (plasma cells) are specialised in the production and excretion of Abs. Their maturation, specifically the cleavage of the CD40 ligand, causes them to be terminally differentiated (Arpin et al., 1995). This presented a challenge to *in vivo* research into Abs. Researchers couldn't determine which antigen marker the polyclonal population of B cells was expressing Abs against.

The *In vitro* investigation of B cells required the culturing and expansion of monoclonal populations. This was facilitated by scientists at the University of Cambridge who developed hybridoma technology. This advancement involved combining normal B cells from the spleen of an immunised mouse with mouse myeloma cells. The resulting culture of cells proliferated indefinitely and produced a high, detectable expression of Abs. This discovery in 1975 was the first reported instance of the production of a monoclonal antibody (mAb). Its significance was later recognised with the award of the Nobel Prize for Medicine in 1984 (Alkan, 2004).

The Food and Drug Administration (FDA) approved the first recombinant therapeutic protein as a thrombolysis treatment 11 years later (Allen, 1987; Baruah, Dash, Chaudhari, & Kadam, 2006). Therapeutic protein product approvals have been greater than 10 per year (with mAbs consisting of >20%) since 1995. In addition, over the past five years, product approval has increased to ~22 per year, with mAbs representing around 53% of these (Walsh, 2018). This

popularity and continued development of mAbs is due to the wide scope of their utility in therapeutic areas (Pavlou & Belsey, 2005).

The research and development activities have been facilitated by the development of genetic engineering techniques. This has been focused in the fields of molecular cloning and delivery of plasmid DNAs (Al-Moslih & Dubes, 1973; Cohen, Chang, Boyer, & Helling, 1973; Graham & van der Eb, 1973; Svoboda et al., 1973). The publication of the complete human genome (Venter et al., 2001) and continued work on the human proteome (M.-S. Kim et al., 2014) has accelerated molecular understanding of disease. This advancement has allowed researchers to design specific nucleotide sequences to target the disease antigen-binding sites (Filpula, 2007). Commercially, this specificity to target indications with high populations has enabled the market to evolve into a multi-billion dollar per year prospect (J. K. Liu, 2014).

1.3 Host Cell Lines, Expression Systems and Stable Cell Line Generation

The first therapeutic mAbs produced experienced human anti-mouse immune side effects. This was due to the large size of the molecules combined with the host cell lines inability to effectively translate the respective genetic sequence (F. Li, Vijayasankaran, Shen, Kiss, & Amanullah, 2010). Investigations identified glycosylation patterns native to the host cell system on translated antibody products as a cause for this immunogenic response (Q. Zhou & Qiu, 2019). Therefore, it was vital to select host cell lines for their ability to accurately translate humanised glycan structures onto the secreted mAbs (Birch & Racher, 2006). The *E.coli* host cell line is an example of an alternative option to mammalian hosts. It possesses an advanced gene editing toolbox and shorter manufacturing windows (Rosano & Ceccarelli, 2014). However, these benefits are not commonly exploited for mAb production due to the inferior expression of humanised product attributes when compared to mammalian hosts (Spadiut, Capone, Krainer, Glieder, & Herwig, 2014).

The Chinese Hamster Ovary (CHO) cell hosts have been studied and utilised extensively for therapeutic mAb expression since the 1980s (Birch & Racher, 2006). Alternative mammalian host cell systems such as the non-secreting murine myeloma (NS0), Human PER.C6 and Human embryonic kidney (HEK) cell lines are used commercially, and their adoption or continued usage by an organisation is typically based on historic procedures and knowhow (Kunert & Reinhart, 2016). The CHO host cell lines make up >70% of the cell lines used commercial expressed mAbs (Jayapal, Wlaschin, Hu, & Yap, 2007) and this ubiquitous use has led to continued improvements into the bioprocesses they define (Goh & Ng, 2018). This

is highlighted by the reported productivity improvements over the decades, with fed batch process titres of 1g/L, 5g/L and more recently 10g/L achieved and exceeded (F. M. Wurm, 2004).

The improvements in productivity have been realised by combining the host cell lines with a complementary expression system. A popular choice of a host cell line is CHO variants that lack the essential dihydrofolate reductase (DHFR) enzyme. These host cell lines are transfected with a plasmid containing DNA for both the DHFR enzyme and therapeutic protein of interest. The application of selective pressure, through an inhibitor such as methotrexate (MTX) and a thymidine lacking medium, forces the cell to co-express the acquired DHFR gene alongside the therapeutic protein of interest simultaneously to survive (Kaufman & Sharp, 1982).

Comparable selective expression pressure is generated by the CHOK1 variant of the CHO host (developed by Lonza Biologics, Switzerland). This is achieved when the host is used in combination with the complimentary GS (glutamine synthase) Gene Expression System®, exploiting the cell lines essential requirement for glutamine. The GS Gene Expression System takes advantage of the host cell lines essential requirement for glutamine. The endogenous glutamine synthase enzymatic reaction is blocked through the addition of a GS inhibitor such as methionine sulphoximine (MSX). The co-expression of a transfected plasmid containing DNA for both the GS enzyme and therapeutic protein of interest ensures sufficient GS is available for cell survival (L. Fan et al., 2012).

These two expression systems, DHFR and GS, inherently link cellular mAb productivity to cellular survival. This provides a failsafe method of cell line selection as only appropriately transfected cell lines will be able to grow (Dhara, Naik, Majewska, & Betenbaugh, 2018).

Stable transfection is typically performed with the assistance of a viral promoter. An example of such a promoter is the retrovirus murine leukaemia virus (MLV). This promotor enables the integration by transfection of DNA sequences into the host cell genome (T. K. Kim & Eberwine, 2010; Ye et al., 2010). This process of transfection results in the random placement of the plasmid into the host cells' genome (T. K. Kim & Eberwine, 2010).

This random integration generates variability in the performance of clones within each pool. Overtime (through natural selection) those with high survival characteristics will generate large subpopulations within the transfected pools. These survival characteristics may not translate to desired expressed Ab quality or productivity characteristics. To accurately characterise a

bioprocess and reproduce the performance in a commercial manufacturing setting, this variability in expression characteristics must be removed.

Ensuring cell line monoclonality is a critical step in ensuring the robustness of the manufacturing process. Several methods have been adopted to confirm culture clonality (Browne & Al-Rubeai, 2007). Traditionally a labour-intensive method of limited dilution was widely adopted for CHO cells due to its application to cultures grown in suspension rather than on agar plates (Puck & Marcus, 1955). More recently, high investment into commercial cell line construction has introduced flow cytometry, and other single cell sorting, techniques into clone selection (Borth, Zeyda, & Katinger, 2000; Grilo & Mantalaris, 2019; Yim & Shaw, 2018).

Ultimately, vast quantities of monoclonal cell lines will be generated with unique expression and stability characteristics. Extensive screening procedures are conducted to determine the ranking of performance. Statistically, the larger number of cell lines evaluated will result in a higher chance of discovering one with appropriate criteria. Ranking criteria can consist of a combination of (but is not limited to), cell growth characteristics, cell specific productivity, titre, product quality and stability of these attributes as cell age increases (Birch & Racher, 2006).

1.4 Cell Line Response to Bioprocess Control, Development and Optimisation

The evaluation of cell line performance is in relation to specific sensitivities and interactions present in the manufacturing physiochemical environment. Due to the extensive utilisation of CHO hosts, many characteristics have been studied and successfully exploited through tight process control, in the commercial production of mAbs. However, the variety of therapeutic mAb products generated gives rise to increasingly complex cell lines displaying unique characteristics to be investigated in development (De Jesus & Wurm, 2011).

1.4.1 Hydrodynamic Stress

Mammalian cell cultures are isolated from immobile vascularised tissue with very low hydrodynamic stresses. Cells grown in suspension cultures are exposed to shear forces as they are mixed and sparged. Cell line sensitivity to shear has been a focus of researchers when culturing mammalian cells (Godoy-Silva, Chalmers, et al., 2009; Walls et al., 2017).

Hydrodynamic stress has historically been investigated in these two formats: the dissipation of energy from the mechanical agitation of the impeller; and the rupture forces of bursting bubbles originating from the sparging of gases (W. Hu, Berdugo, & Chalmers, 2011). As mammalian

cell cultures are intensified in the quest for higher productivities, agitation rates and gas sparging are set to increase to meet the nutrient demand of the cultures, focusing the need to characterise cell line sensitivity to hydrodynamic stress.

For mechanical agitation, early studies investigating microcarrier/adherent cell suspension cultures shaped an adopted opinion that mammalian cells in suspension displayed a sensitivity at elevated agitation. Increasing the agitation rate resulted in detachment of the mammalian hosts from the microcarriers (Clark, Hirstenstein, & Gebb, 1980; Croughan, Hamel, & Wang, 2000; Venkat, Stock, & Chalmers, 1996).

In review of hydrodynamic stress on mammalian cultures (W. Hu et al., 2011), evaluations of bench scale (G. Zhou & Kresta, 1996) and manufacturing scale (Wernersson & Trägårdh, 1999) vessels are conducted. The hydrodynamic stress experienced and investigated was at substantially lower levels than those shown to be detrimental to CHO host growth and productivity performance (Godoy-Silva, Mollet, & Chalmers, 2009; Ma, Koelling, & Chalmers, 2002; Mollet, Godoy-Silva, Berdugo, & Chalmers, 2007). This comparative analysis provides operational flexibility to increase the agitation rates as the culture densities increase and the culture physiochemical environment requires it.

Sparging gasses into the culture results in bubble formation that becomes a local focus of hydrodynamic stress when rupture occurs. These bubbles will ultimately undergo a detachment process at liquid-air surfaces (MacIntyre, 1972). This sudden release of air from the bubble has been shown to release high localised hydrodynamic forces that are inversely proportional to bubble size (Chisti, 2000), and equivalent to those generated in manufacturing scale STRs mechanical agitation (Wernersson & Trägårdh, 1999).

The addition of a non-ionic surfactant (such as Pluronic F-68 (Polyoxyethylene-polyoxypropylene)) has provided a multi-faceted improvement in reducing the hydrodynamic impact on cells from bubbles (Tharmalingam, Ghebeh, Wuerz, & Butler, 2008). Firstly, the surfactant associates with the cell-surface lipid bilayer to increase the physical robustness of the membrane. Secondly, the association with the cell membrane generates an increased hydrophobicity of the cell. This enables the cell to more readily disassociate from the bubble surface, before any detachment or bursting event. The increase in the distance reduces the exposure of the cells to peak hydrodynamic forces during rupture events (Walls et al., 2017).

The potential sensitivities of CHO host cell lines to shear forces requires process control to adopt a conservative strategy to allow successful process operation. Firstly, given its apparent

protective qualities, the medium formulation is regularly supplemented with Pluronic F68. Secondly, to maintain the culture dissolved oxygen (DO) level as required, gas flow rates are restricted to an upper limit and agitation only increased incrementally when the current gas transfer rates do not meet the set DO level. The hydrodynamic forces are thus minimised whilst providing sufficient mixing and maintaining the physiochemical environment.

1.4.2 pH Control

Mammalian cultures rely on the exchange of hydrogen ions for the function of their enzymatic processes. The sub-optimal pH of a culture will impact these interactions and, in turn, can decrease the culture performance. The growth performance of CHO cells can be sensitive to as little deviation as 0.1 from the optimal pH (F. Li et al., 2010).

A sodium bicarbonate ($NaHCO_3$) buffering component is often included in the medium formulations and the carbonic acid readily produced by the metabolically produced carbon dioxide (CO_2) serve as an acid/base pair. The pH is then maintained at an optimised value through controlled addition of gaseous CO_2 and shot additions of $NaHCO_3$, as required.

Incorporated into cultures is an online pH probe that provides data to a proportional-integral (PI) control loop. The PI controller first determines the distance from setpoint (Proportional term) and then sums the duration it has been there (accumulated Integral term). Outputs from the PI controller will be converted into calculated flow rates of either CO_2 or $NaHCO_3$ to bring the pH back within the dead-band.

The exposure to varied pH setpoints has been observed to contribute, at least in part, to variable process performance. Specifically, this has been recognised where a decrease in pH displays a decline in growth and productivity parameters (Brunner, Fricke, Kroll, & Herwig, 2017). In addition, undesirable mAb product quality attributes have been shown to correlate with suboptimal control of culture pH (Goldrick et al., 2017). The impact of pH on culture performance is not universal for all CHO host derived cell lines, and each may present a unique response to pH control (Trummer et al., 2006).

1.4.3 Temperature Control

Temperature, like pH, has a universal impact on enzymatic activity within living organisms. Mammalian culture systems work optimally within a physiological range, between 36 and 38°C. Temperature is maintained within cultures to a predetermined setpoint within this range. This control is performed with the combination of an online temperature probe and heating elements (typically a heated element positioned around the perimeter of the vessels).

The effects of temperature on the performance of mammalian culture systems have been extensively studied. The majority of the focus has been on the impact of hypothermic (<35°C) conditions on culture performance (Fogolín, Wagner, Etcheverrigaray, & Kratje, 2004). A reduction in the growth rates, maximal culture concentrations and culture metabolism has been observed when culture temperature is reduced (Borth, Heider, Assadian, & Katinger, 1992; Furukawa & Ohsuye, 1998; Reuveny, Velez, Macmillan, & Miller, 1986; Sureshkumar & Mutharasan, 1991; Weidemann, Ludwig, & Kretzmer, 1994).

In addition, there are specific benefits to operating in a hypothermic range that translates to therapeutic mAb production. A lower temperature has been shown to decrease the percentage of cultures in the S phase of the cell cycle, enabling cells to accumulate in G1 (Moore et al., 1997). This increased instance of G1 phase results in a delayed onset of culture apoptosis and therefore a prolonged culture duration. Additionally, the temperature mediated reduction in cell metabolism prevents the build-up of potentially toxic waste metabolites (Xu et al., 2019).

The observation of this delayed onset of apoptosis has been shown to increase productivity (Moore et al., 1997) and will be of particular benefit for cell lines that display an increased mAb production in G phase (Dutton, Scharer, & Moo-Young, 2006). However, given that cell specific productivity is typically assumed to be higher in S phase (Lloyd, Holmes, Jackson, Emery, & Al-Rubeai, 2000), the benefits associated with extending batch or fed-batch culture duration are not always realised and are likely cell line specific (Bloemkolk, Gray, Merchant, & Mosmann, 1992).

An increase in temperature above the physiological range evokes stress responses in mammalian cultures. Studies at the transcriptional level indicate the overexpression of heat shock proteins (HSPs) at temperatures maintained above the physiological range (Kregel, 2002). These HSPs provide a protective environment to reduce the amount of protein aggregation that occurs during periods of high temperature stress. However, this protection is not sufficient to counteract the conformational changes and a high rate of protein degradation that occurs at high culture temperatures (Parag, Raboy, & Kulka, 1987). Furthermore, suppressed growth was observed in cultivations at temperatures as high as 42°C (Sureshkumar & Mutharasan, 1991). Recently, studies involving mild hyperthermic exposures have indicated a “eustress” response that acts in the absence of HSPs. This has been observed to result in acquired thermotolerance presenting through maintaining membrane homeostasis, activating lipid remodelling, and redistributing chaperone proteins (Peksel et al., 2017).

This cumulative response to increased culture temperature emphasises the importance of maintenance within physiological ranges when operating production cultures. Potential benefits have been investigated when operating a shift in temperature from physiological to hypothermic at the end of exponential growth (Hendrick et al., 2001; Kaufmann, Mazur, Fussenegger, & Bailey, 1999). In addition, investigations have displayed a doubling of productivity utilising a hypothermic temperature shift, and have also presented beneficial mRNA stabilising effect of the hypothermic condition (Oguchi, Saito, Tsukahara, & Tsumura, 2006).

1.4.4 Dissolved Oxygen and Carbon Dioxide Saturation

The saturation levels of dissolved oxygen (DO) and CO_2 within a culture are critical elements of the physiochemical environment. Dissolved oxygen maintenance is coupled to the culture agitation, sparging of oxygen, vessel geometry and minimisation of foam formation (as mentioned above, Section 1.4.1 Hydrodynamic Stress). Levels of DO within cultures are maintained by altering a single, or combination, of these contributing factors (Amer, Feng, & Ramsey, 2019; Hanson et al., 2007).

Observations have determined mammalian cells display an impact on cellular metabolism at or below five percent culture saturation, with a critical level observed at one percent saturation (Heidemann, Lütkemeyer, Büntemeyer, & Lehmann, 1998). Additionally, hyperoxia conditions (approx. 200% saturation) have been shown to reduce the culture growth rate. Finally, operation outside a range of 10 to 100% saturation can result in undesirable product quality attributes (Restelli et al., 2006), and have a negative impact on culture productivity (Handlogten, Zhu, & Ahuja, 2018).

During culture operation, to mitigate the risk of operating at a saturation below 5%, a set point of around 50% is typically maintained. This provides a contingency for the process control systems (adjustment of agitation rates and volume of sparged oxygen) to respond if oxygen demand of the culture changes. Increases may occur when the culture progressing through exponential growth or when a surfactant such as antifoam is added that alters the gas transfer rates (Pappenreiter, Sissolak, Sommeregger, Striedner, & biotechnology, 2019).

Increases of carbon dioxide (CO_2) saturation within mammalian cell cultures is provided for the maintenance of culture pH (Section 1.4.2 pH Control). Additional CO_2 is generated as a metabolic by-product of respiration. Mammalian cells can tolerate CO_2 build-up, but do experience inhibitory thresholds where adverse effects are encountered. Levels increasing

from 50 to 140-150 mmHg has been reported to impact growth and productivity (deZengotita, Schmelzer, & Miller, 2002; Zhu et al., 2005), with values greater than 111 mmHg reported to impact product quality (Xing, Li, Chow, & Lee, 2008).

These inhibitory thresholds are of particular interest as they represent the levels experienced in the large volume culture vessels, due to the longer bubble residence time and decreased mixing velocities in larger, taller vessels (Sieblist et al., 2011).

Investigations can be conducted in laboratory scale cultures, such as increased CO_2 sparging, to determine the sensitivity of a particular culture or cell line. However, solutions are typically identified in the large manufacturing scale cultures, specifically in bioreactor design (altering vessel geometry to increase gas transfer rates) and pH control strategies (Mostafa & Gu, 2003; Xing, Lewis, Borys, & Li, 2017).

1.4.6 Nutrient Availability and Waste Accumulation

The appropriate maintenance of available nutrients is a vital component of culture control and optimal culture operation. This control involves the exacting supply of carbohydrates, amino acids, lipids, nucleic acid precursors and rare metal ions, throughout stages of culture operation. Iterative improvements in medium and feed development over the past 30 years have resulted in multi g/L processes achieved (F. M. Wurm, 2004).

Whilst the correct medium formulation provides the potential for culture success, incorrect formulations can be equally impactful. In addition to the growth and productivity performance measures (Rodrigues, Costa, Henriques, Azeredo, & Oliveira, 2012; Simpson, Singh, Perani, Goldenzon, & Al-Rubeai, 1998), product quality variation is observed by incorrect control of culture nutrient supply (Costa et al., 2013; Hossler, Khattak, & Li, 2009).

Fetal bovine serum (FBS) has been a widely used mammalian culture supplement in academic and commercial applications. However, due to ethical and safety concerns, and lot-to-lot variation, fully chemically defined medium and supplement formulations have been developed and are an accepted standard in the commercial manufacture of mAbs (Gstraunthaler, 2003). These chemically defined medium can vary widely in their constitutive components but must facilitate the glyco-glutaminolysis activity that characterises mammalian cell culture (Pan, Streefland, Dalm, Wijffels, & Martens, 2017; Quek, Dietmair, Krömer, & Nielsen, 2010).

Glyco-glutaminolysis is the cellular uptake and processing of glucose and glutamine, combined with the secretion of ‘waste’ metabolites, such as lactate and non-essential amino acids. The

toxic build-up of waste metabolites and bi-products can result in premature culture termination. Specifically, lactate has been observed to accumulate through the stationary phases of culture growth. This accumulation presents pressures on pH maintenance control that can result in a loss of control, stress to the culture and negative performance (Quek et al., 2010; Zagari, Jordan, Stettler, Broly, & Wurm, 2013).

High aerobic glycolysis within cells can generate a redox potential that contributes to these elevated lactate concentrations (Halestrap & Wilson, 2012), this process is known as the Warburg effect (Warburg, Wind, & Negelein, 1927). Many carbon feeding strategies have been explored to mitigate this accumulation (Claudia Altamirano, Illanes, Becerra, Cairó, & Gòdia, 2006; C. Altamirano, Paredes, Illanes, Cairó, & Gòdia, 2004; J. Li, Wong, Vijayasankaran, Hudson, & Amanullah, 2012). However, due to the culture supply demands of glucose and glutamine for high product quality (Y. Fan et al., 2015; Hayter et al., 1992; Nyberg, Balcarcel, Follstad, Stephanopoulos, & Wang, 1999; Reinhart, Damjanovic, Kaisermayer, & Kunert, 2015), and the inherent complexity and crosstalk of the metabolic network (Grüning, Lehrach, & Ralser, 2010), no universal control strategy has been developed. It has been shown that by reducing this Warburg effect, cultures display improved growth and productivity (Buchsteiner, Quek, Gray, & Nielsen, 2018). A review of the literature indicating mechanisms driving the consumption and production of lactate has indicated that control of the cytosolic redox potential may be key to controlling cellular lactate concentrations (Hartley, Walker, Chung, & Morten, 2018).

Finally, it is critical to carefully monitor culture viability when controlling waste accumulation in the culture. At the onset of culture apoptosis, there will be an increase in intercellular host cell proteins that may impact the product quality characteristics of the expressed mAb (Hogwood, Bracewell, & Smales, 2014; Park et al., 2017). Therefore, strict culture harvest criteria are set, and the utilisation of low shear primary recovery devices are designated (Y. Fan, Ley, & Andersen, 2018) to ensure consistent product quality is achieved if cellular apoptosis cascades are initiated (Tait, Hogwood, Smales, & Bracewell, 2012).

1.5 Modes of Operation

Culture operation is managed through strategic control of the aforementioned nutrient demands and management of cellular waste. The below subsections present the variety of cultivation modes employed, each offering advantages and drawbacks in the production of mAbs.

1.5.1 Batch

The batch growth of cultures can be a robust mode of cultivation due to the simplicity of its operation. Cells are inoculated into a nutrient rich medium and the culture expands, utilising available resources until they are depleted. As a critical culture component becomes limiting, the culture will transition from exponential growth into a decline phase. Nutrient limited cultures will quickly reach harvest criteria and the production mode terminated as viability decreases.

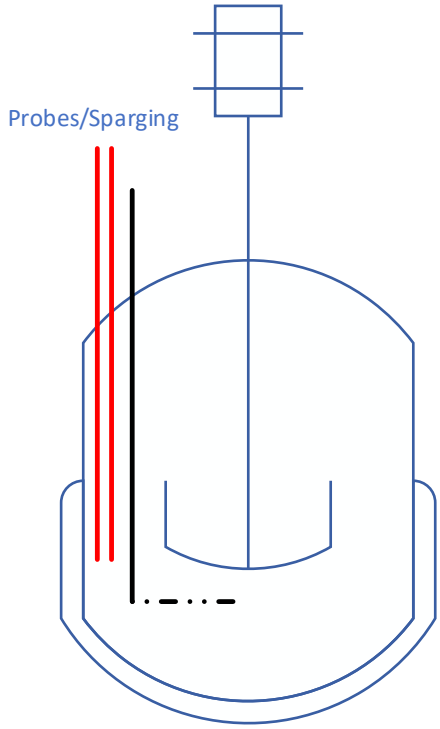

Figure 2 Example of batch culture operation setup
The diagrammatic example contains required components for operation of a batch culture including impeller, probes (e.g. pH and DO) shown in red, gas sparging line shown in black and jacket around the vessel to control temperature.

The simplicity of batch culture enables its use as a low resource method of screening cell line performance. The translation of this performance to other cultivation methods relies on the assumption that cell specific productivity (grams of protein produced/cell/day) is retained and any percentage change in productivity is accounted for by changes in culture duration and or density (Longobardi, 1994).

1.5.2 Fed-Batch

As the name suggests, fed-batch cultivation involves strategic feeding of key nutrients to batch cultures. Fed-batch (FB) methods have proven the most popular method for therapeutic mAb production over the past 30 years, and continued refinement has contributed to 100-fold

improvements in overall bioprocess productivity (Chu & Robinson, 2001). These improvements have been realised by increasing the duration a culture spends in each phase of growth to maximise productivity and maintain product quality.

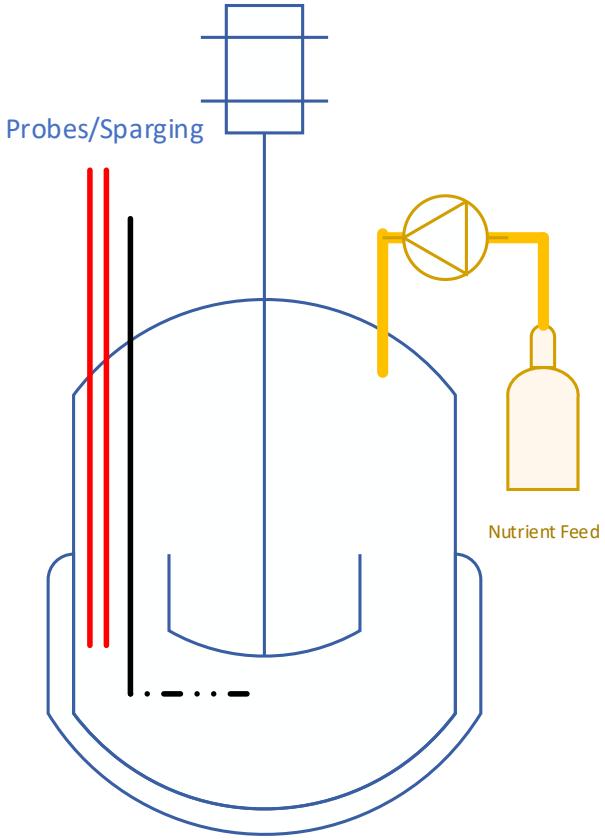

Figure 3 Example of fed batch culture operation setup
The diagrammatic example contains required components for operation of a fed batch culture including impeller, probes (e.g. pH and DO) shown in red, gas sparging line shown in black, jacket around the vessel to control temperature and the nutrient feed bottle in yellow.

Early investigations within cell culture identified the phases of culture progression that are the focus in fed-batch culture, in the present day (Monod, 1949). These phases include inoculation, exponential growth, stationary and decline/death phases, and are presented in Figure 4, below.

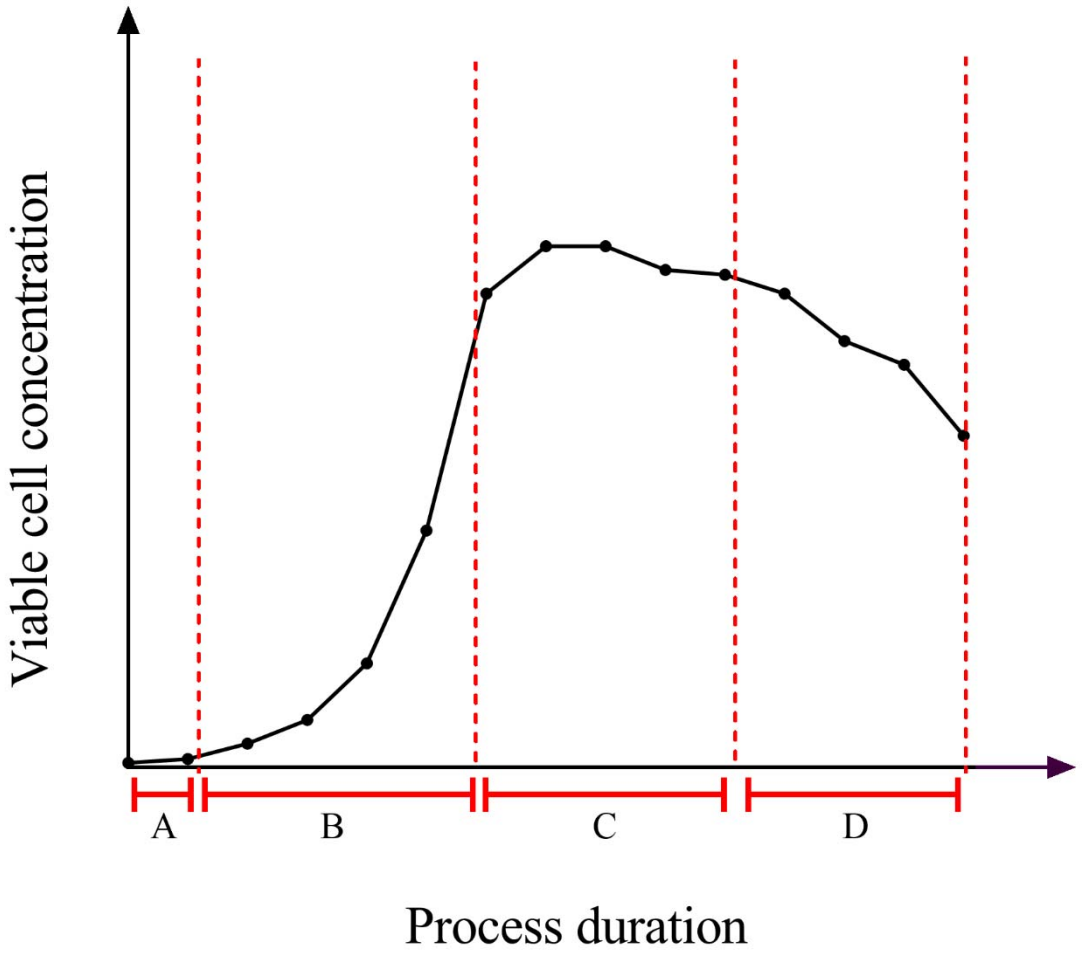

Figure 4 Example presentation of a typical growth profile over a batch or fed-batch bioprocess operation.
Example growth profile plots viable cell concentration over increasing process duration, with intersecting dashed lines designating specific phases of culture progression. (A) Inoculation/Lag following inoculation. (B) Exponential growth. (C) Stationary. (D) Decline/death

Metabolic flux analysis of cultures operated in batch and fed-batch has defined characteristics of these 4 stages of culture progression and identified the complexity involved at each stage (Ahn & Antoniewicz, 2012; Dorka, Fischer, Budman, & Scharer, 2009; Gao, Gorenflo, Scharer, & Budman, 2007; Provost & Bastin, 2004; Templeton, Dean, Reddy, & Young, 2013).

The duration of the exponential growth phase, and the resulting culture cell density, is dependent on the abundant supply of nutrients. Metabolite analysis of medium removed during exponential growth can identify the key nutrients that are required to prolong the exponential growth (Butler & Jenkins, 1989). Ultimately, the exponential growth will become limited by a depleted nutrient and the cultures will display a decline in growth rate and transition into a stationary phase.

The determination of the exponential growth phase can be performed by plotting the log transformation of the viable cell concentration against the process duration. During exponential growth this will result in a linear relationship between the log(Y) and X, enabling consideration of the phase of growth the culture is exhibiting during the process. An example plot is provided in Figure 5, displaying this relationship with linear regression through the points considered in exponential growth.

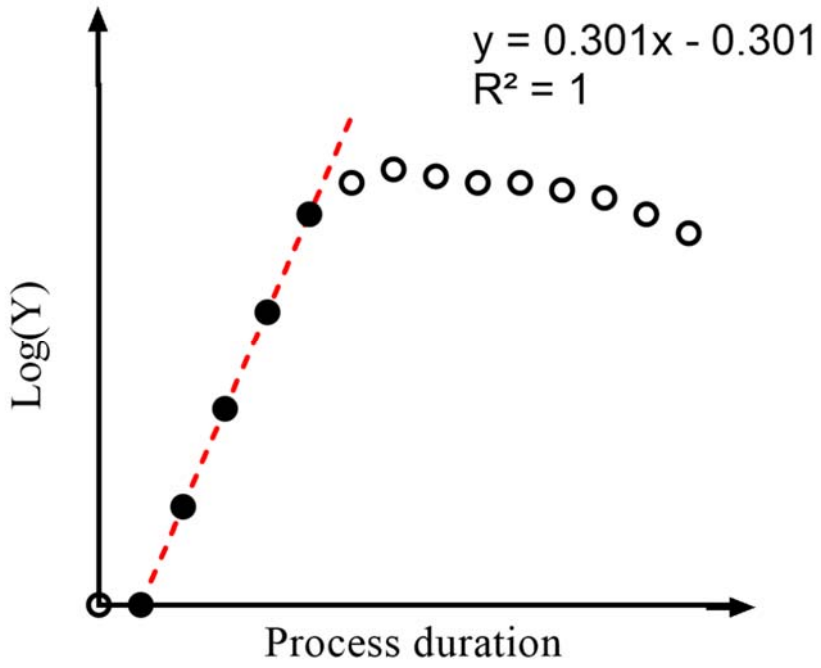

Figure 5 Example presentation of a log(Y) growth profile during bioprocess operation.
Example Log(Y) profile plots Log(Y) over increasing process duration, with the timepoints considered to be in exponential growth highlighted by

As illustrated in Figure 5, the linear relationship will not be represented as the culture progresses into the stationary phase. This estimation of the end of exponential growth and the beginning of the stationary phase are clearly defined in this example presentation. The practical determination of this phase boundary is challenging and can be influenced by factors such as sampling frequency, culture heterogeneity, and analytical variation. True exponential growth can only be considered in the centre of the defined exponential growth phase as the influence of the initial lag and onset of the stationary phase will be minimally impacting the culture.

Characteristics of the stationary phase include a physical increase in cellular size that has been coupled with an increase in cell specific productivity (Pan, Dalm, Wijffels, & Martens, 2017). In addition, this phase is characterised by an accumulation in lactate concentration as its consumption declines, and glucose is continued to be consumed (Martinez et al., 2013).

Ultimately, the environment is a heterogeneous mixture of cells in exponential growth, and those that have committed themselves to apoptosis. To prolong the duration of the stationary phase, this complex and reactive physiochemical environment must be maintained.

The final stage in a batch or fed batch culture is the decline/death phase, where culture viability is observed to decline. Strategies such as the use of temperature (Moore et al., 1997), and the close monitoring of available metabolites, aim to prolong the duration of the culture and maximise productivity (Singh, Al.-Rubeai, Gregory, & Emery, 1994). As the cultures progress into this decline phase, non-viable cells begin to rupture, and undesirable cell debris enters the cell culture supernatant. This debris may impact the efficiency of the harvest and quality of the expressed product. A limit is set for viability that defines when the culture is to be harvested.

1.5.3 Continuous Culture – Non Cell Retention

In contrast to the multiple growth phases experienced in batch and fed-batch culture, continuous culture is considerably simpler. The chemostat is a popular method for continuous

culturing and was defined by researchers in 1950 (Monod, 1950; Novick & Szilard, 1950).

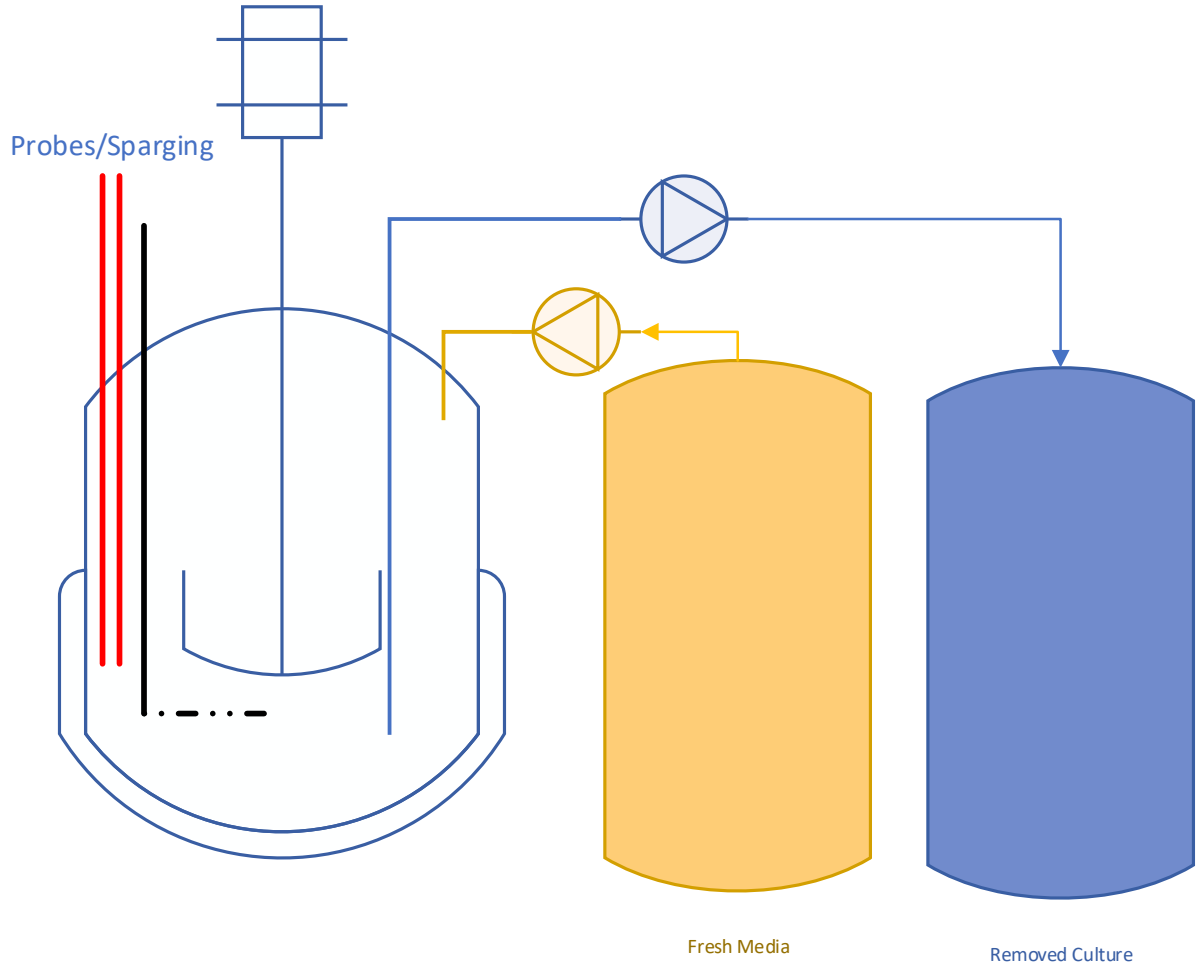

Figure 6 Example of chemostat culture operation setup
The diagrammatic example contains required components for operation of a chemostat culture including impeller, probes (e.g. pH and DO) shown in red, gas sparging line shown in black, jacket around the vessel to control temperature, the fresh media in yellow and removed culture in blue.

Following inoculation, chemostat cultures are grown in batch operation for a nominal time with the goal to establish exponential growth. The continuous exchange of fresh medium and removal of culture (cells plus conditioned medium and expressed protein) is then initiated.

This continuous exchange maintains the physiochemical environment and a cellular 'steady state' is reached where the growth rate matches the death rate for a given dilution rate. These defined growth/death rates at a dilution rate will be realised by the culture because of a limiting nutrient within the medium formulation. Changing the medium formulation will result in a new steady state to be established to reflect changes in the rate limiting nutrient. This control of the physiochemical environment enables high experimental reproducibility and makes chemostat culturing a popular choice for researchers investigating a variety of cellular characteristics (Hoskisson & Hobbs, 2005).

In addition to chemostat culture, is the turbidostat culture method of operation. This method aims to operate at, or as close to the culture maximum specific growth rate as possible, without experiencing culture 'wash-out'. This is achieved by closely monitoring the culture density, and adjusting the dilution rate respectively to increases or decreases in cellular concentration (Watson, 1972).

Differences between the two methods are highlighted by the resulting selective pressure placed on polyclonal populations. The chemostat method will select those cells with the highest efficiency for the limiting nutrient for the given dilution rate. Turbidostat method will select those cells with the highest maximum specific growth rate (Flegr, 1997).

1.5.4 Continuous Culture – Cell Retention

The operation of a chemostat or turbidostat results in the continuous removal of cells and expressed product from the culture. This restricts the culture cell density from reaching its potential maximum. Opportunities exist in cell culture systems, where cell specific productivity is retained over time, to generate a highly productive process by retaining cells within the culture as they expand exponentially.

This method of cell culture is generally defined as perfusion. Perfusion methods of continuous culture operation have been developed that take advantage of the medium exchange of continuous culture, whilst retaining cells (and product if desired) within the culture.

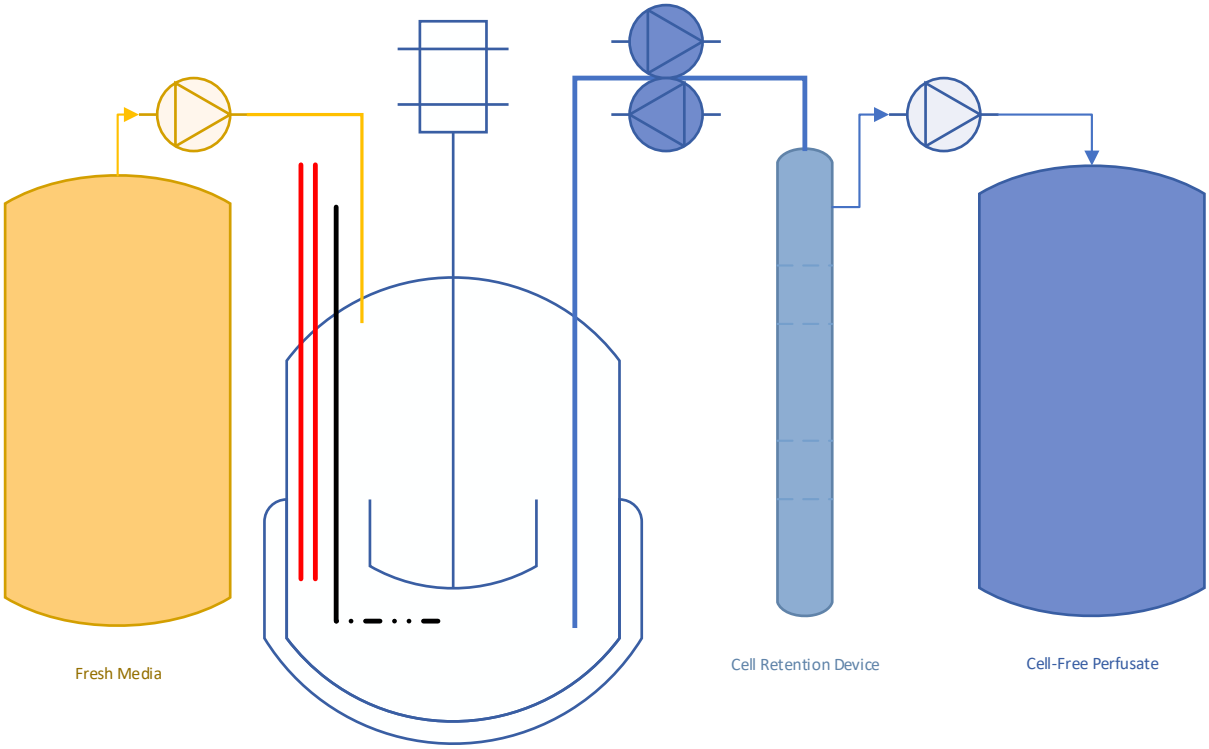

Figure 7 Example of a perfusion culture operation setup
The diagrammatic example contains required components for operation of a perfusion culture including impeller, probes (e.g. pH and DO) shown in red, gas sparging line shown in black, jacket around the vessel to control temperature, the fresh media in yellow, removed culture in blue and the cell retention device.

Commercially applied examples of continuous bioprocessing methods can exist in perfusion production or the utility of a rolling inoculum. Whilst not as popular as fed batch, the principles of perfusion offer highly productive bioprocesses with the ability to produce the wide variety of unstable, 'difficult to express' (DTE) molecules emerging from commercial research pipelines (Alves & Dobrowsky, 2017; Bonham-Carter & Shevitz, 2011).

It is this ability of perfusion to remove volatile protein products from the culture environment that is coveted when a perfusion bioprocess is conceptualised over fed batch best practices. This has been demonstrated in the production of haemoglobin Factor VIII substitute for haemophilia A patients (Pollock et al., 2013).

The operation of a cell retention device adds resource and complexity to the culture operation. The complexity translates into increased risk of failure that is considered when selecting perfusion as a method of cultivation over other methods. Additionally, if perfusion is selected, there is a variety of cell retention methods that must be considered, each with their respective advantages and disadvantages.

1.5.4.1 Cell Retention Devices

For a cell retention device to be considered appropriate, it must retain cells whilst not negatively impacting the culture viability or productivity. In addition, the performance of the device should not deteriorate over time. This deterioration may occur through the build-up of culture by-products, such as cellular particles generated through apoptosis. In achieving efficient cell retention, devices exploit the physical properties of cells. This is conducted through techniques based on one of two main methods, filtration or sedimentation (Voisard, Meuwly, Ruffieux, Baer, & Kadouri, 2003; Woodside, Bowen, & Piret, 1998).

Filtration devices, such as spin filters and hollow fibre columns, must be carefully selected. Selection criteria are based on filter pore size, considering the cellular size to enable cell retention (upper limit) whilst not risking filter fouling (lower limit). Additionally, any requirement to retain the expressed product within the culture must be considered in the filter sizing and increases the risks to filter fouling.

Cultures are exposed to different growth environments depending on the cell retention method. In filtration methods, a cell free perfusate stream is drawn through a filter. This generates hydrodynamic forces on the cells that will increase as the culture density increases or as the filter begins to foul. This may cause undesirable shear forces leading to cellular lysis (S. Wang et al., 2017).

Early filtration devices were based on the spin filter technology, whereby the filter device was situated axially in the stir tank reactor (STR) (Avgerinos et al., 1990). The popularity of this device was restricted by the inability to replace the filter in the event of filter fouling. Additionally, there is high complexity in scaling up the spin filter technology into commercial scale bioreactors (Bonham-Carter & Shevitz, 2011).

In contrast, sedimentation devices, such as incline and vertical settlers, aim to exploit the difference in density of the cell and medium components of the culture. This method generates a cell-free perfusate without the risk of filter fouling.

In sedimentation methods, the culture is influenced firstly through the selective removal of lower density cells (typically non-viable or immature (Searles, Todd, & Kompala, 1994)), and secondly through the heterogeneous environments generated during settling.

In addition to incline and vertical settlers, methods exist that utilise centrifugation and acoustic wave separation to achieve sedimentation. Whilst relative success had been achieved with

these methods, technological challenges and investment to operate the systems at larger scales have prevented further investigation (Woodside et al., 1998).

The lower economic and technological investment needed for cell settlers has provided an entry to explore perfusion for researchers and industry alike. This exploration has expanded into characterisation and industrial processes taking advantages of the simplicity of operation and scalability of the method (Choo et al., 2007; Hülscher, Scheibler, & Onken, 1992; Searles et al., 1994; Z. Wang & Belovich, 2010).

More recent investment and advancements into cell retention devices have focused on filtration based methods. Specifically, hollow fibre filters external to the STR have been coupled with a recirculating pump to provide tangential flow across the filter surface. Pumping the culture ensures a holdup volume is not experienced within the hollow fibre filter and homogenous culture is achieved. In addition, existing externally from the reactor allows the option to replace the filter in the event of failure.

A popular commercial system is the ATF system manufactured by Repligen (USA). This is operated with a pressurised diaphragm inside a bulb structure. An alternating tangential flow (ATF) is generated by the contracting and relaxing diaphragm. This flow is directed from the culture, across a prefabricated hollow fibre column to enable the removal of cell free perfusate.

Aiding its popularity is the fact the ATF system generates very low shear forces in comparison to peristaltic inline pumps (S. Wang et al., 2017), enabling scalability from a 1L STR model up to 500L STRs (Bonham-Carter & Shevitz, 2011). This scalability is critical in enabling the bioprocess development work conducted at bench scale to be quickly translated to larger manufacturing scales.

1.6 Scales of Operation

In the commercial production of mAbs and other therapeutic protein products, manufacturers are bound by strict regulatory guidelines. These guidelines are published by the International Council for Harmonisation (ICH) and adopted by each regional regulatory entity.

Within the regulatory guidelines, the exploration of the culture operational space is promoted. This is to understand the robustness of the system, specifically the impact of culture control variation ('Critical Process Parameters' (CPPs)) on culture outputs ('Critical Quality Attributes' (CQAs)). This investigation is known as 'Quality by Design' (QbD) and to provide the required detail, will entail high experimental resources. To economically complete the

necessary experiments, varying degrees of scale down systems have been adopted that have been characterised to inform commercial manufacturing scale cultures. The scales represented in the following sections are depicted for reference of physical dimensions in Figure 8, below.

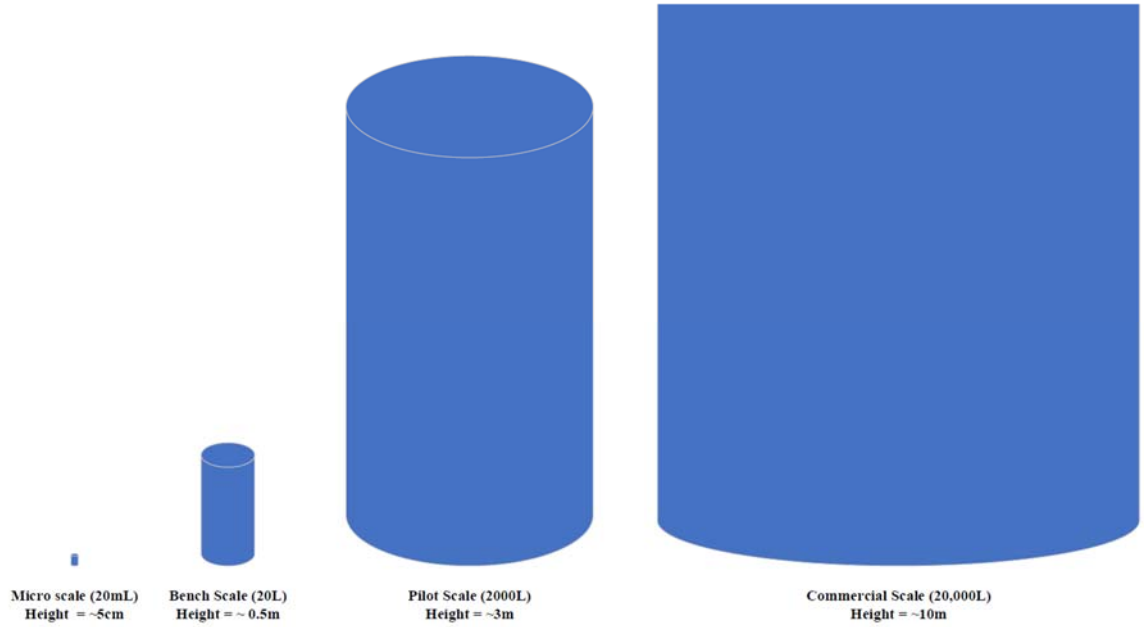

Figure 8 Example volumes and dimensions for bioreactors at different scales
The reported heights and visual depiction of the scales is provided for reference and variation can occur between different manufacturers and vessel geometries. The height of the commercial scale vessel is not fully represented as its height is more than three times that of the pilot scale.

The development of commercial manufacture of fed batch processes utilises operating volumes from 200µl up to 20,000L. Justification and rationale for the operation of these scales are provided in Sections 1.6.1 to 1.6.4, below.

To operate a commercial scale bioreactor with a fed batch process developed at microscale requires careful consideration and balance of scale dependant variables (mixing, shear force and gas transfer rates). The first reported instance of a 20,000L bioreactor by Lonza Biologics in 2005 (Birch & Racher, 2006) reaffirmed that mammalian cells can be grown in suspension at larger scales and that they did not display such high sensitivity to shear as was once feared due to the lack of a cell wall (Nienow, 2006)

Therefore, the process would look to match scale independent variables (such as Nutrient Conc, DO & CO_2, pH, and Temperature) in the scale up operation. Unfortunately, scale dependent variables can negatively impact the scale independent variables if not balanced appropriately. The exacting balance of mixing, shear, and gas transfer rates is not always possible when scaling up, and optimisations at each scale may be required. Recently, advancements in micro

and bench scale bioreactor operation have enabled a more efficient transition to commercial scale vessels with process characterisation aligning for growth and product quality attributes across scales (Manahan et al., 2019).

The increase in gas sparging rates in 20,000L vessels is an example of the compromise used to make this balance. This is performed to minimise the increased mixing speed to achieve the required gas transfer rate, therefore minimising the shear forces exerted on the culture (Xing, Kenty, Li, & Lee, 2009). Unfortunately, there is no uniform bioreactor or impeller design and GMP manufacturing facilities are unlikely to switch away from established systems due to the need for requalification and approval processes. This required process engineers to balance the scale-up of a process for the specific vessel identified (Sieblist, Jenzsch, & Pohlscheidt, 2016).

1.6.1 Commercial Manufacturing (Commercial Scale)

The success of mAbs and other therapeutic proteins during the 1990s resulted in high demand. In order to meet this demand, facilities were constructed to operate multiple vessels that reached operational volumes of up to 20,000 litres. These vessels are now accepted as the norm for a manufacturing facility and process design in development is now carried out to meet this production scale (Gronemeyer, Ditz, & Strube, 2014; Kelley, 2009).

The operation of a commercial manufacturing scale vessel presents the opportunity to produce vast quantities of product. Therefore, operational time in a facility is a valuable commodity and is meticulously planned to maximise outputs.

The time required for the operation of a vessel includes the culture duration and activities that support it, such as facility downtime for cleaning and sterilisation in-between runs and the preparation of medium and inoculum cultures. Strategies have been adopted to minimise these associated activities. These include the use of pre sterilised, single use systems (Eibl, Löffelholz, & Eibl, 2014; Shukla & Gottschalk, 2013).

The expansion of inoculum cultures is not an activity that can be accelerated as it relies on the growth rate of the cells. Each production vessel is initiated from a single 1-2mL cryogenically stored vial, and substantial efforts are directed into growing cells as per process operating criteria to ensure batch to batch reproducibility. For a production vessel of 10,000L in size, this will include the operation of multiple large scale vessels of increasing volume and complexity (Kloth, Maclsaac, Ghebremariam, & Arunakumari, 2010).

1.6.2 Clinical Supply (Pilot Scale)

The development pathway of any new drug involves progression through clinical trials to assess the toxicological and pharmacological characteristics in support of approval and commercialisation. The success rate for new drugs to reach commercial release is low. Therefore, scale must be considered when supplying material for clinical trials and avoid excessive wastage if a new drug is unsuccessful.

Pilot scale vessels are operated at volumes between 10 and 50% of the designated commercial scale. In addition to material supply, the data generated is critical in translating the understanding generated at smaller scale into the successful operation of commercial scale cultures.

The focus of this understanding has been in culture responses to vessel dynamics, hydrodynamic forces and maintaining consistency in process monitoring systems (Marks, 2003; Nienow, 2006).

Process optimisations have been successful in recent years and industrial mAb producers are focusing at larger pilot scale vessels for commercial production in exchange for the typical 20,000 litre scale vessels. This trend in smaller vessel size is reinforced by the popularity of single use disposable bioreactor systems. These are now reaching 2,000L scale and present significant manufacturing facility flexibility and reduction in setup costs (De Jesus & Wurm, 2011).

1.6.3 Process Development (Bench Scale)

Process development and characterisation activities have typically been performed in bench scale vessels, with working volumes between 1 and 20 litres. This scale, therefore, represents a critical step in the development of bioprocess as experiments required cannot feasibly be performed at larger scales (F. Li et al., 2006).

However, the operation at bench scale may not provide the capacity to conduct the experiments required by the QbD paradigm. The experimental resource desired has been further increased through the popularity of the ‘design of experiments’ (DoE) concepts and Plackett Burman statistical design to screen process parameters (González-Leal et al., 2011).

1.6.4 Process Development (Micro Scale)

In the fulfilment of the experimental demand, microscale systems (generally defined as up to 50mL operating volume) have been adopted. The translation of scale down technologies is far more challenging below bench scale, as the previous commonality between monitoring and sampling systems is no longer appropriate. A variety of microscale systems exists with varying degrees of complexity, operational throughput, automation, and robustness (Betts & Baganz, 2006; B. J. Kim, Diao, & Shuler, 2012).

Microtitre plate based systems, originally designated for cellular based assays, have been used to rapidly accelerate bioprocess development screening in a low cost setting (Barrett, Wu, Zhang, Levy, & Lye, 2010).

Whilst conceptually they are an extension of flask based models with their reliance on humidified, shaking incubators for process conditions control, microtiter plates provide additional function through their high throughput nature. Agitation is provided to the cultures through orbital shaking platforms, to ensure culture homogenisation. The cultures are then maintained within a climate controlled incubator (temperature, humidity, and gas composition), enabling critical temperature, pH, and DO maintenance to be achieved. This application has been furthered by the successful adoption of a bespoke automation system to handle the majority of plate interaction steps (Markert & Joeris, 2017).

This process parameter control is crude as there is no associated online monitoring or maintenance. This limits the complexity of screening possible within the systems. In addition, requirements to have cultures exposed to the incubator generates scenarios of evaporation and critically, culture contamination risk.

Nevertheless, comparable evaluations of growth and productivity in microtitre plate systems to shake flask counterparts have been performed. These justify the utility for microtitre plate systems to improve the early bioprocess development screening, where manually operated flask based systems are extensively used (Barrett et al., 2010; Bos et al., 2015; Girard, Meissner, Jordan, Tsao, & Wurm, 2002).

The Duetz Microflask system was developed by Applikon Biotechnology as a commercially available microtitre plate based system. It incorporated a membrane cover combination to the 24 well plates. This generated semi-closed systems that enable sufficient gas transfer with a lower risk of evaporation or contamination. Evaluations have confirmed that, given its

throughput and low resource, this is a vital tool in the early screening of bioprocessing activities (Warr, Patel, Ho, & Newell, 2011; Warr, White, Chim, Patel, & Bosteels, 2011).

Online monitoring and advanced control over a culture's respective CPPs is critical in generating a robust, scalable process. Newly developed microscale systems utilise non-invasive, pre sterilised and calibrated fluorometric spot sensors for the monitoring of pH and DO. Commercialised by PreSens Precision Sensing GmbH (Germany), these sensors are integrated into the flask, plate or vessel wall. The sensors are read non-invasively at pre-set intervals through the excitation of reference dyes in the sensor. The functionality of the sensors uses the Dual Lifetime Referenced (DLR) method (Boniello, Mayr, Bolivar, & Nidetzky, 2012).

One system to adopt these pH and DO sensors is the Biolector® (M2P Labs, Germany) system and Micro24 system (Applikon), providing online pH and DO monitoring in existing, familiar microtitre plate environment (Warr, Betts, Ahmad, Newell, & Finka, 2013; Wewetzer et al., 2015). This monitoring ability is paired with an automated sparging and or microfluidic manifold to enable highly desirable automated control of pH and the provision of metabolic substrates to operate a fed-batch methodology (Funke et al., 2010; Warr, 2014).

Whilst showing promise in their capacity and reproducibility for bioprocessing screening applications, the investment into microtitre plate based systems has been limited. This can be partially accredited to their need to be operated as open systems, to facilitate sufficient gas transfer, and their risk of spilling when agitation is increased in line with gas transfer demands (Betts & Baganz, 2006).

Ultimately, the comparison of functionality of these enhanced microtitre plate based systems is contrasted with advanced microscale STR systems. The microscale STR systems aim to provide linearity in performance, from microscale systems to the STR bench, pilot, and commercial manufacturing scale systems.

One such system, invented by The Automation Partnership (Royston, UK), now part of the Sartorius Group, is the Advanced Microscale BioReactor (ambr®15) system. The system utilises single use disposable sparged miniature STRs, prefabricated with fluorometric spot sensors for pH and DO, and pre-irradiated for sterility. These miniature STRs are paired with the bespoke control system that offers the vessels parallel automated control of pH, DO, temperature, and feeding regimes through a liquid handling robotic arm. Each vessel is operated as a closed system, with only the pipetting interactions exposing the vessel through a

sampling port. To ensure sterility, the entire fabricated bioreactor system must be placed inside a laminar flow cabinet.

The ambr®15 system comprises of either 24 or 48 vessels (depending on the variant) with vessels arranged into culture stations (CSs) of 12 vessel blocks. In each CS, the temperature and agitation are controlled universally, facilitated by the sharing of the head plate and agitation plate for each CS. Other process conditions can be set specifically for each vessel independently. The automated sampling and liquid addition combined with the automated control systems presents a very powerful tool for bioprocess development activities such as DoE, cell line or medium screening (Sandner, Pybus, McCreath, & Glassey, 2018).

The ambr®15 system has been validated through extensive characterisation, which renders the system comparable to large scale STR vessels (Nienow et al., 2013). This investigation has been further extended to the evaluation of bench scale and ambr®15 vessels in commercial bioprocesses (Hsu, Aulakh, Traul, & Yuk, 2012; Lewis, 2010; Moses, Manahan, Ambrogelly, & Ling, 2012; Rameez et al., 2014). Due to the success of these evaluations, ambr®15 has been widely adopted in industrial settings. The systems fine control of CPPs, and the inherent high experimental capacity, has enabled it to be utilised to address problems that required comprehensive and exhaustive experimental designs to determine suitable operating ranges (Goldrick et al., 2017; Janakiraman, Kwiatkowski, Kshirsagar, Ryll, & Huang, 2015).

1.6.5 Continuous Process Development Scales

The scales of operation detailed above must be replicated for continuous cultures to facilitate a commercial manufacturing process. For perfusion cultures, this is readily achieved through the association of ATF systems with existing STR vessels from commercial manufacture to process development.

However, the ATF system is limited to operate at bench scale for process development. The lack of a robust micro scale, high throughput technology for perfusion process development is an obstruction for the wider evaluation of perfusion culture (e.g. for new cell lines or process optimisations).

Additionally, without a micro scale technology, the vast medium requirements of all continuous culture result in limited scope development activities. Furthermore, the lack of high throughput systems prevents the parallel observation of steady states during optimisation and screening evaluations.

Options for conducting microscale evaluations for perfusion bioprocesses are limited and primitive when compared to the bespoke technology designed for fed batch. Adaptation of existing fed-batch microscale cell culture systems to continuous cell culturing applications is an option for achieving a microscale continuous process development tool.

Due to the highly engineered nature of microscale systems, it is difficult to repurpose them for perfusion by retrofitting a cell retention device. Microtitre plate-based systems such as SimCell™ platform (Seahorse) (Legmann et al., 2009) and BioLector® (Blesken, Olfers, Grimm, & Frische, 2016) offer high experimental capacity, however, these systems would require significant operator interaction to mimic perfusion through an adapted cell retention methodology.

Additional industrial investigations (Du et al., 2015; C. J. Huang, Lin, & Yang, 2015) have looked at small scale perfusion models for medium development. These evaluations cannot dynamically measure and control process parameters (such as pH) in real time, such that extensive bioprocess development activities can be conducted.

More recently, microscale systems have been developed that were specifically designed to operate in perfusion mode (Mozdzierz et al., 2015) but they have not yet been evaluated with mammalian expression systems and, as novel applications, inherently will require significant economic and technical investment to fully characterise the system as a scale down model.

The ambr®15 system has a high prevalence in FB bioprocess development due to its advanced ability at process control and automation. If a method for cell retention was refined for this system, its high throughput nature and small (10-15mL) working volumes presents an interesting proposition for investigating the ambr®15 system as a microscale option for perfusion development.

One cell retention strategy that has been proposed for the ambr®15 system is gravity cell settling within the culture vessel, this would allow perfusion operation without the requirement to retrofit a cell retention device. Early studies conducted using traditional gravity settling devices (Searles et al., 1994) can successfully be adopted in the design of a microscale cell settling method. An early application using this strategy (Goletz, Stahn, & KREYE, 2016) and several industrial investigations (Conference abstracts presented with supplementary files (BioMarin Pharmaceutical, 2017; MilliporeSigma, 2017)) highlighted interest in the method adoption, although no specific reports exist on a thorough comparative evaluation of this adapted system.

1.7 Research Aims and Objectives

This thesis aims to present the development and characterisation of a novel methodology for microscale perfusion cell culture. Through the characterisation of the method, its functionality as a bioprocess development tool will be highlighted.

This development and characterisation will be achieved by operating the automated micro-bioreactor (ambr®) system in perfusion cultivation by utilising sedimentation to retain cells within the culture. Interrogating the perfusion operating parameters at microscale, and conducting equivalent bench and microscale evaluations will highlight nuances of continuous perfusion culture operation within the system.

Additionally, this thesis aims to investigate the suitability of control and operation strategies for continuous cultures. As a primary motivation, novel control strategies that are sympathetic to the characteristics of continuous cultures will be investigated.

This aim will be achieved by analysing the performance of perfusion culture and identifying characteristics that do not align with typical control strategies developed for fed-batch manufacturing. Characteristic identification includes focusing on the exponential growth phase of cultures, common of both fed batch and continuous perfusion systems, respectively. The prolonged period that the perfusion culture exists in exponential growth increases the level of consideration needed in control strategies for continuous operation and increases the focus of culture characteristics present during this phase. Therefore, leading to insight into novel control strategies, appropriate for continuous bioprocessing.

Chapter 2 Materials and Methods

For comprehension and concise formation of results chapters, the following information is presented. Alterations to materials and methods are explicitly outlined at the instance where the change is made.

2.1 Experimental numbering system

The given chapter numbering enables a coherent decimal-based experimental numbering system. For example, the first experiment in Chapter 3 is numbered Experiment 3.1, and the second Experiment 3.2, and so forth. A further division within an experiment is donated by an alphabetical suffix and stated explicitly at the first occurrence. The experiments conducted within this thesis and their respective details are summarised in Table 1.

Table 1 Summary of experiments contained within this thesis.

Experiment		Scale	Outline
3.1	a	micro	Evaluation of micro scale perfusion methodology (30min cell settling, 1.0VVD dilution rate).
	b	bench	Biological replicate of 3.1a, operated at bench scale, with ATF hollow fibre cell retention system (1.0VVD dilution rate).
3.2	a	micro	Technical replicate of 3.1a, with 33.5min cell settling (1.0VVD dilution rate).
	b	micro	Technical replicate of 3.1a, with 37min cell settling (1.0VVD dilution rate).
4.1	a	micro	Fed batch cultures operated with cells derived from micro scale perfusion cultures (1.0VVD dilution rate).
	b	bench	Fed batch cultures operated with cells derived from bench scale perfusion cultures (1.0VVD dilution rate).
4.2	-	bench	Fed batch cultures operated with cells derived from bench scale perfusion cultures at decreasing dilution rates (1.0, 0.75 and 0.5 VVD)
5.1	a	micro	Fed batch evaluation of the impact of cell aging in continuous systems, compared to ongoing subculture.
	b	micro	Fed batch evaluation of cell line sensitivity to pH at and post inoculation.
5.2	-	micro	Fed batch evaluation of multi-parameter cell line sensitivity post inoculation.

Plotting of data and generation of figures from these experiments were performed using the commercial scientific 2D graphing and statistics software, Prism (GraphPad Software Inc, USA). Error bars are provided as ± SD, where the error bars are physically smaller than the donated symbol, no error bar is presented.

2.2 Cell line, Medium and Bioreactor systems

A proprietary, Chinese hamster ovary (CHO) cell line expressing a low concentration of novel bispecific monoclonal antibody (Cell line 1) was employed throughout all chapters.

Two animal component free proprietary medium compositions were used; a proprietary medium developed specifically for passaging cultures and fed-batch operation (basal), and another proprietary medium developed for supporting high cell concentrations associated with perfusion systems (enriched). The glucose concentrations in the basal and enriched medium was 5 and 15 g/L, respectively.

Cell line and medium were provided with permission, and thanks, by MedImmune, Cambridge.

The cell line was developed within the environment of the basal medium. Optimal setpoints for pH and temperature were provided as pH 7.2±0.1 and 36.5°C, respectively.

Where a fed-batch culturing method was applied either within the production phase operation in perfusion evaluation of Chapter 4, or within traditional fed-batch in Chapters 5 and 6, the basal medium was complemented with propriety concentrated nutrient feeds. These feeds were added to cultures as bolus additions, as detailed in the respective chapter's experimental design.

Glucose concentrations in perfusion experiments (Chapters 3 and 4) was maintained through the perfusion of enriched medium. For fed-batch processes (Chapters 4 and 5) glucose was fed back on demand as detailed in associated experimental design sections, utilising a 500g/L stock solution.

Each experiment was initiated with cells revived from vials of a common frozen cell stocks. A common frozen cell stock was utilised (referred to as Development Cell Bank 1 (DCB1)) for Cell Line 1. Detailed in Chapter 5 is the expansion of DCB1 to generate the cell banks DCB2, DCB3, and DCB4.

Before inoculation the revived cells were sub-cultured twice per week, in basal medium, in vented shake flasks (Corning, USA) in a humidified orbital shaker incubator maintained at 36.5°C and 5% CO_2.

All reference to microscale experiments within this thesis refers to work conducted in the ambr®15 bioreactor system (Sartorious Stedim, UK). The 24 and 48 variants were used interchangeably depending on the capacity required and availability.

All reference to bench scale experiments within this thesis refers to work conducted in glass 7L bioreactors (Applikon, UK), with working volumes ranging between 3 and 6L. For operation in perfusion at bench scale integrated bioreactor controllers (DasGip, DE) were combined with additional pump units (Electrolab Biotech, UK). This combination maintained culture volume by pumping fresh medium back to the vessel on demand, as it was removed at a constant rate by the bioreactor controller.

Online oxygen and pH measurements were made with fluorescent spot sensors (Presens, DE) and traditional probes (Mettler Toledo, UK), for micro and bench scale experiments, respectively.

The dissolved oxygen saturation was controlled to 50% through the sparging of O_2 on demand, along with an increase in agitation, as required.

The 2-way control of pH to set point ± dead band was performed through automated integrated PI or PID loops for micro or bench scale systems, respectively. Feedback was actioned by the addition of liquid base addition or sparging CO_2 gas on demand. Perfusion experiments or periods of perfusion through hybrid processes utilised 1-way control of pH through sparging of CO_2, relying on the buffering capacity of the perfused medium to control acidic conditions.

Temperature was controlled to 36.5°C through the combination of an integrated temperature probe and a heated head plate or heated jacket for micro and bench scale, respectively (Sartorius and DasGip, respectively)

Material was harvested from experiments for at-line and offline analysis through aseptic removal from bioreactor vessel, centrifugation, and where appropriate, analysed immediately, or stored at -80°c for later processing.

2.3 At-line and Offline Sample Analysis

The execution of sample analysis throughout this thesis is designated as ‘at-line’ in instances where the data produced is used directly in the observations and operations of the process. Sample analysis conducted ‘offline’ includes those where data is utilised for assessing performance but due to the time delay associated with the acquisition of results, cannot be used directly in the observations and operations of the process.

Instruments conducting ‘at-line’ analysis include;

ViCell XR cell counter (Beckman Coulter, USA) for the cellular analysis of samples from all experiments, via the trypan blue exclusion method.

From microscale experiments where there are low sample volumes present, the YSI 2900 (Xylem Analytics, UK) was used for the biochemical analysis of Glucose and Lactate concentration. Similarly, in microscale experiments, the ABL90 FLEX Analyser (Radiometer, UK) was used for pH sensor calibration and offset adjustment.

From bench scale experiments where larger sample volumes exist, the Nova FLEX (Nova Biomedical, USA) was used for comparative glucose, lactate, and pH measurements. As a benefit of the modular Nova FLEX system, samples analysed here also generated osmolality measurements by freezing point method.

Instruments conducting ‘off-line’ analysis include;

For experiments conducted in Chapter 3, to provide additional comparative data, time course samples were submitted for full amino acid analysis. For amino acid profile analysis, cell free perfusate was run on AccQTag Ultra C18 column (ACQUITY UPLC system, Waters). Amino acid peaks were integrated against commercial standards (Waters) and all values were scaled to respect commercial confidentiality of cell line and medium. This sample analysis was generously offered and performed by the BioProcess Analytics team, at Medimmune, Cambridge.

The mAb concentration was determined using Protein A ’dip-and-read’ Biosensors on the Octet System (Pall ForteBio). A serial dilution of the purified mAb product was performed and run in parallel with inter assay controls to determine the titre and control run variation.

The mAb aggregation was determined by SEC-UPLC for both pre and post purification. Unpurified, clarified cell culture supernatant and Protein A purified material was filtered through a 0.22µm AcroPrep™ plate filter (Pall) prior to loading the supernatant to the automated injection by UPLC (Waters) on SEC column (Acquity UPLC® Protein BEH SEC 200Å, Waters), peak detections were made at wavelengths 220nm and 280nm.

2.4 Rate Calculations

Integral viable cell concentration, specific glucose consumption, and specific net lactate change is calculated by equations reported by others (Adams, Korke, & Hu, 2007; Villiger-Oberbek, Yang, Zhou, & Yang, 2015).

The integral viable cell concentration (IVCC) for each culture is calculated by:

$$IVCC_n = IVCC_{n-1} + \left(\left(\frac{VCC_n + VCC_{n-1}}{2}\right) \times (t_n - t_{n-1})\right)$$

Whereby the integral viable cell concentration (IVCC) and viable cell concentration (VCC) for time (t), t_n and t_{n-1}, are represented by $IVCC_n$, $IVCC_{n-1}$, VCC_n and VCC_{n-1}, respectively.

For Fed Batch

Utilising $IVCC_n$, the specific glucose consumption ($q_{c,n}$) is calculated by:

$$q_{c,n} = \frac{\left((cp_{x,n-1} - cp_{x,n}) + ca_{x,n-1}\right)}{\Delta IVCC_n \times V_n}$$

Where cp_x, ca_x and V are the glucose present (g), glucose added (g) and volume (L), respectively.

The specific lactate net change ($q_{l,n}$) is calculated by:

$$q_{l,n} = \frac{(lp_{x,n} - lp_{x,n-1})}{\Delta IVCC_n \times V_n}$$

Where lp_x and V are the lactate present (g) and volume (L), respectively.

The specific production rate $q_{p,n}$ is calculated by:

$$q_{p,n} = \frac{p_{x,n}}{\Delta IVCC_n \times V_n}$$

Whereby p_x and V are the product present (g) and volume (L), respectively.

For Perfusion

Utilising $IVCC_n$, and the specific glucose consumption ($q_{c,n}$) is calculated by:

$$q_{c,n} = \frac{\left(c_{x,n-1} \times (1 - D_n) + (m_x \times D_n)\right) - c_{x,n}}{\Delta IVCC_n \times V_n}$$

Where D, m_x and c_x are the daily dilution rate (VVD), measured glucose in fresh medium added per day (g) and measured glucose in culture (g), respectively.

Similarly, where measured lactate in culture (g) is p_x, the specific lactate net change ($q_{l,n}$) is calculated by:

$$q_{l,n} = \frac{p_{x,n} - (p_{x,n-1} \times (1 - D_n))}{\Delta IVCC_n \times V_n}$$

No product retention occurred and thus cell specific productivity ($q_{p,n}$) was calculated by:

$$q_{p,n} = \frac{p_{x,n}}{\Delta IVCC_n \times V_n} \times D_n$$

Chapter 3 The Design, Execution, and Evaluation of a High-Throughput Continuous Microscale Environment

3.1 Introduction

In the production of therapeutic proteins, mammalian cell lines are selected for their ability to accurately express the desired product. Whilst popular for their accurate expression, mammalian cell lines have comparatively slow growth rates (22-24 hours doubling) to other organisms, for example, bacterial cells (approximately 20-120 minutes doubling). Therefore, investigating the performance of a mammalian cell line requires supporting prolonged culture durations.

This time investment is compounded when investigating continuous cultures. Traditional steady state evaluation requires the culture to be maintained at steady state for three to seven residence times to confirm the steady state is not a transient stage of the culture (this results in up to two weeks for each condition) (Pirt, 1975). Extended continuous cultures require large medium volumes to support the dilution rate operated. These large medium volumes are physically restrictive and not economically viable when compared to the cost of fed-batch culture investigation.

High throughput experimental environments allow for a comprehensive and exhaustive investigation of biological systems. Specifically, this high throughput environment is of interest to mammalian systems as it enables the experiments to be conducted in parallel. If this is combined with a microscale system, it presents a low medium resource environment that has application in the investigation of continuous culturing.

A popular system for high throughput microscale investigation of fed-batch culturing is the ambr®15 system. Several adjustments must be made to exploit the capabilities of the ambr®15 system for the operation of continuous culturing. To facilitate perfusion operation within the ambr®15 system (as a commercially relevant mode of continuous culturing), an efficient cell retention device must be employed.

The ambr®15 system has been designed with highly sophisticated control systems and automation functionality. The system operation requires vessels to be permanently fixed within the robotics during operation, with frequent interaction occurring with the sample port located on top of each vessel. Therefore, the operation of an externally located, retrofitted cell retention device would be extremely challenging and seemingly unfeasible.

Gravity cell settling, as previously presented for its potential for refunctioning the ambr®15 system (1.6.5 Continuous Process Development), allows the vessels to remain in their designated positions whilst employing a sedimentation method of cell retention. Gravity cell settling is achieved *in situ* by stopping gassing and agitation of vessels, allowing cells to settle in preparation for liquid exchange. This operation presents a potential impact on cell viability or productivity, and operator priority must be the swift return to process control following the cell settling procedure.

In addition, and in relation to settling time, the volume to be exchanged post cell settling was a considered design parameter for this method development. As semi-continuous medium exchange is performed, to best mimic the operation at larger scales an approach must be sought that minimises the volume exchanged per cell settling, whilst not sacrificing the ability to conduct higher order dilution rates through inefficient use of the system capacity.

This chapter presents the development and evaluation of a sedimentation based method of cell retention utilised within the ambr®15 system.

To understand the magnitude and holistic impact of these frequent interruptions to normal operating conditions, evaluations are conducted extending the cell settling time incrementally beyond what is required from a cell retention efficiency perspective. This experimentation highlights critical operating ranges and identifies the extent of cell line sensitivity when these periods of settling are exceeded.

Understanding the robustness of the methodology will highlight its suitability to identify cellular and or biochemical characteristics specific to continuous bioprocess systems. This robustness will be compared with a highly developed, commercially adopted technology in the form of the ATF system.

The method of gravity cell settling within the vessel generates a universal, culture wide exposure to an uncontrolled environment at each cell settling event. The ATF system aims to eradicate any heterogeneous locations or events within the process through continuous recirculation of culture from the vessel to the retention device. Therefore, sampling from each system will represent the heterogeneous impact of the respective mode of cell retention.

3.2 Method Development

In the ambr®15 system, automated interaction with the installed vessels is conducted by a robotic liquid handling arm equipped with either a 1mL or 5mL pipette tip (working volumes

of 0.9 and 4mL, respectively). In addition to the inherent differences in volume capacity between the two tips, the diameter of the 5mL tip prevents it from being submerged into the vessel through the access port (depicted below in Figure 9). In developing a perfusion methodology, this difference presented a reliance of the ambr®15 system on the 1mL pipette size in achieving cell free medium removal, following a period of gravity sedimentation.

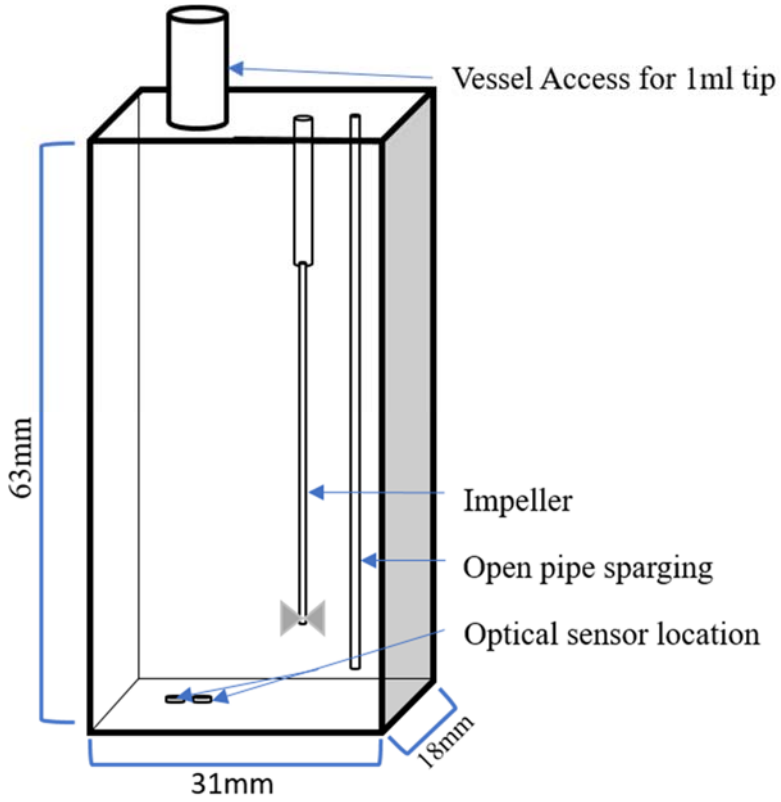

Figure 9 Diagrammatic depiction of the ambr®15 vessel geometry and highlighted operational components
Highlighted components include the access port for 1mL tip insertion, the impeller, sparger, location of optical sensors for pH and DO monitoring, and the simplified three-dimensional geometry measurements (mm).

Optimal operation of the cell retention methodology required accurate incremental removal of the uppermost fraction of culture as it became 'cell free'. This step was repeated to achieve the required dilution rate. Therefore, precise control of the robotic liquid handling arm was of interest. Achievement of minimal immersion prevented impacting the cell settling process and enabled perfusate removal at the earliest possible time point post initiation of cell settling.

The system functionality inherently facilitates fine control over the height at which the pipette travels into the vessel (to the precision of 0.01mm). Unfortunately, this fine control is not contextualised by the manufacture, as no correlation is provided for the relationship between the pipette height (mm) and vessel fill volume (mL). To enable this functionality, the relationship was explored.

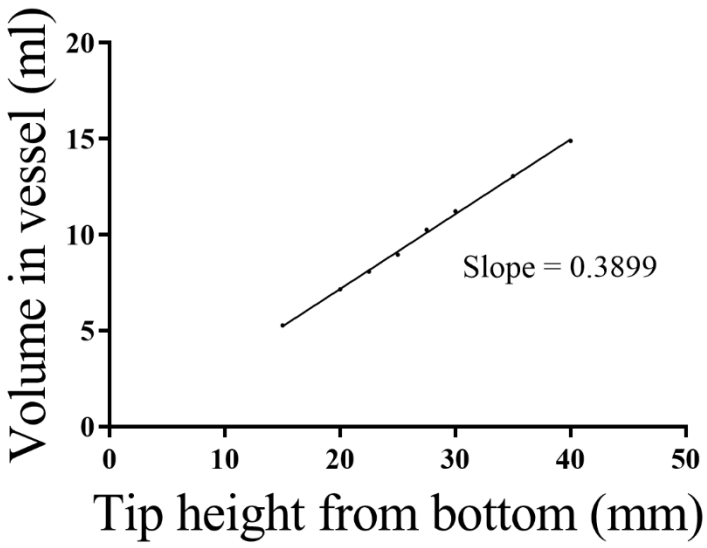

Figure 10 The relationship between, volume in vessel (mL) versus height of tip (mm)
The linear relationship between the two variables is presented by the slope of the fitted line, 0.3899 (R^2=0.9987).

The relationships presented above (Figure 10) were acquired experimentally through the controlled deployment of the 1mL pipette tip into the vessels to predetermined heights above the system platform, on which the vessels reside. Repeated aspiration was conducted at each height until the pipette returned dry and the remaining volume in the vessel was weighed. An understanding of the linear relationship between the two variables allowed the deployment of the pipette tip to heights that represented top fractions at any culture operational volume.

The next step in method development was to calculate feasible volumes to attempt to exchange in a single cell settling step whilst achieving relevant dilution rates for cultures. This was achieved through considering the geometry of the microscale vessel (Nienow et al., 2013), applying the relationship between height and culture volume (Figure 10) and considering the theoretical settling velocity of 1.4 cm/h for CHO cells (Searles et al., 1994). This theoretical velocity combined with spatial measurements suggested the top 2.7 mL of the culture would be 'cell free' after 30 minutes. Volumes of this magnitude would enable three sequential medium removal interactions (operating at 90% capacity of the 1mL tip) to be performed at a single cell settling step.

Experimental testing of the theoretical cell settling efficiency *in situ* enables the confirmation of assumptions made with regards to the cell settling velocity and any delay of transitioning from turbulent to gravity driven laminar flow in producing a reliable and reproducible cell settling methodology for further characterisation.

This testing was conducted through filling twenty-six ambr®15 vessels from a common culture of known cell concentration and installing them into the microscale system, with the control systems activated (Agitation, temperature, and gas flow). Vessels were then divided into four sets, and each set was designating incrementally increasing settling times for evaluation. The settling times evaluated were 15, 20, 25, and 30 minutes, respectively.

Following the respective settling times, sampling was performed from the top 2.7mL fraction, and analysed for its cellular concentration, in comparison to the starting cell concentration to provide a cell retention efficiency for the given fraction removed.

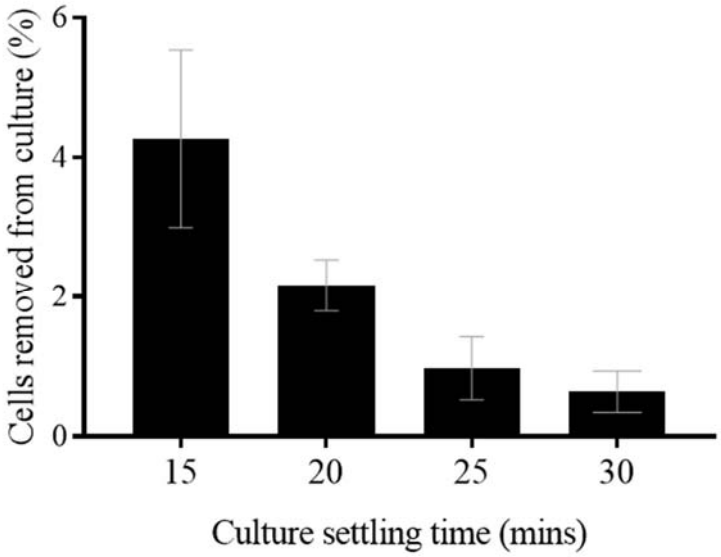

Figure 11 Plotted histogram of cell removal from culture (%) at culture settling times (mins)
Percentage cell loss from microscale reactor vessel following cell retention by incrementally increasing the gravity settling time from 15 minutes to 30 minutes, with a starting concentration of 6.08×10^6cells/mL across replicates. Data shows mean ± SD, n=6

The percentage of cells removed was observed to decrease as the culture settling time increases (Figure 11). The values decrease with (4.3±1.3), (2.2±0.4), (1.0±0.5) and (0.6±0.3) percent, representing 15, 20, 25, and 30 minutes, respectively. This performance displayed at 30 minutes cell settling, indicated a >99% cell retention. To preserve the concept of perfusion mimic when applying this cell settling methodology, settling times <30 minutes were not evaluated further to avoid a resulting 'chemostat like' environment, due to their lower cell retention percentage.

Many factors contribute to the capacity at which the ambr®15 system can operate perfusion. This capacity is ultimately defined by the time required to perform the culture exchange steps combined with the number of steps to be performed per day.

To provide an example, at 1.0 VVD and one third of the culture volume exchanged at each step, a CS operating at 50% capacity (six vessels out of a possible 12) required additional 30 minutes to handle the robotic liquid exchange. Operating four CSs (in the 48 vessel ambr®15 variant) at 50% capacity required settling or sampling to be scheduled for 12 hours per day and at-line measurements such as automated cell counting carried out required an additional four hours. This time requirement remained safely below the maximum capacity to allow downtime for system maintenance that typically must be performed for around 30 minutes daily when the robotic liquid handling arm is idle. This setup allowed the operation of 24 vessels simultaneously in the 48-vessel variant of the ambr® microscale system, which yields a sufficiently large number to make Design of Experiments (DoE) studies of continuous systems possible.

The existing setup and capacity could allow operation of the system running at a higher volume exchange rate than 1.0 VVD. Increasing the fraction of the vessel exchanged per step would limit the physical space that the cells were expected to settle into, thus the number of iterations of liquid exchange steps per day would ideally be increased. The current setup allowed experiments to be conducted at as high a volume exchange rate as 1.5 VVD, corresponding to a specific growth rate (μ) of $0.062h^{-1}$. Since this exceeded the maximum specific growth rate ($\mu_{max} = 0.05\ h^{-1}$) reported for CHO cells (López-Meza et al., 2016), the present setup was suitable for the range of all reported specific growth rates that CHO cells could operate under.

3.3 Experimental Design

This chapter consists of two independent revivals of frozen cell stocks and thus two independent experiments, Experiments 3.1 and 3.2, respectively. In Experiment 3.1, two 7L stirred-tank reactors (STR) 'bench scale' vessels and an ambr®15 'microscale' system were inoculated from the same source culture. The cells were cultured in basal medium, with a starting volume for bench and micro scale of 3.5L and 15mL, respectively.

Upon initiation of perfusion the working volumes are adjusted to 3L and 10.7mL for bench scale and microscale vessels, respectively. All vessels were operated at 1.0 vessel volume exchanges per day (VVD).

In Experiment 3.2, an additional ambr®15 micro scale system was inoculated with cells in basal medium for parallel operation and from the same source culture. These were also operated, as detailed above, at 1.0 VVD dilution rate.

The micro scale reactors were operated at 1.0 VVD with the developed gravity settling methodology detailed above (Section 3.2 Method Development). These cultures were allowed three partial medium exchange steps per day, conducted at eight hour intervals to equal the target VVD.

All cultivations were perfused with enriched medium starting from the initiation of perfusion mode, approximately 96 hours post inoculation. The bench scale vessels were operated in perfusion mode using an alternating tangential flow (ATF2) device (Repligen, USA) in combination with 0.22µm hollow fibre filter for cell retention, and continuous perfusion rate of 1.0 VVD.

In Experiment 3.1 a direct comparison is made between the culture performance within the developed microscale cell settling perfusion methodology and a bench scale ATF system.

In Experiment 3.2 the microscale perfusion methodology was challenged beyond 30 minutes settling time. The initial settling time of the CSs was increased to 33.5 and 37 minutes. This experiment was conducted to comprehensively explore the effect of extended exposure of the cells to micro-aerated and nutrient-limited conditions on their viability. These two conditions in Experiment 3.2 are highlighted as 3.2a and 3.2b for 33.5 and 37 minutes, respectively.

3.3.1 Data Analysis

Where replicates are reported, means and standard deviations (SDs) are provided in the format mean ± SD. The number of replicates from a single culture station in Experiment 3.1, Experiment 3.2a, and Experiment 3.2b microscale setup were n = 6, n = 4, and n=6, respectively. Paired or unpaired two tailed t-tests were used, where appropriate, to determine significance across conditions, and each specific application is referred to in the text. Comparison from microscale to bench scale (n = 2) was made using one way ANOVA. Vessels within a single culture station were treated as replicates for reporting statistical significance except when the vessel position effect was investigated, where no replicates were present.

3.4 Results

3.4.1 Resuspension of the Culture and Recovery to the Set Points

The operation of gravity cell settling required turning off the gassing and agitation control for the cultures. The measurements of pH and DO were observed to reproducibly decline during the settling period and return to the operating range following resuspension throughout the duration of the cultures (Figure 12).

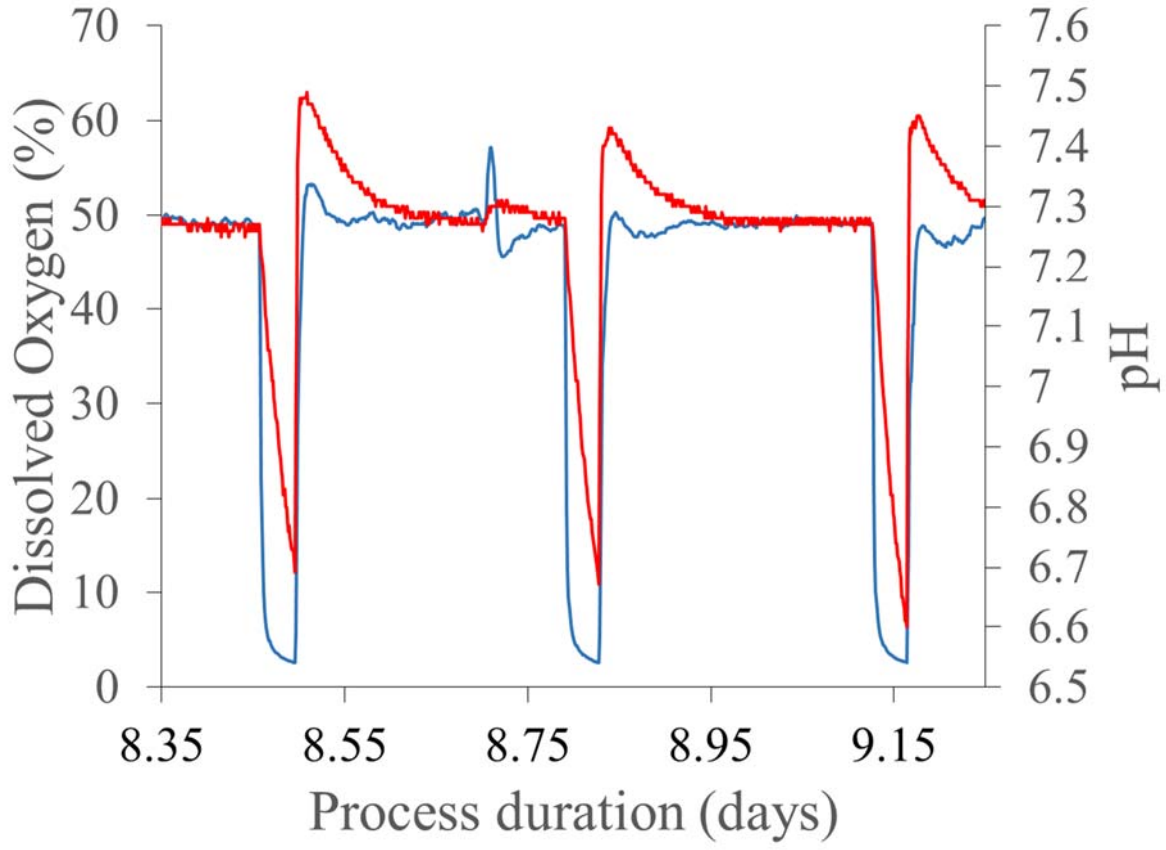

Figure 12 Sample traces of pH and dissolved oxygen in response to cell settling over a 1 day period
Sample traces from one microscale vessel in Experiment 3.1; online DO (Blue) and pH (Red) measurements recorded during the process. Both parameters are plotted on their respective axes against the process duration (days). Variation in the acidity and oxygenation during one day of cultivation, which entails three exchange steps (1.0VVD volume exchange rate), displayed the recovery between liquid exchange steps back to control set points

In the achievement of 1.0 VVD dilution rate, the tactic was employed to conduct three independent cell settling steps and exchange one third of the vessel volume in each instance with fresh enriched medium. As presented in Figure 12, a period of stabilisation was required for pH and DO before they reached levels experienced prior to cell settling. This period between cell settling steps allowed cultures to normalise before the initiation of the next cell settling.

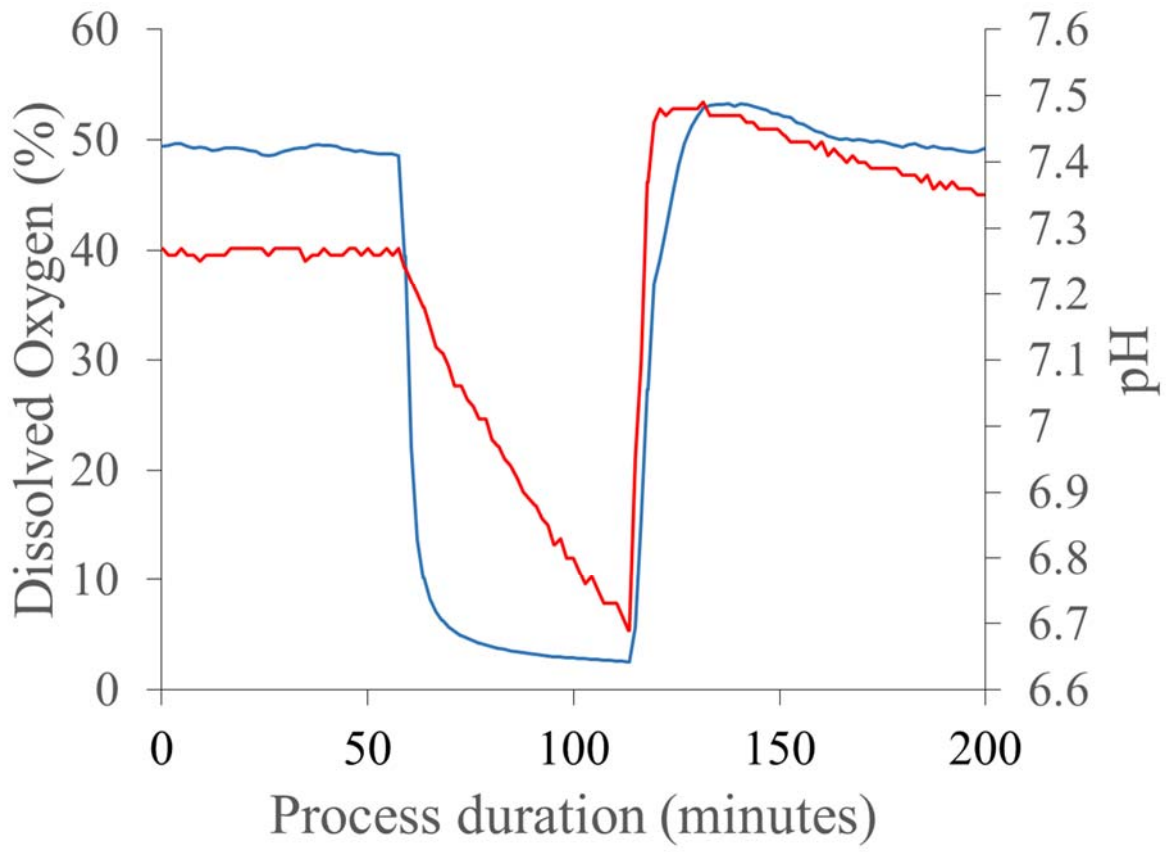

Figure 13 Sample traces of pH and DO from a single cell settling step
Sample traces from one microscale vessel in Experiment 3.1, displaying a single cell settling step; online DO (Blue), and pH (Red) measurements recorded during the process. Both parameters are plotted on their respective axes against the process duration (minutes).

A closer interrogation of an individual cell settling step reveals the different responses in pH and DO over time, in the process of cell settling (Figure 13). The pH observably dropped by approximately 0.8 units over 30 minutes and the decline in pH started immediately after the agitation was stopped (at approximately 60 minutes), slowing towards the end of the settling time. The DO immediately and very sharply declined from the set point (50%) down to below 5% saturation within 10 minutes and readings plateaued between 2 and 5% saturation. pH and DO did not recover to the set points until resuspension (at approximately 110 minutes).

3.4.2 Growth Performance

Evaluation of the perfusion culture's response to the cell retention methodology is presented in Experiment 3.1, as a comparison to bench scale ATF cultures, and in Experiment 3.2 as the extension of cell settling time at micro scale. Deviations in culture performance were observed in the respective growth characteristics, and in the following figures replicates from all experiments are overlaid to highlight the differences experienced in each condition.

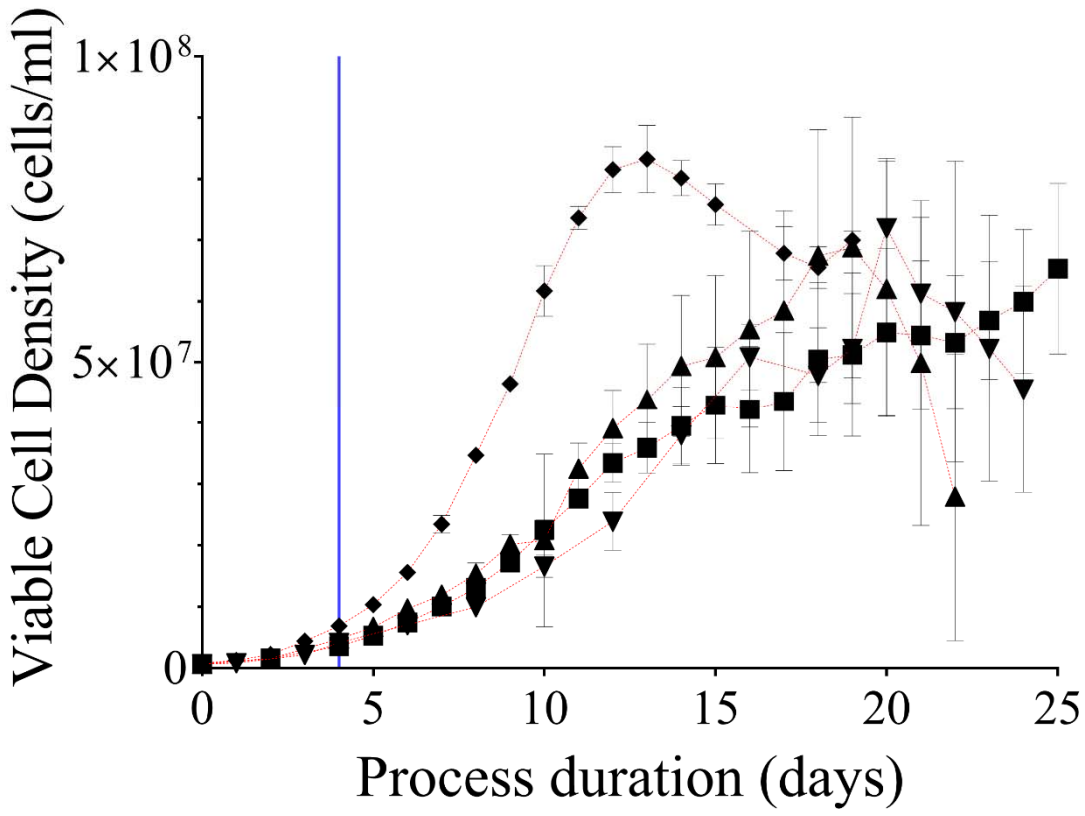

Figure 14 Viable cell density of perfusion cultures over process duration in response to cell retention method.
Microscale reactors: (▲) Experiment 3.1, n=6 (30 minutes settling); (▼) Experiment 3.2a, n=4 (33.5 minutes settling); (■) Experiment 3.2b, n=6 (37 minutes settling); Bench scale reactors: (♦) Experiment 3.1, n=2. Data shows mean ± SD. Blue intersecting line indicates the start of perfusion.

All cultures progressed through the initial batch growth and entered exponential growth following the initiation of perfusion on day four (indicated by the intersecting blue line, Figure 14). In the performance of culture from Experiment 3.1, microscale vessels (operating with a 30 minute cell settling time) reached the maximum viable cell concentration of (7.20 ± 1.14) x10^7 cells/mL 20 days post inoculation. Equivalent bench scale cultures (operated with an ATF, hollow fibre cell retention device) showed an improvement in the duration taken to reach maximum viable cell concentration (13 days post inoculation), and the maximum viable cell concentration was (8.32 ± 0.55) x10^7 cells/mL. The difference in the maximum viable cell concentrations of the cultures was not significant (p-value = 0.24).

Experiment 3.2 looked to investigate the impact of increasing the cell settling on the cultures performance. Increasing the settling time from 30 to 33.5 minutes did not yield a significant change (p-value = 0.91) in the maximum viable cell concentration, although the average maximum value attained was slightly lower, (6.88 ± 2.13) x10^7 cells/mL. A further increase from 30 and 33.5 minutes to 37 minutes did not yield a significant change (p-value = 0.38 and

0.45, respectively) in maximum viable cell concentration either; the average was lower than that for 30 and 33.5 minutes (6.53 ± 1.40) x10^7 cells/mL.

There was variation in the time taken to reach the maximum viable cell concentration in Experiment 3.2a. The average duration of (19.5±1.73) days was earlier than the uniform 20 days post inoculation observed for all replicates in Experiment 3.1. However, this difference was not significant (p-value = 0.49). Vessels across Experiment 3.2b did not reach this maximal cell concentration until later in the culture duration (Day 25), and this difference was highly significant (p-value < 0.001).

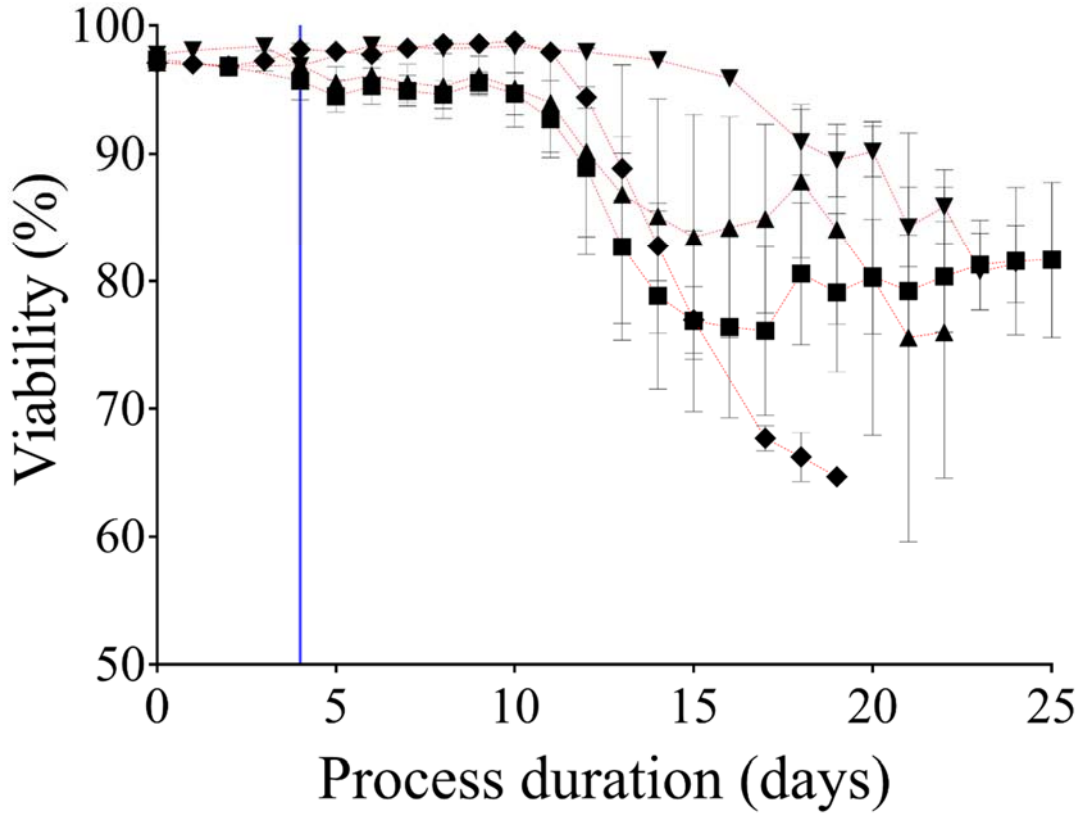

Figure 15 Viability percentage of perfusion cultures over process duration in response to the cell retention method.
Microscale reactors: (▲) Experiment 3.1, n=6 (30 minutes settling); (▼) Experiment 3.2a, n=4 (33.5 minutes settling); (■) Experiment 3.2b, n=6 (37 minutes settling); Bench scale reactors: (♦) Experiment 3.1, n=2. Data shows mean ± SD. Blue intersecting line indicates the start of perfusion.

The culture viability remained high for bench scale cultures throughout their exponential growth (Figure 15). On day 12 post inoculation the maximal viable cell concentration was reached and the growth rates plateaued. After the point of maximal viable cell concentration, the viability began to decline, and by day 17 post inoculation it had declined to below 70%.

The microscale evaluation in Experiment 3.1 (30mins settling) also presented high viability (>90%) throughout the exponential expansion. This was observed at (90.2±2.0) on the day of maximal viable cell density.

A non-significant decrease (p-value = 0.15) was observed in viability on the day of the maximum viable cell concentration as the settling time was increased to 33.5 minutes (86.9±4.5) %. The decrease in cell viability was not significant either (p-value = 0.18) when the settling time was further increased from 33.5 minutes (86.9±4.5) % to 37 minutes (81.7±6.1) %. However, the total decrease in viability observed with increasing the settling time from 30 minutes to 37 minutes was statistically significant (p-value < 0.01), indicating that increasing the culture settling time had an adverse effect on culture viability.

After culture settling, the microscale vessels were serviced sequentially by the robotic arm to replace the perfusate with fresh medium, and this introduced further lag on each vessel situated on positions 2-6 on each CS. The evaluation of individual vessel cell settling times in the operation CSs designated times (e.g. 30, 33.5, and 37 minutes) provides additional granularity on the impact of settling time on culture performance. Interrogation of this positional impact on settling time, and in turn growth performance is presented in Figure 16.

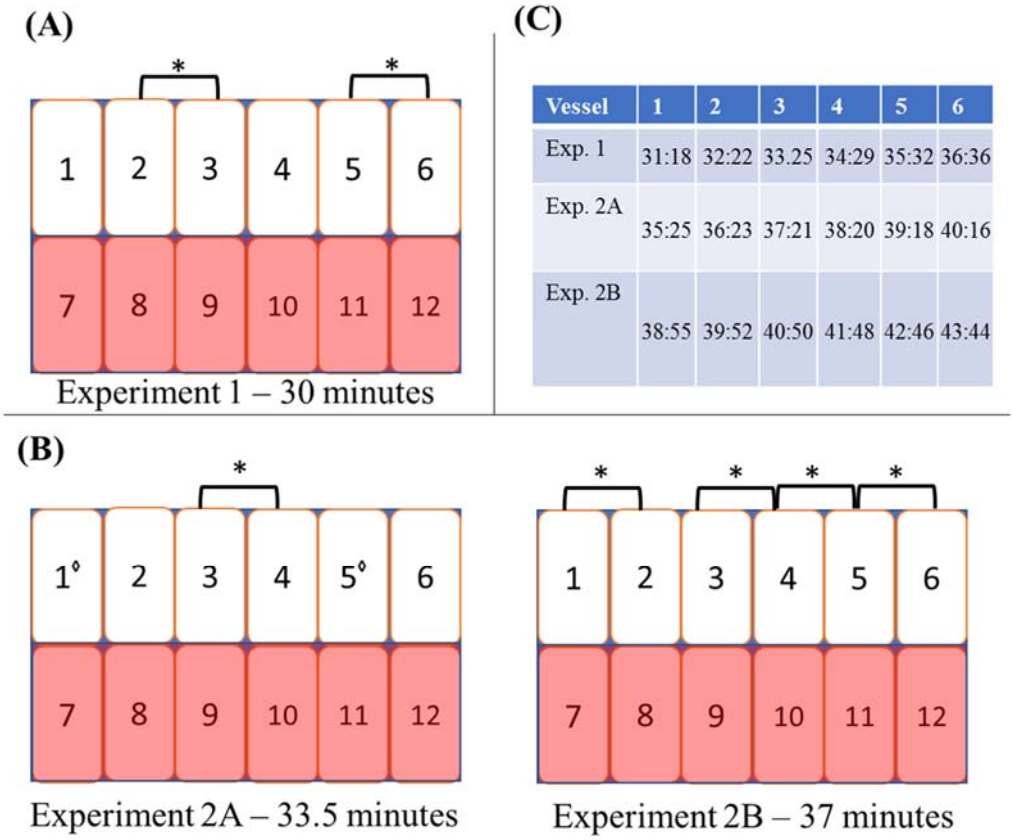

Vessel	1	2	3	4	5	6
Exp. 1	31:18	32:22	33.25	34:29	35:32	36:36
Exp. 2A	35:25	36:23	37:21	38:20	39:18	40:16
Exp. 2B	38:55	39:52	40:50	41:48	42:46	43:44

Figure 16 Position of the microscale vessels within their respective culture stations, and the actual settling times for each vessel observed prior to automated robotic liquid exchange
(A) – (B) Microscale vessel location on each culture station in Experiments 3.1 and 3.2. Differences in the viable cell concentration of neighbouring vessels determined by paired t-test at a significance threshold of ($P<0.05$), denoted by *, where significant. (C) Actual settling times (minutes: seconds) for each vessels in their respective positions 1-6 on the CSs to the initiation of automated liquid exchange, caused by the robotic arm servicing one vessel at a time. ◊ Vessels 1 and 5 in experiment 3.2a were terminated on Day 10 due to hardware failure.

The vessel positions with similar settling times in Experiment 3.1 and Experiment 3.2a were considered as biological replicates, whereas those in Experiment 3.2a and Experiment 3.2b were evaluated as technical replicates (Figure 16). In Experiment 3.1 (30 minutes), a significant difference ($P<0.05$) is seen in the viable cell concentration profiles of vessels 2 & 3 and 5 & 6, respectively. In addition, Experiment 3.2a (33.5 minutes) displays this significant difference between vessels 3 & 4, and in Experiment 3.2b between vessels 1 & 2, and 3 & 4, 4& 5 and 5 & 6, respectively. Although significant positional effects were observed in the viable cell concentrations between the neighbouring vessels in each CS, the biological and cultural replicates with similar settling times did not display significant differences consistently. However, the subsequently serviced vessels in Experiment 3.2b exhibited significant variability in the viable cell concentrations as the settling times increased.

3.4.3 Cellular Content of the Perfusate

The cell content of the perfusate was analysed to investigate the retention performance of the microscale experiments as they progressed.

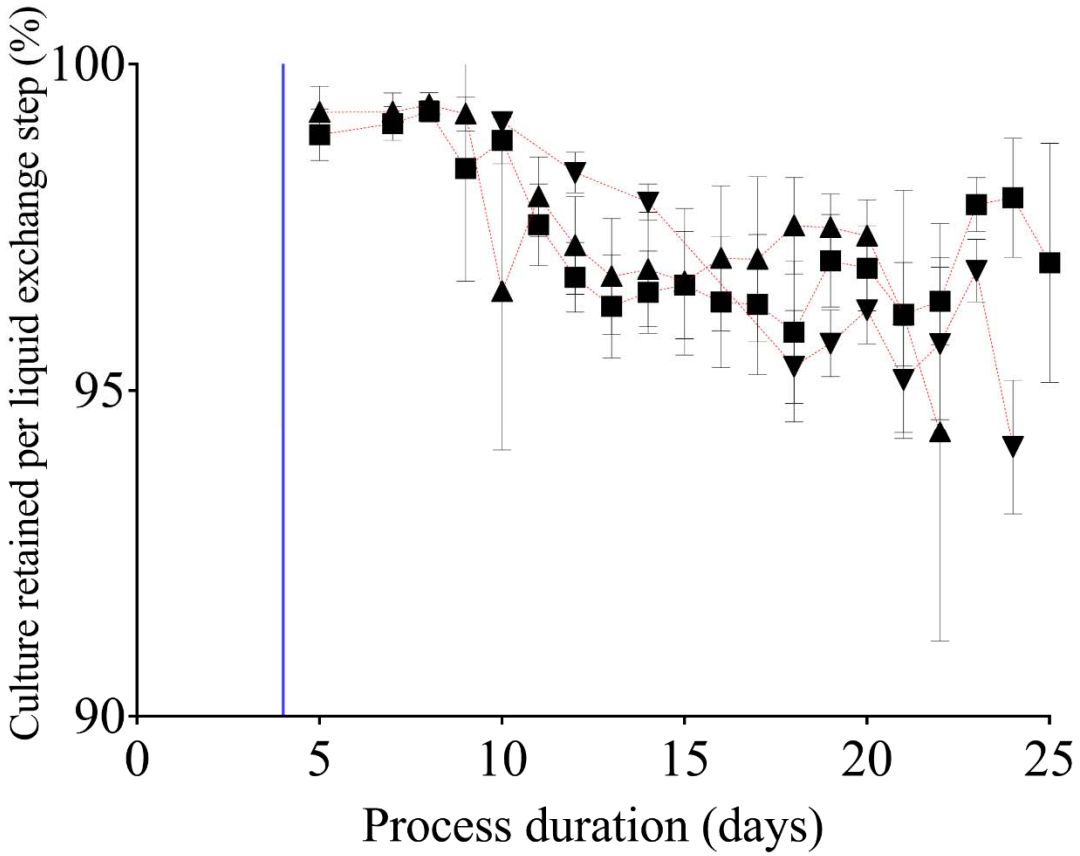

Figure 17 Cell retained per liquid exchange step (%) for microscale vessels.
Retention percentage determined as the ratio of the total cell content of perfusate to the total cell count for its respective culture suspended, plotted against process duration. (▲) Experiment 3.1, n=6 (30 minutes settling); (▼) Experiment 3.2a, n=4 (33.5 minutes settling); (■) Experiment 3.2b, n=6 (37 minutes settling). Data shows mean ± SD.

The average cell retention percentage was retained above 95% for the majority of the cultures (Figure 17). This retention was maintained throughout the fold increases in cellular concentration occurring between inoculation and maximum viable cell concentration. On the day of maximum viable cell concentration, the average cell retention was (96.2 ± 0.5) %, (97.5 ± 0.5) %, and (97.0 ± 1.8) % for Experiments 3.1, 3.2a, and 3.2b, respectively.

As cultures progressed into the late exponential growth phase (18 - 21 days post inoculation), Experiment 3.2 cultures with extended settling times displayed a statistically significant increase in average cell retention (%) (Experiment 3.1 vs 3.2a, and Experiment 3.1 vs 3.2b (p-value < 0.05)). No significant difference was observed between the two CSs in Experiment 3.2.

The ViCell XR (Beckman Coulter, US) cell counter provided for average cell diameter data in addition to automated cell number and viability counting. This average cell diameter value provides insight into the size of the cells present in the perfusate in comparison to those in the culture.

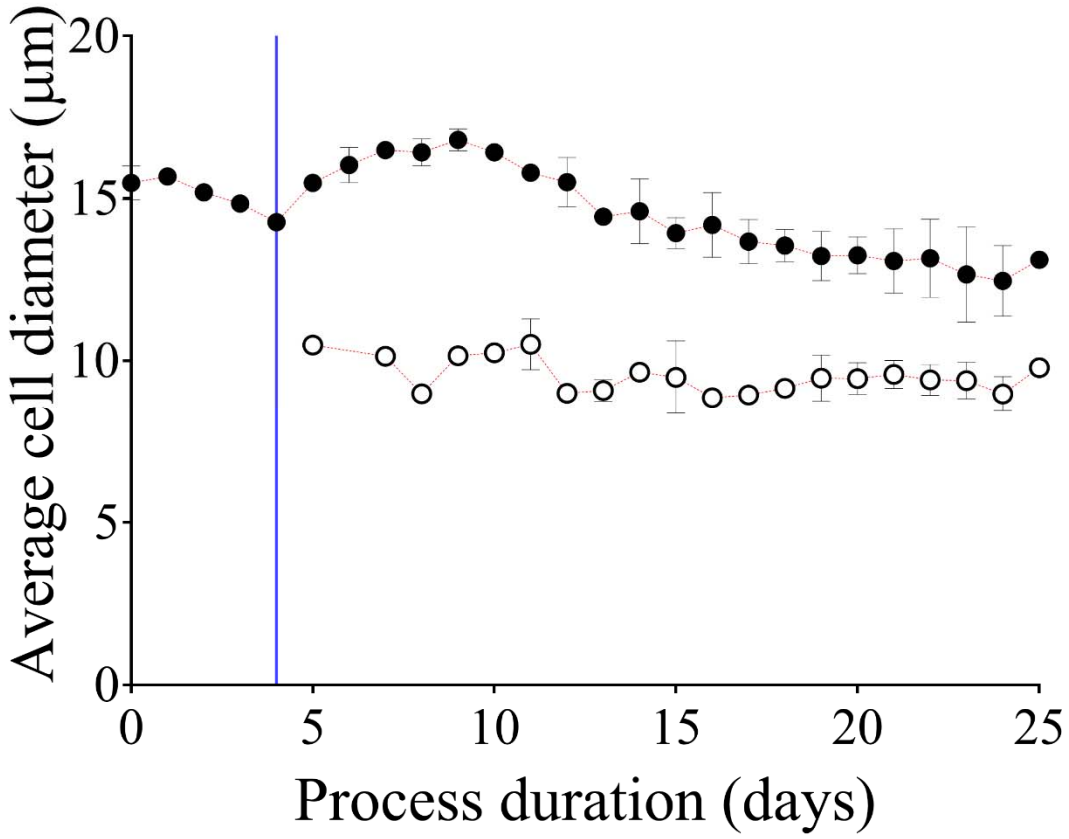

Figure 18 Comparison of Average cell diameter (µm) plotted for microscale cultures and respective perfusate.
Average cell diameter is plotted against process duration (days) for the cell samples in the microscale cultures (●) and in the perfusate (○). Plot represents the mean for all microscale samples (n=16) with SD shown when the variation was greater than 3.5% of the mean.

A highly significant difference (p-value < 0.001) in the average diameter of the cells across all culture samples and perfusate samples was observed (Figure 18), (13.27 ± 0.95) and (9.50 ± 0.50) µm, respectively. This difference indicates that the individual cells analysed in the perfusate samples that are inherent of a lower density are also smaller in diameter.

In addition, the viability measurements of the perfusate samples at maximum viable cell concentration (93.1 ± 4.8) % was consistently higher than that of the homogenous microscale cultures (86.2 ± 5.5) % (n=16) (p-value < 0.001).

3.4.4 Controlled Process Parameters

Evaluation of the monitoring associated with the culture control parameters enables further characterisation and comparison of the culture performance within micro and bench scale perfusion methodologies, respectively.

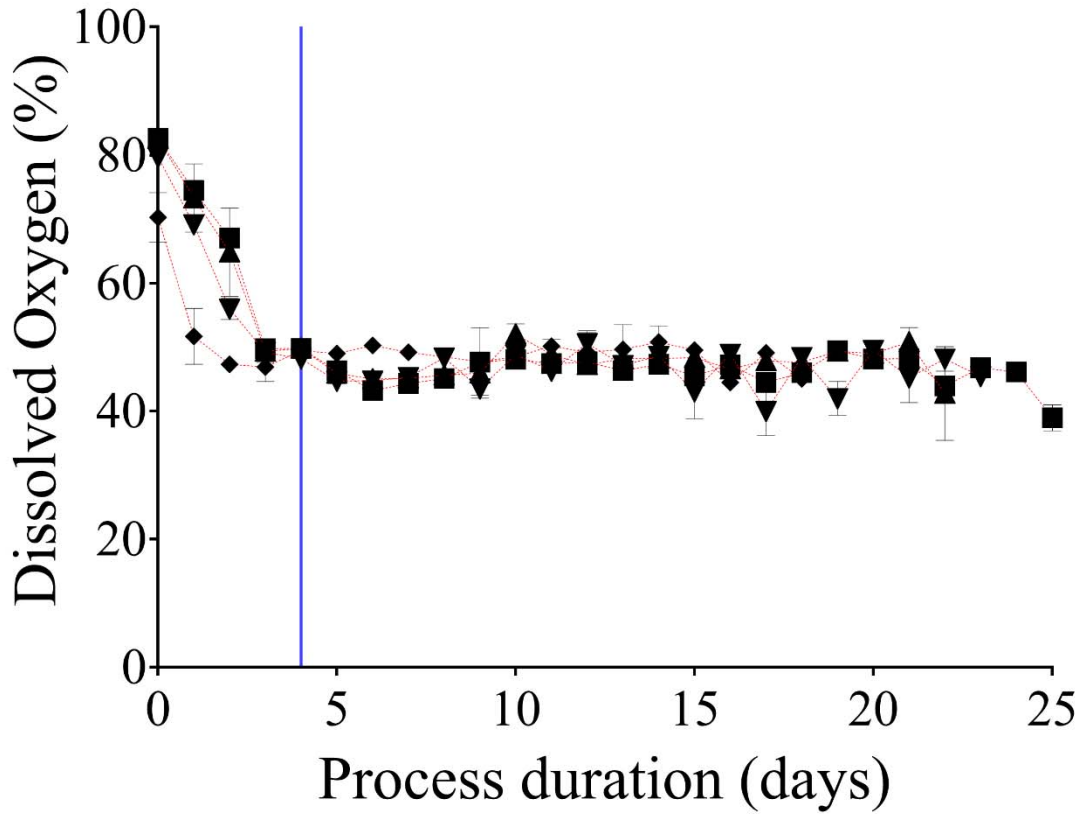

Figure 19 Culture response in online measured dissolved oxygen (%) plotted against process duration. Online microscale vessel readings have been averaged over their respective 24-hour periods to provide a representative value for the period. Microscale reactors: (▲) Experiment 1, n=6 (30 minutes settling); (▼) Experiment 2, n=4 (33.5 minutes settling); (■) Experiment 2, n=6 (37 minutes settling); (♦) Bench scale reactors: Experiment 1, n=2. Data shows mean ± SD. Perfusion initiation is indicated with an intersecting blue line.

The online readings for dissolved oxygen (%) from micro and bench scale vessels are displayed in Figure 19. In order to provide representative readings, the microscale vessels in an environment fluctuated by periods of no control (during cell settling, see Figure 13) an average is reported for each 24 hour period. Following inoculation, the oxygen demand in the cultures gradually increased, as the cell count increased, and the high starting DO percentage was gradually depleted towards the set point (50%). The point at which oxygen sparging was needed to supplement the oxygen transfer provided by agitation alone was met by day two and day three post inoculation for bench and microscale vessels, respectively. For the remainder of culture duration, dissolved oxygen was maintained at the set point throughout both the micro

and bench scale operations. The systems were both able to supply sufficient oxygen to support the culture growth at the high viable cell concentrations observed (Figure 14).

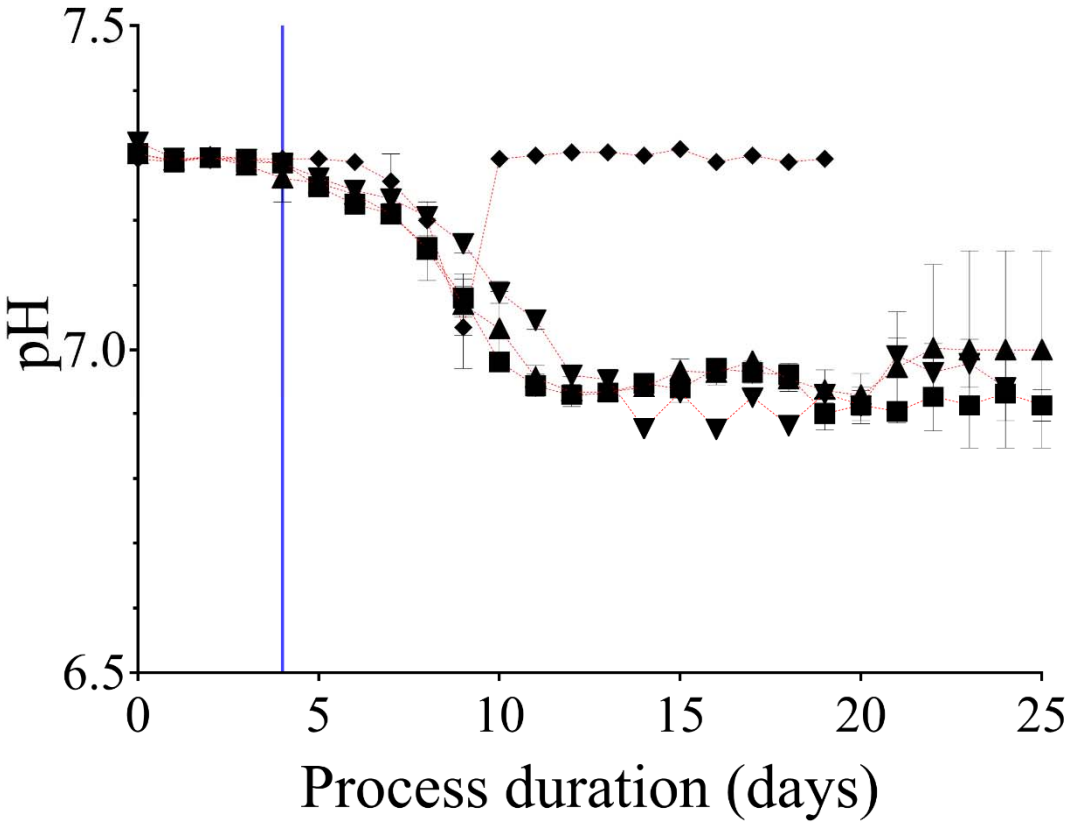

Figure 20 Culture response in online measured pH plotted against process duration.
Online microscale vessel readings have been averaged over their respective 24-hour periods to provide a representative value for the period. Microscale reactors: (▲) Experiment 1, n=6 (30 minutes settling); (▼) Experiment 2, n=4 (33.5 minutes settling); (■) Experiment 2, n=6 (37 minutes settling); (♦) Bench scale reactors: Experiment 1, n=2. Data shows mean ± SD. Perfusion initiation is indicated with an intersecting blue line.

The observed pH for micro and bench scale cultures is presented in Figure 20. The pH of both microscale and bench scale cultures accumulated acidity but were observed within ±0.1 pH units of set points for seven to ten days post inoculation.

At day 10 post inoculation the decreasing pH trend of the bench scale cultures was reversed and pH control was returned to the CO_2 sparging on demand, in the upper range of pH 7.2 to 7.3. The culture pH for microscale vessels continued to become more acidic and consistently remained within the pH range of 7.0 to 6.9.

This difference in pH profiles indicated a cellular adjustment occurring in the bench scale cultures, which was not observed in microscale cultures. Closer inspection of biochemical measurements conducted throughout the culture and retrospectively can highlight causation for

this difference in pH and offer insight into the level of impact it may have on process screening applicability.

3.4.5 Biochemical Analysis

The analysis of the cultures consumption of available carbon sources provides insight into the culture performance, highlighting potential areas for improvement when optimisation is sought. Central to the metabolism of mammalian cultures is the utility of glucose as the primary carbon source.

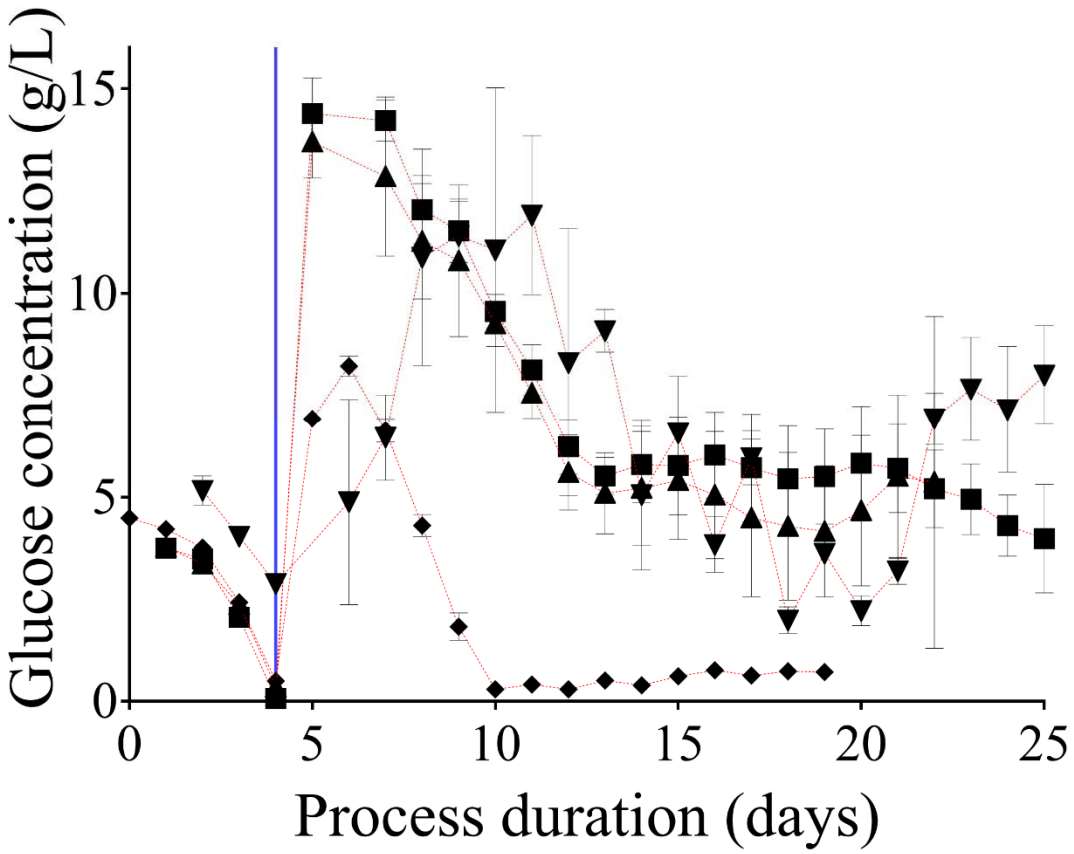

Figure 21 Culture response in at-line measured glucose (g/L) plotted against process duration.
At-line microscale and benchscale vessel readings for glucose (g/L). Microscale reactors: (▲) Experiment 1, n=6 (30 minutes settling); (▼) Experiment 2, n=4 (33.5 minutes settling); (■) Experiment 2, n=6 (37 minutes settling); (♦) Bench scale reactors: Experiment 1, n=2. Data shows mean ± SD. Perfusion initiation is indicated with an intersecting blue line.

The measured glucose that was observed in the vessels throughout the micro and bench scale evaluations is presented in Figure 21. The fluctuations observed are a function of cellular consumption of residual glucose and the influx and removal of glucose through the perfusion cultures. The starting glucose concentration, of approximately 5g/L, was gradually consumed in all cultures before perfusion being initiated on day four. Once perfusion was initiated, the influx of enriched medium increased culture glucose concentrations.

Excess glucose was available for the cultures in all bench and microscale vessels on the day of maximum viable cell concentration; (0.50±0.04), (2.22 ± 0.37), (3.07 ± 1.02) and (3.98 ± 1.33) g/L, for Experiments 3.1a, 3.1b, 3.2a, and 3.2b respectively. The presentation of glucose concentration across scales does not align with reference to culture progression. However, the time differences in reaching maximal cell concentrations enables a normalisation of the data and therefore a comprehensive comparison to be made. This normalisation is presented in Figure 22 as cell specific glucose consumption rate (g/cell/day).

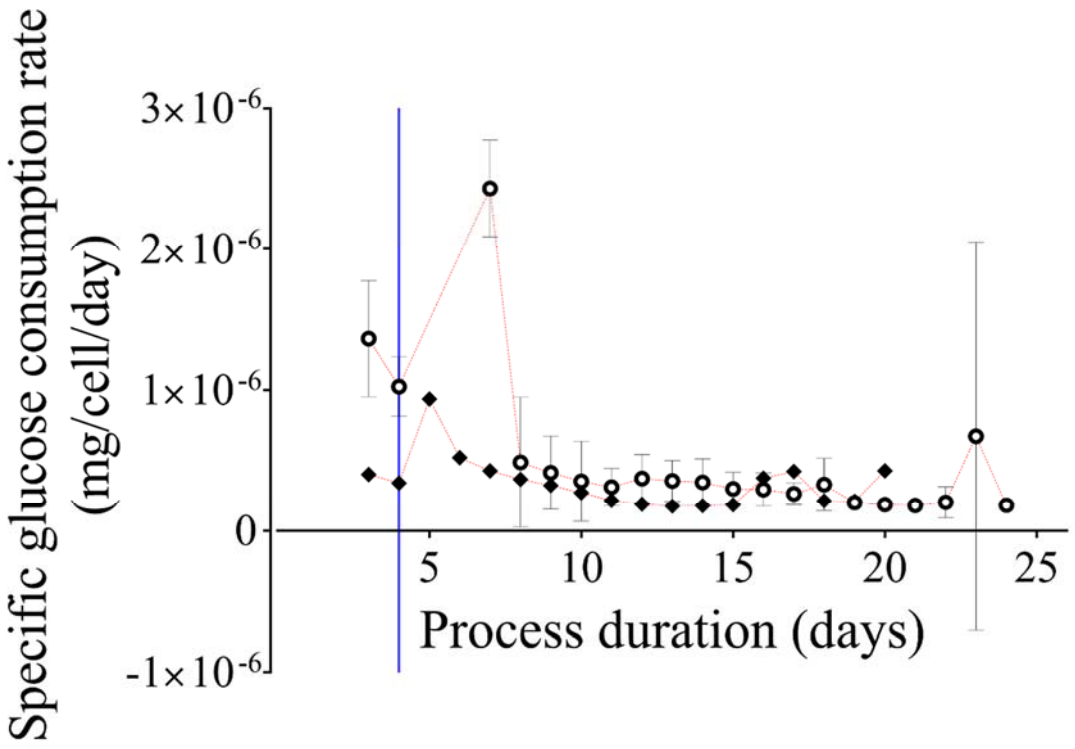

Figure 22 Culture cell specific glucose consumption rate (mg/cell/day) in response to scale over process duration (days).
Plotted cell specific glucose consumption rate over process duration, (○) combined microscale from Experiment 3.1 and 3.2, n=16; (♦) Bench scale reactors: Experiment 3.1, n=2. Data shows mean ± SD. Perfusion initiation is indicated with an intersecting blue line.

Whilst variation does exist, cultures follow similar trends over the first seven days post inoculation, dropping slightly as perfusion is initiated (day four) and then peaking shortly thereafter (day five). The variation observed appears to plateau by day eight post inoculation as all cultures are established in exponential growth, with (4.88±4.61) and (3.68±2.12) $x10^{-7}$ mg/cell/day for micro and bench scale vessels, respectively. This comparability between scales continued through the day of maximal growth and as cultures began to decline in viability, up to harvest.

Alongside glucose consumption, lactate production and consumption must be considered to gain a more comprehensive understanding of the biochemical status of the cultures, starting to explain some of the variation observed in pH.

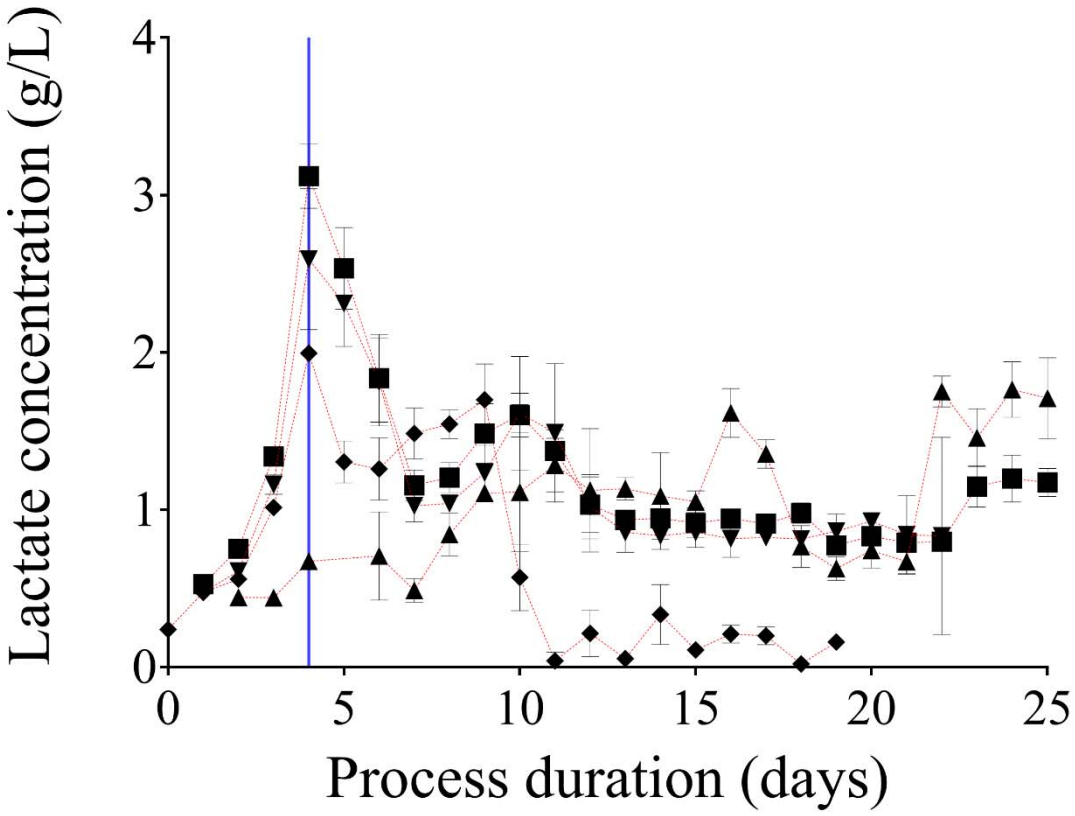

Figure 23 Culture response in at-line measured lactate (g/L) plotted against process duration.
At-line microscale and benchscale vessel readings for lactate (g/L). Microscale reactors: (▲) Experiment 1, n=6 (30 minutes settling); (▼) Experiment 2, n=4 (33.5 minutes settling); (■) Experiment 2, n=6 (37 minutes settling); (♦) Bench scale reactors: Experiment 1, n=2. Data shows mean ± SD. Perfusion initiation is indicated with an intersecting blue line.

The concentration of lactate (g/L) was measured from micro and bench scale cultures in Experiments 3.1 and 3.2, and is plotted in Figure 23. Starting at less than 0.5g/L, the lactate concentration accumulated in the cultures during the initial batch phase of the microscale cultures. This accumulation resulted in lactate concentrations on day four post inoculation of (0.67 ± 0.05), (2.59 ± 0.48), and (3.12 ± 0.20) g/L for experiments 3.1, 3.2a, and 3.2b, respectively. The lactate concentrations of microscale vessels aligned during perfusion operation and maintained at approximately 1g/L throughout the remainder of the perfusion phase.

The lactate concentrations for bench scale cultures peaked along with the microscale cultures on day four post inoculation and remained elevated >1g/L until the ninth day post inoculation

when it deviated from the microscale cultures and began to decline. This decline correlated with glucose availability in the culture, presented in Figure 21.

The glucose concentration of bench scale cultures declined from a peak at the sixth day post inoculation (8.22 ± 0.25) g/L and was fully utilised starting from the tenth day post inoculation (0.29 ± 0.01) g/L. A metabolic shift was observed as the cultures also metabolised the available lactate, dropping from (1.70 ± 0.23) g/L on the ninth day post inoculation, to (0.04 ± 0.06) g/L by the 11th day post inoculation.

A correlation was also observed between this glucose and lactate consumption event and the increased culture pH, presented in Figure 20, whereby pH is shown to recover back to the initial set point in the bench scale cultures. This metabolic switch did not occur in any of the microscale vessels and consequently, the pH remained depressed (Section 3.4.4 Controlled Process Parameters).

To further detail this metabolic variation, a retrospective analysis was conducted on retained samples from Experiments 3.1 and 3.2. This looked to quantify the individual amino acid levels within the medium and this highlights the metabolic pathways preferences of the cultures in the events presented above.

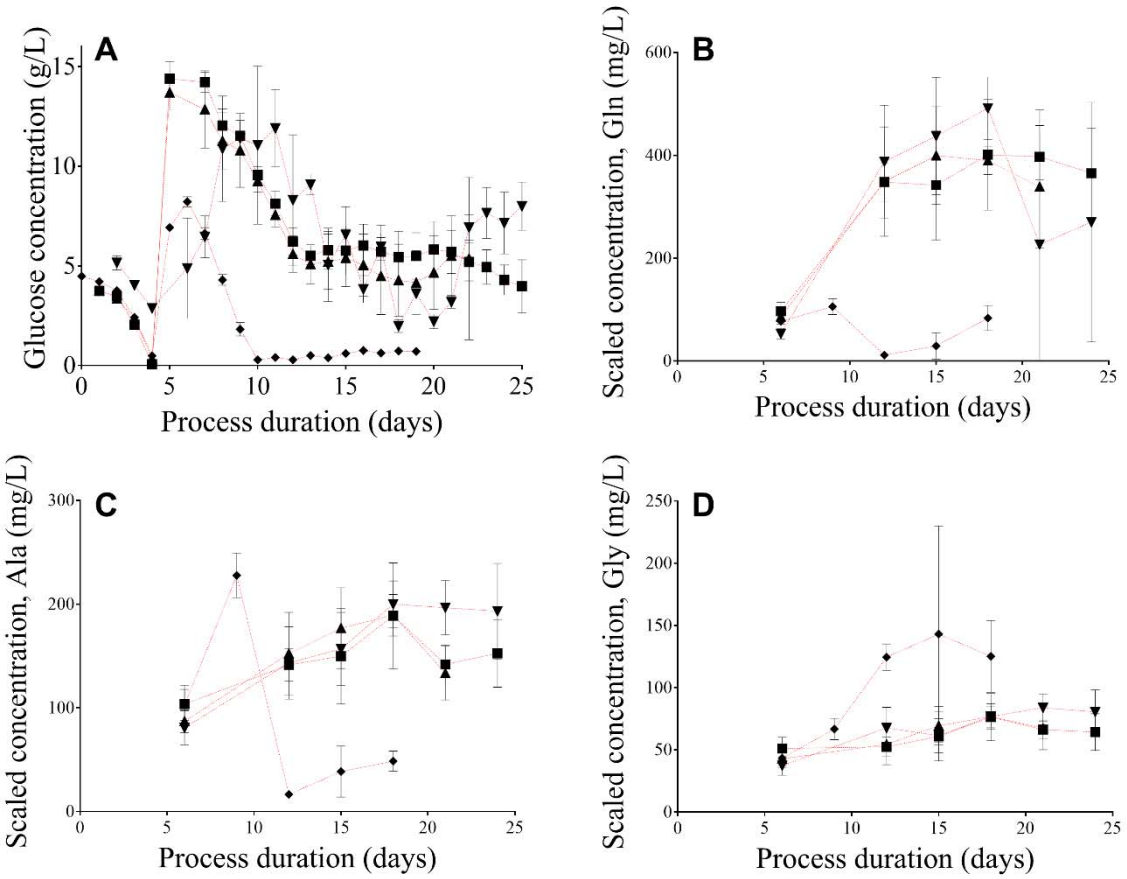

Figure 24 Glucose (g/L) presented with Amino Acid (mg/L) concentrations highlighting the metabolic shift in bench scale cultures plotted over process duration (days)
Microscale and bench scale vessel readings for (A) Glucose (g/L), (B) Scaled glutamine (mg/L), (C) Scaled alanine (mg/L) and (D) Scaled glycine (mg/L). Concentrations were scaled randomly in the interest of protecting the IP of the proprietary medium and are reported as "Scaled concentrations (mg/L)". Microscale reactors: (▲) Experiment 1, n=6 (30 minutes settling); (▼) Experiment 2, n=4 (33.5 minutes settling); (■) Experiment 2, n=6 (37 minutes settling); (♦) Bench scale reactors: Experiment 1, n=2. Data shows mean ± SD.

To succinctly present the biochemical response present in the bench scale vessels in comparison to the microscale vessels, Figure 24 contains culture concentrations of glucose (g/L), glutamine (mg/L), alanine (mg/L) and glycine (mg/L) in positions A, B, C, and D, respectively. Figure 24A presents the measured glucose concentrations (g/L) to provide a corresponding time course for responses in amino acid abundances within the cultures.

Presented in Figure 24B and C, a difference is observed in the concentrations of glutamine and alanine in the bench scale vessel compared to other cultures. Observed on day 12 post inoculation the bench scale cultures simultaneously begin consuming additional glutamine and alanine. Concurrently, a significant increase is observed in the concentration of glycine for bench scale cultures when compared to microscale (Figure 24D). Statistically, a significant difference (p-value < 0.05) was observed in the glycine, alanine, and glutamine between the bench scale and microscale cultures starting from the 12th day post inoculation.

In conclusion of the amino acid analysis and in addition to the trends presented in Figure 24, both bench scale and microscale systems concentrations of asparagine, cysteine, and serine were shown to concurrently deplete over time. The concentration of the remaining amino acids remained constant and not statistically different (p-value > 0.05) (Appendix Figure I).

3.4.6 Productivity and Product Quality

Culture productivity was measured throughout the exponential expansion of perfusion cultures. Alongside the productivity assessment, samples were tested for product quality by SEC for aggregation of the expressed mAb.

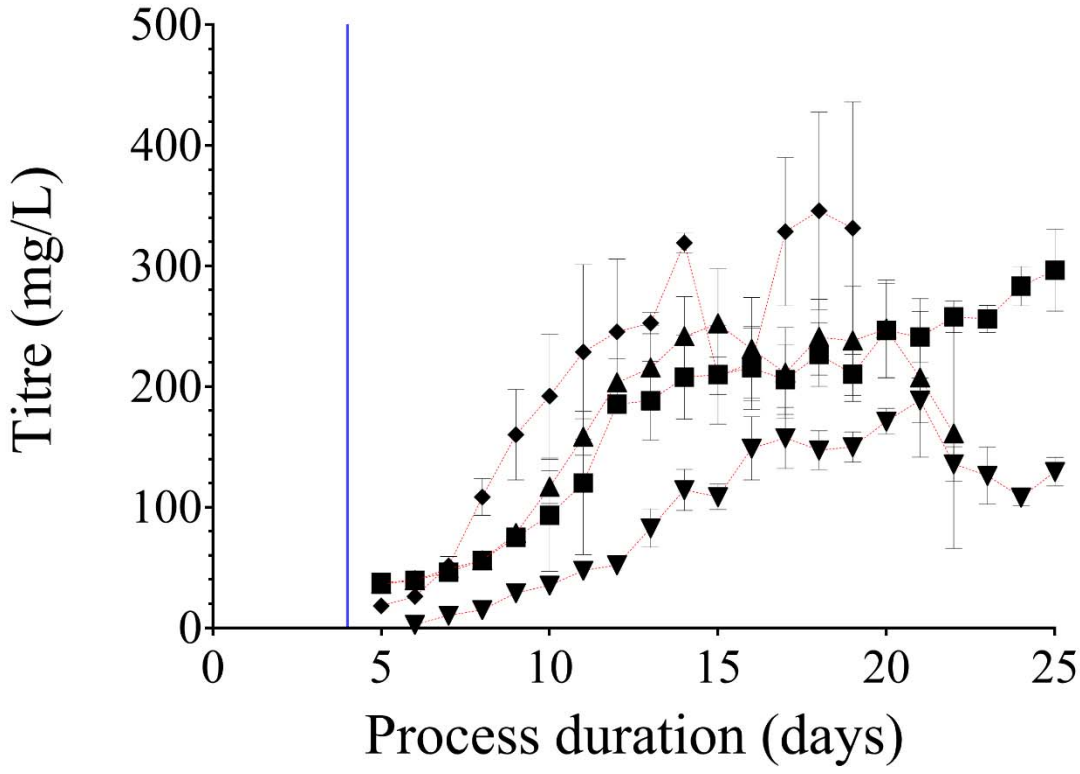

Figure 25 Titre (mg/L) of micro and bench scale cultures plotted across process duration (days)
Microscale reactors: (▲) Experiment 1, n=6 (30 minutes settling); (▼) Experiment 2, n=4 (33.5 minutes settling); (■) Experiment 2, n=6 (37 minutes settling); (♦) Bench scale reactors: Experiment 1, n=2. Data shows mean ± SD

The measured mAb concentration within cultures is low over the first few days of culture (Figure 25), due to the low cell density over this period (Figure 14). The average mAb concentration increased in line with the viable cell concentration across all cultures to the respective maximum viable cell concentration. On the day of the maximum viable cell concentration, the product concentration was (189 ± 19), (267 ± 18), and (267 ± 13) mg/L for microscale Experiments 3.1, 3.2a and 3.2b, respectively. The differences observed between Experiments 3.1 and 3.2a, as well as between Experiments 3.1 and 3.2b were significant

(p-value < 0.001, for both). The mAb concentration in the bench scale vessels was (253 ± 9) mg/L at the point of maximum viable cell concentration and the difference between the microscale and the bench scale product concentration was not significant (p-value = 0.92).

Due to observed differences in cell concentration (Section 3.4.2 Growth) between scales, and the inherent link between cell concentration and mAb titre, objective performance evaluation requires the calculated cell specific productivity. The cell specific productivity measurements for bench and microscale cultures were performed as detailed in Section 2.4 Rate Calculations.

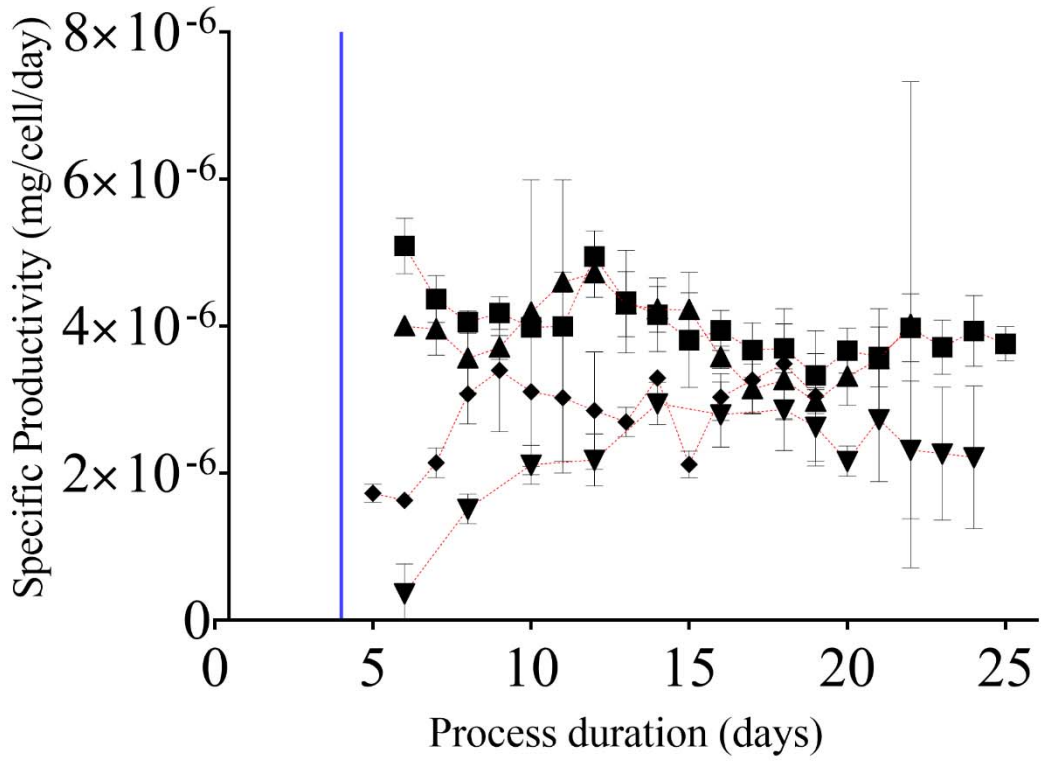

Figure 26 Cell specific productivity (mg/cell/day) of micro and bench scale cultures plotted across process duration (days)
Microscale reactors: (▲) Experiment 1, n=6 (30 minutes settling); (▼) Experiment 2, n=4 (33.5 minutes settling); (■) Experiment 2, n=6 (37 minutes settling); (♦) Bench scale reactors: Experiment 1, n=2. Data shows mean ± SD

The bench scale cultures displayed no marked improvement over microscale cultures in their cell specific productivity measurements (Figure 26). Additionally, variation was observed in cell specific productivity across cultures during the first 10 days of culture. This variation was observed to reduce as the cultures approached similar phases of operation, such as exponential growth in advance of the culture maximum cell density.

The average specific productivity (3.05 ± 1.1) on day eight post inoculation narrowed to (3.06±0.17) x10^{-6} mg/cell/day on day 19 post inoculation, displaying a non-significant difference between scales (p-value = 0.86).

Table 2 Monomer percentages of micro and bench scale cultures taken pre and post protein A purification

Experiment	Pre-purification monomer (%)	Post-purification monomer (%)
3.1a	44.8±0.7	94.0
3.1b	61.0±0.7	93.3
3.2a	54.6±8.7	95.1
3.2b	53.3±6.5	94.0

Protein A purified perfusate was collected and evaluated for monomer purity for each microscale and the bench scale experiment. Samples were taken from the vessels at maximal viable cell concentration (Table 2). The product purity achieved by cultivation at microscale was 93.3%, 95.1%, and 94.0% for the microscale Experiments 3.1, 3.2a, and 3.2b, respectively, and that achieved at bench scale was 94.0%, indicating comparability across microscale and bench scale cultures.

In addition to this, the average monomer content of the perfusate was measured pre Protein A purification, indicating the quality of the mAb product was (61.0 ± 0.7), (54.6 ± 8.7), and (53.3 ± 6.5) % for the microscale Experiments 3.1, 3.2a, and 3.2b, on the days 19, 19 and 24 post inoculation, respectively. The differences observed between Experiments 3.1 and 3.2a and between Experiments 3.2a and 3.2b were not statistically significant (p-values = 0.1 and 0.8, respectively). However, the product quality was significantly lower in Experiment 3.2b than in Experiment 3.1 (p-value < 0.05). The long settling times were observed to be associated with lower product quality that was nevertheless higher than the monomer content of the bench scale cultures at 14 days post inoculation ((44.8 ± 0.7) %). This difference between the bench scale and microscale cultures was highly significant (p-value < 0.001, Experiment 3.1).

3.5 Discussion

The operation of perfusion cultures within the ambr®15 system required the sedimentation of the cultures *in situ* to allow the exchange of a cell free fraction of medium. In retaining cells within vessels to perform liquid exchange steps, periods of uncontrolled bioprocess activity

were experienced. Fortunately, these uncontrolled periods were not unmonitored, and they appeared reproducibly throughout the microscale perfusion bioprocess operation.

These periods were highlighted by drops in DO and pH, likely to be caused by the metabolic activity of the cells consuming residual oxygen and producing CO_2 and lactate. As oxygen became limited (approximately after 10 minutes of cell settling) the slowing down of the cellular metabolic activity through reduced oxidative phosphorylation at low (<5%) DO saturations (Heidemann et al., 1998) could consequently have slowed down the rate of pH drop, since CO_2 production would slow down.

The location of the optical sensors at the bottom of the vessel was thought to contribute to the magnitude of these observed changes. As cells settled down at the bottom of the vessel, the sensors only picked up the parameters associated with an oxygen depleted and by-product accumulated local environment. Thus, hypoxic stress was thought not to be as extreme across the entire culture.

Efficient resuspension of the cultures was important to recover the system back to its control set points. This allowed the culture to evade the adverse effects of the microenvironment such as hypoxia or toxicity. Hydrodynamic investigation of the mixing time within microscale vessels indicate < 5 seconds is required for resuspension (Nienow et al., 2013). Upon resuspension, this short resuspension time was realised as the immediate recovery of pH back towards set point was observed.

The initially recovered values were higher than those measured prior to settling. The DO rapidly responded to the re-introduction of aeration and agitation, however, the values were observed to overshoot immediately after resuspension, only to recover to the set points within the first hour. Increased sparging of oxygen into the vessel to recover the DO back to 50% was thought to remove CO_2 from the culture, resulting in the slight elevation of the pH, an issue commonly mitigated in scale up applications (Matsunaga, Kano, Maki, & Dobashi, 2009).

Observations of the cell settling methodology in isolation can only present the recorded cellular environment experienced by the cultures. Feasibility for its application to a perfusion process is hampered by the critical levels of DO attained, and drastic pH deviations, during the cell settling.

However, considering the holistic, process wide impact of the cell settling methodology and how these perturbations impact the growth, viability, and production of the cultures provides valuable insight into method performance.

At microscale, the retention efficiency depended on settling cells from the surface of culture. A drop was observed in the percentage of culture retained during each liquid exchange step, this was from 99% initially tested, towards 95% as the cell concentration increased and culture progressed. The cell retention performance values (>95%) were higher than the values reported earlier (90% retention, (MilliporeSigma, 2017)) indicating improved performance in the present setup. However, this small percentage loss was thought to be a small and frequent cell bleed that could contribute to depressed growth rates and lag time in reaching maximum cell concentration.

Additional information was gained on the performance of the cell retention methodology by analysing the small subpopulation that was being removed at each perfusion step. Although the viability of cells has been reported to affect their settling velocity (Searles et al., 1994), with non-viable cells moving 30 – 50% slower than viable cells (Z. Wang & Belovich, 2010), the cultures investigated here did not adhere to the earlier observations. However, given the difference in physical size, the cells removed were more likely those which displayed lower specific productivity due to their stage in the cell cycle, as reported earlier (Lloyd et al., 2000).

In the conduction of the cell settling methodology, vessels within each CS were serviced sequentially post settling period, such that incremental increases in the respective settling times were experienced. This occurrence of variation in settling time enabled the closer investigation of the impact of the uncontrolled period on the perfusion bioprocess. An increase in statistically significant variation was observed in line with settling time. Thus, a combination of this interrogation combined with initial method development work presenting minimum settling times of above 30 minutes and suggesting an operational maximum settling time of this cell line to be kept shorter than 41 minutes.

It is noted however, as cell size distributions will vary between individual cell lines and clones these figures should be investigated in each new application and the operating range investigated here provides a wide investigative space to find operational space for future cell lines, well within the operational limits or boundaries.

The growth performance of microscale perfusion cultures presented statistically comparable maximum cell concentration to bench scale operation. The cultures were observed reaching high cell concentrations exceeding 7.0 x10^7 cell/mL in bench and microscale alike.

However, differences were observed in the achievement of these maximal cell densities that the further characterise the microscale methodology. An extended phase of exponential growth observed for the cultures growing at microscale and was thought to be at least partially related to the efficiency (very small, frequent cell bleeds) or periods of uncontrolled cultivation, experienced in gravity cell settling. In contrast, cells operated at bench scale were considered to be retained at 100% efficiency as the 0.2µm pore size within the hollow fibre filter was sufficiently small to prevent the passage of cells, without periods of uncontrolled cultivation.

In addition to a lag period in reaching maximal cell concentration, microscale perfusion vessels also experienced differences in the pH environments generated when compared to bench scale cultures. Following an initial growth period, bench and micro scale cultures began to see an accumulation of lactate and sequential drop in pH. This was reversed in bench scale cultures as the improved growth characteristics enabled the cultures consumption of residual glucose and increased back metabolism of lactate. This metabolic scenario was confirmed by further amino acid analysis.

In the bench scale cultures, data suggest pyruvate was selectively converted into alpha-ketoglutarate, which entered the TCA cycle, and excess pyruvate was be converted into glycine. The concurrent increase in the by-product alanine concentration provided further support for the activation of this pathway. Glutamine concentration was shown to decrease supporting that the glutamate pool was utilised in alpha ketoglutarate production, rather than glutamine.

Despite these differences, in pH, the specific glucose consumption and lactate production of the microscale and bench scale systems were similar (Figure 22 and Figure 23, respectively). Earlier reports indicated that even a small variation such as 0.1 in pH could significantly impact culture growth and metabolism, in particular glucose consumption and lactate production (F. Li et al., 2010). The cell line employed in this study was very robust, withstanding a pH variation of 0.3 without demonstrating any observable differences in two major indicators of metabolic activity after the 10^{th} day following inoculation; glucose utilisation and lactate production. However, the sensitivity of the cell line to variations in pH needs to be considered in designing the system, e.g. introducing two-point pH control in the system.

Comparison of the micro and bench scale systems is furthered with the evaluation of productivity and product quality assessments. Cell specific productivity does not appear to be impacted by the method of cell retention, with comparability presented in cell specific productivity once cultures are established. This supportive productivity data is paired with comparable product quality outcomes, where aggregation was consistently below 6% across micro and bench scale cultures post protein A purification. In addition, monomer content achieved in microscale pre protein A was significantly higher than bench scale, suggesting that the unique microscale perfusion environment did not negatively impact product quality when compared to the characterised ATF bench scale perfusion environment (Kelly et al., 2014; Walther, McLarty, & Johnson).

In conclusion, the microscale system supported statistically comparable maximum cell concentration to that displayed in bench scale operation specific for this experimental cell line, with cultures reaching very high cell concentrations exceeding 7.0 $x10^7$ cell/ml; the cultures were not limited by oxygen, and the pH of the system was maintained at a stable level. The differences in culture pH between the microscale and bench scale cultures did not yield differences in the CHO cell physiology, with the specific glucose consumption and net specific lactate production rates remaining similar.

The present setup could utilise either the 48-vessel or the 24-vessel variants of the microscale system at 50% capacity with half of each culture station being utilised at a time. At a liquid exchange rate of 1 vessel volume per day, this setup allowed suitable maintenance downtime and a single operator intervention per day. This evaluation has shown the potential and applicability of this setup in conducting multifactorial DoE to effectively evaluate perfusion process set points, media optimisation, or as a cell line screening tool.

Chapter 4 The Evaluation of Micro and Bench Scales Perfusion Cultures as Tools for Production Culture Inoculum Expansion

4.1 Introduction

Perfusion culturing of Cell line 1 at microscale, as presented in Chapter 3, achieved a maximum density of (7.20 ± 1.14) x10^7 cells/mL. Due to the continuous dilution of the cultures with fresh medium, this high cell density did not result in a highly concentrated mAb product.

The observed high volume and low concentration harvest of perfusion is a contrast to the low volume, and high concentration typically observed in fed batch methods. The low concentration prevents prevalent commercial production of mAbs through continuous culturing methods.

However, the high cell density observed in continuous culture has a direct application to the supply of cells for inoculation in commercial scale vessels. Each commercial scale inoculation is initiated by thawing cryopreserved cell stocks (from a single vial of a common source). This culture is expanded in incrementally increasing culture volumes until sufficient cells are present to achieve the desired seeding density. This expansion is achieved by multiple subcultures per week followed by multiple pilot scale (or larger) vessels (Shukla & Thömmes, 2010). An example of this expansion process is presented in Figure 27, below.

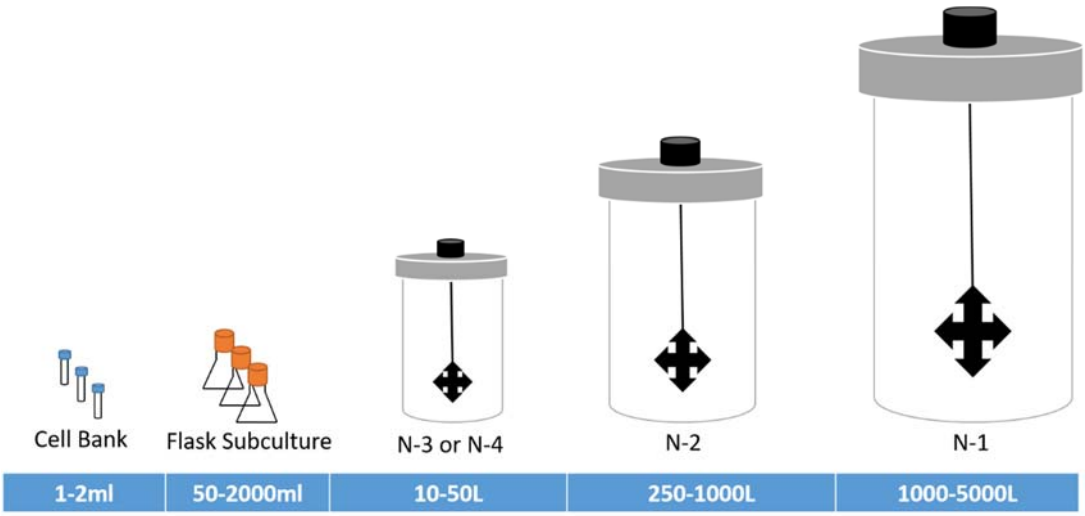

Figure 27 Diagrammatic representation of typical inoculum expansion
Presented in this figure is the typical expansion process and volume requirements for a fed batch bioprocess inoculum, in order to operate high volume manufacturing scale vessels. At each step cells are grown to between 2 and 10 x10^6cells/mL prior to inoculation of the next stage.

Perfusion cultures maintain exponential growth up to a maximum density (Clincke et al., 2013). This exponential growth can be maintained indefinitely as a pseudo-steady state with the application of regular culture 'cell bleeds', reducing cellular concentration below the critical density. The cellular state present in perfusion exponential growth is thought to be similar to what would be targeted during the inoculum expansion subculture (Kloth et al., 2010). Therefore, high density perfusion cultures may streamline inoculum expansion by reducing the number of incrementally increasing scale-up vessels required (Figure 27).

The use of perfusion cultures for inoculum expansion shifts the focus of evaluations from the quantity and quality of the expressed mAb to the health and viability of cells within the culture. The impact of the continuous expansion can be simultaneously experienced across multiple cellular processes, including the transcriptome (Fomina-Yadlin et al., 2015), metabolome (Sellick et al., 2011) and proteome (Nissom et al., 2006). Simultaneous characterisation of the impact on these cellular frameworks within a perfusion culture is challenging for a single culture, and unfeasible in a high throughput setting.

Therefore, experiments within this chapter aim to first characterise the cellular content present in micro and bench scale perfusion cultures. This is conducted holistically by utilising the perfusion cultures as inoculum expansions, inoculating production cultures. Observed differences in the subsequent production cultures will be expected to have origins in the perfusion methodology. This dual mode strategy for investigation has been highlighted previously by conducting batch and fed-batch to alter the metabolism and progressing the cultures to a continuous system to evaluate the impact (Europa, Gambhir, Fu, & Hu, 2000).

Variation observed in inoculum expansion is documented to impact culture performance in production cultures (Kallos & Behie, 1999). Differences were highlighted in the growth rates of the respective micro and bench scale perfusion methods (Chapter 3). Sub- populations that grow slower were thought to be promoted in the microscale perfusion cultures, as the fast growing populations were expected to 'over-grow' during the cycling of nutrient availability (Stephens & Lyberatos, 1987). Therefore, utilising the microscale perfusion methodology for the generation of n-1 inoculation cultures presents the opportunity to further characterise the methodology and compare it to bench scale systems.

Secondly, the cell line sensitivity to decreasing perfusion dilution rates was evaluated at bench scale. This auxiliary investigation served to characterise and attribute any variation observed at micro scale with sensitivity to dilution rate.

4.2 Materials, Methods, and Experimental Design

Materials and methods utilised for both perfusion and fed batch operation are as presented in Chapter 2 Materials and Methods. The two investigations and their unique design characteristics are outlined below and in Table 3.

Table 3 Experimental outline for evaluations contained in Chapter 4

Experiment	Scale	Cell line	Dilution rate (VVD) of perfusion phase	Seeding density for production phase	Fed-batch condition
4.1a	Micro	1	1.0	2.5, 5, 10, 15	1X, 2X
4.1b	Bench	1	1.0	2.5, 10	1X, 2X
4.2	Bench	1	1.0, 0.75, 0.5	10	1X

To aid the comprehension of the experimental design, a discussion is offered following each experimental subsection (e.g. Results for Experiment 4.1 are followed by Discussion for Experiment 4.1, then Results for Experiment 4.2 are followed by Discussion for Experiment 4.2).

The first of these investigations (Experiment 4.1a) followed the microscale methodology for gravity cell settling, presented in Chapter 3. The microscale perfusion cultures were used to inoculate microscale fed-batch production cultures. The operation of the production cultures was performed at multiple production conditions. These conditions varied the seeding density and feeding regime to highlight the cellular characteristics of the proceeding perfusion cultures.

Parallel evaluations in bench scale cultures were conducted (4.1b) to highlight scale dependent characteristics present in Experiment 4.1. Due to the high throughput nature of the microscale system, additional conditions were conducted at microscale, compared to those evaluated at bench scale.

The second investigation (Experiment 4.2) was conducted at bench scale. The dilution rate of the inoculum perfusion vessels was varied, whilst the process conditions of the production phase are kept consistent. This design highlighted cellular characteristics related to different dilution rates of the perfusion cultures.

The bolus addition of the nutrient feed was conducted daily from day 1, in production cultures. This frequency was selected to ensure that the nutrient demands of the high cell density present at inoculation was supported.

Given the proprietary nature of the medium and feed compositions, only a simplified adjustment of feeding ratios, rather than informed medium optimisation investigations, were utilised. Presented in this Chapter is the culture response, at different scales and seeding densities, to a platform 2-part feed volume (1x condition) and one that is volumetrically doubled (2x condition). Respective seeding densities for following production vessels and the feed conditions applied on each day are detailed in Table 3.

Cultures were progressed through the production phase up to day 14 post inoculation or until viability declined below 60%, whichever came first.

4.2.1 Transition of Cultures From Perfusion to Production

The transition of cells into production cultures was initiated when perfusion vessels were within exponential growth. An understanding of maximal cell density was gained from work conducted in Chapter 3. Therefore, the target cell density for the transition was determined to be at 40 $x10^6$ cells/mL to ensure cells were established in exponential growth.

The experiments detailed in Table 3 require the inoculation of the production cultures with cells originating from the respective perfusion cultures. The incorrect operation of this inoculation step can result in extended periods of time where the physiochemical environment of inoculum cultures is uncontrolled. Characteristics associated with high density culture, such as net high accumulation of waste and inherently high oxygen demand, have potential to negatively impact on the production vessel performance unless the transition is managed appropriately.

4.2.1.1 Pooling Cultures – Production Phase Evaluation

For Experiment 4.1, the screening of seeding density and feeding ratio in the production phase cultures required large quantities of high concentration inoculum to be generated. To supply this, multiple perfusion vessels were operated for the micro and bench scale experiments, respectively. Comparable replicate perfusion cultures (n=9 and n=2 for micro and bench scale, respectively) from within the same scale were pooled together in the transition step. The pooling step highlighted specific scale-related challenges.

At microscale, the combination of nine vessels from n-1 perfusion resulted in a total culture volume of approximately 90mL. The pooling was performed utilising a vented shake flask (Corning®) and a humidified incubator to provide rudimentary temperature, CO_2, and O_2 maintenance conditions while the inoculation was conducted.

At bench scale, two perfusion vessels were combined to provide approximately six litres of culture volume. The main concern was to ensure agitation of the pooled inoculum whilst inoculation was conducted. The cultures were extracted from the perfusion vessels into a 20L culture bag. This bag was then placed on a rocking platform (WAVE25, GE) whilst transition was performed. Agitation through the rocking action of the culture ensured homogenisation during inoculation and aided the culture to maintain viability.

In order to conduct the transition without delay, it was important to have pre-prepared production vessels for inoculation. Such preparations include ensuring the inoculation medium is within operating ranges for temperature and pH, alongside performing at-line sensor calibration checks and applying offsets.

Experiment 4.2 evaluated different dilution rates in the perfusion cultures before inoculating the production cultures. This required segregation of dilution rate conditions and alleviated the need for pooling material. This experiment was conducted at bench scale to accurately control the designed dilution rate continuously rather that the incremental semi-continuous dilution rate offered in the microscale system.

4.3 Results

4.3.1 Experiment 4.1 The Cellular Characteristics of Micro and Bench Scale Perfusion Present in Production Cultures

4.3.1.1 Growth Performance and Biochemical Characteristics of Perfusion Cultures

The micro and bench scale perfusion cultures were inoculated at a target seeding density of $0.8x10^6$ cells/mL, respectively. The measured viable cell concentrations from the operation of these vessels are presented in Figure 28, below.

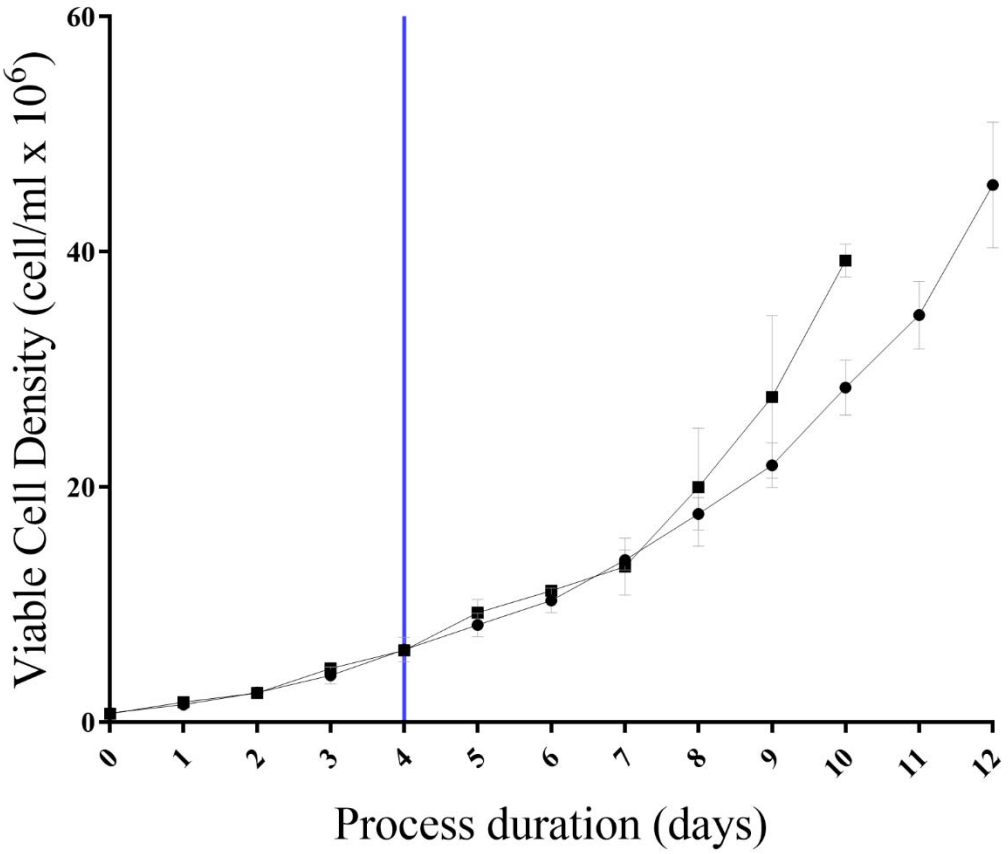

Figure 28 Growth of perfusion vessels operated at micro and bench scale over process duration (days)
Viable cell density (cells/mL x10^6) of perfusion vessels. Viable cell density is plotted against process duration (days), (●) and (■) represent micro (n=9) and bench (n=2) scale vessels, respectively. Perfusion initiation is indicated with an intersecting blue line.

Following inoculation, cells were grown in batch for the first four days of culture. The viable cell density during this period reached (6.17±1.03) and (6.13±0.21) x10^6 cells/mL for micro and bench scale vessels, respectively. The initiation of perfusion systems on the fourth day post inoculation (indicated by the intersecting blue line) enabled the cultures to extend this period of exponential growth. A similar growth profile is experienced in the micro scale vessels when compared to bench scale.

The two scales display no significant difference throughout the process duration, however, the level of significance decreases when values up to day seven are expanded to day ten (P-value = 0.23 and 0.10, respectively). This decrease in significance is representative of the microscale vessels taking an additional two days to reach the target density (40x10^6cells/mL) set for transfer into the production vessels. Cell densities at transfer were (45.71±5.34) and (39.27±1.40) x10^6cells/mL on days 12 and 10, for micro and bench scale vessels respectively.

Additional process monitoring displays comparability between bench and microscale perfusion vessels, up to their transition into production operation. This is highlighted by the key process variables pH and dissolved oxygen, in addition to key metabolites glucose and lactate.

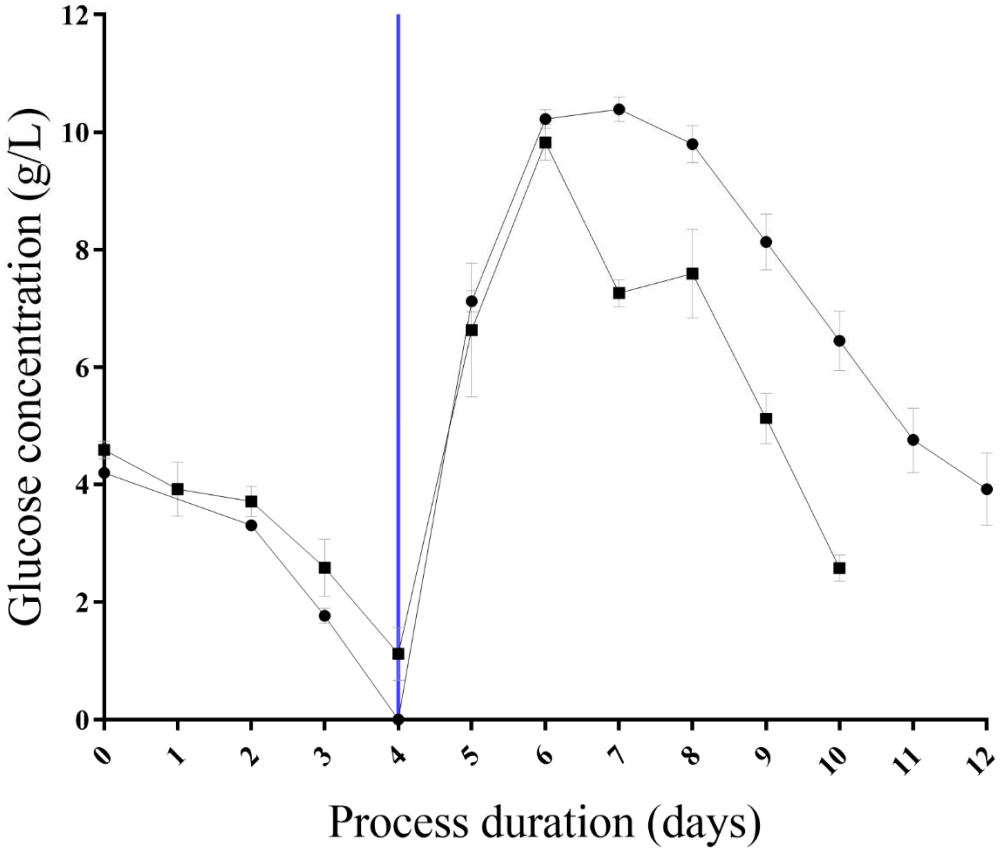

Figure 29 Measured glucose of perfusion vessels operated at micro and bench scale over process duration (days)
Glucose concentration (g/L) of perfusion vessels. Glucose concentration is plotted against process duration (days), (●) and (■) represent micro (n=9) and bench (n=2) scale vessels, respectively. Perfusion initiation is indicated with an intersecting blue line.

The measured glucose (g/L) present within micro and bench scale cultures during the perfusion phase of operation is highlighted in Figure 29. A decline in glucose concentration was observed over the first four days of batch culture. The concentrations decreased from initial values of approximately 4g/L, to (0.01±0.01) and (1.12±0.45) g/L for micro and bench scale vessels, respectively. Following the initiation of perfusion, and the influx of fresh medium, these glucose concentrations rapidly increased, reaching (10.2±0.2) and (9.8±0.3) g/L by day six for micro and bench scale, respectively. No significant difference was observed between glucose concentrations over this period of time (p-value= 0.3).

On day seven, a decline was observed in glucose concentration for bench scale vessels, to (7.3±0.2) g/L, where microscale vessel glucose concentration remained above 10g/L.

Increased culture glucose consumption aligned with viable cell concentration in Figure 28, whereby an increase was observed for bench scale cultures. As cultures progressed towards transition criteria ($40x10^6$ cells/mL) the residual glucose concentration within the vessels continued to decline, but was never limiting, with measured values at transition at (3.9±0.6) and (2.6±0.2) g/L for micro and bench scale, respectively.

In close relationship to measured glucose levels within the vessels, Figure 30 presents the measured lactate (g/L) that was present in the vessels through a function of the cells' production, consumption, and perfusion process dilution.

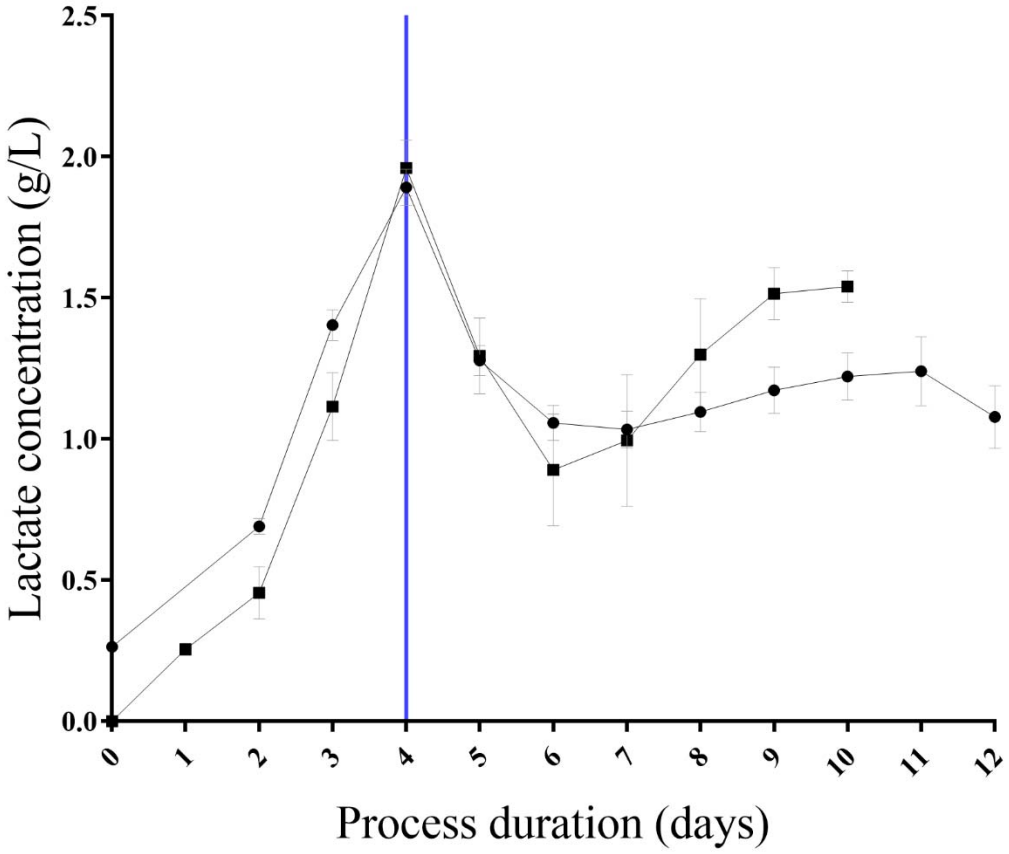

Figure 30 Measured lactate of perfusion vessels operated at micro and bench scale over process duration (days)
Lactate concentration (g/L) of perfusion vessels. Lactate concentration is plotted against process duration (days), (●) and (■) represent micro (n=9) and bench (n=2) scale vessels, respectively. Perfusion initiation is indicated with an intersecting blue line

Observed lactate concentration within vessels begun at concentrations >0.3g/L for both micro and bench scale systems. During the initial batch period, an inverse relationship was observed between glucose and lactate levels. The concentrations of glucose are observed gradually depleting from initial starting points of (4.19±0.04) and (4.59±0.15) g/L, respectively.

Lactate concentrations within the cultures are seen to increase to a maximum of (1.89±0.06) and (1.96±0.10) g/L, respectively. Following this maximum, and the initiation of perfusion, lactate concentrations were observed to reduce, establishing homeostasis between 1 and 1.5 g/L. Measured lactate concentration at culture transition is (1.08±0.11) and (1.54±0.06) g/L for micro and bench scale vessels, respectively.

The metabolic demand that drives these changes in measured glucose and lactate places pressure on control systems associated with maintaining process setpoints, namely dissolved oxygen percentage and pH.

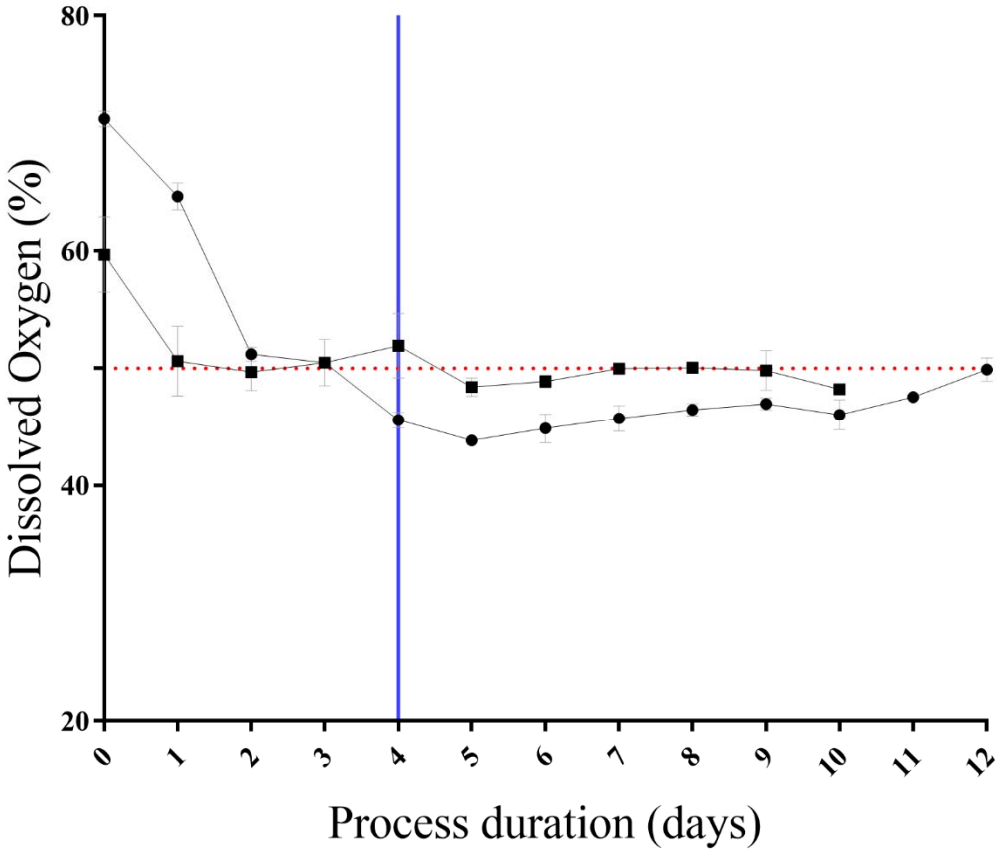

Figure 31 Dissolved oxygen (%) of perfusion vessels operated at micro and bench scale over process duration (days)
Dissolved oxygen (%) of n-1 perfusion vessels in preparation of inoculum for hybrid process production vessels. Dissolved oxygen is plotted against process duration (days), (●) and (■) represent micro (n=9) and bench (n=2) scale vessels, respectively. Values for microscale vessels are averaged over 24 hour periods to provide representative values incorporating cell setting. Perfusion initiation is indicated with an intersecting blue line.

Following inoculation, where oxygen saturation is elevated within vessels, cellular demand for oxygen quickly brought saturation towards the controlled 50% threshold (as indicated by the dashed red line, Figure 31), by day 1 and 2 for bench and microscale respectively.

Dissolved oxygen was maintained above 43% saturation for all cultures throughout the perfusion step, with cellular demand never exceeding supply. The cumulative impact of the micro scale cell settling retention protocol on average oxygen saturation is represented in Figure 31 with a consistently lower oxygen saturation observed for the micro scale cultures when compared to the bench scale cultures.

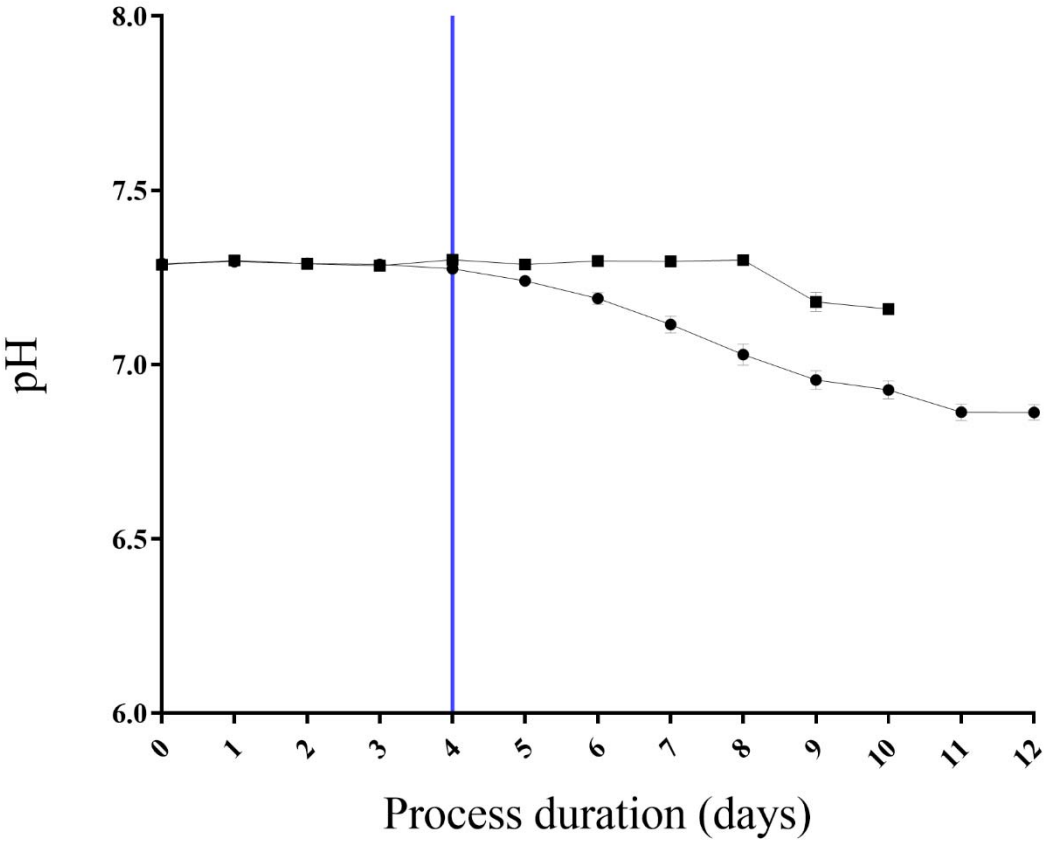

Figure 32 The pH of perfusion vessels operated at micro and bench scale over process duration (days)
pH is plotted against process duration (days), (●) and (■) represent micro (n=9) and bench (n=2) scale vessels, respectively. Values for microscale vessels are averaged over 24 hour periods to provide representative values incorporating cell setting. Perfusion initiation is indicated with an intersecting blue line.

At inoculation, pH was accurately controlled to pH 7.2±0.1 with the utility of sparged CO_2 preventing elevation above 7.3. This control strategy was maintained through to the point of perfusion initiation on day four. On day 4, a deviation in pH for micro and bench scale cultures was presented.

In accordance with data presented in Figure 31, lower averaged pH measurements for microscale vessels were caused by the low culture pH experienced during the method of cell retention. However, declines in pH were observed for both micro and bench scale cultures, as they progressed towards transition.

This was highlighted by a decrease in culture pH, presented between days five and 12 post inoculation in the micro scale vessels where monitored pH is seen to decrease from (7.24±0.01) to (6.86±0.02), respectively. In bench scale it appeared that the culture impact on process control is suppressed and a pH decline is not experienced until nine days post inoculation, where a decline from (7.30±0.00) to (7.16±0.02) is initiated.

4.3.1.2 Production Culture

The perfusion cultures reached the target cell density (40 x10^6 cells/mL) on days 10 and 12 for bench and micro scale vessels, respectively. Following this, the inoculation of production cultures was conducted (see, Section 4.2.1 Transition of Cultures From Perfusion to Production).

The successful inoculation of the production vessels at micro scale was highlighted by the maintenance of high viability in the pooled cultures and post inoculation production culture cell counts.

Measured viability of pooled cultures prior to microscale transition was (94.5±1.7) % and post inoculation the from cell counts on days 0, 1 and 2 post inoculation were (92.7±1.5), (91.1±1.9) and (91.2±2.2), respectively. The breakdown of percentage viability for 1x and 2x feed conditions are provided in Figure 33 and Figure 41, respectively. This maintenance of viability over the initial culture period represented a successful transition from perfusion to production vessels at micro scale.

Viability of bench scale vessels prior to transition was (98.1±0.7) % and those post inoculation from cell counts on days 0, 1 and 2 were (97.2±0.7), (97.6±0.6) and (96.9±1.0), respectively. This maintained viability over the initial culture period also represented a successful transition from perfusion to production vessels for bench scale. Analysis of viability progression throughout bench scale production cultures is provided in Figure 50.

4.3.1.2.1 The 1x Feed Condition in Microscale Production Culture

Viability measurements from microscale vessels operated in the 1x feed condition were stable up to day four for all seeding densities. They are observed to maintain viability from (92.4±2.0) % at inoculation to (89.8±0.4) % on day four (Figure 33).

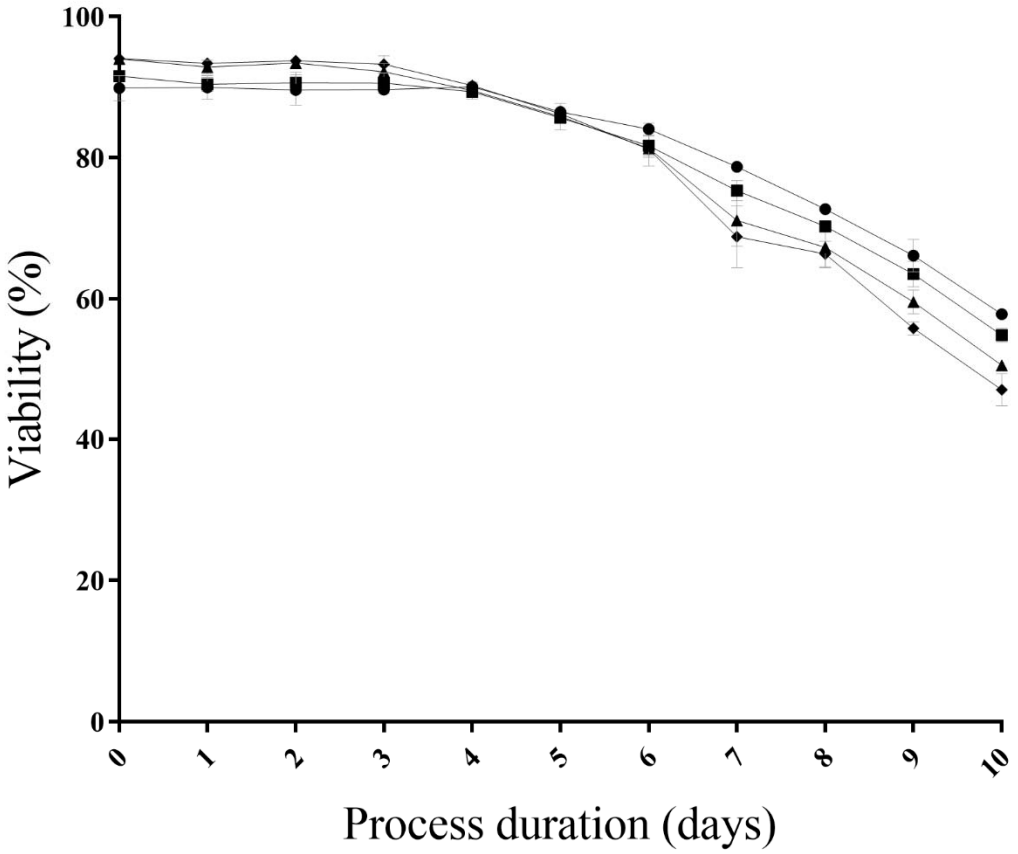

Figure 33 Viability (%) of production phase micro scale vessels operated at incremental seeding densities at the 1x feed condition (Experiment 4.1a)
Viability is plotted against process duration (days); symbols ♦, ▲, ■ and ● represent seeding densities 15, 10, 5 and 2.5 x10^6cells/mL, respectively (n=3 for each).

From day five onwards, a decline in viability (86.1±0.4) was observed. This decline in viability was consistent across all cultures. Whilst all cultures were declining simultaneously towards harvest viability (60%), an inverse relationship was observed between the starting seeding density and the viability. Viability at harvest highlighted this with seeding densities 2.5, 5, 10 and 15 x10^6 cells/mL presenting viabilities of (57.9±0.5), (54.9±1.0), (50.6±0.8) and (47.1±2.3) %, respectively.

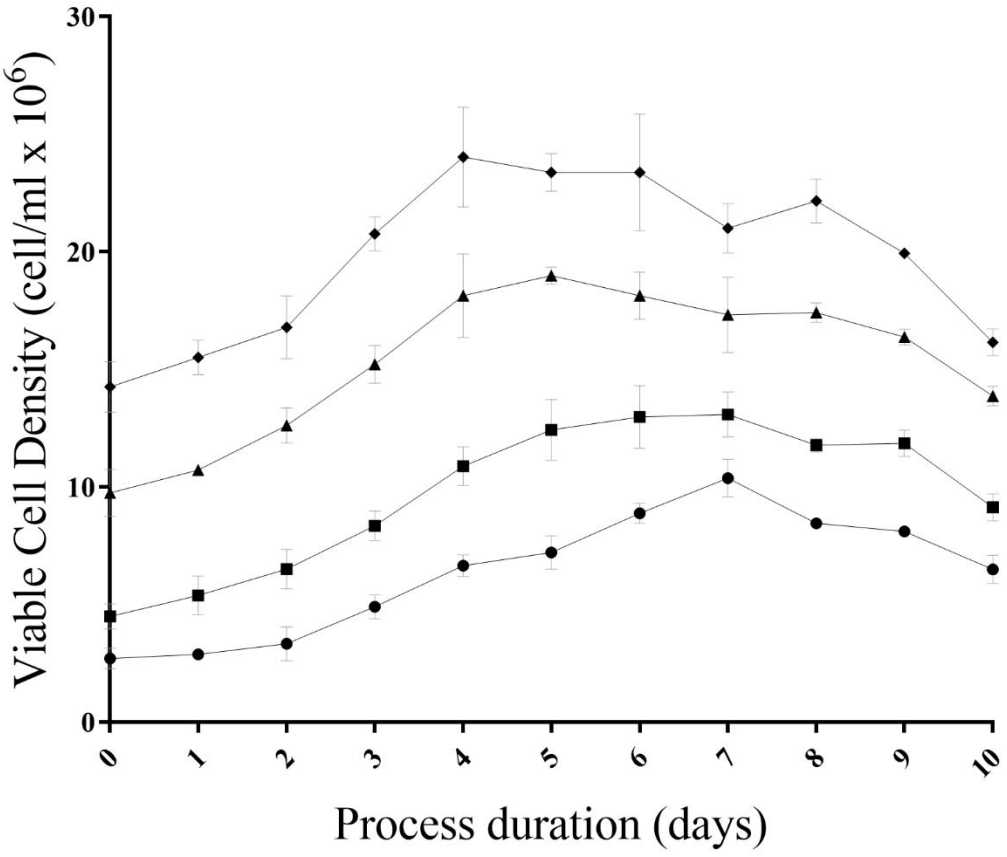

Figure 34 Viable cell density (cells/mL x 106) of production phase micro scale vessels operated at incremental seeding densities at the 1x feed condition (Experiment 4.1a)
Viable cell density is plotted against process duration (days); symbols ♦, ▲, ■ and ● represent seeding densities 15, 10, 5 and 2.5 x10^6cells/mL, respectively (n=3 for each).

Following the inoculation of production microscale vessels in the 1x feed condition, exponential growth was successfully established (Figure 34). All cultures progressed towards a transition into a stationary phase between days four and seven. This transition was highlighted by peak viable cell density, observed to correlate to the magnitude of seeding density. The peak viable cell density was (10.37±0.80), (13.89±0.96), (18.99±0.36) and (24.03±2.13) x10^6cells/mL, for conditions 2.5, 5, 10 and 15 x10^6 cells/mL, respectively.

Following the peak viable cell density, an accelerating decline in cell viability was observed. Cultures were observed to decline to harvest criteria (<60% viability) at day 10 post inoculation (Figure 33). Analysis of the viable cell density profiles highlighted statistically significant increases in performance correlating to increases in seeding density (P-values<0.05 for each respective paired combination).

Routine at-line monitoring of culture glucose and lactate concentrations are presented in Figure 35 and Figure 36, respectively.

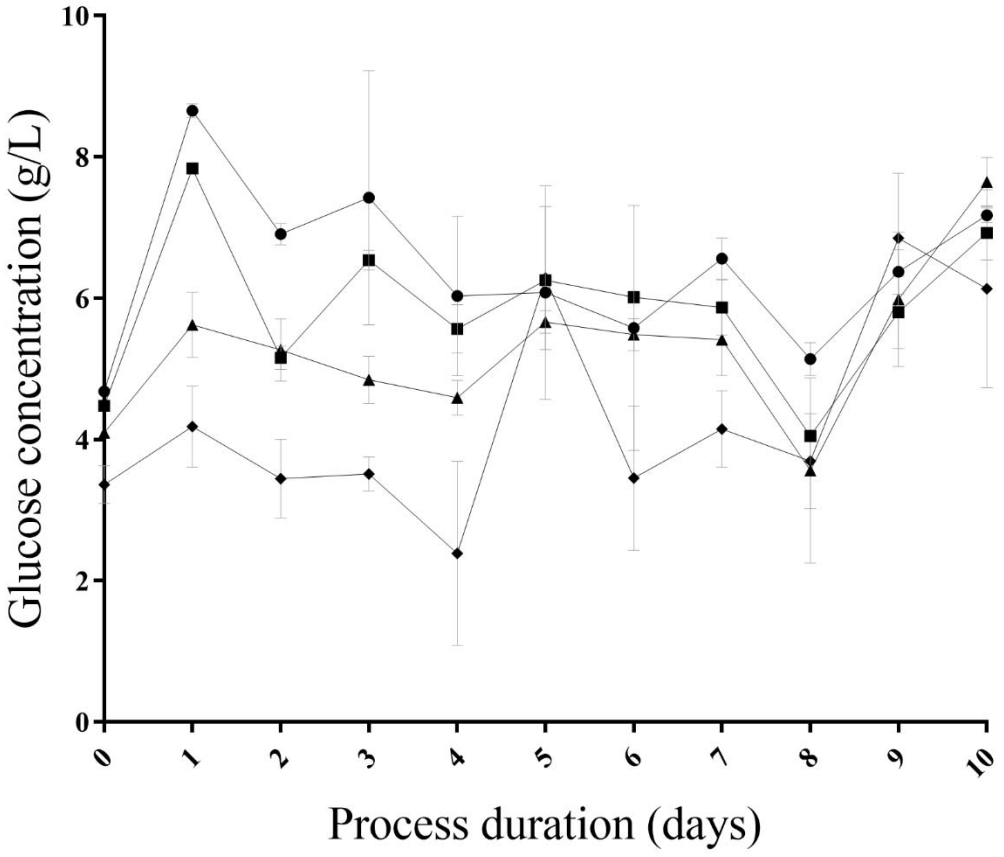

Figure 35 Glucose concentration (g/L) of production phase micro scale vessels operated at incremental seeding densities at the 1x feed condition (Experiment 4.1a)
Glucose g/L plotted against process duration (days); symbols ♦, ▲, ■ and ● represent seeding densities 15, 10, 5 and 2.5 x10^6cells/mL, respectively (n=3 for each).

A concentrated glucose stock (500g/L) is fed back into the cultures on demand, the profile presented (Figure 35) reflects the accuracy of operation and ability of the control system to maintain the glucose concentration within the cultures.

Glucose concentration was observed to be accurately controlled within the design parameters throughout the process with the following exceptions. Glucose concentration slightly exceeded 8g/L in the 2.5 x10^6cells/mL seed density culture on day one, the value recorded was (8.7±0.1) g/L. Glucose concentration was observed to drop below 2g/L on day four for triplicate cultures in the 15 x10^6cells/mL seed density condition, leading to an average value of (2.4±1.3) g/L. These high and low glucose concentrations were examples of the highest and lowest culture glucose demands, correlating with viable cell density (Figure 34) and were consistent glucose consumption rates (Figure 37, below).

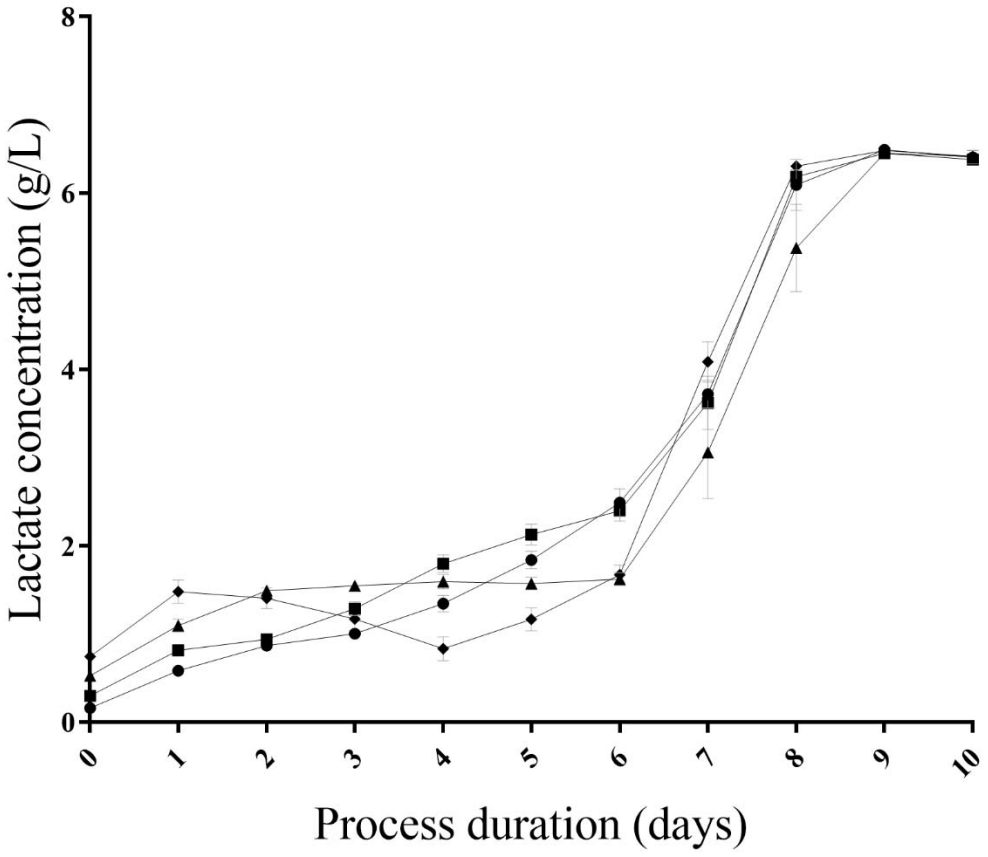

Figure 36 Lactate concentration (g/L) of production phase micro scale vessels operated at incremental seeding densities at the 1x feed condition (Experiment 4.1a)
Lactate (g/L) plotted against process duration (days); symbols ♦, ▲, ■ and ● represent seeding densities 15, 10, 5 and 2.5 x10^6cells/mL, respectively (n=3 for each).

The trend of lactate concentration over the culture duration represented a sigmoidal fashion, whereby residual lactate levels increase slowly over the first six days of culture, from a starting concentration of (0.4±0.3) g/L at inoculation, to (2.1±0.5) g/L on day 6 post inoculation (Figure 36).

Lactate concentrations are then observed to triple, increasing to (6.0±0.4) g/L by day eight. Following this sharp increase in concentration, lactate levels plateau over the final days of culture, (6.5±0.02) and (6.4±0.02) g/L for days nine and ten, respectively. These changes in lactate concentration can be indicative of the cellular processing of available glucose (presented earlier, Section 3.4.5 Biochemical Analysis).

The calculation of cell specific consumption rates for glucose (Figure 37) and lactate (Figure 38) within the cultures takes into account the glucose added to maintain the controlled process range, the measured concentration, and the viable cell density between daily measurements.

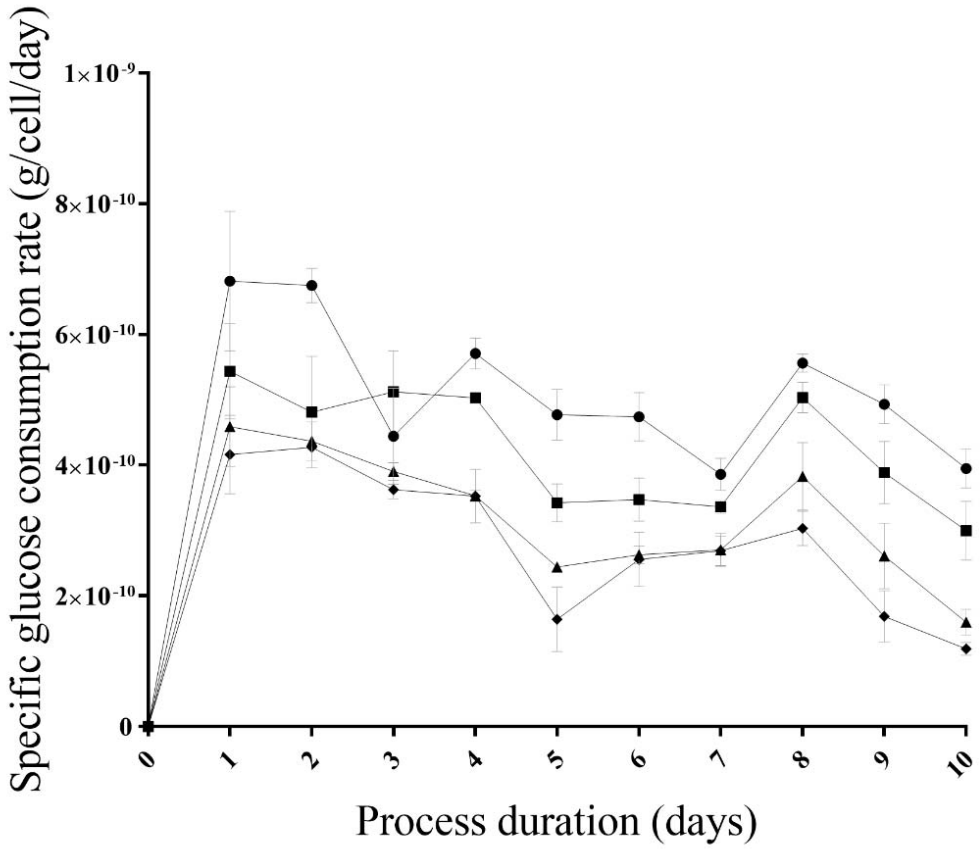

Figure 37 Cell specific glucose consumption rate (g/cell/day) of production phase micro scale vessels operated at incremental seeding densities at the 1x feed condition (Experiment 4.1a)
Glucose consumption (g/cell/day) plotted against process duration (days); symbols ♦, ▲, ■ and ● represent seeding densities 15, 10, 5 and 2.5 x10^6cells/mL, respectively (n=3 for each).

On the first day of culture, the rates of glucose consumption reached peaks of (6.8±1.1), (5.4±0.7), (4.6±0.6) and (4.2±0.6) x10^{-10} g/cell/day for seeding densities 2.5, 5, 10 and 15 x10^6cells/mL, respectively (Figure 37).

Whilst fluctuations occurred in the consumption rates throughout the cultures, this elevated level was maintained up to day eight post inoculation, where an average of (4.4±1.2) x10^{-10} g/cell/day was observed across all seeding densities. Following day eight, consecutive declines in average glucose consumption rates in-line with a decrease in culture viability were observed (Figure 33). The average glucose consumption rate on days nine and ten was (3.3±1.4) and (2.4±1.3) x10^{-10} g/cell/day, respectively.

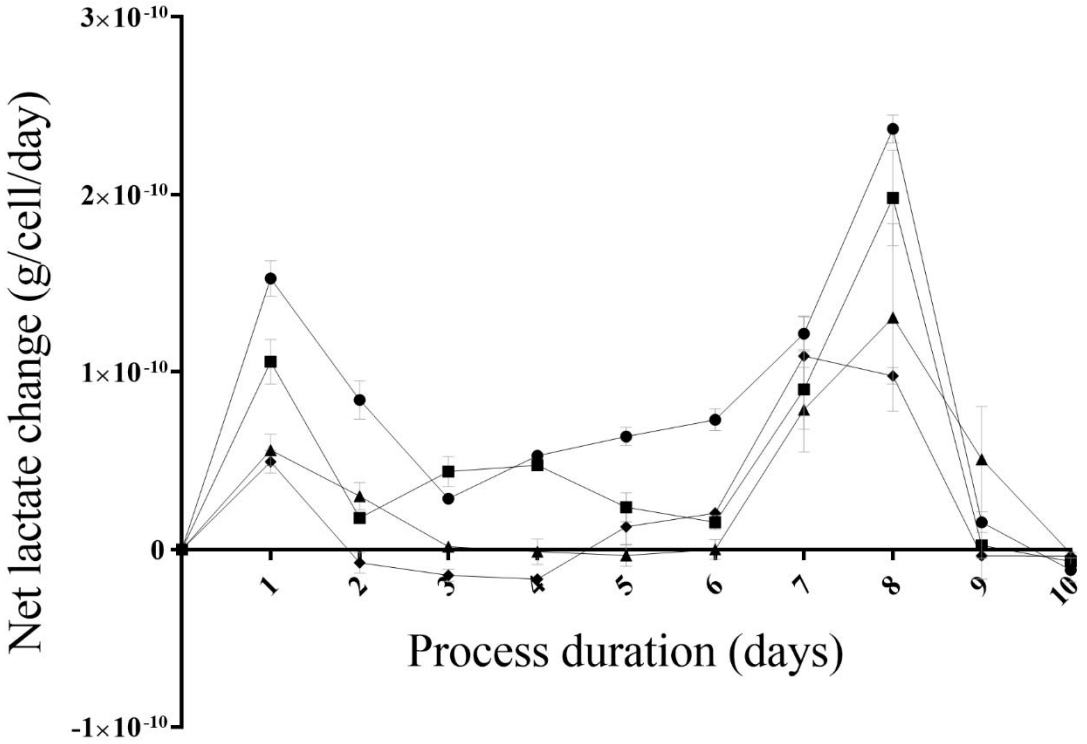

Figure 38 Cell specific net lactate change (g/cell/day) of production phase micro scale vessels operated at incremental seeding densities at the 1x feed condition (Experiment 4.1a)
Cell specific net lactate change (g/cell/day) is plotted against process duration (days); symbols ♦, ▲, ■ and ● represent seeding densities 15, 10, 5 and 2.5 x10^{6}cells/mL, respectively (n=3 for each).

The cell specific net lactate change represents the simultaneous lactate production and consumption occurring in the microscale cultures (Figure 38). There were two defined peaks presented in the positive net change in specific lactate rates, with the first occurring on day one.

The calculated rates at the first peak are (1.5±0.1), (1.1±0.1), (0.6±0.1) and (0.5±0.1) x10^{-10} g/cell/day for seeding densities 2.5, 5, 10 and 15 x10^{6}cells/mL, respectively. Following the first peak, the cell specific net lactate change rates were observed to decrease. The rates were observed to be low until day six of culture. On day six, the rates for all cultures increased towards the second peak on day eight.

The other culture biochemical monitoring and control was the pH and dissolved oxygen saturation. No deviation from the control range (pH 7.2±0.1) was observed between seeding densities in the 1x feeding condition. The residual lactate present in vessels (Figure 36) resulted in the pH trending towards the bottom of the control range for the duration of the culture. This maintenance was achieved through the addition of sodium bicarbonate.

Similarly, the agitation and O_2 sparging on demand maintained the dissolved oxygen level at 50% of the saturation point.

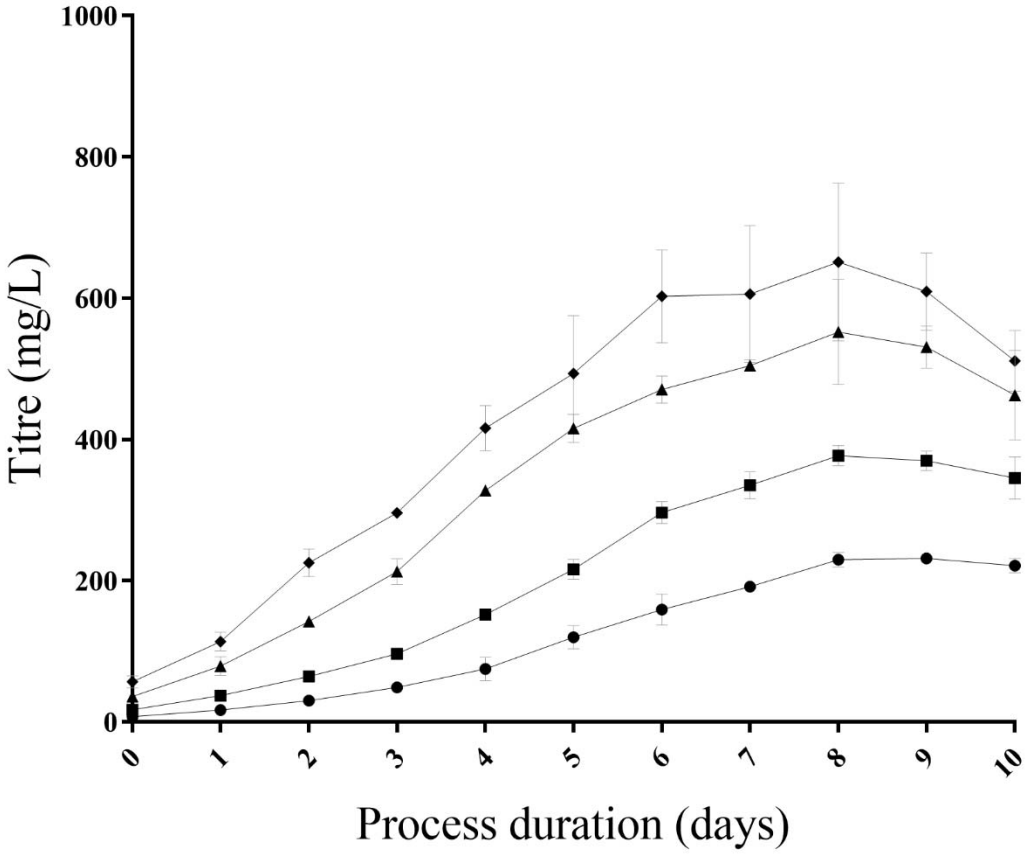

Figure 39 Titre (mg/L) representing the process performance of production phase micro scale vessels at 1x feed condition (Experiment 4.1a)
Titre plotted against process duration (days); symbols ♦, ▲, ■ and ● represent seeding densities 15, 10, 5 and 2.5 x10^6cells/mL, respectively (n=3 for each).

Measurements for mAb concentration (Titre) increased over time in line with viable cell density (Figure 34), peaking at day 8 post inoculation (Figure 39). Peak titre values were (230.0±10.2), (377.0±14.2), (552.0±74.5) and (651.3±111.7) for seeding densities 2.5, 5, 10 and 15 x 10^6cells/mL, respectively.

This stepwise increase in titre and correlation with viable cell density results in the maintenance of calculated cell specific productivity across seeding densities (Figure 40, below).

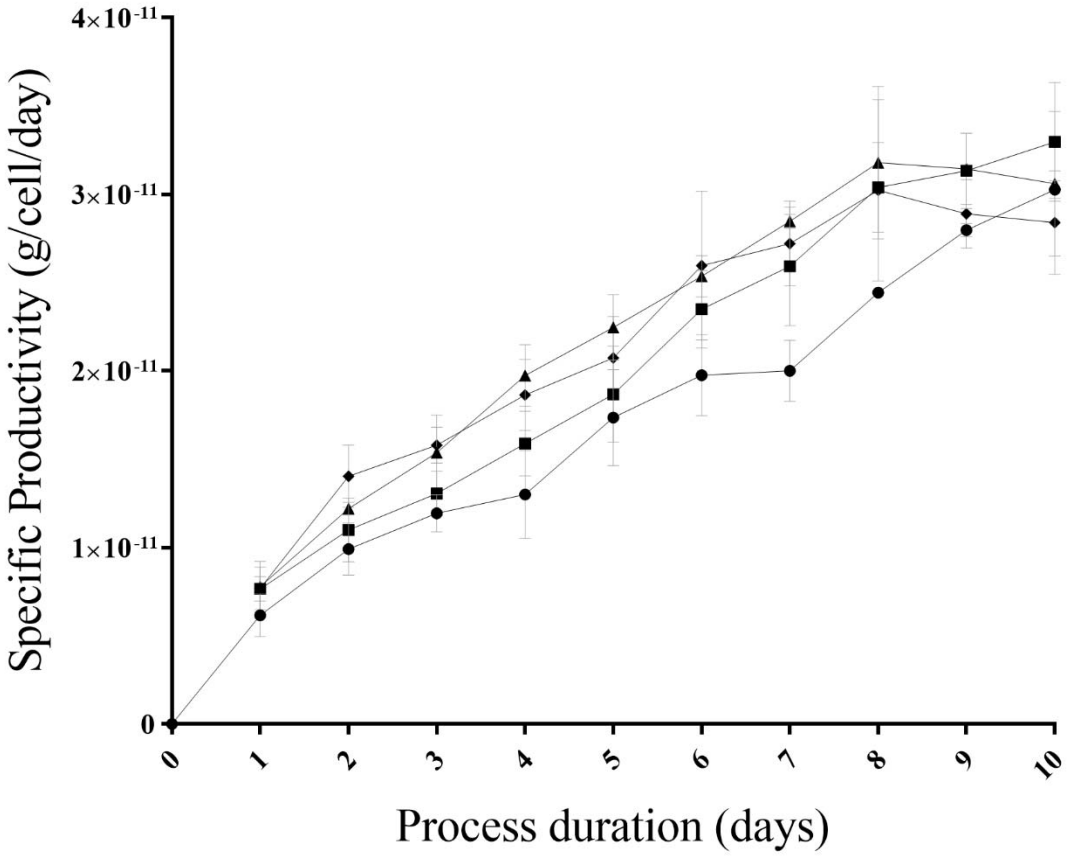

Figure 40 Cell specific productivity (g/cell/day) representing the process performance of production phase micro scale vessels at 1x feed condition (Experiment 4.1a)
Cell specific productivity (g/cell/day) plotted against process duration (days); symbols ♦, ▲, ■ and ● represent seeding densities 15, 10, 5 and 2.5 x10^{6}cells/mL, respectively (n=3 for each).

The cell specific productivity experienced was consistent across seeding densities 5, 10, and 15 x10^6 cells/mL. Variation was observed in the cell specific productivity for the 2.5 x10^6 cells/mL seeding condition. This is highlighted by a suppressed rate present on day eight of culture. The peak average cell specific productivity for all cultures was (3.1±0.3) x10^{11} g/cell/day, on day 10.

Table 4 Percentage monomer post Protein A purification of microscale cultures at 1x feed condition

Seeding Density (x10^6 cells/ml)	Monomer (%)
2.5	(96.6±0.5)
5	(97.0±0.1)
10	(97.3±0.6)
15	(97.1±0.2)

The product quality of the mAb expressed from Cell line 1 was not observed to be impacted by seeding density in the 1x feed condition. Monomer percentage observed post Protein A purification was greater than 96% for all dilution rate cultures (Table 4)

4.3.1.2.2 The 2x Feed Condition in Microscale Production Culture

The 1x and 2x feed condition microscale cultures were inoculated simultaneously from the same high cell density pooled culture.

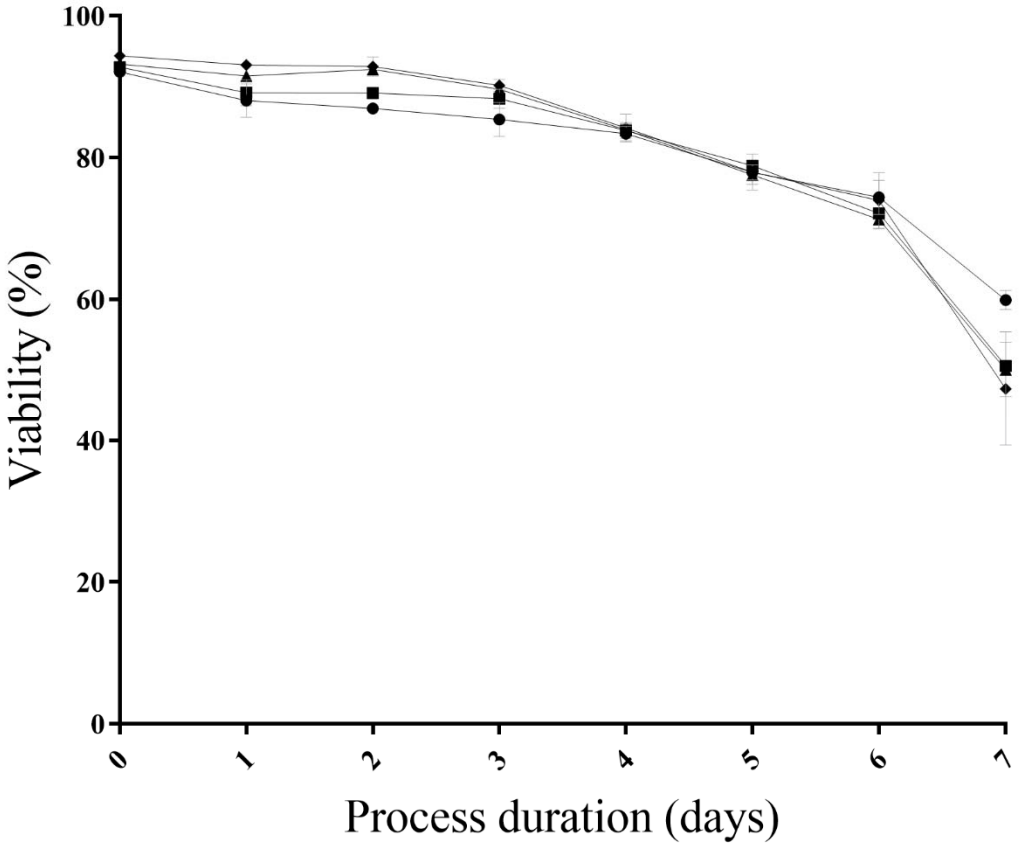

Figure 41 Viability (%) representing the process performance of production phase micro scale vessels at 2x feed condition (Experiment 4.1a)
Viability (%) plotted against process duration (days); symbols ♦, ▲, ■ and ● represent seeding densities 15, 10, 5 and 2.5 x10^6cells/mL, respectively (n=3 for each).

High culture viabilities were observed at inoculation, (92.1±0.7), (92.8±0.0), (93.3±0.5) and (94.4±0.6) reported for seeding densities 2.5, 5, 10 and 15 x10^6 cells/mL, respectively (Figure 41). This high viability was not maintained and a decrease in viability was observed on day one of culture. The decline in culture viability was observed and continued in all seeding density conditions as cultures progressed. Culture viability declined below the harvest criteria (<60%) on day seven in all cultures. Therefore, the process duration for the 2x feed condition

was three days shorter than that experiences for the 1x feed condition, seven days and ten days, respectively.

Viable cell concentrations indicated a deviation in performance from the 1x condition as early as day one of culture (Figure 42). Cultures seeded at the lower seeding densities had lower viable cell concentrations on day one post inoculation than their counts at inoculation, (2.32±0.40) to (2.21±0.11), and (4.59±0.47) to (4.26±0.37), for 2.5 and 5 x10^6 cell/mL target seeding densities, respectively.

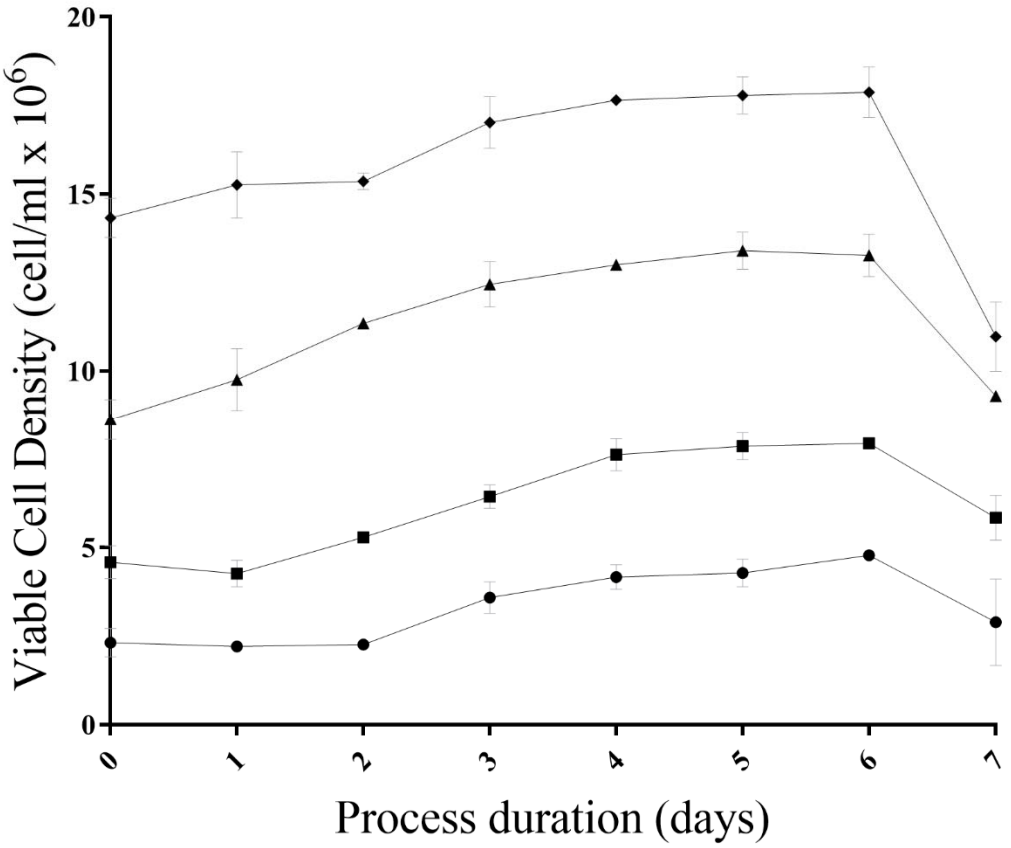

Figure 42 Viable cell density representing the process performance of production phase micro scale vessels at 2x feed condition (Experiment 4.1a)
Viable cell density plotted against process duration (days); symbols ♦, ▲, ■ and ● represent seeding densities 15, 10, 5 and 2.5 x10^6cells/mL, respectively (n=3 for each)

Following this lag period of approximately two days, cultures appeared to return to growth. An exponential growth phase was not observed for any 2x feed condition cultures, and they entered a stationary phase where viable cell densities gradually peaked on day six. The observed peak viable cell densities were (4.8±0.1), (7.9±0.03), (13.3±0.6) and (17.9±0.7) for seeding densities 2.5, 5, 10, and 15, respectively.

The difference in average growth profiles was observed to significantly increase (p-value < 0.05) in line with seeding density, as was experienced in the 1x condition. All cultures experienced a decrease in viable cell density on day seven and were harvested as the culture viability harvest criteria was achieved.

Comparative viable cell density observed up to day seven of cultures represented statistically significant decreases (p-value < 0.05) across all 2x condition cultures when paired to equivalent seeding densities in the 1x feed condition.

Throughout the production cultures, glucose concentrations were accurately controlled above 2g/L and never dropped into a glucose-limited environment (Figure 43).

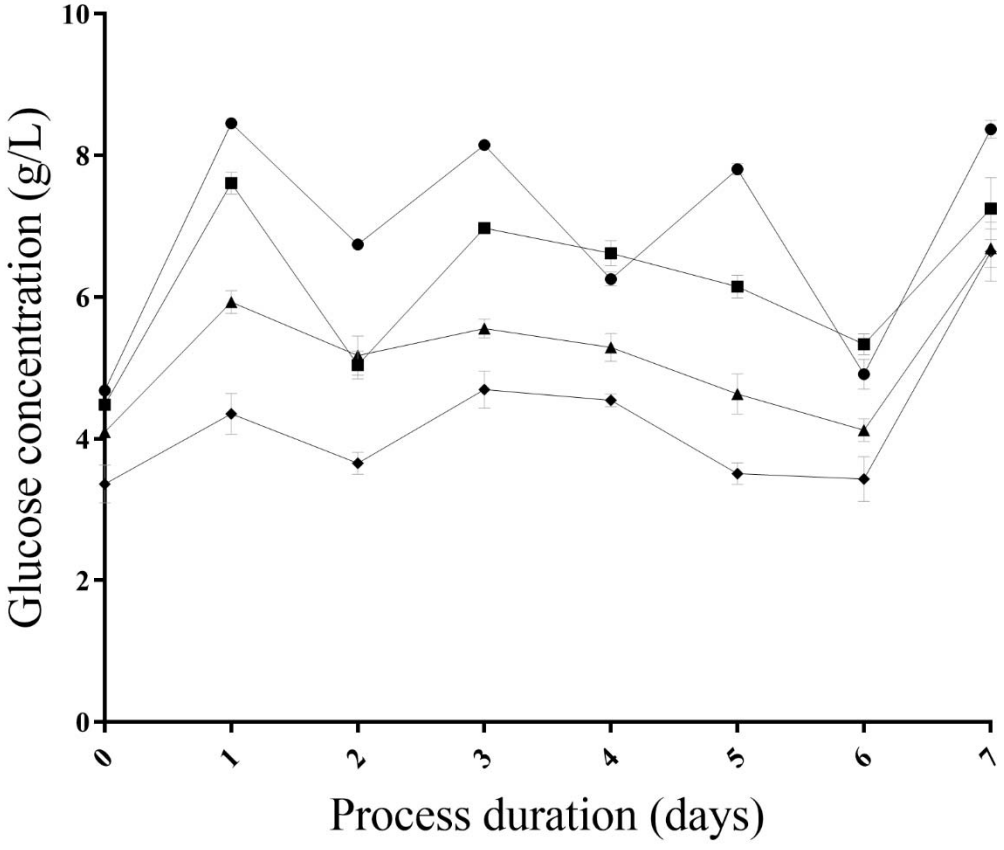

Figure 43 Glucose concentration (g/L) representing the process performance of production phase micro scale vessels at 2x feed condition (Experiment 4.1a)
Glucose concentration (g/L) is plotted against process duration (days); symbols ♦, ▲, ■ and ● represent seeding densities 15, 10, 5 and 2.5 x10^6cells/mL, respectively (n=3 for each).

The glucose monitoring standard deviations in the 2x condition were visibly lower at each data point than those observed in the 1x feed condition. Cellular content of the 2x condition (Figure 42) was lower for respective cultures in the 2x condition and resulted in a lower demand being placed on the feeding of glucose back into the system to reach maintenance concentrations.

The measured glucose concentrations were representative of the highest and lowest culture glucose demands, correlating with an inverse relationship with cellular density (and seeding density, Figure 42) assuming constant cell specific glucose consumption rates.

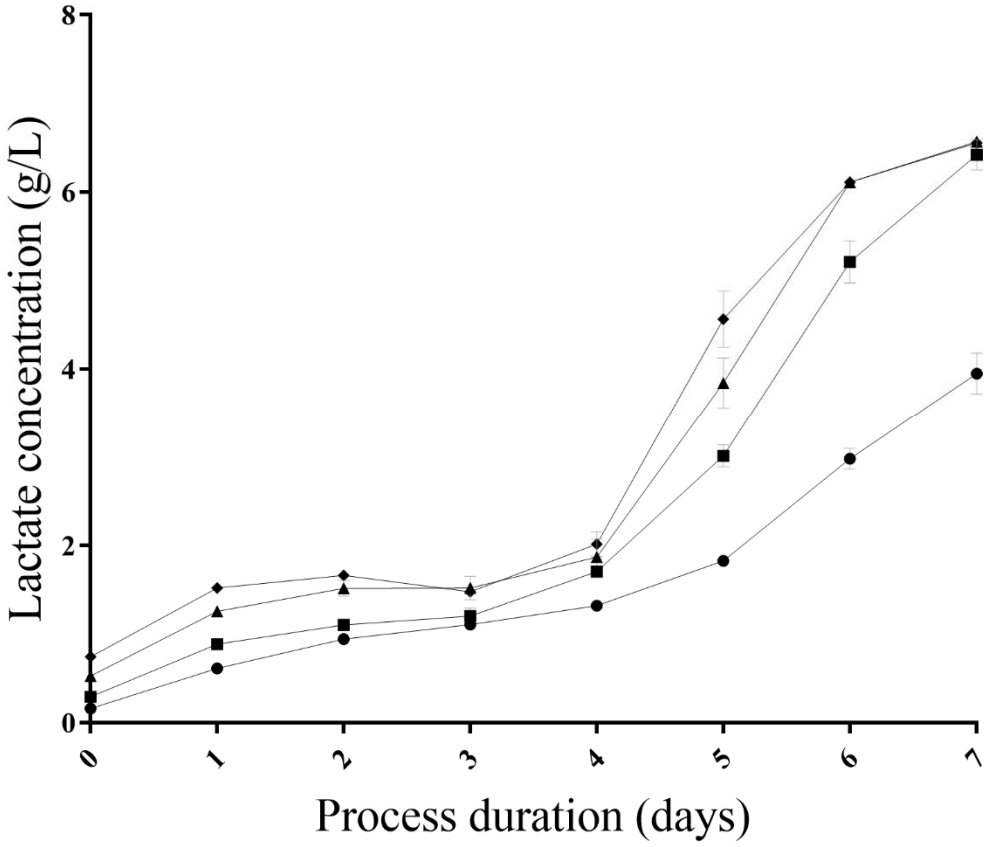

Figure 44 Lactate concentration (g/L) representing the process performance of production phase micro scale vessels at 2x feed condition (Experiment 4.1a)
Lactate concentration (g/L) is plotted against process duration (days); symbols ♦, ▲, ■ and ● represent seeding densities 15, 10, 5 and 2.5 x10^6cells/mL, respectively (n=3 for each).

The lactate concentrations began at <1g/L for all seeding densities within the microscale 2x feed condition at inoculation. During the first four days of culture, these levels slowly increased for all cultures, towards but remaining below 2g/L.

Between days four and seven, the concentrations of lactate within cultures increased. The lactate concentrations for seeding densities 5, 10, and 15 x10^6cells/mL increased from <2g/L to >6g/L on days four and six, respectively. Similarities are drawn between these profiles and those presented in the 1x feed condition with a peak concentration being reached at culture harvest, where viability is low.

An outlier was observed in the 2 x10^6 seeding density culture, whereby lactate concentrations reached (3.95±0.23) g/L at harvest. The lower cell concentration and poor growth of this condition (Figure 42) were thought to partially contribute to this presentation.

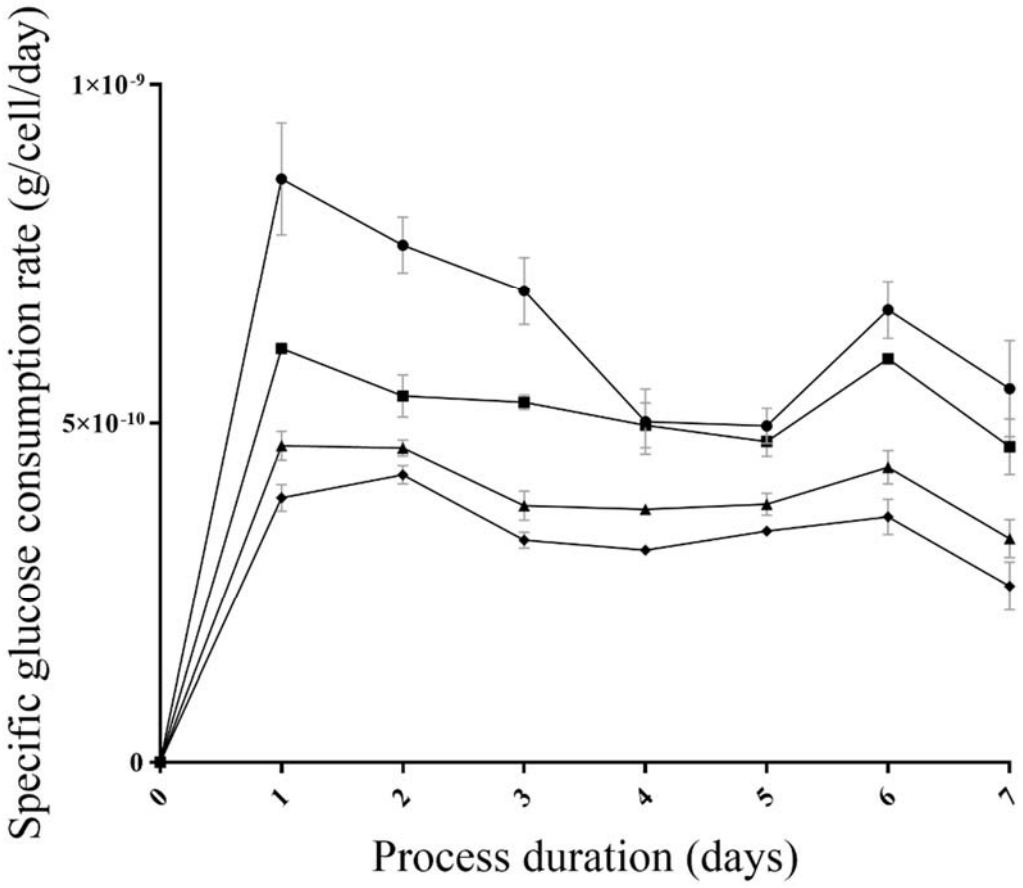

Figure 45 Cell specific glucose consumption rate (g/cell/day)
Glucose consumption rate (g/cell/day) is plotted against process duration (days); symbols ♦, ▲, ■ and ● represent seeding densities 15, 10, 5 and 2.5 x10^6cells/mL, respectively (n=3 for each).

The cell specific glucose consumption rate is presented in Figure 45. On the first day post inoculation the rates for seeding densities 2.5, 5, 10 and 15 x10^6cells/mL, were (8.6±0.8), (6.3±0.3), (4.7±0.2) and (3.9±0.2) x10^{-10} g/cell/day, respectively. The order of highest to lowest cell specific glucose consumption rates was maintained from the first day post inoculation through to harvest. Whilst variation existed in cell specific consumption rates, this decreased as cultures progressed and on day 5 post inoculation, the average across all seeding densities was (4.2±0.7) x10^{-10} g/cell/day.

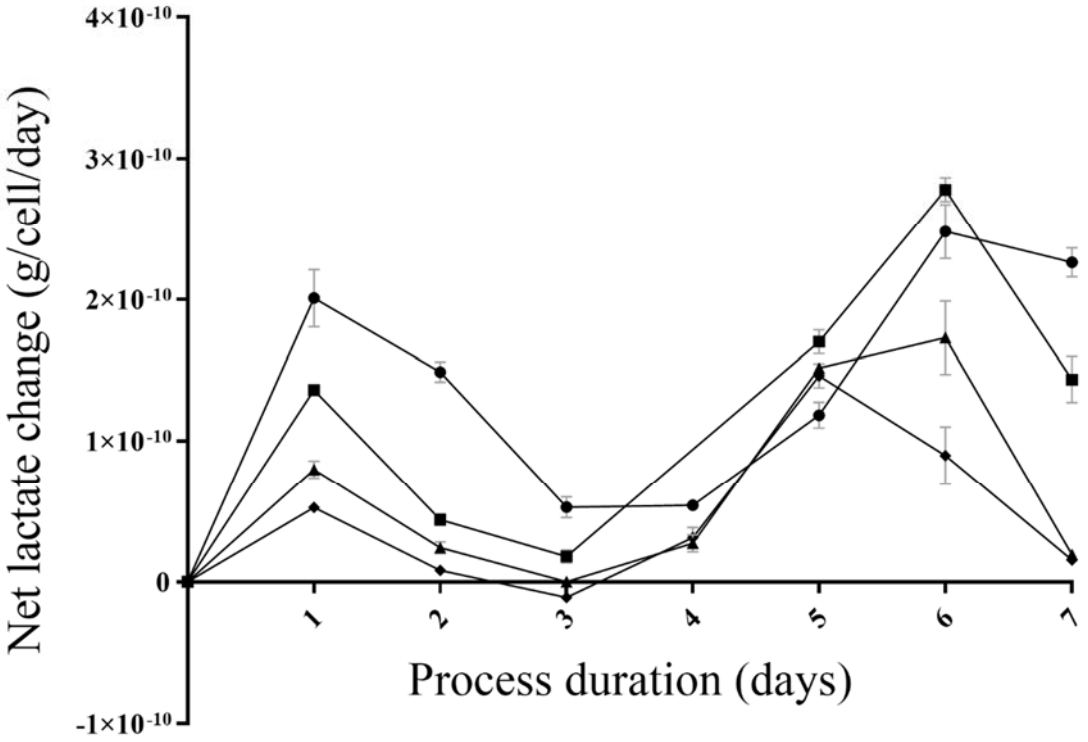

Figure 46 Cell specific net lactate change (g/cell/day) representing the process performance of production phase micro scale vessels at 2x feed condition (Experiment 4.1a)
Cell specific net lactate change (g/cell/day) is plotted against process duration (days); symbols ♦, ▲, ■ and ● represent seeding densities 15, 10, 5 and 2.5 x10^{6}cells/mL, respectively (n=3 for each).

Whilst not possible to observe exact rates of production or consumption as they occur simultaneously within the culture, the net change is presented in the daily lactate measurements (Figure 44)

An initial peak in cell specific net lactate change was calculated, with values of (2.0±0.2), (1.4±0.03), (0.8±0.06) and (0.5±0.03) x10^{-10} g/cell/day for seeding densities 2.5, 5, 10 and 15 x10^{6}cells/mL, respectively (Figure 46). This cell specific rate on day one decreased as the culture progressed and on day 3 the cell specific rate had declined to between (0.5±0.07) and (-0.1±0.03), for seeding densities 2.5 and 15 x10^{6}cells/mL, respectively.

The lactate concentrations for all cultures peaked in the final few days of culture (Figure 44), this change was represented in the cell specific net lactate change, with values increasing up to day six post inoculation and becoming depressed on the final day of culture, as cellular activity began to decrease in line with falling viability (Figure 41).

pH control, as previously outlined for the 1x feed condition, was maintained within the process limits of 7.2±0.1. Given the high lactate concentration experienced in both the 1x and 2x

conditions, the pH was controlled along the bottom of this process limit through the addition of sodium bicarbonate, on demand.

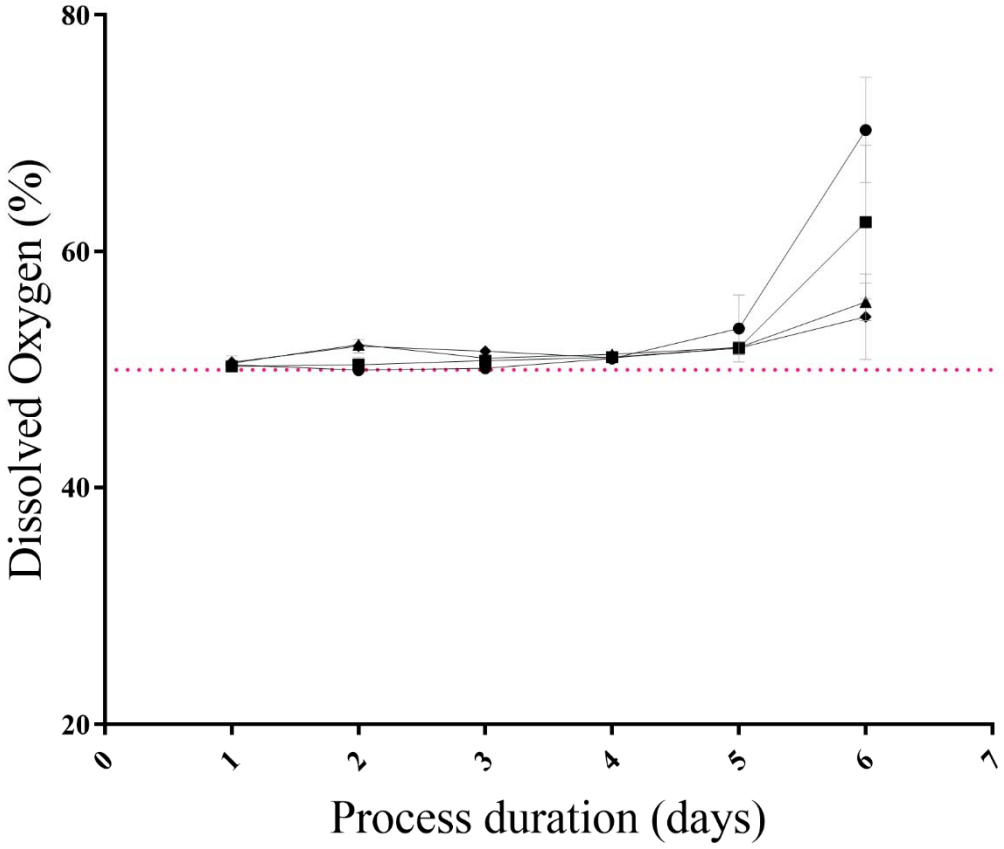

Figure 47 Dissolved oxygen (%) representing the process performance of production phase micro scale vessels at 2x feed condition (Experiment 4.1a)
DO plotted against process duration (days); symbols ♦, ▲, ■ and ● represent seeding densities 15, 10, 5 and 2.5 x106cells/mL, respectively (n=3 for each).

The observed dissolved oxygen saturation was well maintained at or above the 50% level throughout the 2x condition cultures (Figure 47). These profiles were observed to increase towards the last days of culture, with values >70% experienced on day six for the 2.5 x10^6 cells/mL seeding density culture. This increase in the final days can be representative of the declining culture viability (Figure 41) and, in turn, lower oxygen demand.

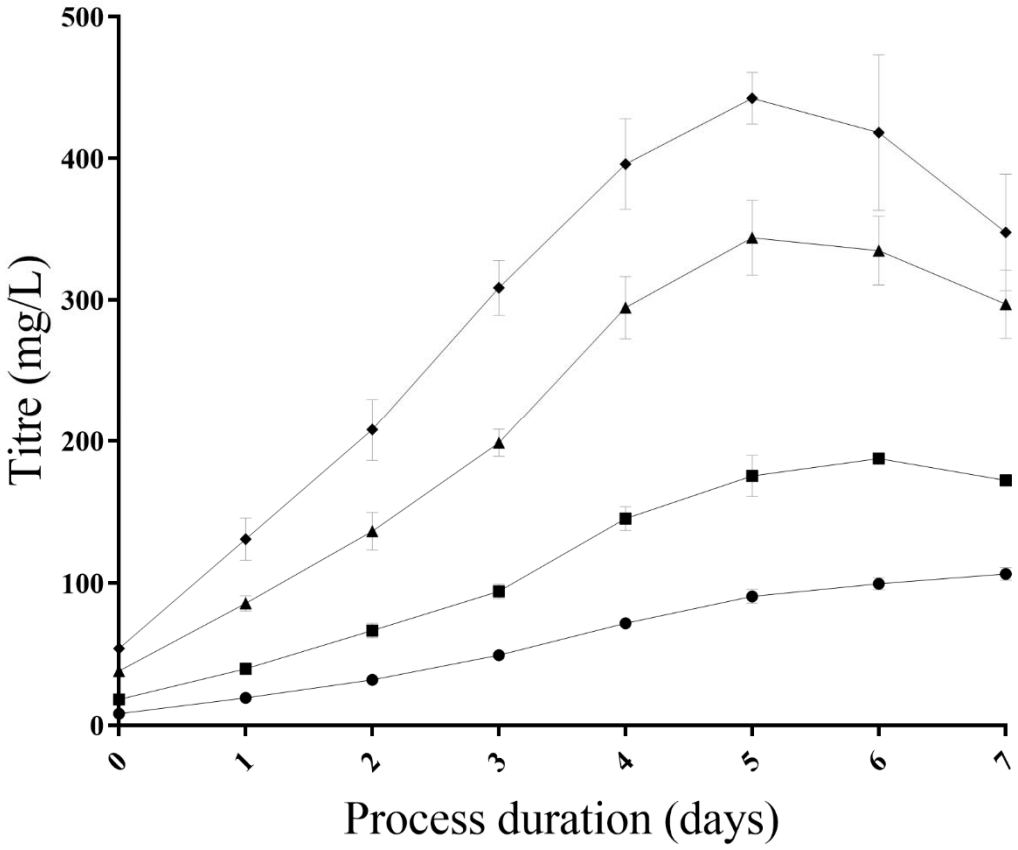

Figure 48 Titre (mg/L) representing the process performance of production phase micro scale vessels at 2x feed condition (Experiment 4.1a)
Titre plotted against process duration (days); symbols ♦, ▲, ■ and ● represent seeding densities 15, 10, 5 and 2.5 x106cells/mL, respectively (n=3 for each).

As experienced previously for the 1x feed condition, the measured mAb concentration was observed to increase as cultures progressed (Figure 48). A separation was observed in the titre measurements between seeding densities within the 2x feed condition. An analysis of the average profiles displayed a significant difference between each respective seeding density. The highest peak within the 2x feed condition was achieved by the 15 x10^6 cell/mL seeding density, where concentration was observed to reach (442±18) mg/L on day five.

A similar profile was observed in the 10 x10^6cell/mL seeding density, whereby a peak was also observed on day five, (344±26) mg/L. In comparison, the cultures of 2.5 and 5 x10^6 cell/mL achieved significantly lower peak titres, with values less than 200 and 100mg/L for conditions 5 and 2.5 x10^6 cells/mL, respectively.

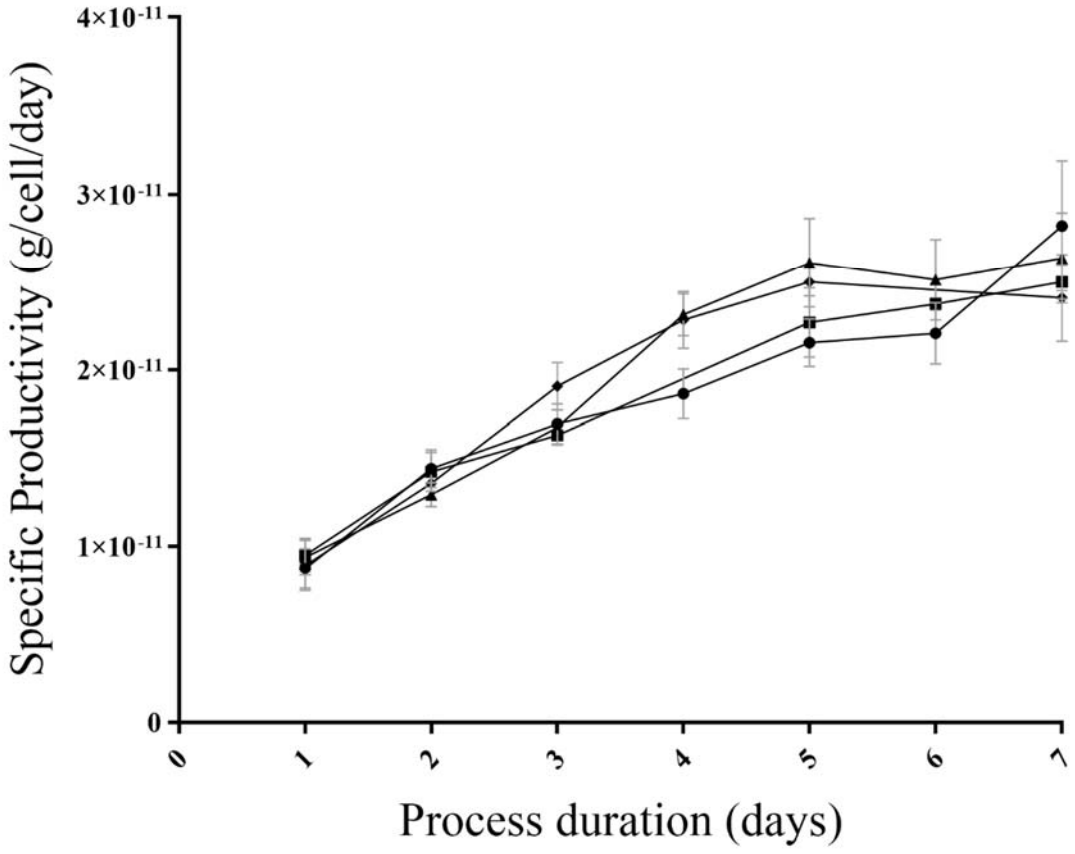

Figure 49 Cell specific productivity (g/cell/day) representing the process performance of production phase micro scale vessels at 2x feed condition (Experiment 4.1a)
Cell specific productivity plotted against process duration (days); symbols ♦, ▲, ■ and ● represent seeding densities 15, 10, 5 and 2.5 x106cells/mL, respectively (n=3 for each).

During the first few days of culture, comparable cell specific productivities were calculated for all cultures, with average productivity (0.9±0.04) and (1.4±0.07) $x10^{-11}$g/cell/day for cultures on days one and two, respectively (Figure 49). As the cultures progressed, lower specific productivity was observed with the lower seeding densities (2.5 and 5 $x10^6$ cells/mL, respectively), when compared to others operated in the 2x feed condition. Average cell specific productivity at harvest was (2.6±0.3) $x10^{-11}$g/cell/day.

Table 5 Percentage monomer post Protein A purification of microscale cultures at 2x feed condition

Seeding Density ($x10^6$ cells/ml)	Monomer (%)
2.5	(97.7±2.1)
5	(87.7±13.6)
10	(96.3±0.2)
15	(96.4±0.0)

The observed monomer percentage was > 96.2 % for three of the four seeding densities evaluated for the 2x condition cultures. The post protein A monomer percentage for the three cultures inoculated at 5 x10^6 cells/ml was 96.82, 95.34, and 71.99 %, respectively. Statistical analysis of all triplicate values reveals no significant differences between any pairs of samples (p-value >0.05).

4.3.1.2.3 Bench Scale Production Cultures

Given the high throughput nature of microscale systems, it was not feasible to conduct an investigation at bench scale that contained the variety and replication of conditions selected in microscale. The conditions conducted at bench scale included (n=2) of seeding densities 2.5 and 10 x10^6 cells/ml, both operated at 1x and 2x feed conditions, respectively.

Unfortunately, a replicate vessel was terminated shortly after inoculation due to equipment failure, and thus the 1x condition inoculated at 2.5 x10^6 cells/mL is reported as n=1.

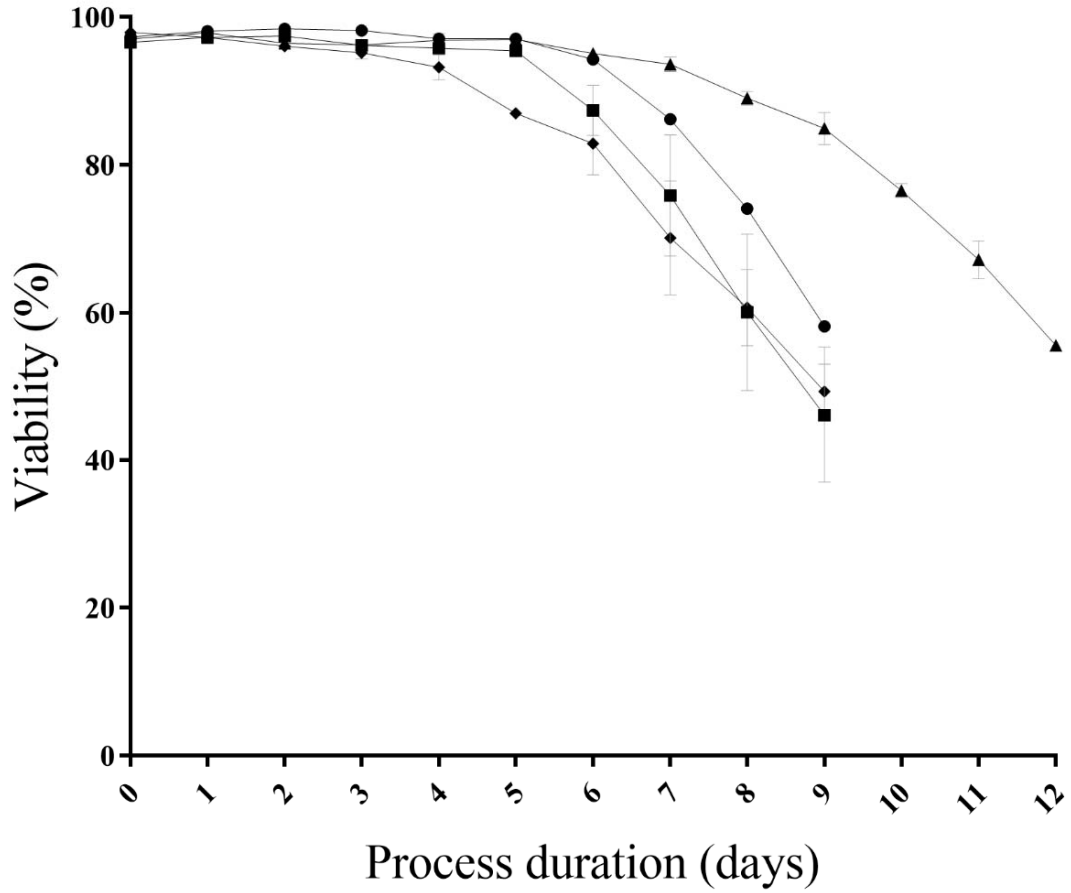

Figure 50 viability representing the process performance of production phase bench scale vessels at 1x and 2x feed condition (Experiment 4.1b)
Viability plotted against process duration (days); symbols, ■, ▲, ♦ and ● represent seeding densities (feed condition); 10 (2x), 10 (1x), 2.5 (2x) and 2.5 (1x) x10^6cells/mL, respectively. (n=2 for each)

The viabilities over the initial few days of the bench scale cultures were maintained above 95% across all conditions (Figure 50). A decline in viability is first observed in the 2x feeding condition, seeding density 2.5 x 10^6cells/mL, where readings of (93.2±1.7) and (87.0±0.0) % were experienced for days four and five, respectively.

This decline in viability was observed in the other 2x feed condition (seeding density 10 x10^6 cells/mL) on day six, where viability of (87.4±3.4) % was recorded. Following this, the 2x feed condition cultures displayed no difference in their rates of decline and reached harvest criteria on day nine.

Cultures operated in the 1x feed condition displayed an improved culture viability profile throughout the experiment. A decline in viability was observed on day seven in the 10 x 10^6cells/mL seeding density condition. The condition still reached harvest criteria on day nine. The performance of cultures seeded at 2.5 x10^6cells/mL, with the 1x feed condition displayed improvement over all other conditions evaluated at bench scale. Not only was the decline in viability initiated later, day eight, but the rate of decline was slower, enabling the culture to remain above the harvest criteria until day 12.

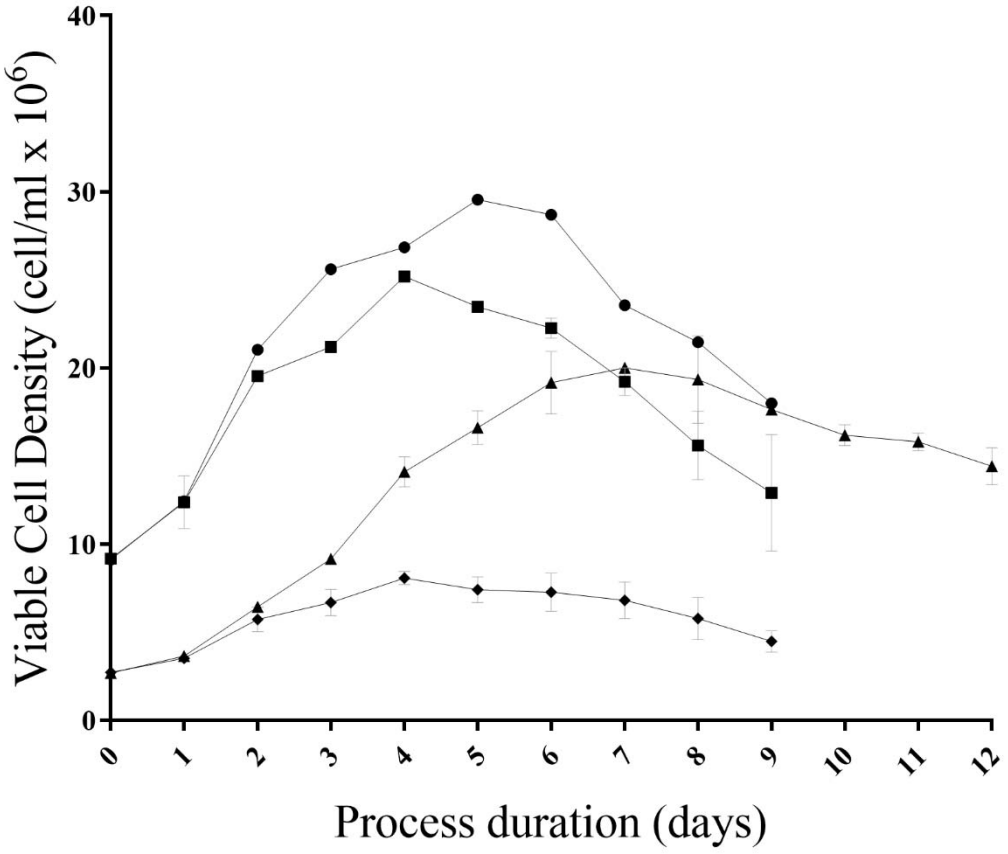

Figure 51 Viable cell density representing the process performance of production phase bench scale vessels at 1x and 2x feed condition (Experiment 4.1b)
VCD plotted against process duration (days); symbols, ■,▲, ♦ and ● represent seeding densities (feed condition); 10 (2x), 10 (1x), 2.5 (2x) and 2.5 (1x) x10^{6}cells/mL, respectively. (n=2 for each)

From inoculation (day zero) to day one all cultures were observed to increase their viable cell density (Figure 51). On day one, consistency is achieved in cell concentrations within respective seeding densities, with (12.4±0.04) and (3.59±0.09) reported for 10 and 2.5 x10^{6}cells/mL, respectively. Following this, deviation occurs based on the feeding regime, with improved performance originating from cultures operated in the 1x feeding regime.

Peak viable cell densities were experienced on day four for the 2x feed condition, with values (8.1±0.4) and (25.2±0.3) x10^6 cells/mL for seeding densities 2.5 and 10 x10^6 cells/mL, respectively. In the 1x feed condition peak viable cell density was experienced on days seven and five for seeding densities 2.5 and 10 x10^6 cells/mL, with (20.0±0.01) and (29.6±0.00) x10^6 cells/mL, respectively.

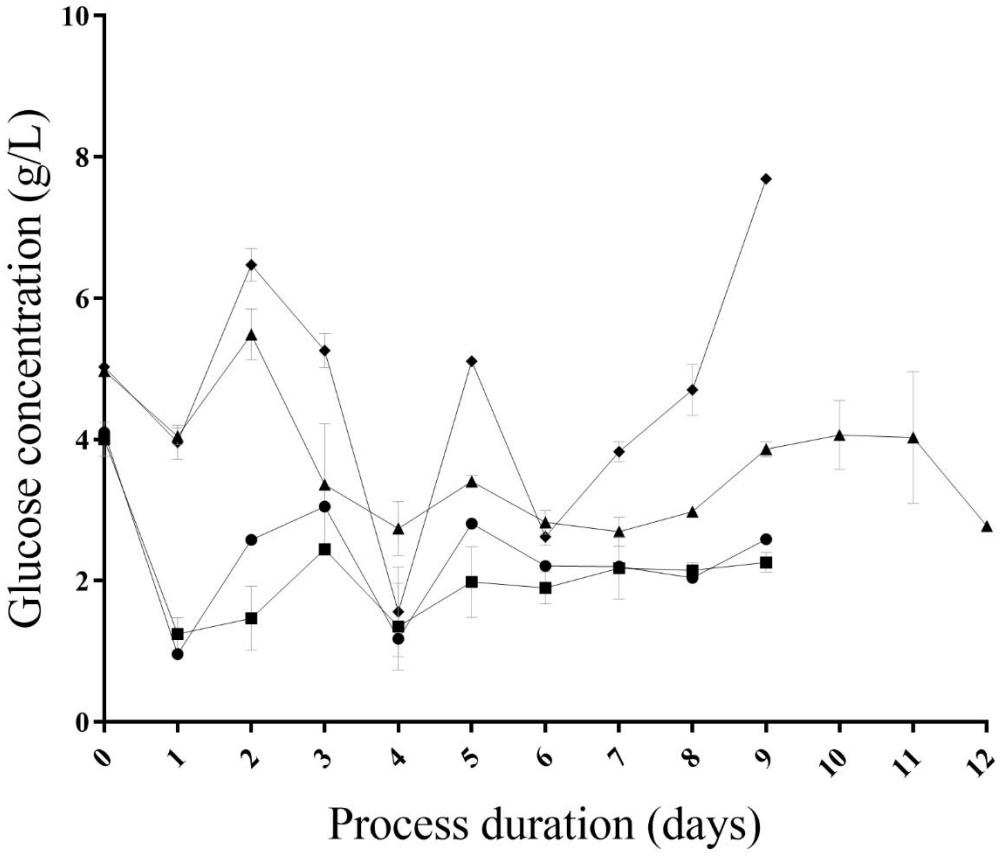

Figure 52 Glucose concentration (g/L) representing the process performance of production phase bench scale vessels at 1x and 2x feed condition (Experiment 4.1b)
Glucose plotted against process duration (days); symbols, ■,▲, ♦ and ● represent seeding densities (feed condition); 10 (2x), 10 (1x), 2.5 (2x) and 2.5 (1x) x10^6cells/mL, respectively. (n=2 for each)

The availability of glucose was maintained throughout the duration of the culture, with the lowest recorded concentration (0.96g/L) occurring on day one of the cultures for the 10 x10^6cell/mL seeding density culture, operated at 1x feed condition (Figure 52).

Due to the high cellular concentration, and resulting culture glucose demand, both feeding conditions operated from the 10 x 10^6cells/mL seeding density regularly dropped below 2g/L. The glucose added following this measurement was sufficient on each day to provide the key metabolite over the subsequent 24 hour period.

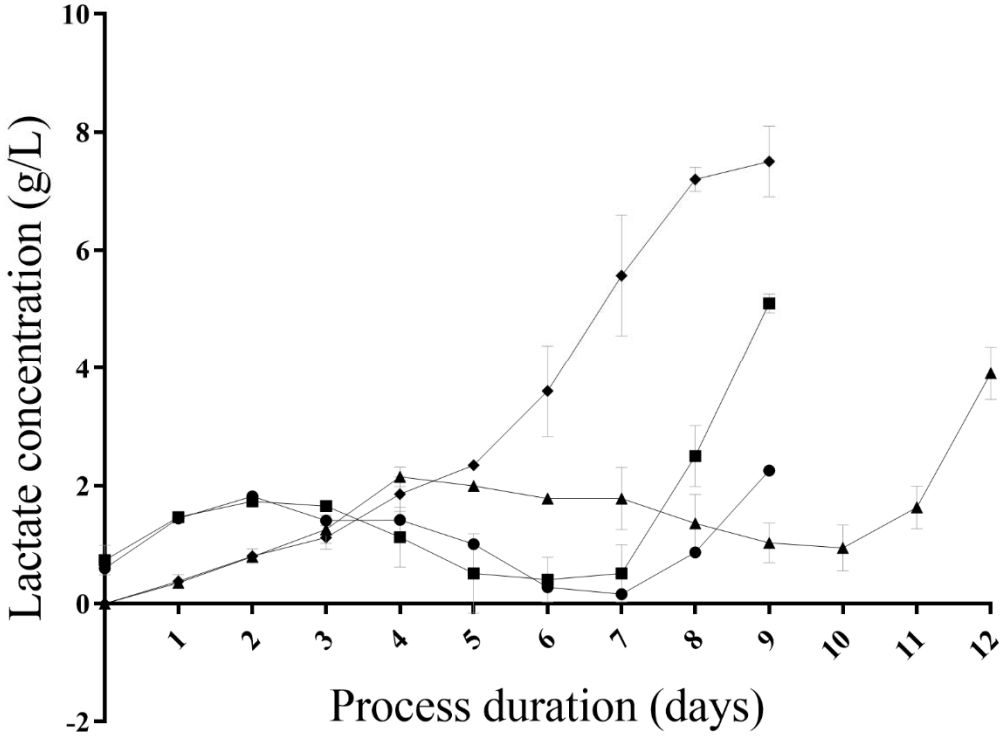

Figure 53 Lactate representing the process performance of production phase bench scale vessels at 1x and 2x feed condition (Experiment 4.1b)
Lactate plotted against process duration (days); symbols, ■,▲, ♦ and ● represent seeding densities (feed condition); 10 (2x), 10 (1x), 2.5 (2x) and 2.5 (1x) x10^6cells/mL, respectively. (n=2 for each)

The concentration of lactate was observed to increase on the final days of culture for all conditions Figure 53. The observed values for the 1x feed condition were (3.9±0.5) and (2.3±0.0) g/L for seeding densities 2.5 and 10 x10^6 cells/mL, respectively. The 2x feed condition concentrations were (7.5±0.6) and (5.1±0.2) g/L for seeding densities 2.5 and 10 x10^6 cells/mL, respectively.

Lactate concentrations in bench scale cultures displayed two distinct trends that differ from those observed at microscale. Firstly, the lower seeding density 2x feed condition presents an exponentially increasing lactate concentration. This increase is observed throughout the culture duration up to day eight and plateaus on the final day of culture (day nine). This trend is similar to that generated in the respective microscale culture (Figure 44), whereby lactate accumulation is persistent throughout the culture duration.

The second trend observed begun with an initial accumulation of lactate within vessels. This occurred over the first four days of culture, and the concentration increased up to approximately 2g/L. Following this initial accumulation, lactate concentration was then observed to decrease as the cultures grew exponentially. On the final two days of each respective culture, a sharp

increase in lactate concentration was observed. This increase in concentration resulted in peak lactate concentration on the final day of culture.

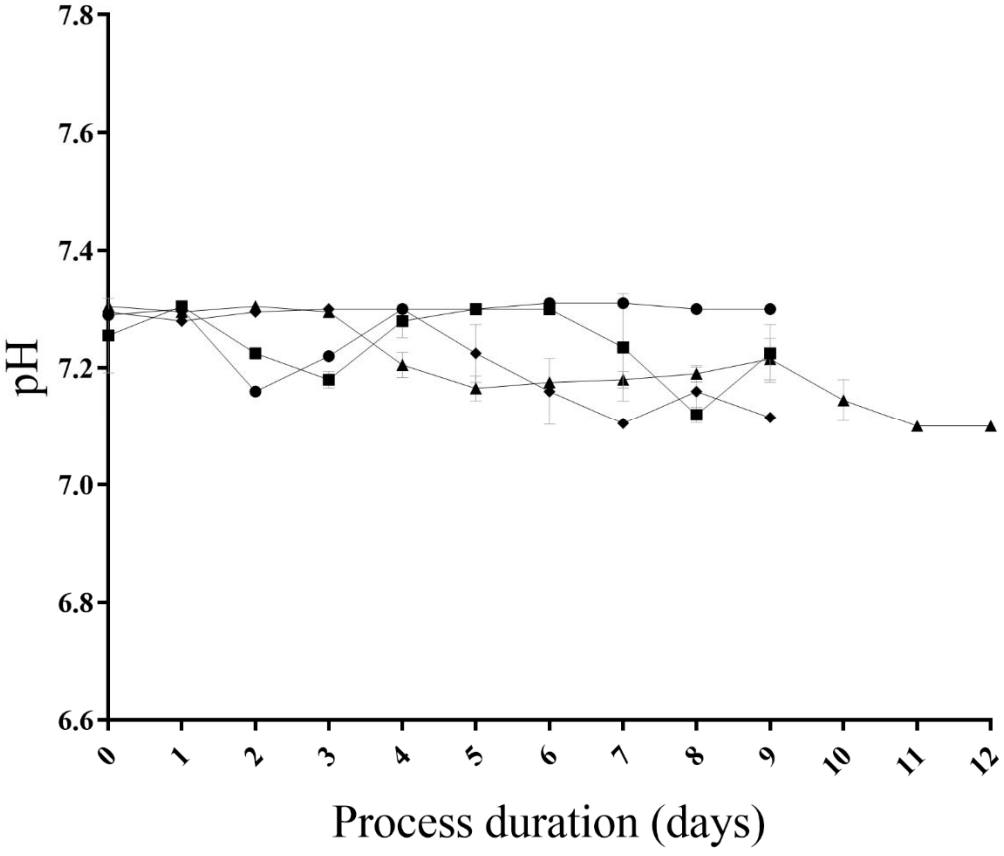

Figure 54 Online pH measurements representing the process performance of production phase bench scale vessels at 1x and 2x feed condition (Experiment 4.1b)
pH plotted against process duration (days); symbols, ■,▲, ♦ and ● represent seeding densities (feed condition); 10 (2x), 10 (1x), 2.5 (2x) and 2.5 (1x) x10^6cells/mL, respectively. (n=2 for each)

Throughout the culture duration, the control strategies successfully maintained pH and oxygen saturation to the respective setpoints (pH 7.2±0.1, DO 50%). Fluctuations occurred within this culture biochemical environment that presented themselves as pH measurements moving between the top and bottom of the deadband (Figure 54).

In a correlation to evolving lactate concentration within the culture (Figure 53), the pH started at the top of the deadband was observed to decline as lactate concentration increased. This trend was observed to oscillate as lactate levels within cultures decreased and then peaked at the last days of culture.

Cultures with low cellular growth, and in turn low oxygen demand, saw a rise in dissolved oxygen percentage in the final few days of culture as oxygen supply from agitation alone was in excess of demand.

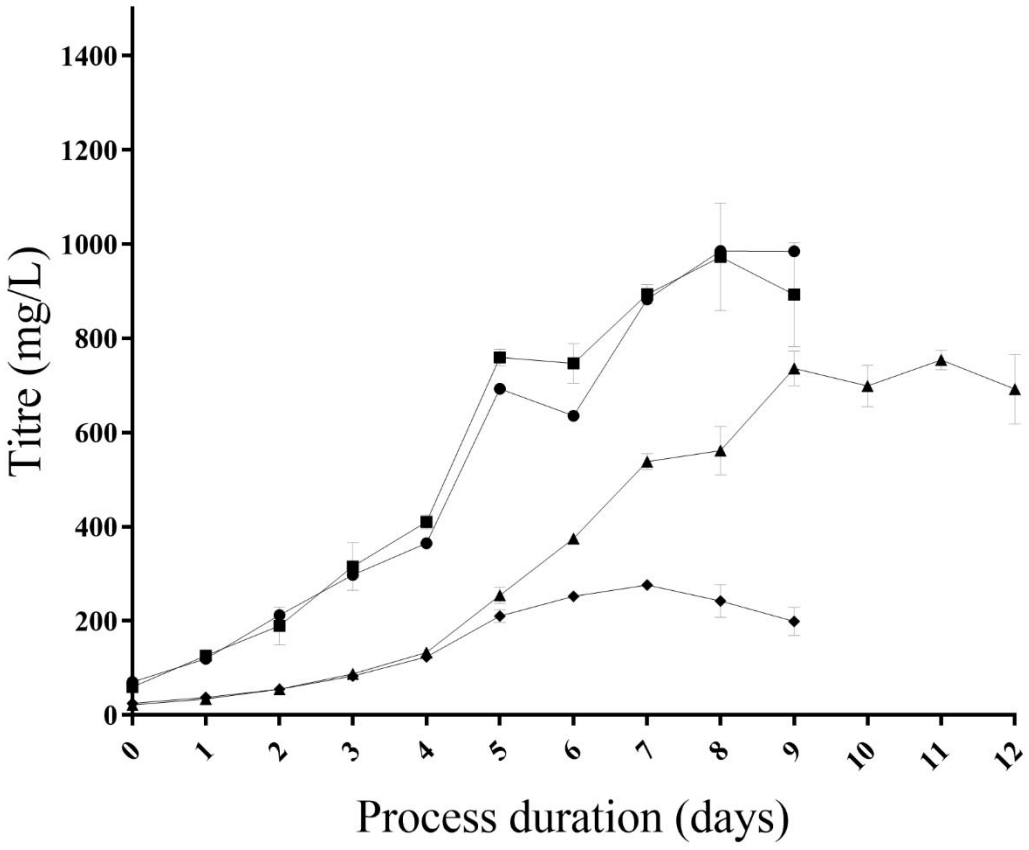

Figure 55 Titre representing the process performance of production phase bench scale vessels at 1x and 2x feed condition (Experiment 4.1b)
Titre plotted against process duration (days); symbols, ■,▲, ♦ and ● represent seeding densities (feed condition); 10 (2x), 10 (1x), 2.5 (2x) and 2.5 (1x) x10^6cells/mL, respectively. (n=2 for each)

Over the first four days of culture, there are two distinct titre profiles generated, separated with relation to their seeing density (Figure 55). Cultures inoculated at 10 x10^6cell/mL displayed titre measurements of 365.3 (n=1) and (410.7±14.9) mg/L for 1x and 2x feed conditions, respectively. These values are in contrast to the vessels inoculated at 2.5 x10^6cells/mL, where titre was achieved as (133.2±6.6) and (123.9±4.5) mg/L for conditions 1x and 2x, respectively.

Following day four, cultures seeded at 2.5 x 10^6cells/mL were observed to deviate as the feeding condition applied impacted the titre measurement. The vessels in the 1x feed condition continued onto a peak titre measurement of (754.3±20.9) mg/L on day 11, whereas the 2x feed condition only reached (276±10.3) mg/L, occurring on day seven.

For the higher seeding density cultures, higher titre measurements observed on day four was continued throughout the remainder of the culture. A high correlation was observed between titre profiles operated at different feed conditions, with both reaching peak titre on day eight, 985.5, and (972.9±114.4) mg/L for 1x and 2x, respectively.

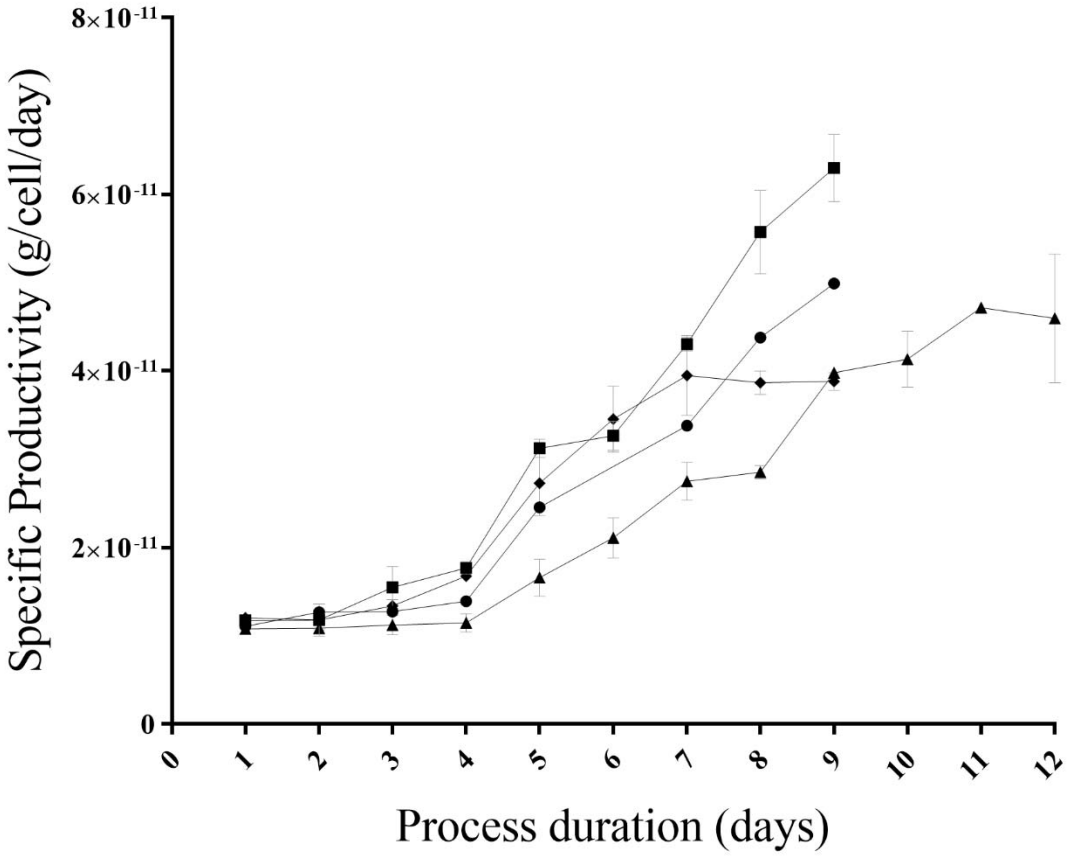

Figure 56 Specific productivity representing the process performance of production phase bench scale vessels at 1x and 2x feed condition (Experiment 4.1b)
Specific productivity plotted against process duration (days); symbols, ■,▲, ♦ and ● represent seeding densities (feed condition); 10 (2x), 10 (1x), 2.5 (2x) and 2.5 (1x) x10^{6}cells/mL, respectively. (n=2 for each)

The cell specific productivity did not display excessive variation over the first four days, however following this point there were distinct trends in performance observed (Figure 56). These differences were highlighted by the performance in the 10 x10^{6}cell/mL seeding density conditions. Improved specific productivity was observed in the 2x feed condition, with specific productivity measurements 5.0 and (6.3±0.4) x10^{-11} g/cell/day achieved on day nine for feeding conditions 1x and 2x, respectively.

The 2x feed condition also promoted comparable cell specific productivity in the 2.5 x10^6 cell/mL seeding density cultures up to day seven. Specific productivity of (4.3±0.07) and (4.0±0.5) x10^{-11} g/cell/day was observed for the 10 and 2.5 x10^{6}cell/mL seeding density conditions, respectively. Furthermore, the cell specific productivity for the 2.5 x10^{6}cell/mL seeding density condition plateaued as the culture progressed towards harvest, (3.9±0.1) x10^{-11} g/cell/day was observed on the final day of culture.

Table 6 Percentage monomer post Protein A purification of bench scale cultures at 1x and 2x feed conditions

Seeding density (x10^6 cells/ml)	Feed condition	Monomer (%)
10	1x	96.3 (n=1)
10	2x	(95.8±0.3)
2.5	1x	(95.3±0.5)
2.5	2x	(94.6±0.6)

The product quality of the mAb expressed from bench scale cultures was lower than that observed for microscale. However, no significant difference was observed and the monomer percentage was > 95% post Protein A purification, indicating no impact on product quality.

4.3.2 Interim Discussion (Experiment 4.1)

The microscale perfusion methodology achieved comparable culture Key Performance Indicators (KPIs), e.g. maximum viable cell density and specific productivity, to equivalent bench scale cultures (Chapter 3). Despite this comparability, differences existed in the growth of cultures in microscale perfusion that is in contrast to the accepted robustness and scalability of the ambr® 15 system (Lewis, 2010). Therefore, experiments have been conducted to characterise the method-related impact on culture performance. This information is critical when determining the scalability of process knowledge gained through perfusion operation at microscale.

During Experiment 4.1, a lag in growth was observed between scales (Figure 28). This lag was present in the microscale cultures and resulted in a two day delay in reaching the transition criteria (inoculation of production cultures). These differences are characteristic artefacts of the microscale perfusion methodology (Figure 14). However, the extent of the difference in growth is not significant when paired profiles up to the day of the transition of the shortest cultures are compared (micro and bench scale cultures to day ten; p-value = 0.10).

The glucose concentration was maintained in bench and microscale perfusion cultures throughout Experiment 4.1. This resulted in the utilisation of glucose as an energy source, and the metabolism of lactate was not deemed critical for energy production. The residual lactate concentrations resulted in a slightly basic biochemical environment for both bench and micro scale cultures at the point of transition, respectively.

The cellular characteristics of the two scales of perfusion cultures during exponential growth were evaluated in the performance of respective subsequent fed batch production cultures. Whilst a monoclonal cell line, the act of culturing cell lines generates heterogeneous sub-population of phenotypes with different functional characteristics (Davies et al., 2013). The hypothesis tested was that the semi-continuous method of perfusion at microscale was selectively removing the fast growing phenotypic sub-population of the culture (Stephens & Lyberatos, 1987). The slower growing phenotype would present as a homogeneous population and be realised in the measured performance of the resulting production cultures.

The perfusion cultures were transitioned into production cultures at concentrations between 2.5 and 15 x10^6 cells/ml. These inoculation concentrations were combined with two seeding densities that provided examples of sub-optimal nutrient feeding (1x and 2x). Sub-optimal feeding commonly results in a reduction in culture growth, and subsequently mAb concentration (Kuwae, Ohda, Tamashima, Miki, & Kobayashi, 2005). Conversely, optimising nutrient supply has been shown to increase viable cell concentration up-to 1.9-fold (Chong et al., 2010). The sub-optimal nutrient environments generated will provide contrasting performances that can be replicated across scales and to highlight the holistic method related differences in the cultures.

At microscale the high throughput nature of the ambr® 15 system allowed additional seeding densities (5 and 15 x10^6 cells/ml) to be evaluated for each feed condition. The peak viable cell densities at microscale correlated in magnitude to the culture seeding densities (from lowest to highest 2.5, 5, 10, and 15 x10^6 cells/ml**)**. A significant difference (p-value <0.05) was observed between each paired profile. Microscale cultures were harvested due to a decline in viability on days ten and seven, for feed conditions 1x and 2x, respectively.

The bench scale 1x condition entered exponential growth when inoculated at seeding densities 2.5 and 10 x10^6cells/ml. The cultures achieved peak viable cell density on days seven and five, for seeding densities 2.5 and 10 x10^6cells/ml, respectively. In the 10 x10^6cells/ml seeding density, peak viable cell densities of (18.99±0.36) and (29.6±0.00) x10^6cells/ml, were observed for micro and bench scale cultures, respectively. In the 2.5 x10^6 cells/ml seeding density, peak viable cell densities of (10.37±0.80) and (20.0±0.01) x10^6cells/ml were observed for micro and bench scale cultures, respectively. These peak cell densities at bench scale were significantly higher than those observed for microscale cultures.

Exponential growth was not observed in any microscale cultures operated with 2x feed conditions. Within bench scale cultures the 10 x10^6cells/ml seeding density culture was observed to grow exponentially with 2x feed conditions following inoculation. The peak viable cell density of (25.2±0.3) x10^6cells/ml was observed.

The higher feed condition (2x) resulted in shorter culture durations when compared to the 1x cultures. This feed criteria for 2x is inherently sub-optimal and in excess of what is required by the culture. The microscale operation of the 2x condition was uniform in its duration, harvesting after seven days due to a decrease in viability below 60%. This uniform performance and short culture duration are indicative of a singular phenotype contained within these cultures. The maintenance of a stationary phase over a prolonged duration indicates subpopulations growing and offsetting the non-viable cells present in the culture. Therefore, the short culture duration is an indication of low population variance in the phenotypes present.

The performance of the two 2x conditions at bench scale was not comparable in growth. The 2.5 x10^6 cells/ml inoculated culture was observed to enter exponential growth. When compared to the respective condition at microscale, this culture appeared to have an ability to utilise the high nutrient environment presented by the 2x condition and exhibited an extended culture duration.

Differences were also observed in the lactate profiles between microscale and bench scale cultures. An elevation in lactate concentration was observed on the first day post inoculation for all microscale cultures. An approximate three-fold increase in lactate concentration was observed across all microscale cultures, during or following peak viable cell density. This accumulation of lactate is documented in mammalian bioprocessing and occurs as mitochondrial metabolism alters during the transition from exponential growth to stationary phase (Zagari et al., 2013). It is stated that whilst lactate production is prevalent during exponential growth, the oxidative metabolism of the cell prevents its accumulation, and thus in the stationary phase the level of oxidation is decreased and resulting accumulation occurs.

Similar trends in lactate concentrations were observed in three of the four bench scale cultures. One bench scale culture (2.5 x10^6 cells/ml, 1x feed condition) did not display this increase in lactate concentration towards the end of exponential growth. Literature investigating the expression of anti-apoptotic genes has highlighted the impact their absence has on lactate concentrations within a culture (Dorai et al., 2009)

When evaluating the impact of the 2x feed condition on cultures (micro and bench scale), it appears the increased nutrient availability has accelerated cellular processes into a stationary phase. This is observed in the accumulation of lactate from day four onwards, and the elevation in cell specific lactate production both shortly after inoculation and again from day four onwards. Published work states that an abundance of glutamine within the feed composition could promote the lactate production metabolism pathways (Zagari et al., 2013), indicating the potential source of sub-optimal performance.

In conclusion, the sedimentation method applied to the ambr® 15 microscale system to achieve perfusion produces unique physiochemical conditions for cultures (Section 3.2 Method Development). The production cultures derived from these unique microscale physiochemical conditions have decreased performance when compared to bench scale counterparts. Additionally, under sub-optimal production culture conditions, lower variation in performance is observed in microscale cultures compared to bench scale cultures.

As previously discussed, during cell sedimentation in microscale perfusion, the culture is being exposed to locally extreme pH and DO saturation. In addition, to operate the method there are discrete media exchange steps that will produce a fluctuating nutrient exposure. This discrete media exchange will ultimately result in oscillating variation in the dilution rate applied to the culture. Therefore, it is important to understand if the performance observed in Experiment 4.1 is due to inherent sensitivity to the dilution rate/supply of nutrients to the cultures or if the method of perfusion is generating selective pressure on the culture impacting sub-population expansions.

Experiment 4.2 focused on understanding the cell line's response to a reduced dilution rate. This was conducted exclusively at bench scale utilising the ATF perfusion technology to achieve high accuracy in the dilution rate applied.

4.3.3 Experiment 4.2 Culture Response to Reduced Dilution Rate

Experiment 4.2 evaluated the impact of dilution rate on perfusion culture performance. This was conducted in a similar fashion as Experiment 4.1, by conducting subsequent evaluations of production fed-batch vessels with cells derived from the perfusion cultures. The consideration of the transition operation between perfusion and production (fed-batch) inoculation was simplified in comparison to that outlined, in Section 4.2.1 Transition of Cultures From Perfusion to Production.

Each perfusion vessel operated within Experiment 4.2 was an independent experimental condition and thus, was used to inoculate the respecting duplicate production vessels. This was performed without the requirement for the pooling of multiple cultures before inoculation.

4.3.2.1 Perfusion Expansion

Experiment 4.2 was initiated with the inoculation of three bench scale perfusion vessels, at the target seeding density of 0.8 x10^6 cells/mL.

Previous perfusion evaluations of Cell line 1 indicated glucose concentrations decreasing below 1g/L on the fourth day (Figure 21 and Figure 29). Therefore, in Experiment 4.2 perfusion was initiated on the third day of culture for all vessels. This action mitigated the risk of the culture experiencing a glucose limited environment.

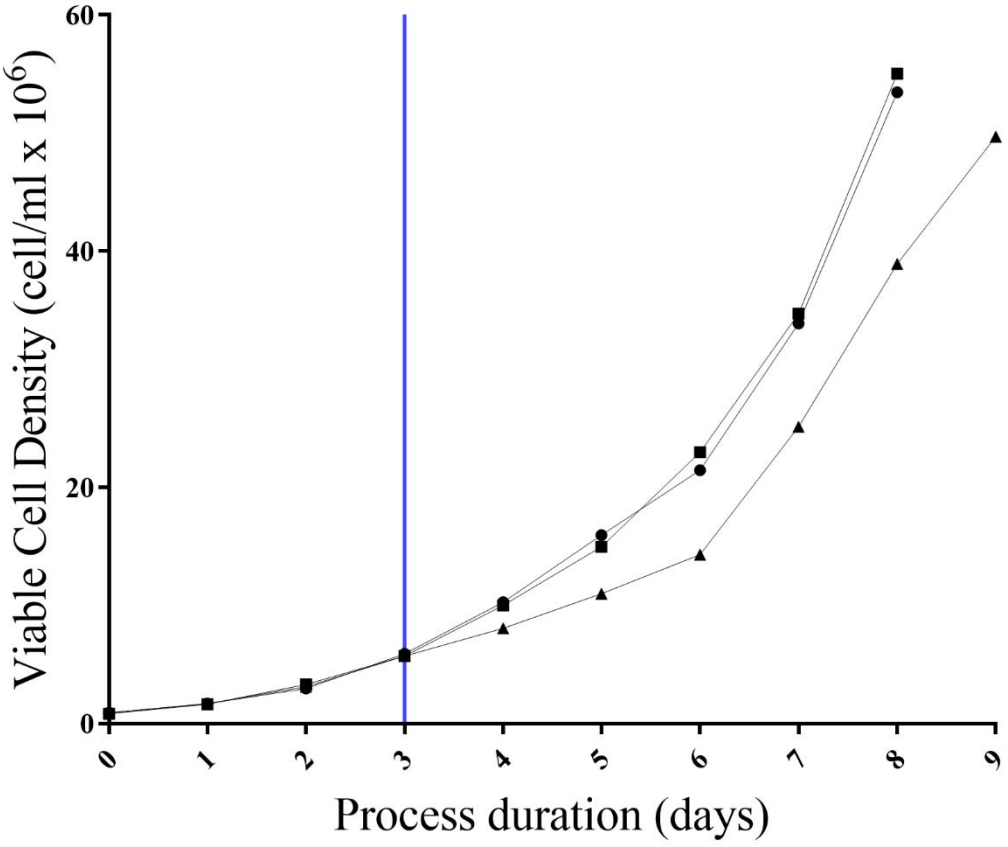

Figure 57 Viable cell density (x10^6 cells/mL) representing the process performance of the n-1 phase vessels in Experiment 4.2
Values are plotted against process duration (days); symbols and ●, ▲ and ■ represent dilution rates 1.0, 0.75, and 0.5 VVD, respectively. Single vessels were operated at each dilution rate. Perfusion initiation is indicated with an intersecting blue line.

The cultures displayed comparable growth over the initial three day batch period, with average cell density increasing in number and variability between days two and three, (3.1±0.2) and (5.8±0.1) x10^6cells/mL, respectively (Figure 57).

Following the initiation of perfusion (indicated in Figure 57 with an intersecting blue line) a separation was observed in the growth profiles of Cell line 1. The perfusion operation resulted in a variation in the growth profile based on the dilution rate. Dilution rates 1.0 and 0.5 VVD reached criteria for the transition on day eight, with values of 53.5 and 55.0 x10^6cells/mL, respectively. The 0.75 VVD dilution rate experienced a lag in growth between days four and six when compared to 1.0 and 0.5 VVD dilution rates. The criteria for the transition were not met until day nine for the 0.75 VVD dilution rate, 49.7 x10^6cells/mL. The 0.75 VVD condition was an example of a mid-point dilution rate, between the other high and low conditions in 1.0 and 0.5 VVD, respectively.

No variation was observed in the viability of the cultures as, throughout the n-1 perfusion step, viabilities did not drop below 97% in any condition.

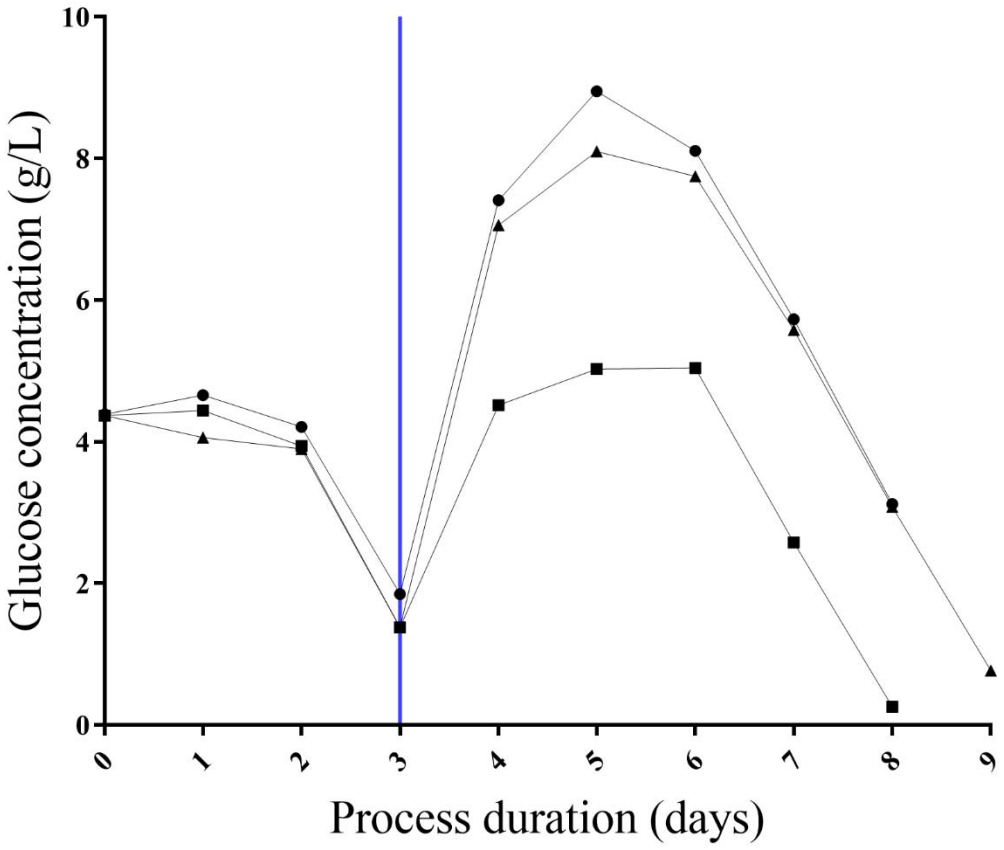

Figure 58 Glucose concentration (g/L) representing the process performance of the n-1 phase vessels in Experiment 4.2
Values are plotted against process duration (days); symbols and ●, ▲ and ■ represent dilution rates 1.0, 0.75, and 0.5 VVD, respectively. Single vessels were operated at each dilution rate. Perfusion initiation is indicated with an intersecting blue line.

Observed over the first three days of culture, is a gradual depletion of glucose concentration as the cells consumed the residual glucose concentration over the batch phase (Figure 58). The average glucose concentration in all cultures on day three before perfusion initiation was (1.5±0.3) g/L.

Following the initiation of perfusion, the culture concentration of glucose was increased to a peak, experienced on day five. The dilution rate could be implied from the resulting glucose concentration with 1.0 VVD, 0.75 VVD and 0.5 VVD measured at 8.95, 8.10, and 5.03, g/L, respectively. The glucose concentration gradually decreased as cultures progressed towards the transition to production cultures.

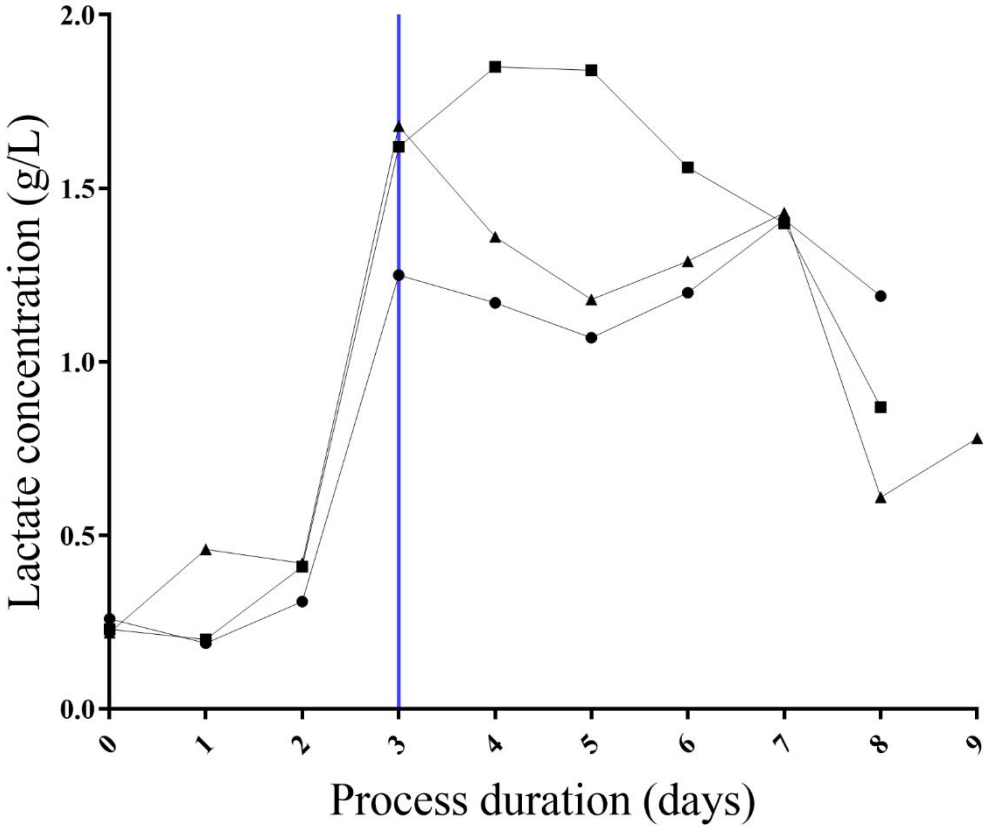

Figure 59 Lactate concentration (g/L) representing the process performance of the n-1 phase vessels in Experiment 4.2
Values are plotted against process duration (days); symbols and ●, ▲ and ■ represent dilution rates 1.0, 0.75, and 0.5 VVD, respectively. Single vessels were operated at each dilution rate. Perfusion initiation is indicated with an intersecting blue line.

Lactate levels were low across all cultures at inoculation, <0.5g/L across all cultures. Cell line 1 lactate concentration was maintained at a low level over the first two days, with values measured 0.31, 0.42, and 0.41 g/L for dilution rates 1.0, 0.75, and 0.5, respectively. On day three, and the last day of batch growth before perfusion initiation, lactate concentrations increased stepwise to >1g/L where they were maintained until day eight when they reduced back to <1g/L.

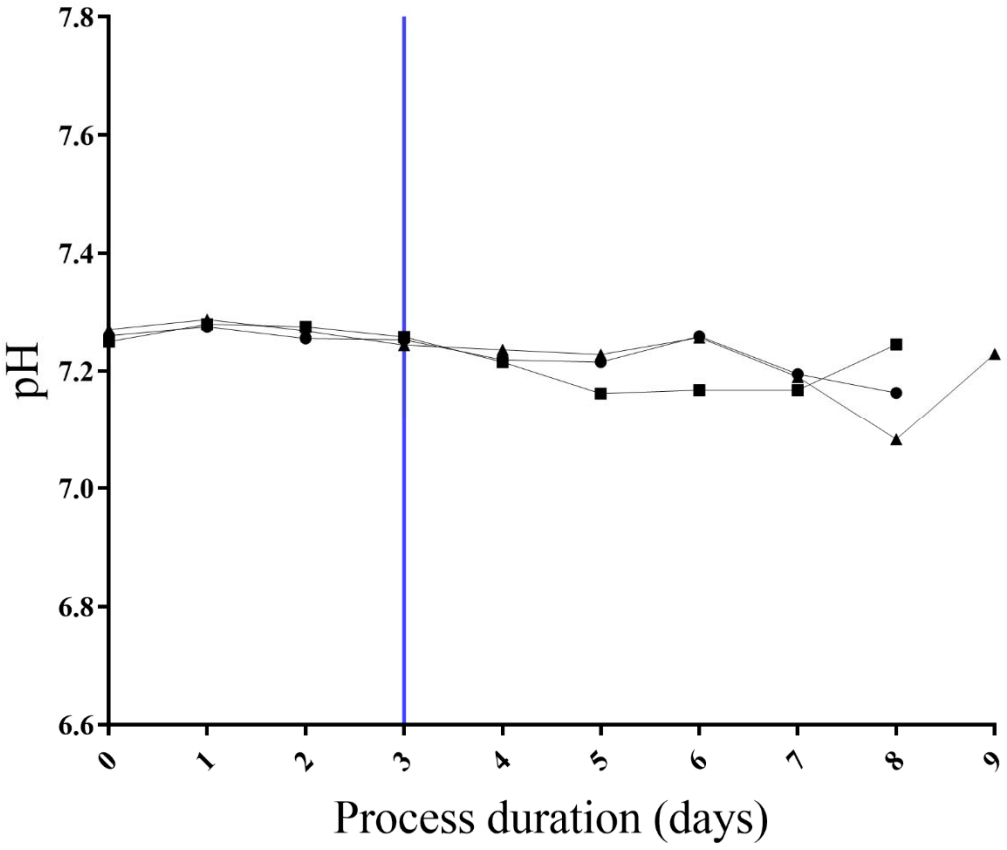

Figure 60 pH representing the process performance of the n-1 phase vessels in Experiment 4.2
Values are plotted against process duration (days); symbols and ●, ▲ and ■ represent dilution rates 1.0, 0.75, and 0.5 VVD, respectively. Single vessels were operated at each dilution rate. Perfusion initiation is indicated with an intersecting blue line.

The pH is observed to remain close to setpoint (pH 7.2±0.1) over the initial three days of batch growth. Following the initiation of perfusion, pH was seen to decrease, in line with the lactate accumulation detailed in Figure 59.

The decrease in pH was not consistent across Cell line 1 cultures, and the transient accumulation, consumption, and dilution of lactate within the vessel caused fluctuations in the pH through to the point of transition into production cultures. Transition to production culture for Cell line 1 occurred with pH within the 7.2±0.1 setpoint, in all dilution rates.

4.3.2.2 Production Phase

The perfusion culture dilution rates (1.0, 0.75, and 0.5 VVD) applied to Cell line 1 cultures were evaluated in production cultures. These production cultures were operated at the 1x feed condition and 10 x10^6cells/mL seeding density. These conditions represented the best performance in bench scale with relation to cell growth and titre from Experiment 4.1.

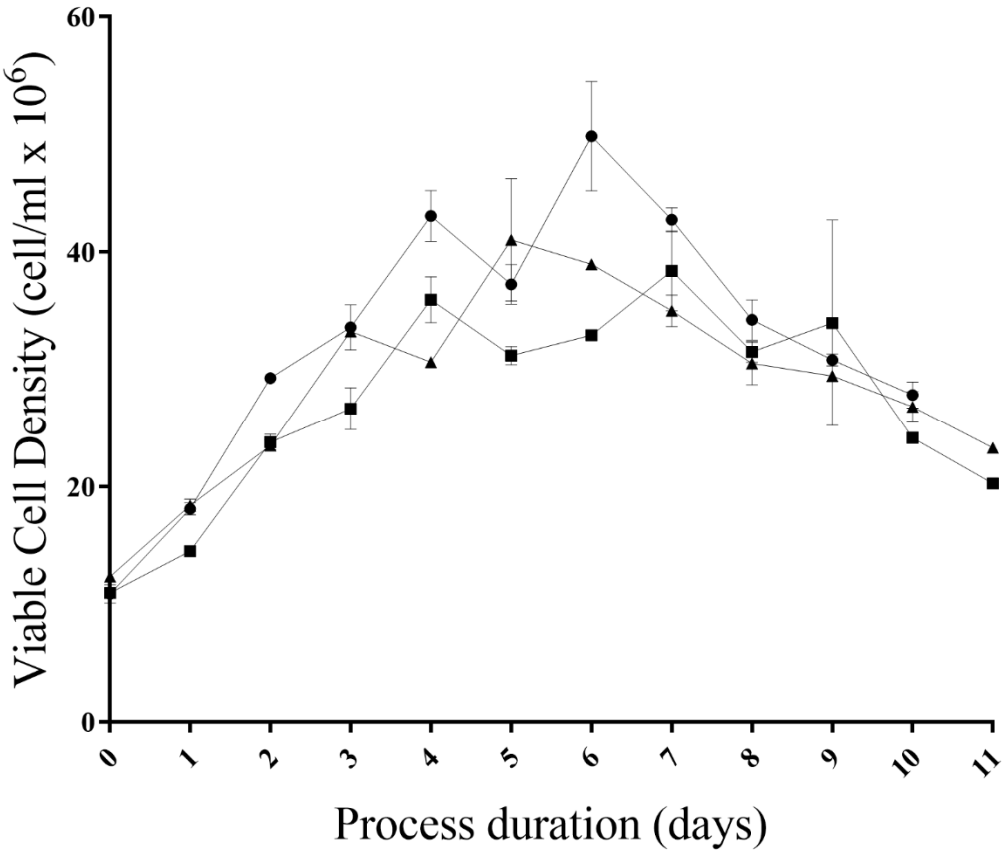

Figure 61 Viable cell density (cells/mL) representing the process performance of the production phase vessels in Experiment 4.2
Viable cell density measurements are plotted against process duration (days); symbols and ●, ▲ and ■ represent dilution rates 1.0, 0.75, and 0.5 VVD, respectively (n=2).

The growth of cultures within production vessels presented comparability in the different dilution rates employed in the perfusion cultures (Figure 61). Inoculation of production phase cultures was successfully conducted to the target seeding density. All cultures appeared to progress concurrently towards a peak viable cell density, reaching it on consecutive days. Peak viable cell densities were (38.4±3.4, day seven), (41.1±5.2, day five) and (49.9±4.7, day six) x10^6cells/mL for 0.5, 0.75 and 1.0 VVD dilution rate cultures, respectively.

Following these peaks, viable cell density decreased to the point of culture harvest that was met on day 10, for 1.0 VVD cultures and day 11 for 0.5 and 0.75 VVD cultures, respectively. As conducted for Experiment 4.1, the culture harvest criteria were set to be when viability reached <60%. Viable cell density at harvest was (20.3±0.0), (23.3±0.4) and (27.9±1.1) x10^6cells/mL for 0.5, 0.75 and 1.0 VVD dilution rate cultures, respectively.

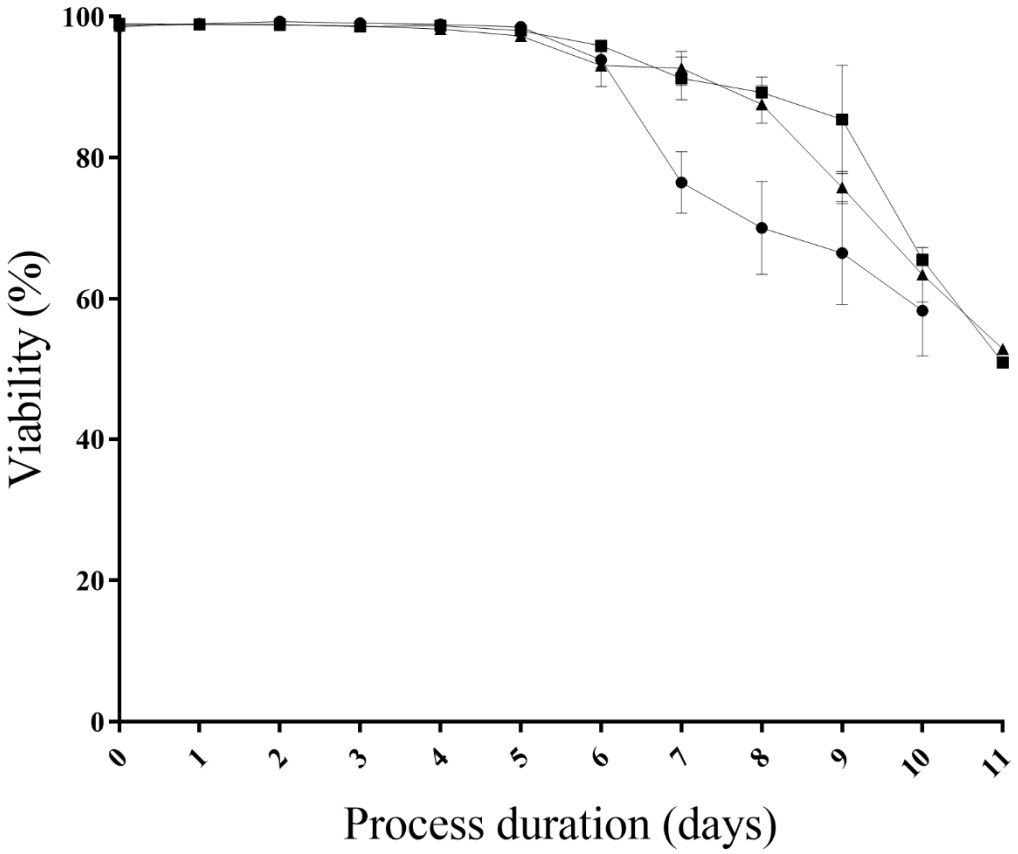

Figure 62 Viability (%) representing the process performance of the production phase vessels in Experiment 4.2
Viability (%) measurements are plotted against process duration (days); symbols and ●, ▲ and ■ represent dilution rates 1.0, 0.75, and 0.5 VVD, respectively (n=2).

High culture viability (>97%) was maintained from inoculation through the first five days of culture (Figure 62). This high viability was coupled with the culture expansion to peak viable cell density, presented in Figure 57, and as the cultures surpassed peak viable cell concentration, viability began to decline.

The decline in viability was first observed on day six. Viability decreased from >97% to (95.9±0.0), (93.1±3.0) and (93.9±1.1) % for 0.5, 0.75 and 1.0 VVD dilution rate cultures, respectively. Starting from day seven, the viability for 1.0 VVD cultures varied when compared to 0.5 and 0.75 cultures, with observed viability of (76.5±4.4) compared to (91.3±3.0) and (92.7±2.4), respectively. This increased rate of decline was slowed and culture duration was only shortened by one day (day 10 post inoculation), in comparison to the other dilution rates (day 11 post inoculation).

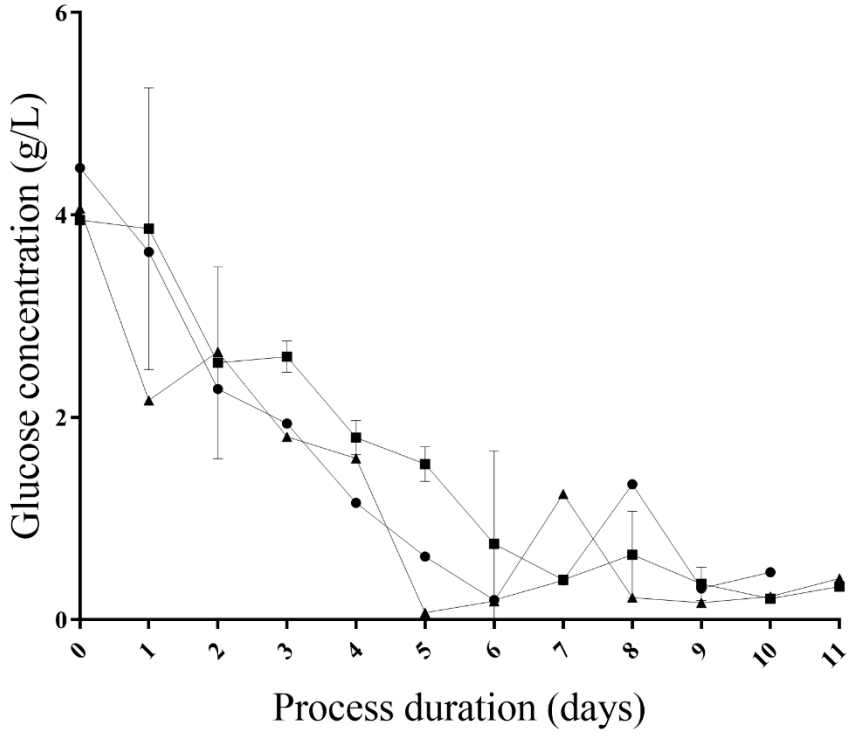

Figure 63 Glucose concentration (g/L) representing the process performance of the production phase vessels in Experiment 4.2
Glucose concentration (g/L) measurements are plotted against process duration (days); symbols and ●, ▲ and ■ represent dilution rates 1.0, 0.75 and 0.5 VVD, respectively (n=2).

In contrast to the cultures conducted throughout Experiment 4.1, glucose concentrations spent a substantial period of time below 2g/L in Experiment 4.2a (Figure 63). This control below 2g/L occurred from day four onwards, coinciding with the highest culture cellular content, around the peak viable cell concentration (Figure 61).

The fed batch target concentration to feed glucose back into the cultures appeared to be insufficient to maintain a daily concentration above 2g/L. This ineffective control resulted in a high chance of cultures experiencing a temporary glucose limited environment. This low glucose environment was observed concurrently across all cultures. Therefore, the comparative analysis of the performance of different cultures' respective responses is valid when analysed in this isolated experiment.

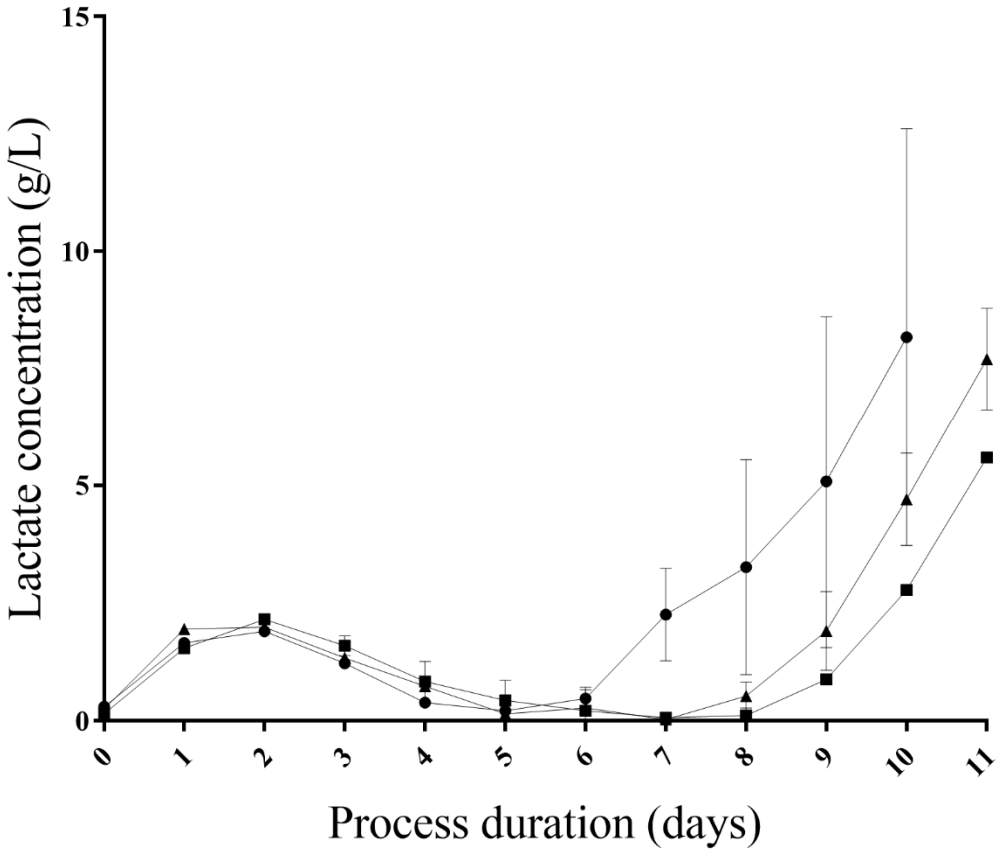

Figure 64 Lactate concentration (g/L) representing the process performance of the production phase vessels in Experiment 4.2
Lactate concentration (g/L) measurements are plotted against process duration (days); symbols and ●, ▲ and ■ represent dilution rates 1.0, 0.75 and 0.5 VVD, respectively (n=2).

The lactate concentration of cultures was observed to rise in all cultures to an initial peak on day two (Figure 64). The overall profile observed for culture lactate concentration aligns with that experienced in Experiment 4.1b (Figure 53). The lactate concentration on day two was (2.2±0.04), (2.0±0.1) and (1.9±0.1) g/L and decreased to concentrations on day five of (0.4±0.4), (0.2±0.0) and (0.2±0.1) g/L for dilution rates 0.5, 0.75 and 1.0 VVD, respectively.

The lactate concentration peaked as culture viability decreased over the final days of culture. This peak was in excess of that displayed on day two. Cultures operated in the 1.0 VVD dilution rate condition appeared to initiate this increase in lactate concentration on day seven, where 0.75 and 0.5 VVD cultures presented at days eight and nine, respectively.

Lactate concentration at harvest was (5.6±0.0), (7.7±1.1), and (8.2±4.4) g/L for cultures operated at dilution rates 0.5, 0.75, and 1.0 VVD, respectively. The pH of cultures was controlled within the ±0.1 deadband around setpoint 7.2.

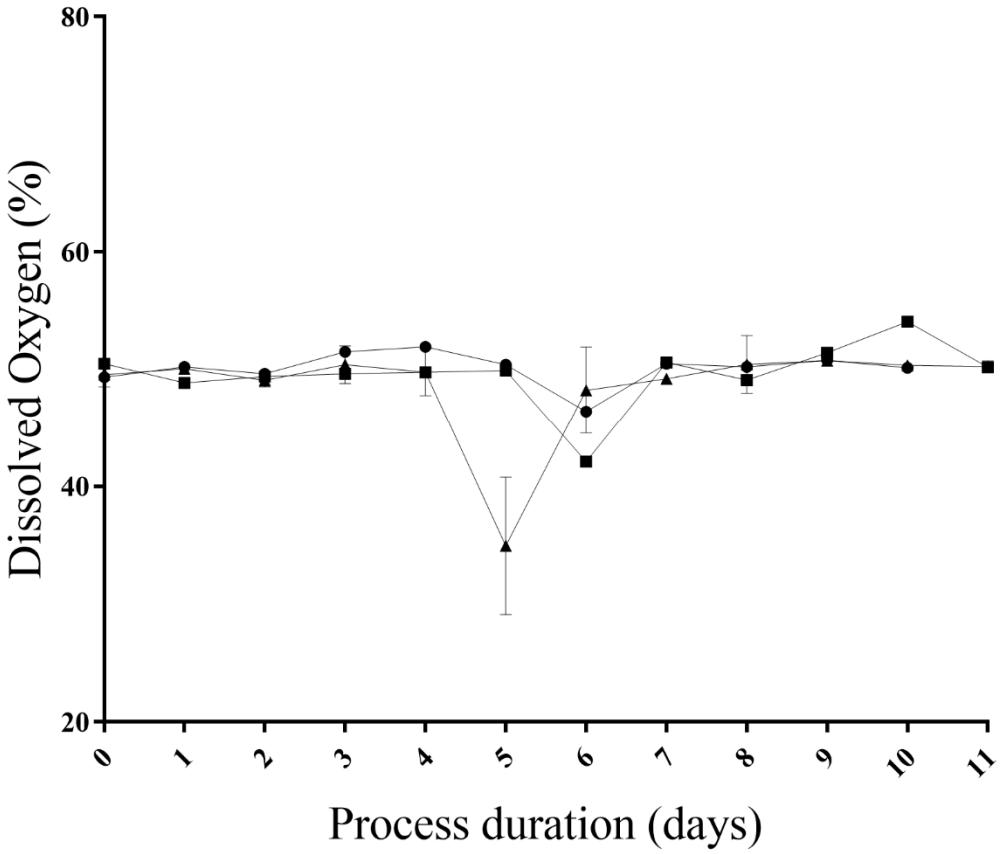

Figure 65 Dissolved oxygen (%) representing the process performance of the production phase vessels in Experiment 4.2
Dissolved oxygen (%) measurements are plotted against process duration (days); symbols and ●, ▲ and ■ represent dilution rates 1.0, 0.75, and 0.5 VVD, respectively (n=2).

Over the first four days, dissolved oxygen saturations were maintained to setpoint (50%) with the combination of culture agitation and sparged oxygen on demand (Figure 65).

On day five, dissolved oxygen saturation was observed to decline to (35.0±5.8) % for cultures operated from the 0.75 VVD dilution rate. This decline was then observed on day six in the 0.5 and 1.0 VVD dilution rate cultures, with values reported (42.1±0.8) and (46.4±1.6) %, respectively.

A combination of factors contributed to these declines. The culture total demand for oxygen is inherently linked to the exponential expansion of the culture. This was increasing during days five and six as cells grew exponentially towards max viable cell density (Figure 61). This high oxygen demand was coupled with the addition of antifoam, decreasing the surface oxygen transfer and requiring additional input of the process control to maintain the saturation setpoint. The process control strategy for oxygen saturation requires operator input to incrementally increase the agitation rate of the culture as maximum sparging rates are experiences. A delay

in this operator interaction was experienced during days five and six, however once culture agitation rate was increased, the control strategy re-established dissolved oxygen saturation to the setpoint. This was maintained for the remainder of the culture duration.

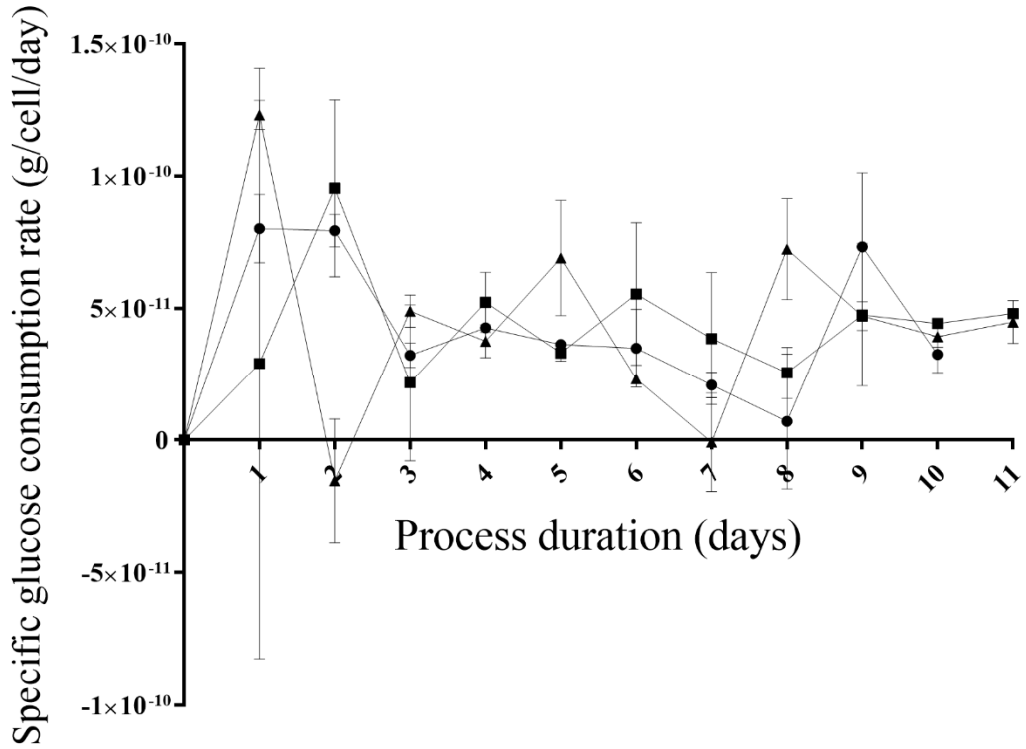

Figure 66 Cell specific glucose consumption rate (g/cell/day) representing the process performance of the production phase vessels in Experiment 4.2
Cell specific glucose consumption rate (g/cell/day) measurements are plotted against process duration (days); symbols and ●, ▲ and ■ represent dilution rates 1.0, 0.75 and 0.5 VVD, respectively (n=2).

Variation is observed in the cell specific glucose consumption rates during the first two days, and through the seventh to ninth days of cultures (Figure 66). The specific glucose consumption rates were comparable through the exponential growth to the maximum viable cell density (days three to six).

Average cell specific glucose concentrations observed on day four matched that at the end of the culture (day ten) with values (4.4±0.8) and (3.9±0.6) x10^{-11}g/cell/day, respectively.

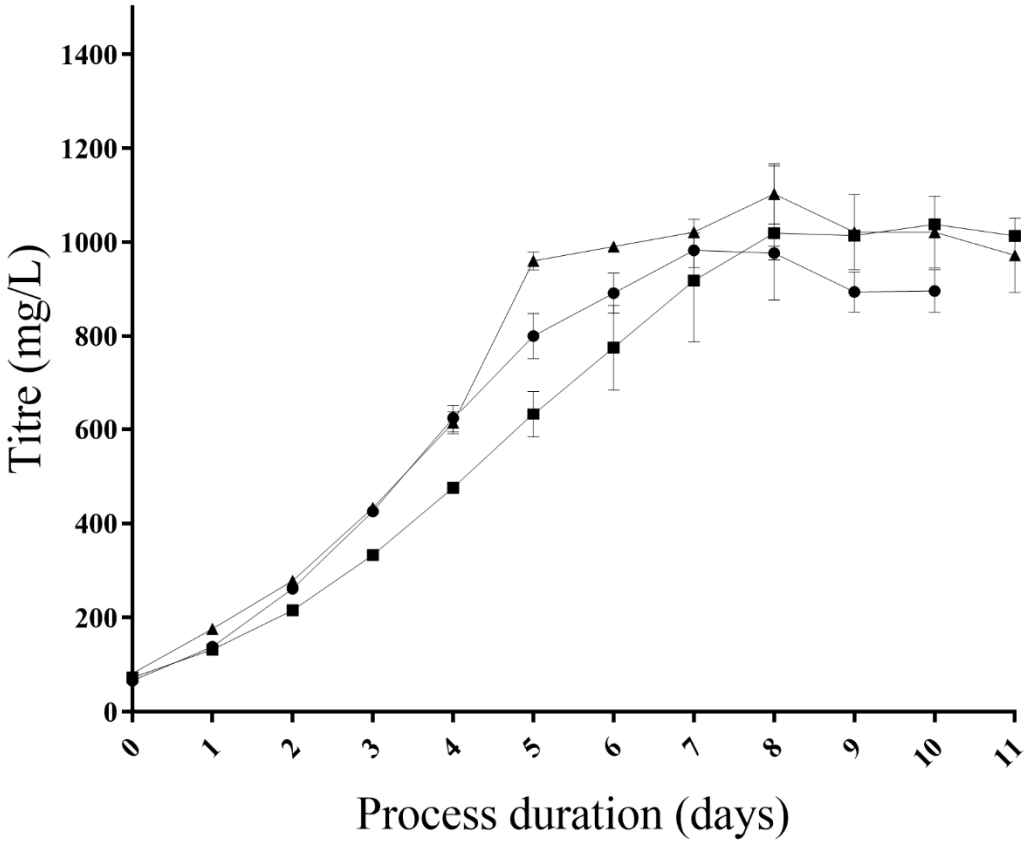

Figure 67 Titre (g/L) representing the process performance of the production phase vessels in Experiment 4.2
Titre (g/L) measurements are plotted against process duration (days); symbols and ●, ▲ and ■ represent dilution rates 1.0, 0.75 and 0.5 VVD, respectively (n=2).

All cultures were observed to increase titre over process duration up to a peak at day eight, with (1019±143), (1102±64) and (977±15) mg/L, for dilution rates 0.5, 0.75 and 1.0 VVD, respectively (Figure 67).

The cultures operated from the 0.5 VVD perfusion vessel displayed a lag in the production of mAb over the first two days. The profile across the full culture duration was significantly lower when paired with the 0.75 VVD perfusion derived cultures ($P<0.05$). Additionally, the 0.75 VVD cultures displayed an increase in titre on day five, where titre measurements thereafter were observed to slowly increase to their maximum on day eight. This deviation from the profile presented by 1.0 VVD culture is significantly different when averaged paired measurements are compared ($p<0.05$). Interestingly, the titre values for the highest dilution culture (1.0 VVD) fell between the other two dilution rate cultures and displayed no significant difference with the lowest dilution culture (0.5 VVD, p-value=0.36), indicating comparability between cultures.

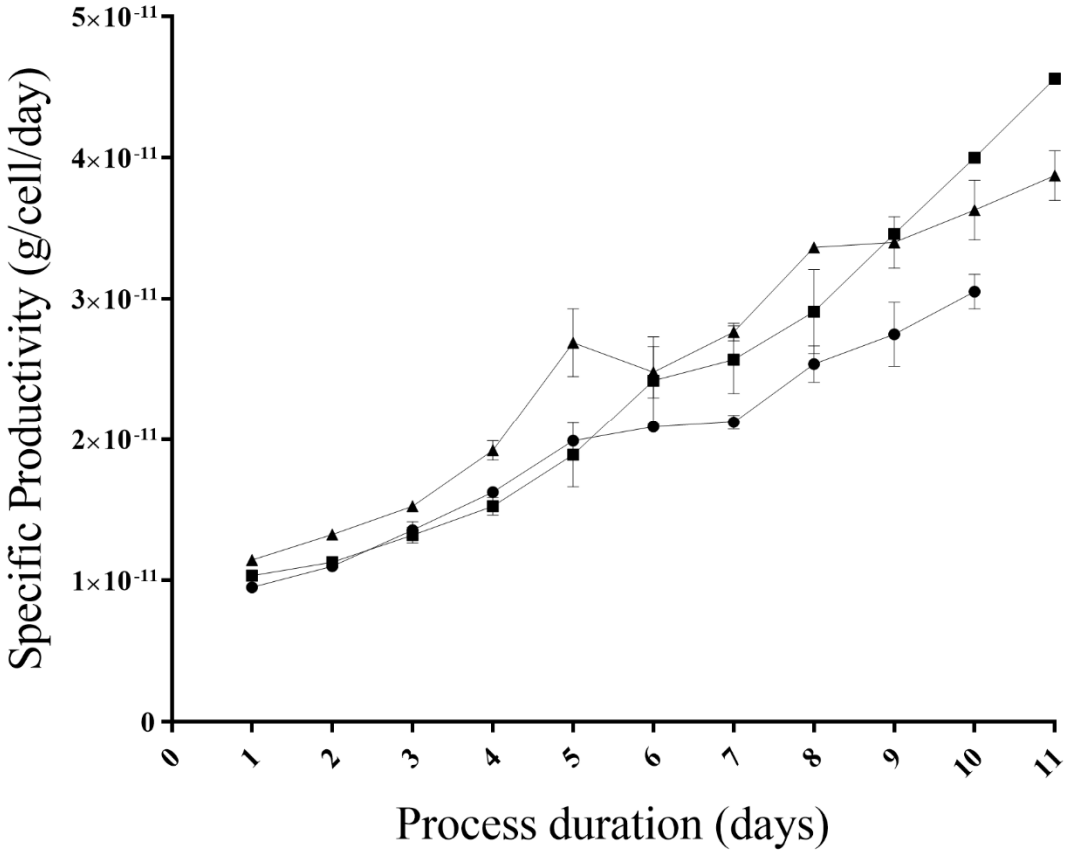

Figure 68 Cell specific productivity (g/cell/day) representing the process performance of the production phase vessels in Experiment 4.2
Cell specific productivity (g/cell/day) measurements are plotted against process duration (days); symbols and ●, ▲ and ■ represent dilution rates 1.0, 0.75, and 0.5 VVD, respectively (n=2).

Specific productivity measurements for all cultures were observed to increase linearly throughout the process duration (Figure 68). During the exponential growth and at maximum viable cell density, day four and eight respectively, the cultures presented higher specific productivity in the 0.75 VVD dilution rate cultures compared with equivalent 0.5 and 1.0 VVD cultures. Specific productivity for 1.0 VVD cultures was consistently lowest throughout the second half of the culture. The observed specific productivity measurements at harvest were (3.0±0.1), compared with (4.5±0.0) and (3.9±1.8) $x10^{-11}$ g/cell/day, for 0.5 and 0.75 VVD cultures, respectively.

Table 7 Percentage monomer post Protein A purification of production cultures at harvest, inoculated with cells from perfusion cultures of respective dilution rates (Experiment 4.2)

Dilution Rate (VVD)	Monomer (%)
1.0	(96.1±2.6)
0.5	97.9 (n=1)
0.75	(95.6±2.4)

Finally, the product quality of the mAb expressed from Cell line 1 was not observed to be impacted by the dilution rate. Monomer percentage observed post Protein A purification was greater than 96% for all dilution rate cultures (Table 7).

4.4 Discussion

Within Experiment 4.1, differences were observed in the performance of microscale production cultures that had previously been cultured in the microscale perfusion methodology when compared to bench scale, ATF perfusion derived cultures. In a dynamic cell culture environment such as perfusion, it is challenging to isolate individual elements contributing to the observed performance differences.

One of the nuances of the microscale perfusion sedimentation methodology is an oscillating supply of nutrients to the culture. If this element was a contributing factor, an inherent sensitivity of the cell line performance to dilution rates may be observed when studied in isolation. Therefore, Experiment 4.2 focused on understanding the cell line's response to reduced dilution rate. This was conducted exclusively at bench scale utilising the ATF perfusion technology to achieve high accuracy in the dilution rate applied.

All perfusion cultures (dilution rates 0.5, 0.75, and 1.0 VVD, respectively) established exponential growth during the initial batch phase. This continued through the operation of the perfusion cultures, before inoculation of production cultures.

The dilution rates are observed in the glucose concentrations present in the cultures immediately after perfusion was initiated. The higher dilution rates supply larger quantities of glucose, in addition to the other key metabolites. The lactate concentrations for all cultures were observed below 2g/L for the duration of the perfusion step, indicating exponential growth was maintained throughout the culture duration.

The highest and lowest dilution rates (1.0 VVD and 0.5 VVD, respectively) both reach the criteria for the transition by the eighth day post inoculation. The 0.75 VVD perfusion condition

lagged behind the other conditions and took an additional day to reach criteria for transition, day nine. No indication for the reasons behind this lag in culture growth was observed in any of the measured parameters. The alignment of the higher (1.0VVD) and lower (0.5VVD) dilution rate culture performances suggest that it is not related to the dilution rate applied. Perfusion cultures all experienced very high culture viability percentages throughout their operation (>98%).

The production phase vessels were successfully inoculated with the respective perfusion cultures. Culture growth performance was comparable to that achieved in the respective bench scale cultures in Experiment 4.1. The cultures grew exponentially to day seven, followed by a stationary phase, and harvest on day 11. Peak viable cell densities were not significantly different (p-value > 0.05), (38.4±3.4, day seven), (41.1±5.2, day five) and (49.9±4.7, day six) $x10^6$cells/mL for 0.5, 0.75 and 1.0 VVD dilution rate cultures, respectively.

All cultures were observed to increase titre over process duration up to a peak at day eight, with (1019±143), (1102±64) and (977±15) mg/L, for dilution rates 0.5, 0.75 and 1.0 VVD, respectively (Figure 67).

This comparability in growth and productivity across dilution rates indicates no sensitivity to dilution rate was observed for Cell line 1. Potential causes for micro scale performance differences, compared with bench scale, may be attributed to a sensitivity to the unique physiochemical characteristics present during the sedimentation process, specifically pH, DO, and a loss of culture agitation.

Chapter 5 The Evaluation of Fed-Batch Culture Performance in Response to Targeted Parameter Deviation Before and After Controlled Inoculation

5.1 Introduction

Transfected, monoclonal CHO cell lines exhibit cell line specific traits and sensitivities that are evaluated during bioprocess development. This is conducted by evaluating critical process parameters (CPPs) and operation ranges through the Quality by Design (QbD) manufacturing principles (Looby et al., 2011). The QbD approach leads to a wealth of information generated on the process robustness and the relative impact on Critical Quality Attributes (CQAs) (A. S. Rathore, 2009; Anurag S. Rathore & Winkle, 2009).

In this risk averse environment, the QbD approach will narrow the operational window; starting from a wide knowledge base gained through iterative investigation, to a smaller investigative space. The approach concludes with a tightly defined operational window specific to the product (Read et al., 2010). This approach safeguards the manufacturing process steps by defining product specific CPP operational ranges. Operation of the process within defined ranges ensures CQAs are achieved (Nagashima, Watari, Shinoda, Okamoto, & Takuma, 2013).

Fed batch bioprocessing exposes the cultures to a progressive evolution of cell cycles. Cultures are assumed to grow exhaustively and transition into stationary and death phases (Selvarasu et al., 2012). The CPP operational range is evaluated from inoculation to harvest. Therefore, this is defined by the phase of operation that exhibits the highest sensitivity to variation or assumes a constant response to variation throughout the culture progression. By simplifying the process in this manner it enables a single operational window to be defined for each CPP, aligning with QbD principles.

Continuous culture operation differs from fed-batch in the sense that it exists primarily in one phase of operation (exponential growth) and culture success is defined by performance within this one phase, rather than across the progression of fed batch operation (Clincke et al., 2013). Therefore, the culture's longevity is enhanced by the application of control strategies specific to the exponential phase, rather than considering the culture characteristics present during inoculation and stationary/decline phases, respectively.

Observed through experimental evaluations in Chapters 3 and 4 is strict adherence to pH setpoint during inoculation (Figure 20, Figure 32, Figure 54 & Figure 60). The fluctuations

discussed in gravity cell settling and perfusion occur once the cultures had established exponential growth, past an initial phase of batch growth (three to four days).

The experiments and discussion presented within this chapter aim to understand the cell line sensitivities present within the progressive phases of operation of fed batch culture. This will inform the creation of CPP control strategies for continuous cultures that emphasises the importance of appropriate control of the exponential growth phase of operation.

Additionally, due to the extended duration of continuous culture, cell line sensitivities that may present through extended operation are investigated. These may exist from the high culture age generated or through exposure to high nutrient environments (Frye et al., 2016). The cell line responses are investigated both in isolation and included in the evaluation of phase sensitivity for a comprehensive understanding of sensitivity.

5.2 Materials, Methods and Experimental Designs

This chapter contains two independent experiments, 5.1 and 5.2. These experiments were both conducted as fed-batch operated ambr®15 systems, in the 24 and 48 vessel system variants for 5.1 and 5.2, respectively. The materials and methods are presented in Chapter 2, with exceptions specifically noted.

5.2.1 Generation of Cell Banks

Three distinct cell banks were generated by the controlled expansion of cells revived from DCB1. These three cell banks are defined as DCB2, DCB3, and DCB4. The expansion of DCB1 and the creation of these cell banks are presented in Section 5.3.1 Preliminary Data, Cell Bank Generation.

5.2.2 Experiment 5.1

Experiment 5.1 contains two distinct experimental designs, Experiment 5.1a, and 5.1b. These were conducted simultaneously on culture stations (CSs) one and two of an ambr®15 system (24 vessel variant), respectively.

In Experiment 5.1a, each condition inoculated in triplicate. The conditions were defined by the use of inoculum derived from the 4 independent cell banks of Cell Line 1 (Section 5.2.1 Generation of Cell Banks).

DCB1 represents the controlled expansion of inoculum from a frozen vial, with minimal generation number accumulation as would be designed in the process description of commercial fed batch bioprocess. DCB2 is an extension of this inoculum expansion over a

period of >100 generations, providing an upper limit or "manufacturing window" for the operation of a commercial bioprocess. The suitability of this 'manufacturing window' is determined by the cultures maintenance of Key Performance Indicators (KPIs) (Alvin & Ye, 2014).

DCB3 and DCB4 represent the preparation of an inoculum utilising continuous methods, both in the exposure to an enriched medium environment (DCB3) and the extension of the generation numbers beyond the 'manufacturing window' (>120 generations, DCB4). All cultures within CS1 are operated at the experimental set points for Cell line 1, as detailed in Chapter 2.

Experiment 5.1b was inoculated with cells from a vial expanded from DCB1. The focus of the experiment was to observe the differences in the cell line's response to changes pH, occurring during inoculation or exponential growth. Presented in the operation of Cell line 1 through Chapters 3 and 4 is an insensitivity to pH variation (>0.4 units) that conflicts expected sensitivity of >0.1 units deviation from setpoint (Brunner, Fricke, et al., 2017).

Four pH conditions were evaluated in triplicate. Three of these conditions were operated from inoculation through to harvest. They are referred to as 'Basic', 'neutral', and 'Acidic', defined by a target pH of (7.2±0.1), (7.0±0.1) and (6.8±0.1), respectively. The fourth condition was inoculated at pH (7.2±0.1), and the pH setpoint was reduced to (6.8±0.1) as the culture progressed through exponential growth. This fourth condition is referred to as 'drift'. A detailed outline of pH setpoint and cell bank used for inoculation is provided below, Table 8.

Table 8 Experimental conditions for vessels in Experiment 5.1
The conditions were conducted in triplicate vessels (V), and the cell bank and pH control setpoints are outlined.

	Experiment 5.1a				**Experiment 5.1b**			
	V1, 2 &3	V4, 5 &6	V7, 8 &9	V10, 11&12	V1, 2 &3	V4, 5 &6	V7, 8 &9	V10, 11 &12
Inoculum Cell Bank	DCB1	DCB2	DCB3	DCB4	DCB1	DCB1	DCB1	DCB1
pH setpoint, at inoculation	(7.2±0.1)	(7.2±0.1)	(7.2±0.1)	(7.2±0.1)	(7.2±0.1)	(7.0±0.1)	(6.8±0.1)	(7.2±0.1)
pH setpoint, at exponential growth	(7.2±0.1)	(7.2±0.1)	(7.2±0.1)	(7.2±0.1)	(7.2±0.1)	(7.0±0.1)	(6.8±0.1)	(6.8±0.1)

5.2.3 Experiment 5.2

During the inoculation of Experiment 5.2, the optimal pH, dissolved oxygen, and temperature setpoints for Cell line 1 (detailed in Chapter 2) were applied to all vessels within an ambr 48® system. Following successful inoculation and transition into exponential growth, the experimental conditions were applied (Table 9). As an extension to the investigation of pH in Experiment 5.1b, Experiment 5.2 explores unexpected variation occurring during the exponential growth phase in order to understand potential impacts on culture longevity in a continuous setting. Understanding of the impacts and potential sources of variation will allow control strategies to be adapted to safeguard bioprocess operation.

Additional context of how these elements of variation may occur in a controlled system is provided (Table 9) as they are classified as 'equipment failure' (EF) or 'operator error' (OE).

Table 9 Experiment 5.2 Conditions and the Classification of the Source of Variation
Equipment Failure (EF) and Operator Error (OE) are defined for each condition, respectively. The conditions were replicated in four culture stations of an ambr®15 48-variant system

Vessel #	Process variation	Classification
1	Control condition	N/A
2	pH drift upwards	EF
3	pH drift downwards	EF
4	Dissolved Oxygen 30%	EF
5	Double antifoam addition	OE
6	Dissolved Oxygen 40%	EF
7	Triple antifoam addition	OE
8	DCB3 Inoculated	OE
9	DCB3 Inoculated	OE
10	Dissolved Oxygen 60%	EF
11	Control condition	N/A
12	Dissolved Oxygen 70%	EF

5.2.3.2 Equipment Failure (EF)

5.2.3.2.1 pH

In vessels 2 and 3, a fluctuating pH profile was generated to simulate the failure of a pH probe. Probes were simulated to drift either upwards or downwards from the operational setpoint over a period of 24 hours. This drift was corrected back to setpoint at the end of each 24 hours, as would occur during routine daily maintenance.

This simulation was conducted by instructing the top deadband to cycle through an increase or decrease of 0.1 units every 24 hours. These steps were repeated for the duration of the

experiment from day 2 onwards. After successful inoculation at setpoint (7.2±0.1), this condition acted on the culture's exponential growth phase and continued into stationary, and death phases.

5.2.3.2.2 Dissolved Oxygen (DO)

In vessels 4, 6, 10, and 12 on each of the four culture stations, dissolved oxygen (DO) setpoint to control at 30, 40, 60, and 70%, respectively. This was performed to simulate an incorrectly calibrated DO probe. Culture oxygen consumption from the saturated environment at inoculation will gradually decrease levels to the defined setpoints. Therefore, the impact of this condition was not represented by cultures until 24-48 hours post inoculation, when the saturation levels stabilise at setpoint.

5.2.3.2.3 Temperature

The impact of hypothermic temperature shifts has been extensively studied for mammalian bioprocessing during or after exponential growth (Bastide et al., 2017; Birch & Racher, 2006; Gomez et al., 2012; Kaufmann et al., 1999). Therefore, within Experiment 5.2 on each of the conditions outlined in Table 9, hyperthermic stress was investigated during late exponential growth.

The hyperthermic temperature condition was achieved through the removal of the active cooling system of the ambr® system on day 12. The measured culture temperature displayed an increase to >38°c for all cultures, maintained over 24 hours.

5.2.3.3 Operator Error

5.2.3.3.1 Antifoam

The control level addition of antifoam (20µl per vessel) was provided to each condition every 48 hours, starting from day two onwards. Vessels five and seven on each culture station received additional antifoam additions, 20µl (double) and 40µl (triple), respectively. This was performed to simulate miscalculation and over-addition of antifoam into the reactor.

5.2.3.3.2 Exposure to Continuous Culturing Environment

Vessels 8 and 9 utilised an inoculum of cells from DCB3. As detailed above (5.2.1 Generation of Cell Banks), this cell bank was generated through exposure to a continuous culture environment, prior to cryopreservation. This condition provides an example of the performance of an exponential phase from a culture operated through a continuous method.

This variation occurring before inoculation may occur either by error or by design. In error, the selection of the wrong medium components or raw material impurities may lead to exposure of the cells to enriched medium prior to inoculation. By design, the utilisation of continuous bioprocessing methods in the inoculum expansion (as detailed in Chapter 4), will expose the cells to enriched medium environment prior to their production vessel inoculation.

5.2.3.4 Data Analysis

During Experiment 5.1, conditions are conducted in triplicate, and data is reported as means and standard deviations (SDs), provided in the format mean ± SD. Paired or unpaired two tailed t-tests were used, where appropriate, to determine significance between conditions.

In Experiment 5.2, the growth performance of the two control vessels per CS (vessels 1 and 11) was analysed with respect to each other. No variation was seen in control vessels across culture stations in the same position within their respective culture station. In addition, a significant difference (p-value < 0.05) was seen in the profiles of viable cell densities of control vessels within the same CS (vessels 1 and 11), throughout the experiment. Variation within each culture station is highlighted as no variation is seen between biological replicates in vessel positions nearby (vessel 8 and 9) on each culture station.

Vessels of the same condition across cultures stations are reported as replicates (n=3) and reported as means and standard deviations (SDs), provided in the format mean ± SD. Comparisons of significance against control are made between conditions and respective control vessel given the position; in either the first half (vessels 1 to 6; control from vessel 1) or the second half (vessels 7 to 12; control from vessel 11) of the CSs. Assessment of significance is made by one-way ANOVA, significance reported where $P < 0.05$.

The fourth culture station was omitted from the analysis as a programming error caused experimental variation in the temperature control when compared to the other three replicate culture stations.

5.3 Results

5.3.1 Preliminary Data, Cell Bank Generation

In DCB2 (high generation cell bank), cells were revived and passaged in basal medium twice to three times weekly, over a period of 102 days. Over this time the generation numbers were tracked and upon exceeding 100 generations a cell bank was laid. This cell bank consisted of 10 vials cryopreserved at 1 $x10^7$ cells/vial, in basal medium containing 10% DMSO.

The sawtooth plot of this expansion is presented in Figure 69, providing a visual representation of the viable cell density achieved at each passage. The vertical lines of the sawtooth link each viable cell density to the seeding density of the following passage.

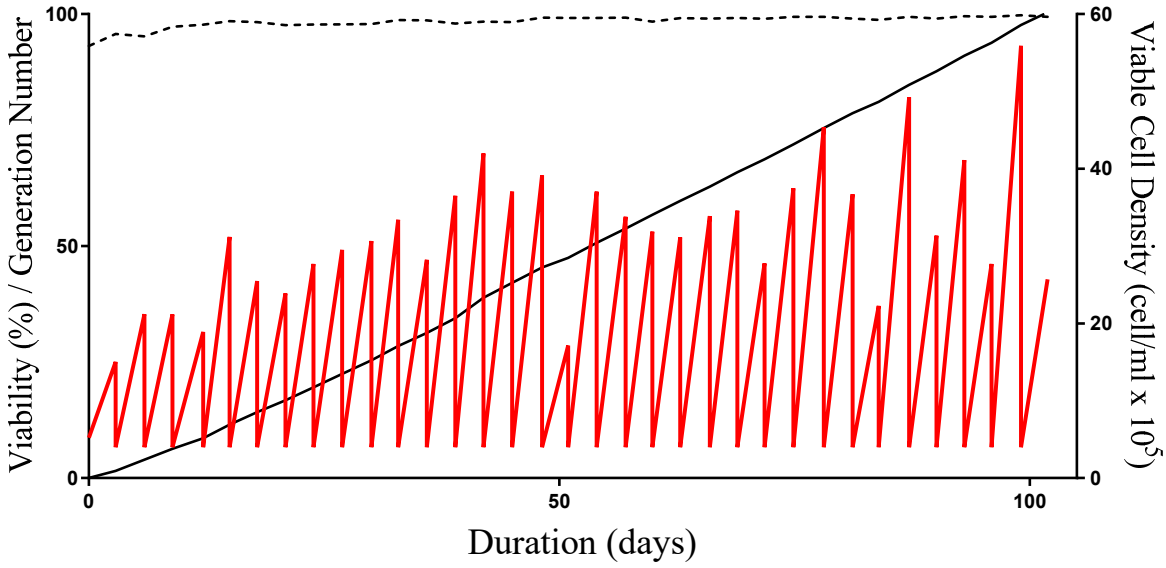

Figure 69 Saw-Tooth plot of the expansion of DCB1 in the generation of DCB2
Viable Cell Density (cell/mL x10^5) (right axis, solid red line), Viability (%) (left axis, dashed black line) and Cumulative Generation Number (left axis, solid black line) are plotted against Duration (days)

The viability of the cultures presented in Figure 69 was consistently maintained above 95% viability for the duration of the expansion. The average viable cell density reached at subculture was (33±13) cell/mL x10^5. The reproducible viability and cell density achieved in repeated subculture as cell generation numbers increased highlights the ability of the cultures to reproducibly enter exponential growth following inoculation.

For DCB3 (Enriched medium exposure cell bank), cells were revived and passaged in basal medium prior to inoculation into a 3L STR vessel (1.5L working volume). This vessel was equipped to remove the culture (cells plus spent medium) through a dip-tube, installed onto the head-plate of the vessel. Any removed culture was replaced with fresh medium to maintain the 1.5L working volume. Cells were grown in batch over the first four days of culture, without any medium removal/replacement. On day five of culture, the dilution rate of the vessel was initiated and was maintained between 0.36 and 0.45 VVD, until DCB3 was cryopreserved.

During inoculation, the volume in the vessel was comprised of basal medium. Basal medium was used for media exchange over the initial 20 days of culture dilution and the culture averaged a cell density of (6.4±1.4) cell/mL x10^6 was observed. Whilst variation is present in the viable cell density measurements, a steady state is determined to be established during this

20 day period. The enriched medium formulation was connected on day 26 of culture. Due to unforeseen challenges with media availability, the culture was required to return to basal media exposure whilst replacement enriched media was prepared. The culture existed in enriched media for 10 days followed by seven days in basal media before returning to enriched media exposure.

On day 42 of culture, the enriched medium was connected to the exchange for a second time and the culture was operated with this medium formulation for a 20 day period as per the initial basal media exposure. The cells were cryopreserved on day 62. The respective viable cell concentration and viability obtained from the culture is presented in Figure 70, below.

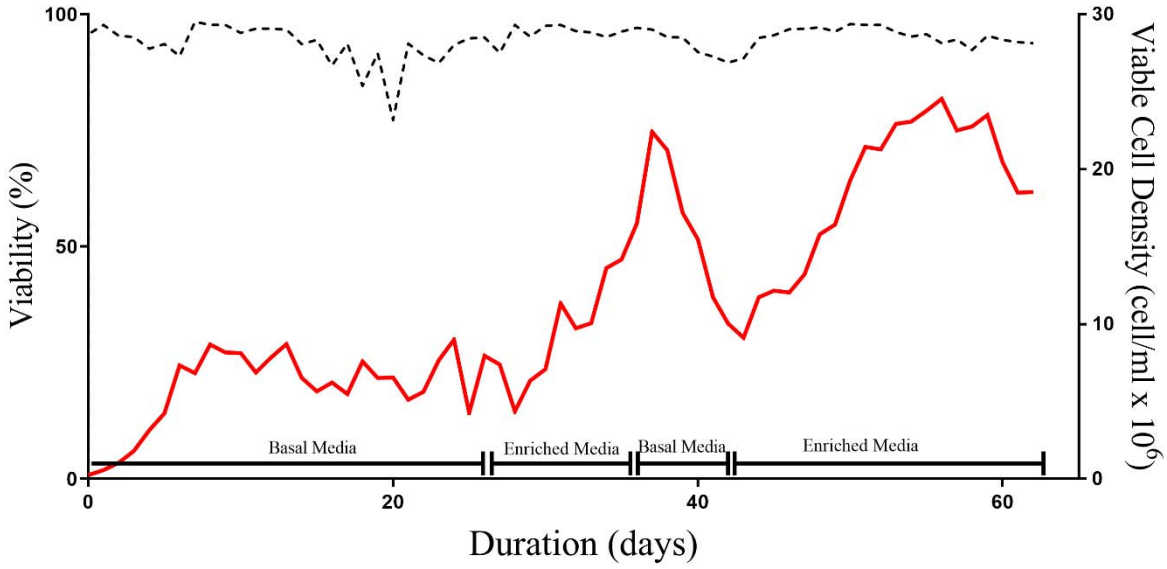

Figure 70 The expansion of DCB1 within a continuous bioprocessing environment, with exposure to enriched medium, in the generation of DCB3
Viable Cell Density (cell/mL x10^6) (right axis, solid red line) and Viability (%) (left axis, dashed black line) are plotted against Duration (days)

Following the 62 day culture, cells were removed aseptically and cryopreserved to generate the cell bank. This cell bank (DCB3) consisted of 10 vials cryopreserved at 1x10^7 cells/vial, in basal medium containing 10% DMSO.

As presented in Figure 70, high viability was observed throughout the expansion. The culture responded to the enriched medium with an increase in viable cell density. This increase occurred during both instances of the enriched medium introduction. The culture reached a peak during the second enriched medium treatment at 23.0 cell/mL x10^6, on day 56.

A further cell bank with a very high generation number, DCB4, was generated by reviving a vial from DCB3 into basal medium.

Following the revival, cells were passaged in basal medium twice to three times weekly, over a period of 102 days. Over this time the generation numbers were tracked and surpassed 120 generations, in addition to those accumulated in the generation of DCB3, at the generation of DCB4. This cell bank consisted of 10 vials cryopreserved at $1x10^7$ cells/vial, in basal medium containing 10% DMSO.

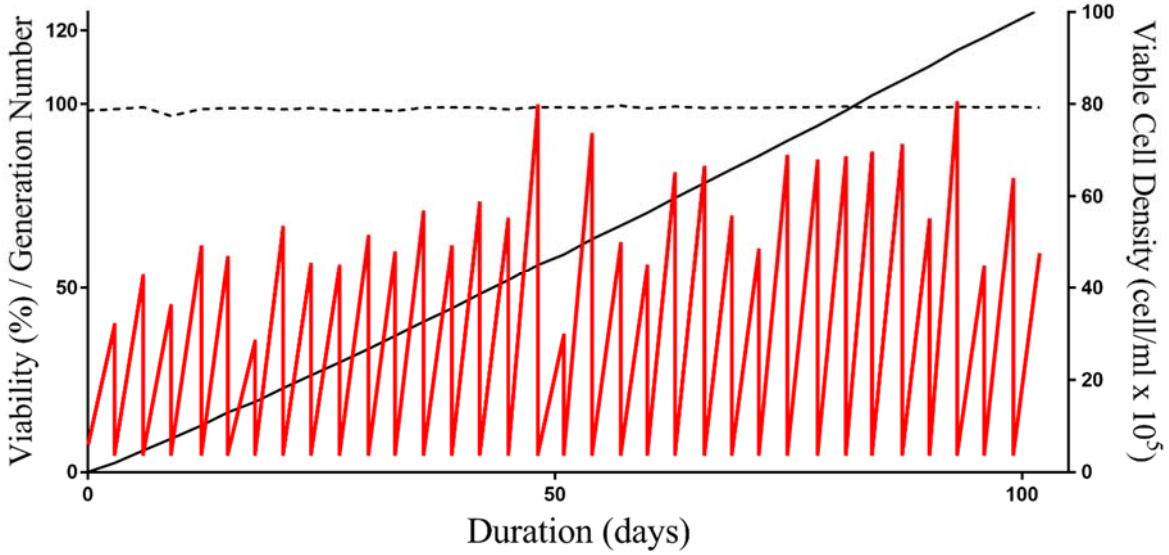

Figure 71 Saw-Tooth plot of the expansion of DCB3 in the generation of DCB4
Viable Cell Density (cell/mL $x10^5$) (right axis, solid red line), Viability (%) (left axis, dashed black line) and Cumulative Generation Number (left axis, solid black line) are plotted against Duration (days)

The viability of the cultures presented in Figure 71 was consistently maintained above 95% for the duration of the expansion. The average viable cell density reached at subculture was higher than that experienced for DCB2, (52.8±15.6) cell/mL $x10^5$. The increased viable cell density at subculture contributed additional generation numbers to be accumulated over the same time period as DCB2.

5.3.1 Experiment 5.1a - Cell Line Sensitivity to Cell Age and Enriched Media Exposure

The inoculum cultures of the four cell banks were all successfully inoculated in triplicate, into CS1 of the ambr® system (as detailed in Table 8). The viable cell density (VCD) measurements observed for cultures in Experiment 5.1a is presented in Figure 72, below

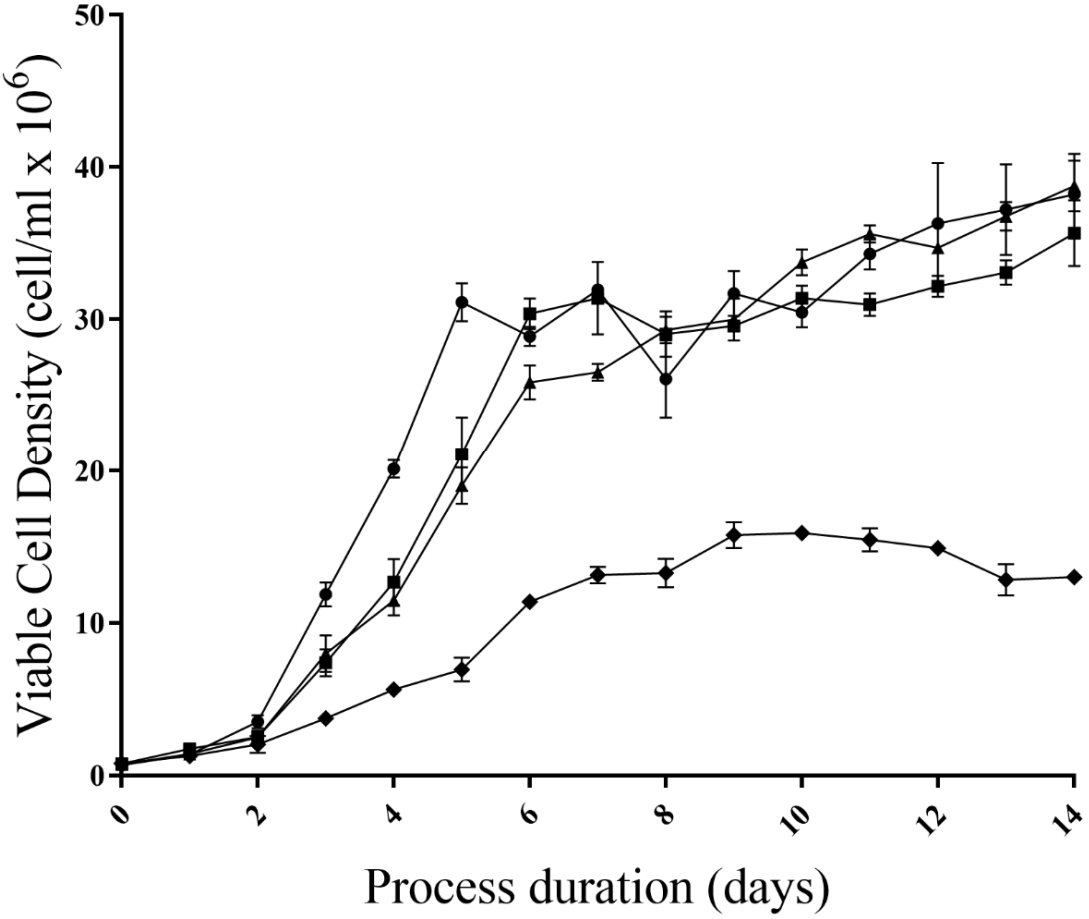

Figure 72 Viable cell density (VCD) of cultures within Experiment 5.1a plotted over duration (days)
Viable cell density, cells/mL x10^6, is plotted for DCB1 (◆), DCB2 (■), DCB3 (▲) and DCB4 (●), respectively.

On the first two days after inoculation comparable growth was observed, with no significant variation (P-value > 0.05) in the VCD between conditions. The average VCD measurements for all cultures was (1.5±0.2) and (2.6±0.6) x10^6 cells/mL for the first and second days, respectively. The addition of the first nutrient feed on the second day, as per the fed-batch protocol (detailed in Section 2.2 Cell line, Medium and Bioreactor systems), supported the exponential growth of the cultures.

On the third day of the process, significant differences were observed between the cultures and this continued throughout exponential growth. Those cultures inoculated with cells from DCB4 displayed the fastest growth rate, reaching a peak viable cell density of (3.1±0.1) x10^7 cells/mL of the exponential growth phase by day five. The VCD measurements for DCB4 were significantly higher (P-value <0.05) than for DCB1, DCB2, and DCB3 on days three to five, respectively.

Following the exponential growth of DCB4, the VCD plateaus and the cultures entered a stationary phase on day six. This stationary phase was maintained until day 10, and the viable cell density on day 10 was not significantly different from that observed on day five (p-value = 0.50). A rise in VCD was observed for DCB4 on the final days (day 11 to 14) of the culture, resulting in a universal VCD peak of (3.8±0.3) $x10^7$ cells/mL, recorded on the day of harvest (day 14).

Cultures inoculated from DCB2 and DCB3 displayed comparable VCD measurements throughout exponential growth, P values = 0.53, 0.31, and 0.26 for days three, four, and five, respectively. Both conditions transitioned into a stationary phase after day six of the process. The DCB2 inoculated cultures reached a significantly higher peak VCD during exponential growth than those from DCB3, (3.0±0.1), and (2.6±0.1) $x10^7$ cells/mL, respectively. Significant differences between the two cultures were also observed on the following day (day seven), (3.1±0.2) and (2.7±0.1) $x10^7$cells/mL, for DCB2 and DCB3, respectively. The VCD measured during the remaining culture duration followed the trend observed for DCB4, whereby an increase was observed during the second half of the process resulting in a peak that exceeds that for the exponential growth phase. On the day of harvest (day 14) the VCD measurements were, (3.6±0.2) and (3.9±0.2) $x10^6$cells/mL for DCB2 and DCB3, respectively.

The DCB1 cultures were observed to enter exponential growth following day two. The VCD through exponential growth and measured peak viable cell density (1.6±0.1) $x10^7$ cells/mL, observed on day nine) was significantly lower than those measured for DCB2, DCB3, and DCB4, respectively. These cultures enter a stationary and death phase following the exponential growth and measured VCD at harvest was (1.30±0.03) $x10^6$cells/mL.

The viability for the cultures in Experiment 5.1a is presented in Figure 73, below.

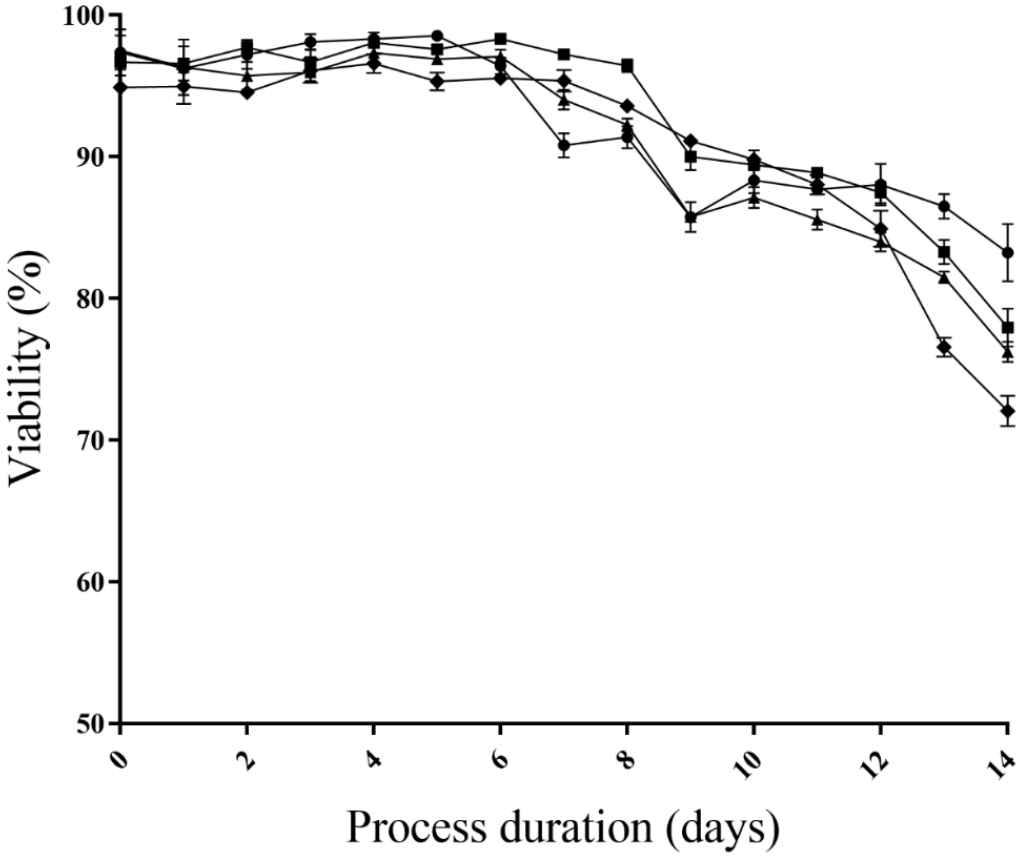

Figure 73 Percentage viability of cultures within Experiment 5.1a plotted over duration (days)
Viability (%) is plotted for DCB1 (◆), DCB2 (■), DCB3 (▲) and DCB4 (●), respectively.

All cultures in Experiment 5.1a were observed to have high viability (>95%) at inoculation. This high viability was maintained as the cultures progressed through exponential growth, until day six. On day seven a decrease in viability was observed in DCB4, to (90.8±0.8) %, whilst other cultures remained high (>95%). On day 9, the viability had decreased in all cultures to < 95%.

As the cultures progressed through stationary and death phases, the viability decreased in all cultures. Viability measurements at harvest (day 14) were significantly lower ($P<0.05$) in all cultures, compared to the respective culture viability measured at the end of exponential growth. The fluctuating rates of decline in viability resulted in harvest viability of (72.0±1.1), (78.0±1.4). (76.2±0.7) and (83.2±2.0) %, for DCB1, DCB2, DCB3 and DCB4, respectively.

As detailed in Section 2.3 At-line and Offline Sample Analysis, glucose was actively maintained within fed-batch cultures through daily measurement and addition. A maintenance range of 2 to 6g/L was targeted. The glucose concentrations (g/L) are reported in Figure 74, and display the maintenance of glucose throughout the experiment.

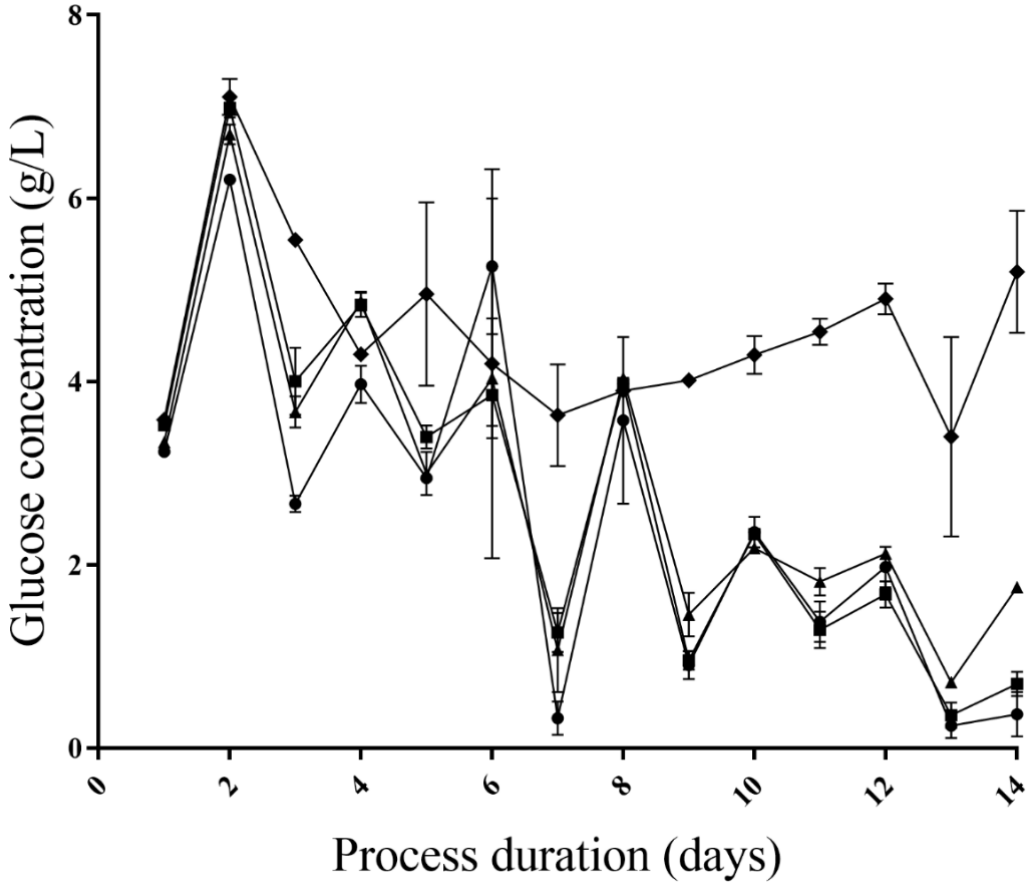

Figure 74 Glucose Concentration of cultures within Experiment 5.1a plotted over duration (days)
Glucose concentration (g/L) is plotted for DCB1 (◆), DCB2 (■), DCB3 (▲) and DCB4 (●), respectively.

Glucose measurements on the first day of culture <5g/L triggered glucose addition in all cultures, and subsequent peak concentrations >6g/L for all vessels were observed on day two of culture. Following this peak, concentrations through exponential growth, up to day six, were controlled within the targeted 2 to 6g/L range for all cultures. On day seven, DCB2, DCB3, and DCB4 all measured glucose concentrations <2g/L. These cultures have previously been identified as showing high VCD (Figure 72). These cultures required improvements in the glucose control strategy to maintain glucose concentration where high viable cell concentration is combined with high cell specific glucose consumption rate. Whilst < 2g/L was a deviation from the target range, the glucose concentration did not enter a limited state (Glucose concentration = 0 g/L).

The glucose feedback control loop was initiated at each timepoint where concentration measurements were conducted. The resulting measurement on day eight, following day seven being below the target range, was within the target range. There is a further decrease in measured glucose to, and below, 2g/L in the subsequent samples on days 9, 11, 12, and 13,

respectively. This fluctuation at the lower target highlights challenges of maintaining glucose concentrations within a high VCD environment.

Conversely, the DCB1 cultures displayed concentrations within the target range throughout the exponential, stationary, and death phases, through to harvest on day 14.

The contribution of VCD to variation in controlled glucose concentration requires that the cell specific glucose consumption rate be consistent across all vessels and phases of the process. The cell specific glucose consumption rate for Experiment 5.1a is presented below, in Figure 75.

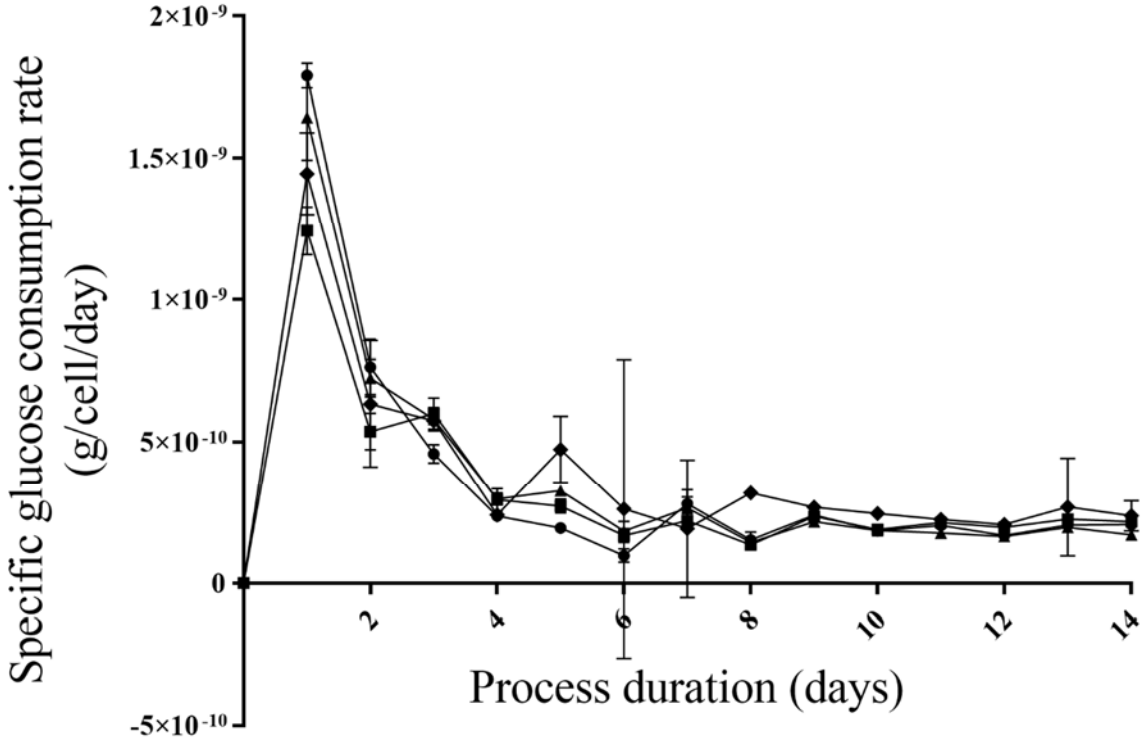

Figure 75 Cell specific glucose consumption of cultures within Experiment 5.1a plotted over duration (days)
Specific glucose consumption rate (g/cell/day) is plotted for DCB1 (◆), DCB2 (■), DCB3 (▲) and DCB4 (●), respectively.

The calculated cell specific glucose consumption rate (g/cell/day) peaked on day one, with values of (1.4±0.2), (1.2±0.1), (1.6±0.2) and (1.8±0.0) $x10^{-9}$ g/cell/day, for DCB1, DCB2, DCB3 and DCB4, respectively. The cell specific rates in all vessels were observed to decrease from day one to day four. On day four, the average cell specific consumption rate for all vessels was (2.7±0.4) $x10^{-10}$ g/cell/day. Similarly, the average for all vessels during stationary phase (day nine) and at harvest (day 14) was (2.4±0.2) and (2.1±0.4) $x10^{-10}$ g/cell/day, respectively.

The rate of cell specific glucose consumption for DCB1 cultures was significantly higher than each of the other cultures on days eight, nine, and ten, respectively.

Measured lactate concentrations within cultures represent the glucose consumption and back metabolism, respectively. The measure lactate concentrations are presented in Figure 76, below.

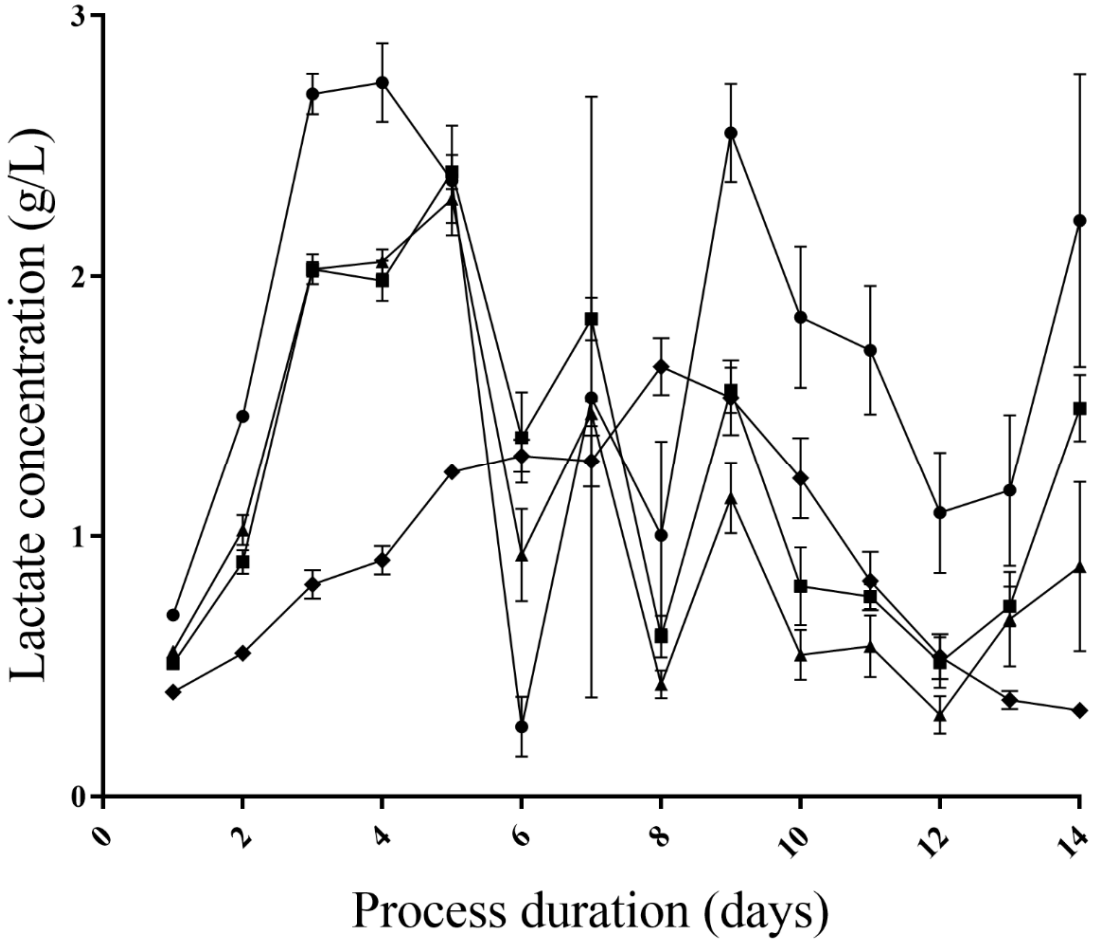

Figure 76 Lactate concentration of cultures within Experiment 5.1a plotted over duration (days)
Lactate concentration (g/L) is plotted for DCB1 (◆), DCB2 (■), DCB3 (▲) and DCB4 (●), respectively.

The lactate concentration for DCB1 cultures increased from (0.4±0.0) g/L on day one, to a peak of (1.7±0.1) g/L on day eight of culture. Following this peak, a decline in the lactate concentration was observed and decreased to (0.3±0.0) g/L at harvest (day 14). The peak concentration and the concentration at harvest were both significantly lower ($P<0.05$) than that observed for DCB2, DCB3, and DCB4, respectively.

The concentration of the DCB2, DCB3 and DCB4 cultures on day one of culture was (0.5±0.0), (0.6±0.0) and (0.7±0.0) g/L, respectively. On day three of culture, the concentration had increased to (2.0±0.0), (2.0±0.1), and (2.7±0.1) g/L for DCB2, DCB3, and DCB4, respectively.

Paired average profiles for DCB2 and DCB3 displayed no significant difference from inoculation to day nine of the experiment (P-value = 0.19). A peak in lactate concentration was observed on day five for DCB2 and DCB3, (2.4±0.1) and (2.3±0.1) g/L, respectively. DCB2 and DCB3 exhibited fluctuations in their lactate concentrations between days nine and 13, in the range of 0 and 2 g/L. The concentration was observed to increase at harvest and was measured as (1.5±0.1) and (0.9±0.3) g/L, respectively.

The DCB4 cultures peaked in lactate concentration, (2.7±0.2) g/L on day four, which was significantly higher than the peak lactate concentrations for DCB1, DCB2, and DCB3, respectively ($P<0.05$). DCB4 cultures had decreased to (0.3±0.1) and increased again to (2.6±0.2) g/L on days 6 and 9, respectively. At harvest, DCB4 was observed to have the highest lactate concentration amongst all cultures, (2.2±0.6) g/L.

The acidic and basic environments generated by the increase and decrease in lactate concentration were observed to impact the online pH readings (Figure 77, below).

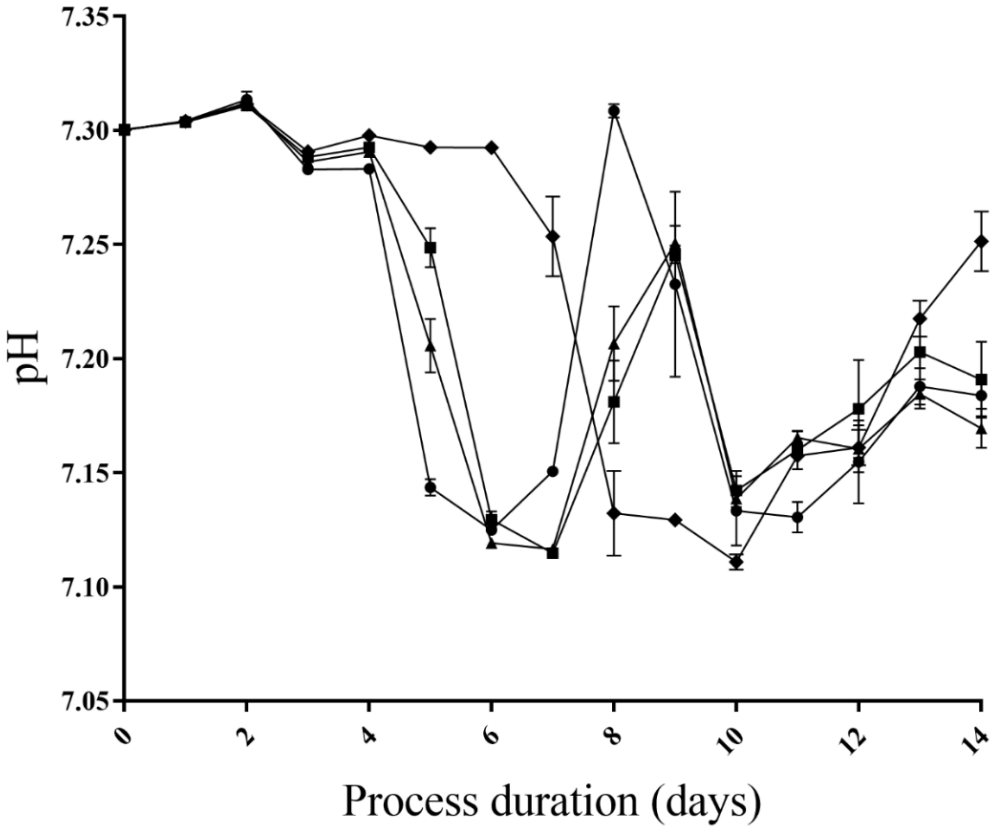

Figure 77 pH of cultures within Experiment 5.1a plotted over duration (days)
Culture pH is plotted for DCB1 (◆), DCB2 (■), DCB3 (▲) and DCB4 (●), respectively.

At inoculation and through the first four days of culture, all vessels were maintained at the upper deadband of the setpoint (7.2±0.1). On day five of culture, the pH of DCB2, DCB3, and DCB4 declined towards the bottom of the deadband, correlating with the increase in lactate concentration (Figure 76). The cultures remained at the bottom deadband (>7.1) through days six and seven, before an increase was observed on day eight. The pH at harvest for DCB2, DCB3, and DCB4 was (7.19±0.02), (7.17±0.01), and (7.18±0.01), respectively.

The pH of DCB1 was controlled within the top deadband until day six, and a decrease in pH was observed that resulted in control within the lower deadband on day eight. From day eight onwards, the pH was observed to increase for the remainder of the process. The pH at harvest for DCB1 was (7.25±0.01), significantly higher than that for DCB2, DCB3, and DCB4, respectively.

The production of the mAb product was analysed from samples taken on day six, and every other day thereafter until harvest. The measured mAb produced (Titre, mg/L) is presented in Figure 78, below.

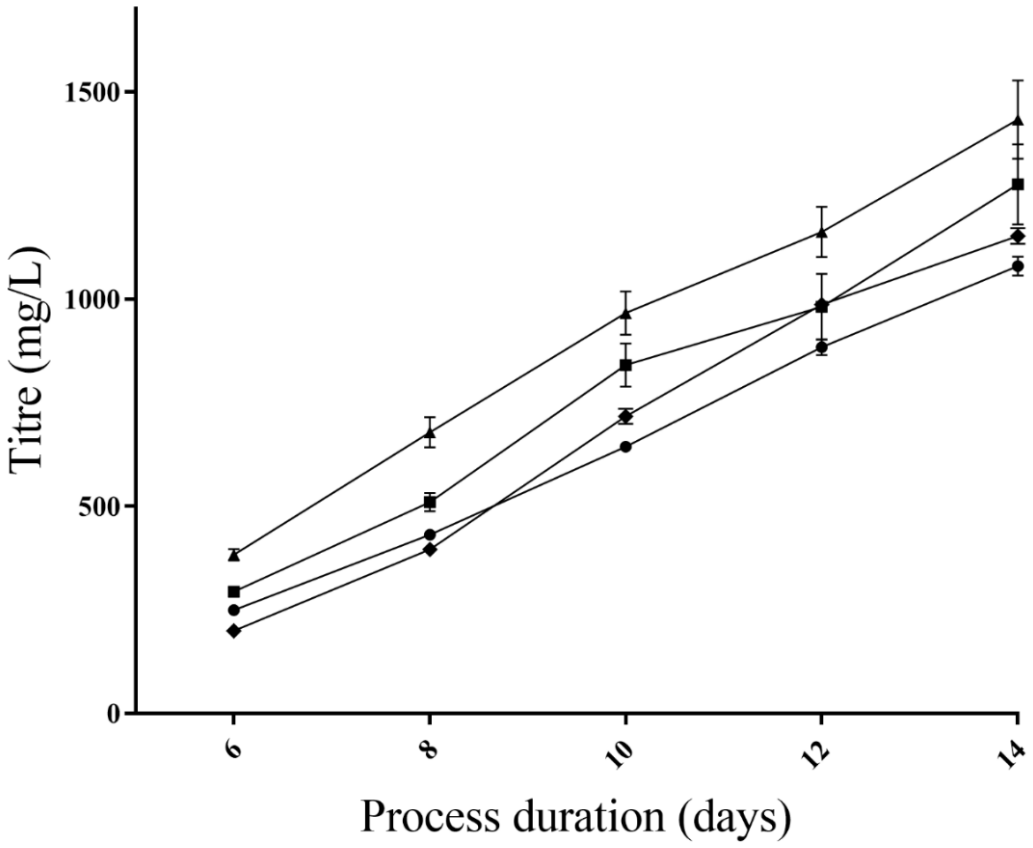

Figure 78 Titre (mg/L) of cultures within Experiment 5.1a plotted over duration (days)
Titre (mg/L) is plotted for DCB1 (◆), DCB2 (■), DCB3 (▲) and DCB4 (●), respectively.

The titre of DCB1, DCB2, DCB3, and DCB4 on day six was (199±2), (294±5), (383±14) and (249±2) mg/L, respectively. The titre of all cultures displayed a linear increase up until harvest, where measurements were (1152±19), (1277±97), (1433±95) and (1079±23) mg/L, respectively. The highest recorded titre on each day was from DCB3, and the value was significantly higher when compared to the second highest value on each day (from DCB2). The lowest value at harvest from DCB4 was significantly lower than that reported for DCB1 ($p<0.05$), (1079±23), and (1152±13) mg/L, respectively.

Ultimately, the higher viable cell density of those cultures derived from DCB1 did not result in an increase in titre. Therefore, the cell banks DCB2, DCB3, and DCB4 were observed to display a decrease in cell specific productivity, compared to DCB1.

Replicate cultures were pooled together and harvested by centrifugation. The clarified supernatant was purified by Protein A HPLC and the mAb product was analysed for aggregation by Size Exclusion Chromatography (SEC). The measured percentage monomer and aggregate for each culture are presented in Table 10, below.

Table 10 Product quality (percentage monomer and aggregates) present for Experiment 5.1a cultures, at harvest, post product capture purification.

Cell Bank	Monomer (%)	Aggregate (%)
DCB1	96.28	3.72
DCB2	97.90	2.10
DCB3	97.16	2.84
DCB4	97.64	2.36

The percentage monomer measured presented low levels of aggregation across culture derived from each cell bank. All cell banks display monomer percentage >96%, and the difference between the lowest and highest is 1.62 %, between DCB1 and DCB2, respectively.

5.3.2 Experiment 5.1b – Culture pH Sensitivity, Magnitude Verses Timing

Experiment 5.1b was successfully inoculated with cells from the DCB1 inoculum cultures. The conditions were conducted in triplicate as outlined in Table 8, above. The VCD measurements from cultures in Experiment 5.1b are presented in Figure 79, below.

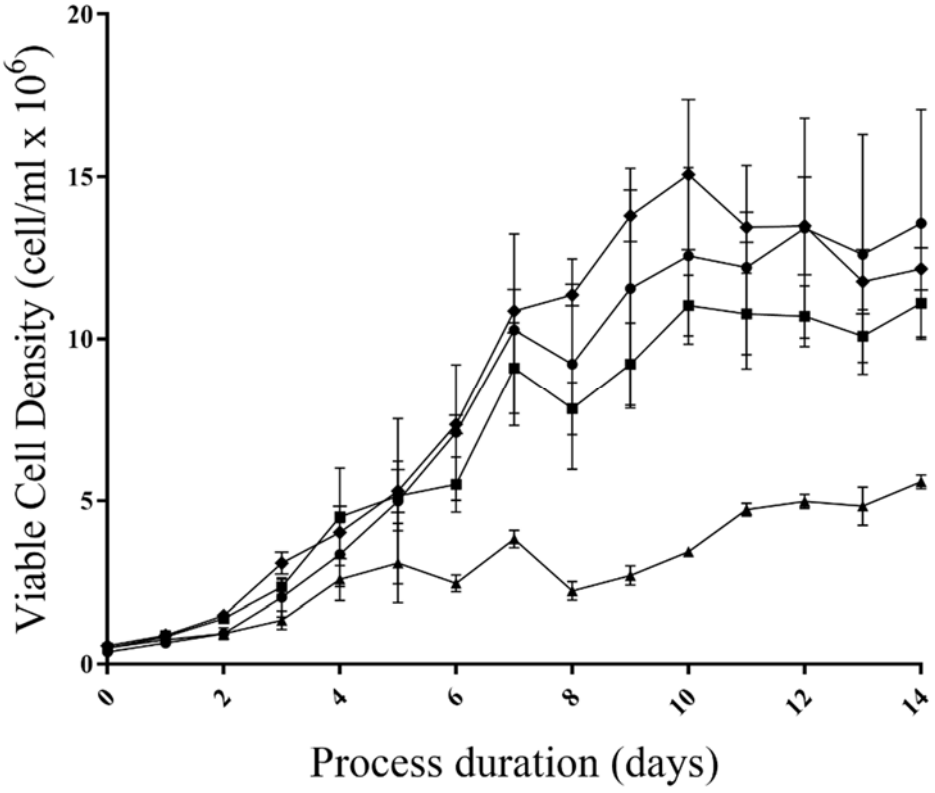

Figure 79 Viable cell density (VCD) of cultures within Experiment 5.1b plotted over duration (days)
Viable cell density, cells/mL x10^6, is plotted for pH conditions 'Basic' (◆), 'Neutral' (■), 'Acidic' (▲) and 'Drift' (●), respectively.

The measured viable cell density of cultures increased over the first two days, reaching an average of (1.2±0.3) x10^6 cells/mL. On day three, the cultures continued their exponential growth. The viable cell density of the 'Acidic' pH condition was observed to be significantly lower than that for the highest 'Basic' condition, (1.3±0.3) and (3.1±0.4) x10^6 cells/mL, respectively. Poor growth of the 'Acidic' condition cultures was observed throughout the duration of the experiment. The measured VCD for the 'Acidic' condition was significantly lower than the next lowest 'Neutral' condition on days six and each day until day 14. The overall poor growth of 'Acidic' condition results is represented by the absence of clearly defined exponential and stationary periods of culture progression, and the viable cell density at day 14 is (5.6±0.2) cells/mL x10^6.

Exponential growth was observed until day seven in the 'Basic', 'Neutral', and 'Drift' cultures and observed VCDs were of (1.1±0.1), (0.9±0.1), and (1.0±0.0) x10^7 cells/mL, respectively. No significant difference is observed between conditions on day seven (p-values= 0.12, 0.75, and 0.56, for 'Basic' to 'Neutral', 'Basic' to 'Drift' and 'Neutral' to 'Drift', respectively). Following day seven, cultures in conditions 'Basic', 'Neutral', and 'Drift' continued to increase their respective VCD through the stationary phase. This continued growth resulted in VCD at harvest (day 14) of (1.2±0.1), (1.1±0.1) and (1.4±0.3) x10^7 cells/mL, for 'Basic', 'Neutral' and 'Drift', respectively. No significant difference in VCD was observed on day 14 between 'Basic' and 'Neutral', 'Basic' and 'Drift' and 'Neutral' and 'Drift' cultures (p-value = 0.22, 0.53 and 0.31, respectively).

The observed changes in viability over the experiment duration are presented in Figure 80, below. High viability (>90%) was maintained by all cultures over the first three days of the experiment.

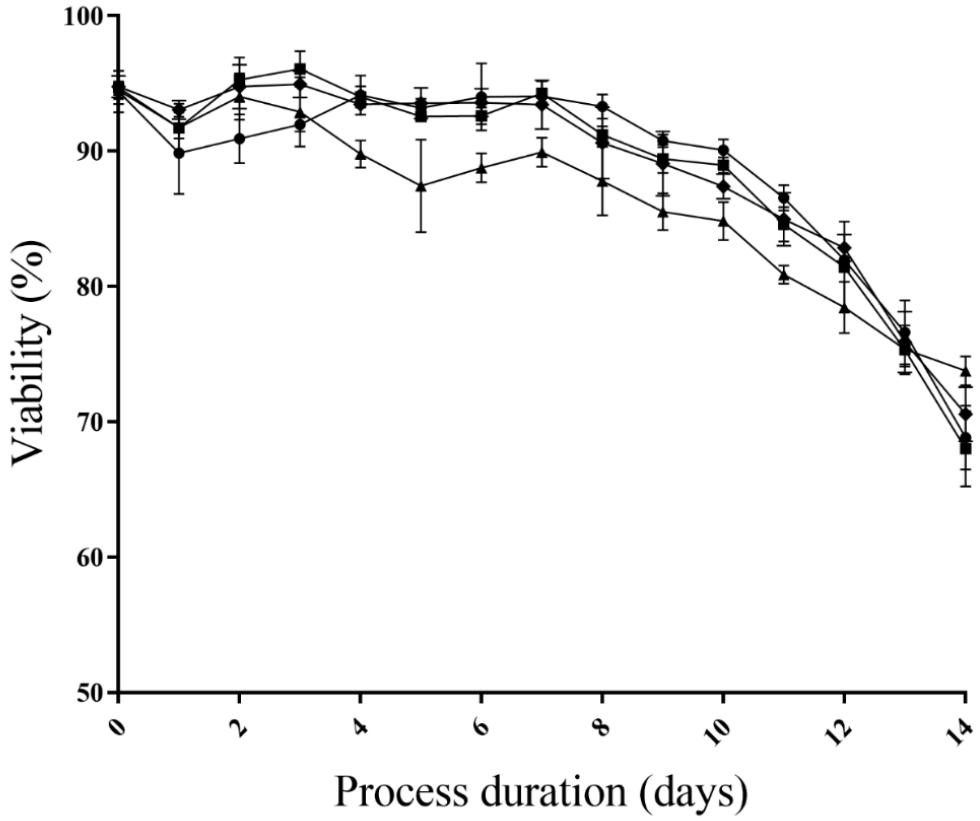

Figure 80 Viability of cultures within Experiment 5.1b plotted over duration (days)
Viability (%) is plotted for pH conditions 'Basic' (◆), 'Neutral' (■), 'Acidic' (▲) and 'Drift' (●), respectively.

On day four the viability of the 'Acidic' condition dropped to (89.8±1.0) %, and the average of the other three conditions remained at (93.9±0.9) %. This represented a significant decrease (P-value < 0.05) in viability that was reproduced on each subsequent day until day 12. On day 13 the rate of decline slowed in the 'Acidic' condition and on the final day of culture it represented the highest viability of all cultures. The viability of the 'Acidic' condition at harvest was (73.8±1.1) %.

The remaining three conditions maintained high viability until day seven, where percentage viability of (93.4±1.8), (94.3±0.9), and (94.1±0.5), for conditions 'Basic', 'Neutral' and 'Drift' was observed, respectively.

Following day seven, the viabilities of conditions were observed to decline simultaneously until harvest, reaching viabilities of (70.6±2.0), (68.0±2.8) and (68.8±2.4), for conditions 'Basic', 'Neutral' and 'Drift', respectively.

Glucose measurements from the cultures displayed control within the 2 to 6g/L target range throughout the experiment, presented below in Figure 81.

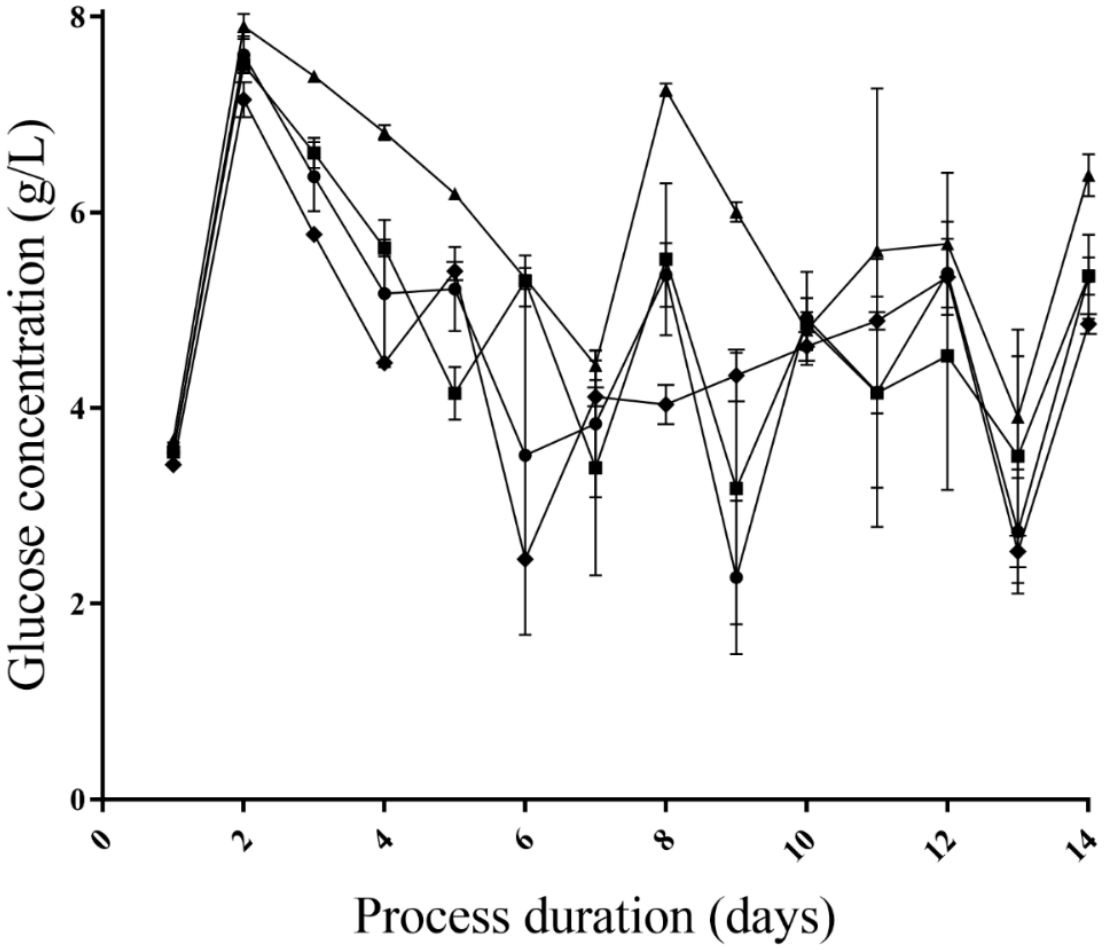

Figure 81 Glucose concentration (g/L) of cultures within Experiment 5.1b plotted over duration (days)
Glucose concentration is plotted for pH conditions 'Basic' (◆), 'Neutral' (■), 'Acidic' (▲) and 'Drift' (●), respectively.

On day two, as observed in Experiment 5.1a, glucose concentrations exceeded the 6g/L upper target. The highest measured glucose concentration was in the 'Acidic' condition, (7.9±0.1) g/L. The lowest observed glucose concentration throughout the experiment was from the 'Drift' condition on day nine, (2.3±0.8) g/L.

The availability and consumption of glucose by the cultures throughout the experiment have resulted in lactate concentration profiles that vary for each condition based on the production and consumption rates of lactate. The measured lactate concentrations (g/L) are presented in Figure 82, below.

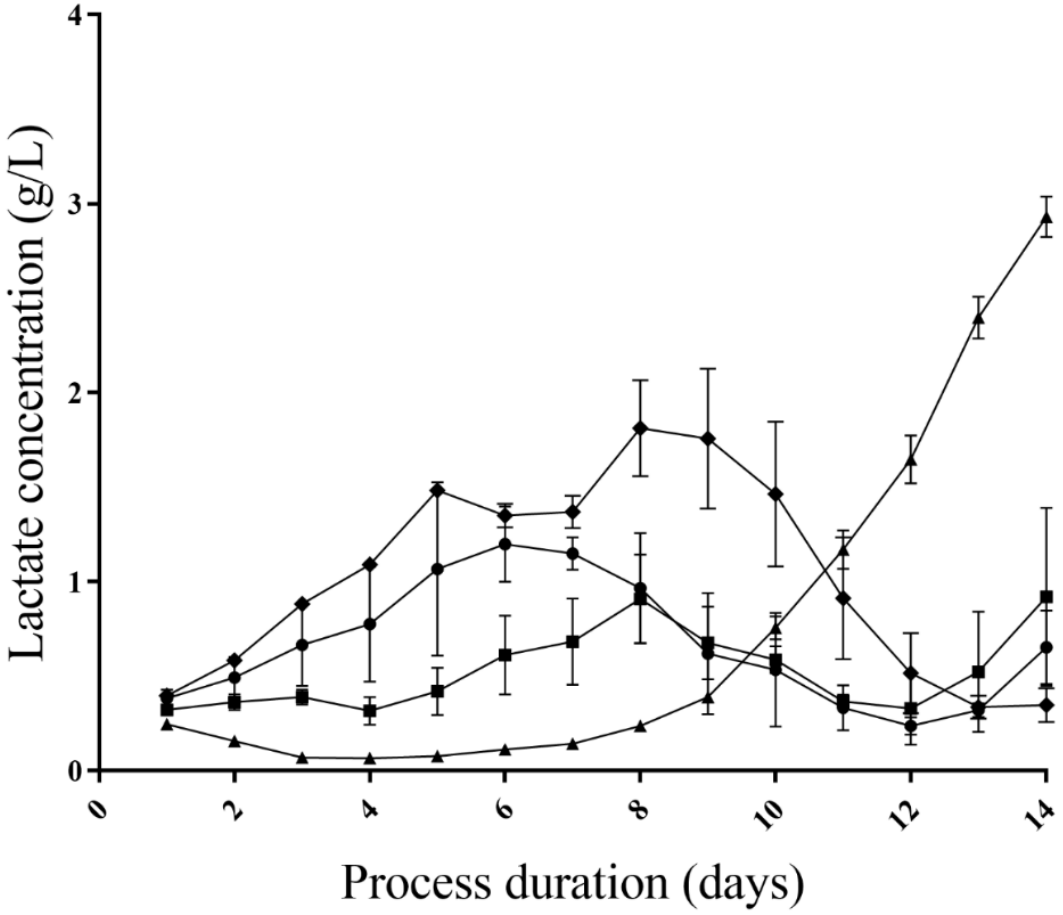

Figure 82 Lactate concentration (g/L) of cultures within Experiment 5.1b plotted over duration (days)
Lactate concentration is plotted for pH conditions 'Basic' (◆), 'Neutral' (■), 'Acidic' (▲) and 'Drift' (●), respectively.

The observed lactate concentration on day one is consistently low in all cultures, with the average concentration at (0.3±0.1) g/L. Following this starting point, the cultures respond to their respective pH conditions, and variation was observed in profiles.

Lactate concentrations were observed to increase initially in the conditions that exhibited a high pH at inoculation, (1.1±0.0) and (0.8±0.3) on day four for pH 'Basic' and 'Drift' conditions, respectively. The concentration continued to increase and resulted in peak lactate concentrations of (1.8±0.3) and (1.2±0.2) g/L on days eight and six for pH 'Basic' and 'Drift' conditions, respectively.

The 'Neutral' condition increased to a peak concentration of (0.9±0.2) g/L on day eight. Following this peak, three culture conditions ('Basic', 'Neutral' and 'Drift') all exhibited a decrease in lactate concentration. The 'Basic' condition decreased to (0.4±0.1) g/L, on day 14. The conditions 'Neutral' and 'Drift' decreased to (0.3±0.2) and (0.2±0.1) g/L, respectively on

day 12, before increasing on the final two days. The concentrations for the 'Neutral' and 'Drift' conditions on day 14 were (0.9±0.5) and (0.7±0.2) g/L, respectively.

Significant differences (P-value < 0.05) were observed in the lactate concentration trend of the 'Acidic' condition throughout the experiment when compared to the other three conditions. During the first eight days, the lactate concentration of the 'Acidic' condition remains significantly lower than all other cultures. The concentrations of (0.3±0.0) and (0.2±0.0) g/L were observed on days one and eight, respectively.

During the second half of the experiment, the measured lactate concentration in the 'Acidic' condition increased to a peak at harvest. Measured lactate concentration on day 8 and day 14 increased from (0.2±0.0) to (2.9±0.1) g/L, respectively.

The pH profiles for each condition are presented in Figure 83 and display the movement of the pH within the deadband. This is presented here to highlight the timing of the 'Drift' condition initiation. Additionally, the natural movement of pH within the deadband is displayed as cultures progress from inoculation through to harvest.

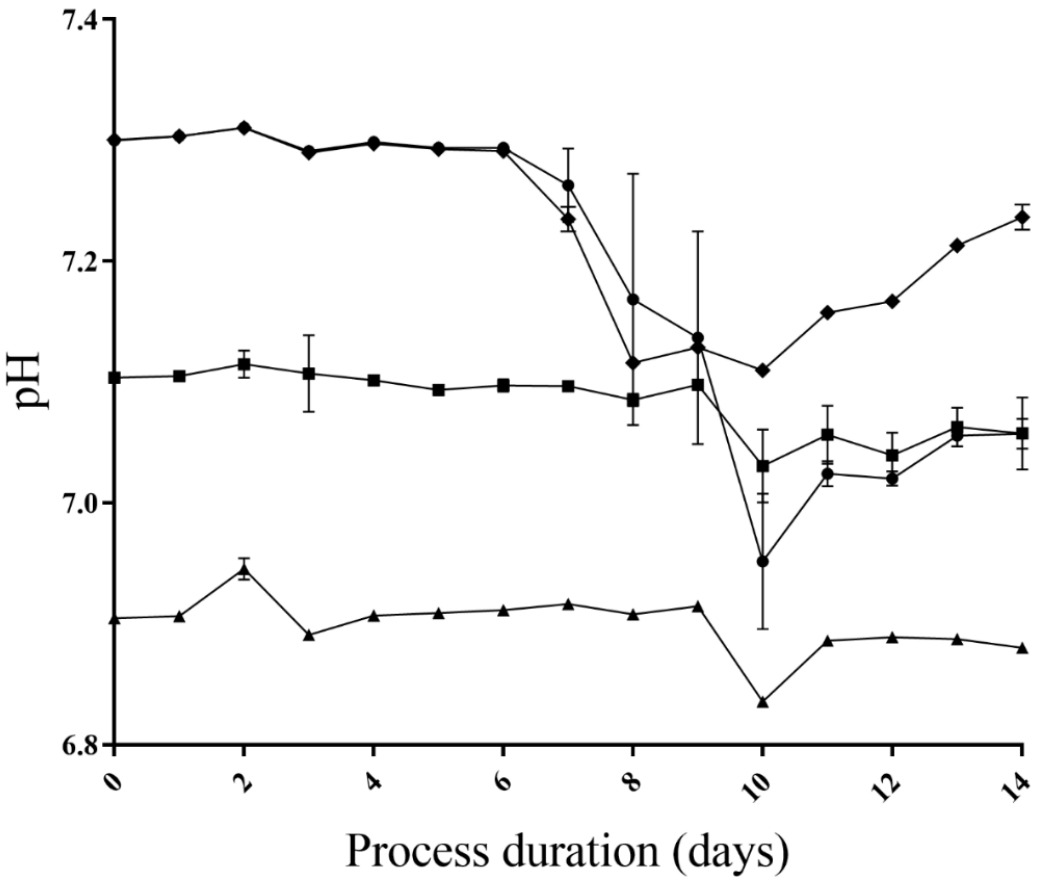

Figure 83 pH of cultures within Experiment 5.1b plotted over duration (days)
Measured pH is plotted for pH conditions 'Basic' (◆), 'Neutral' (■), 'Acidic' (▲) and 'Drift' (●), respectively.

During the first six days of culture, the pH of the conditions tracks along the top of the deadband, controlled by CO_2 sparging. The pH for conditions 'Neutral' and 'Acidic' were controlled at the upper deadband for the duration of the experiment, pH 7.10 and 6.90, respectively. On day seven, the pH of the 'Basic' and 'Drift' conditions both begin to move away from the upper deadband and a decrease in pH was observed. In the 'Basic' pH condition, the pH reached the bottom deadband, pH 7.10 on day 10. On day eight, the pH slowly increased in the direction of the upper deadband, pH 7.30. This pH change correlated with the accumulation of lactate (up to day eight), and removal of lactate prior to harvest (Figure 82, above).

In the pH 'Drift' condition, the pH moved from the 'Basic' condition to the setpoints for the pH 'Acidic' condition. A basic pH was reached for the 'Drift' condition of (6.95±0.05), on day 10. Following day 10, the pH increases to the 7.20 setpoint and is recorded at (7.06±0.01) on day 14.

The measured impact on mAb titre resulting from these conditions is presented in Figure 84, below.

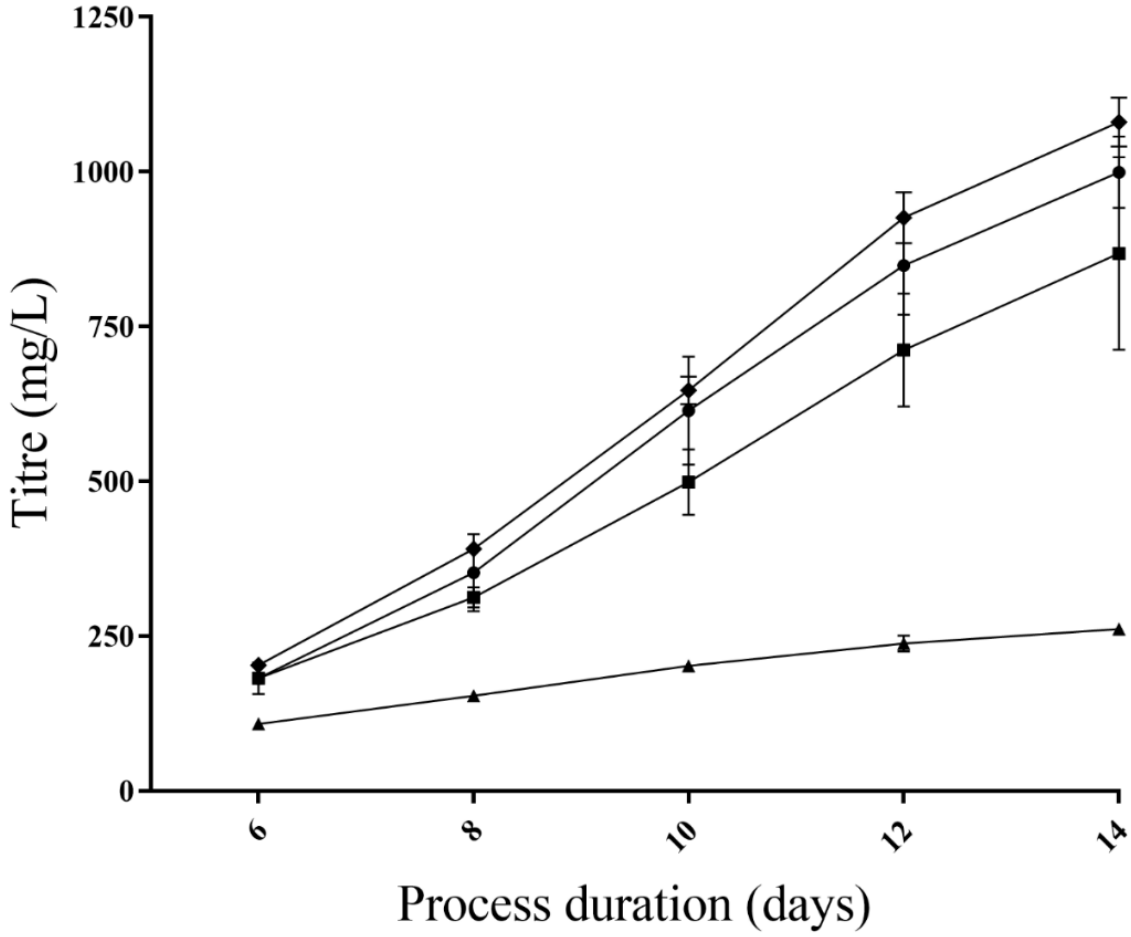

Figure 84 Titre (mg/L) of cultures within Experiment 5.1b plotted over duration (days)
Titre is plotted for pH conditions 'Basic' (◆), 'Neutral' (■), 'Acidic' (▲) and 'Drift' (●), respectively.

The 'Basic' condition displayed the highest titre measurements on each day, respectively at harvest a final titre of (1080±40) mg/L was observed. The titre of the pH 'Drift' increased at the same rates as the 'Basic' condition. The titre at harvest for the 'Drift' condition was lower, (999±58) mg/L, but not significantly different from that observed for the 'Basic' condition. The third ranked condition was the 'Neutral' cultures that reached (868±156) mg/L, by day 14. The titre measurements for the 'Neutral' condition represent significantly lower values (p-value < 0.05) than those for the 'Basic' cultures on days six, eight, 10, and 12, respectively. No significant difference is observed at harvest between the 'Basic' and 'Neutral' cultures (P-value = 0.08). No significant difference was observed between titre measurements in the 'Neutral' and 'Drift' conditions respectively, P values = 0.99, 0.35, 0.12, 0.12, and 0.24 for days six, eight, 10, 12 and 14, respectively.

Titre measurements taken from samples within the 'Acidic' condition were significantly lower than respective timepoint samples from each of the other three conditions. There was a significantly lower final concentration of mAb product observed at harvest, (261±9) mg/L for the 'Acidic' condition. This 'Acidic' titre calculates as 24% of that achieved in the 'Basic' condition.

Product quality measurements from harvest samples provided information on the cumulative impact of the pH condition on the final mAb product. Percentage monomer data for cultures is presented in Table 11.

Table 11 Product quality (percentage monomer and aggregates) present for Experiment 5.1b cultures, at harvest, post product capture purification.

Condition	Monomer (%)	Aggregate (%)
pH Setpoint 'Basic'	95.60	4.40
pH Setpoint 'Neutral'	96.41	3.59
pH Setpoint 'Acidic'	97.60	2.40
pH Setpoint 'Drift'	95.19	4.81

The percentage monomer of the mAb was measured by size exclusion chromatography following Protein A capture purification. The observed aggregation of the mAb was consistently low (< 5%) in each pH setpoint condition. The percentage monomer at harvest for 'Basic', 'Neutral', 'Acidic', and 'Drift' were 95.6, 96.4, 97.6, and 95.2, respectively.

5.3.2 Experiment 5.2 – Culture Robustness During Exponential Expansion

In Experiment 5.2, the conditions (as represented in Table 9) are replicated in each culture station of an ambr®, 48-variant system. The successful operation of three (of a total of four) culture stations (CS) provides triplicate examples of each condition to compare against respective control vessels.

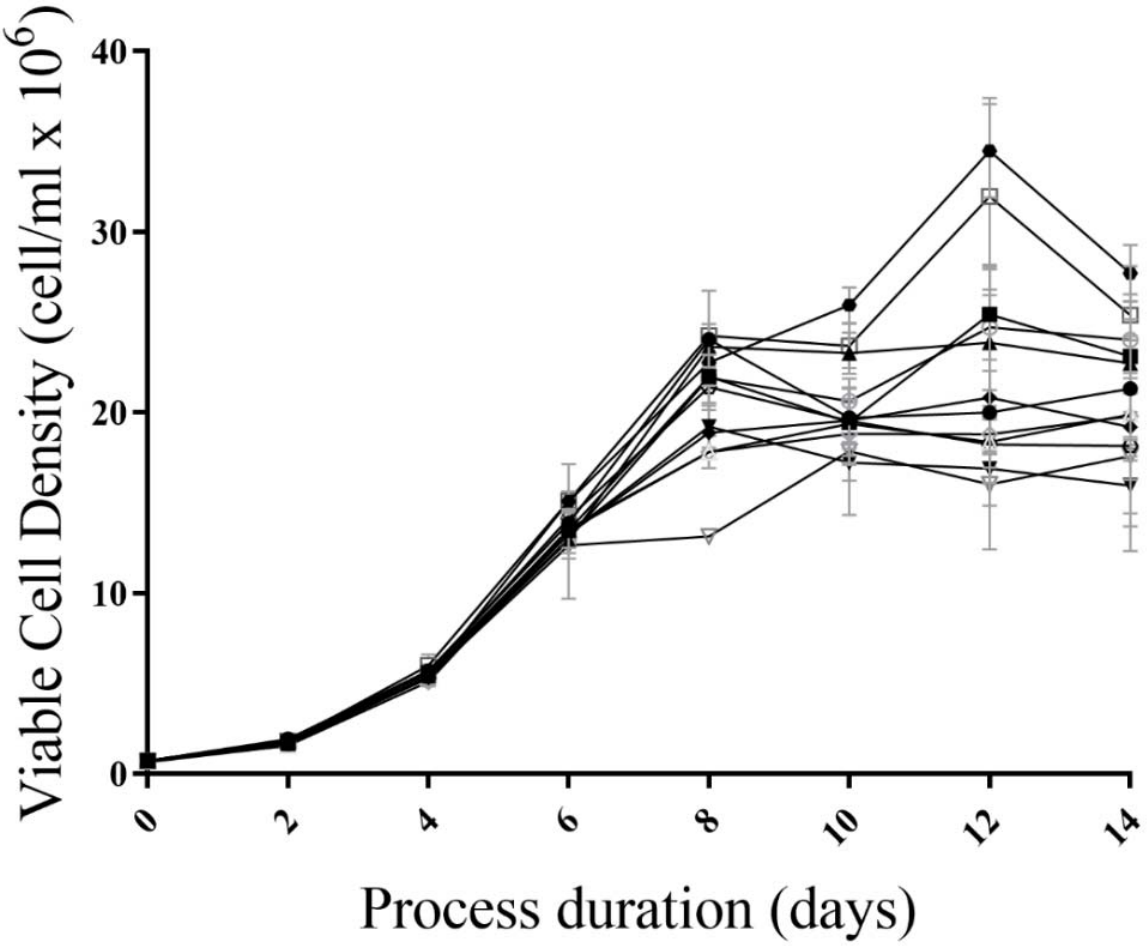

Figure 85 Viable cell density (cells/mL x10^6) of cultures within Experiment 5.2, plotted over duration (days)
Plotted conditions are, Vessel 1 - Control (●), Vessel 2 – pH up(■), Vessel 3 – pH down (▲), Vessel 4 – 30%DO (◆), Vessel 5 – Double Antifoam (⬣), Vessel 6 - 40% DO (○), Vessel 7 – Triple Antifoam (□), Vessel 8 – EM (Δ), Vessel 9 - EM (◊), Vessel 10 – 60%DO (⧏), Vessel 11 (▼), Vessel 12 – 70% DO (▽)

The viable cell density (VCD) measurements from Experiment 5.2 are presented in Figure 85, above. After successful inoculation, all conditions displayed comparable VCDs up to day six. The average VCD on day six was (1.4±0.1) x 10^7 cells/mL. No significant difference was observed in VCD (P-value > 0.05) across all conditions through this period when compared to their respective control.

On day eight, the cultures in Experiment 5.2 reached the end of exponential growth and transitioned into a stationary phase. The VCD observed for control vessels 1 and 11 on day eight was (2.4±0.1) and (1.9±0.1) x10^7 cells/mL, respectively. On this day, a significant decrease compared to control (P < 0.05) was observed in conditions where dissolved oxygen (%) was maximally increased or decreased to 70% and 30% setpoints, respectively.

As the cultures progressed to days 10, 12, and 14, statistically significant increases were also observed in the viable cell density of conditions with additional antifoam, vessels 5 & 7, respectively ($P < 0.05$). In addition, the peak VCD measurements were recorded on day 12 from these two conditions, (3.5±0.3) and (3.2±0.6) $x10^7$ cells/mL for vessels 5 & 7, respectively.

Furthermore, on day 12 there were significant differences in cell density observed between control and the pH up condition and 60% dissolved oxygen condition. Notably, no significant difference was observed between the DCB3 cultures and control cultures on each day from inoculation through to harvest (P values > 0.05).

Observed VCD of control vessels between days 10, 12, and 14, indicated no significant difference resulting from the temperature increases applied during day 12. Control vessels 1 & 11 displayed viable cell densities on day 12 of (2.0±0.2) & (1.7±0.1) and on day 14 of (2.1±0.3) & (1.6±0.2) $x10^7$ cells/mL, respectively.

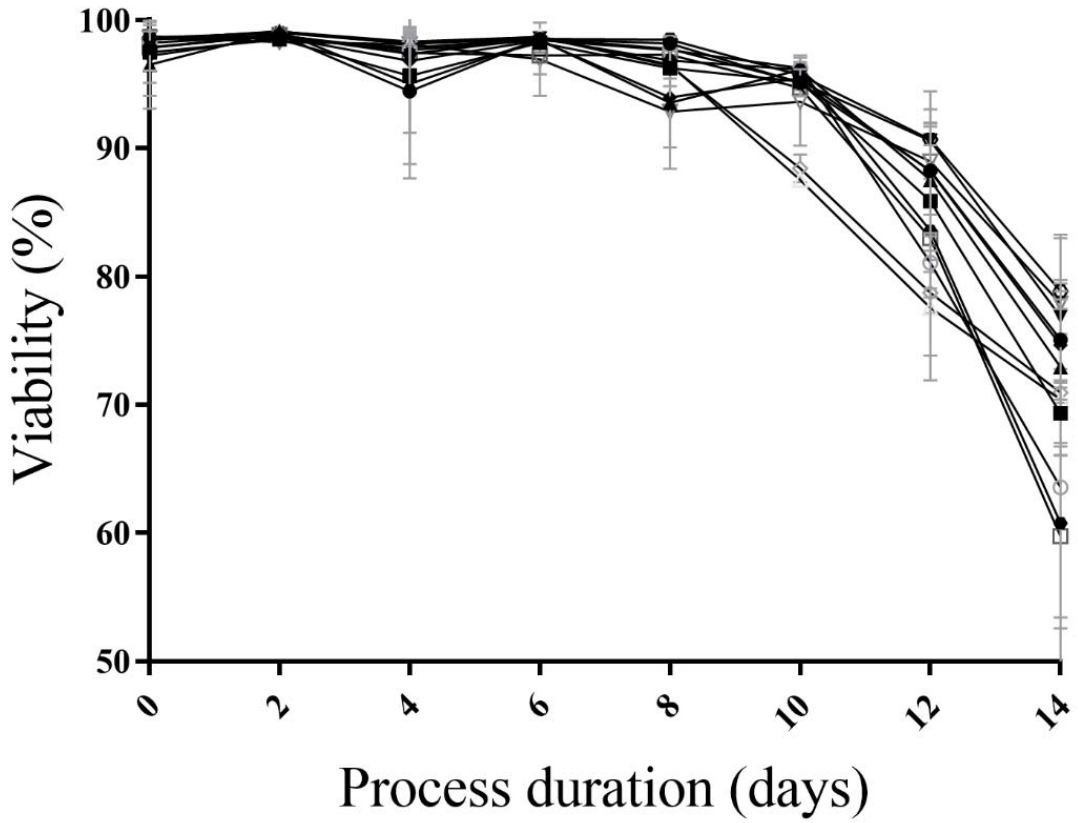

Figure 86 Viability (%) of cultures within Experiment 5.2, plotted over duration (days)
Plotted conditions are, Vessel 1 - Control (●), Vessel 2 – pH up(■), Vessel 3 – pH down (▲), Vessel 4 – 30%DO (◆), Vessel 5 – Double Antifoam (⬣), Vessel 6 - 40% DO (○), Vessel 7 – Triple Antifoam (□), Vessel 8 – EM (Δ), Vessel 9 - EM (◊), Vessel 10 – 60%DO (⧏), Vessel 11 (▼), Vessel 12 – 70% DO (▽)

The percentage viability of cultures in the experiment is presented in Figure 86 above. The average percentage viability at inoculation was (98.0±1.5) %. This high viability was maintained throughout the exponential growth phase and on day six, the average percentage viability for all cultures was (98.3±1.0) %. As cultures transition into stationary phase on day eight, a decline in viability is observed in cultures with high (70% dissolved oxygen) and low (30% dissolved oxygen) dissolved oxygen percentage saturation setpoints, vessels 4 & 12 with (94.0±0.4) and (92.9±0.4), respectively.

The control conditions (vessels 1 and 11) displayed a decrease in viability during the later stages of the culture. A decrease in viability was observed between days 10 and 14, decreasing from (95.1±1.1) and (95.2±0.6) to (75.1±4.7) and (76.9±1.4) %, for vessels 1 and 11 respectively.

Cultures inoculated with DCB3 cells displayed a significant decrease in viability compared to control on days 10 and 12 with average viabilities of (88.0±0.9) and (78.1±2.6) %, respectively. Additionally, viability measurements were lower than control on days 12 and 14 of culture for conditions with additional antifoam additions (vessels 5 and 7), (83.6±4.5) & (83.0±4.7) and (60.8±8.2) & (59.7±6.3) for days 12 and 14, respectively. These differences compared to control were significant ($p < 0.05$) in the triple antifoam condition (vessel 7).

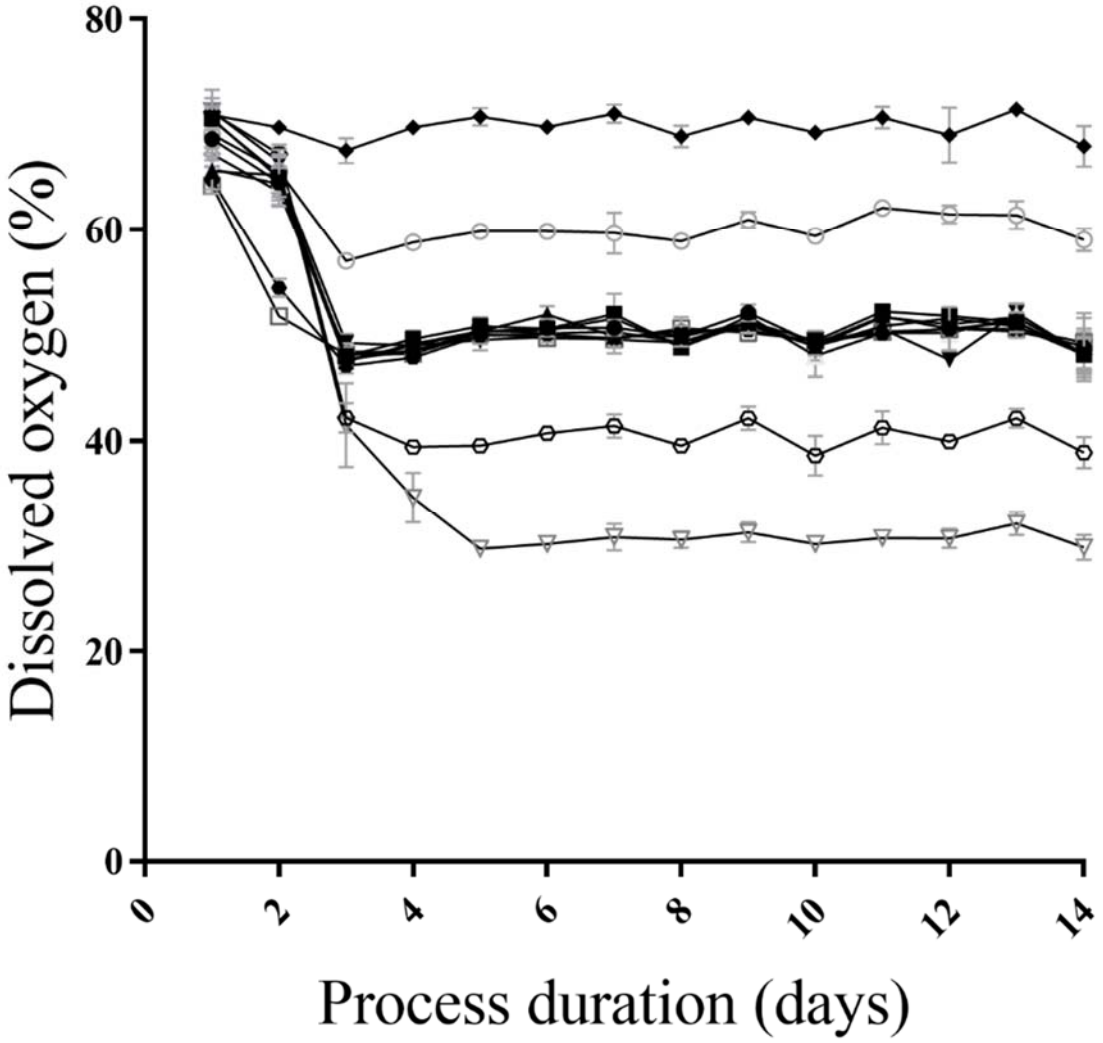

Figure 87 Dissolved oxygen (%) of cultures within Experiment 5.2, plotted over duration (days)
Plotted conditions are, Vessel 1 - Control (●), Vessel 2 – pH up(■), Vessel 3 – pH down (▲), Vessel 4 – 30%DO (◆), Vessel 5 – Double Antifoam (⬣), Vessel 6 - 40% DO (○), Vessel 7 – Triple Antifoam (□), Vessel 8 – EM (Δ), Vessel 9 - EM (◊), Vessel 10 – 60%DO (◃), Vessel 11 (▼), Vessel 12 – 70% DO (▽)

The dissolved oxygen saturation (DO) percentages are presented in Figure 87. Average DO for all cultures on day one was observed as (68.3±2.9) %. The data in Figure 87, highlights the timing of the DO experimental conditions differentiating from the respective control cultures. The experimental conditions are produced sequentially between days 2 and 5, for the highest and lowest percentage saturation, respectively.

The pH was tightly controlled within the (setpoint ± 0.1) deadband for the duration of the experiment. The observed pH measurements are presented in Figure 88.

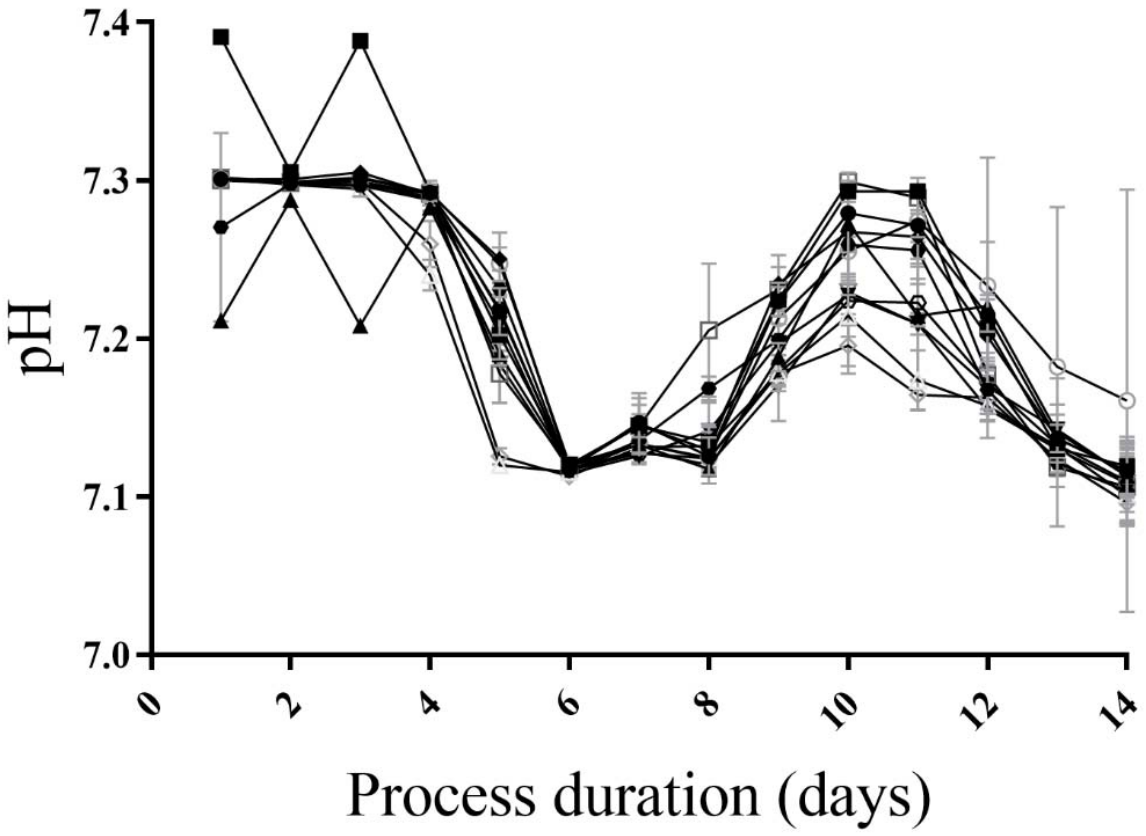

Figure 88 pH of cultures within Experiment 5.2, plotted over duration (days)
Plotted conditions are, Vessel 1 - Control (●), Vessel 2 – pH up(■), Vessel 3 – pH down (▲), Vessel 4 – 30%DO (◆), Vessel 5 – Double Antifoam (⬣), Vessel 6 - 40% DO (○), Vessel 7 – Triple Antifoam (□), Vessel 8 – EM (Δ), Vessel 9 - EM (◊), Vessel 10 – 60%DO (◃), Vessel 11 (▼), Vessel 12 – 70% DO (▽)

In response to the condition tested, the recorded pH in vessels 2 and 3 fluctuated between pH 7.4 and 7.2, over the first 4 days of culture. This occurred when the upper deadband setpoint was increased or decreased, as per the experimental design (Table 9). After day 4, the acidic environment of the cultures resulted in the movement of recorded pH away from the alternating upper deadband, and thus this pH condition did not impact the culture.

On day 5 the pH of the DCB3 derived cells decreased to (7.12±0.00) and (7.13±0.01) for vessels 8 and 9, respectively. On day 6 the pH of all other vessels transitioned from acidic to basic control, as they were maintained at the lower deadband of pH 7.1. This low pH was maintained on day 7 for all cultures.

On day 8 an increase was seen in double (Vessel 5) and triple (vessel 7) conditions, increasing to pH (7.17±0.01) and (7.21±0.04), respectively. This increase was replicated in all other cultures on days 9, 10, and 11, respectively. A decrease in average pH from (7.14±0.01) to (7.11±0.03) was observed in all vessels between days 12 and 14, respectively.

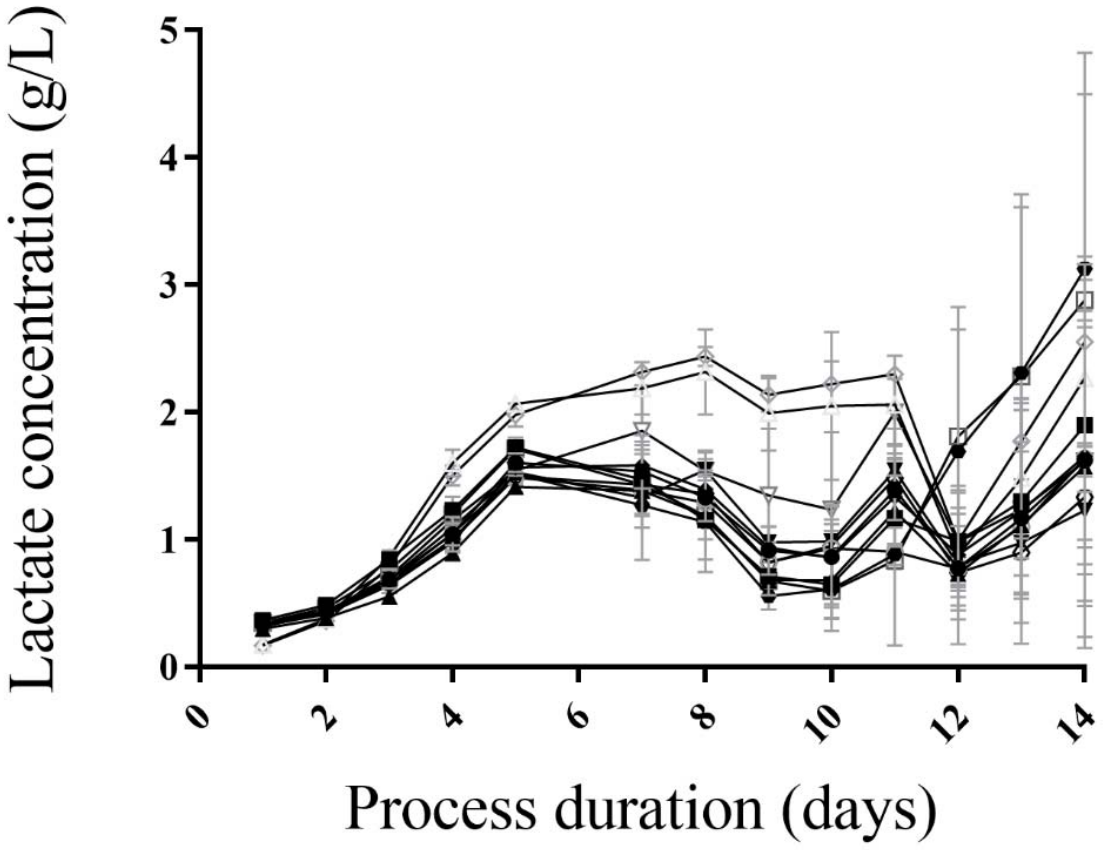

Figure 89 Lactate Concentration (g/L) of cultures within Experiment 5.2, plotted over duration (days)
Plotted conditions are, Vessel 1 - Control (●), Vessel 2 – pH up(■), Vessel 3 – pH down (▲), Vessel 4 – 30%DO (◆), Vessel 5 – Double Antifoam (⬣), Vessel 6 - 40% DO (○), Vessel 7 – Triple Antifoam (□), Vessel 8 – EM (Δ), Vessel 9 - EM (◊), Vessel 10 – 60%DO (⧏), Vessel 11 (▼), Vessel 12 – 70% DO (▽)

The lactate concentration (g/L) observed in Experiment 5.2 is presented in Figure 89, above. An increase in lactate concentration was observed in the control vessels during the first five days of cultures, rising to (1.6±0.1) and (1.5±0.0) for vessels 1 and 11, respectively. The highest concentrations observed until day five were from the DCB3 derived cultures, displaying (2.1±0.1) and (2.0±0.1) for vessels 8 and 9, respectively.

The DCB3 vessels (8 & 9) also exhibited a significant increase compared to control, maintaining a concentration of approximately 2g/L each day from day five to 11, respectively. All other cultures displayed initial peaks on day five of between (1.4±0.1) and (1.7±0.1) g/L, for vessels 3 and 2, respectively. Following this peak, the concentrations were observed to decrease, reaching <1g/L on days nine and 10, respectively.

The lactate concentration on days 12 to 14 was observed to increase across all conditions. The magnitude of the lactate concentration increases in vessels 5 and 7 was significantly higher

than control. The lactate concentration at harvest ranged from between (3.1±1.4) and (1.2±0.5) g/L for vessels 5 and 11, respectively.

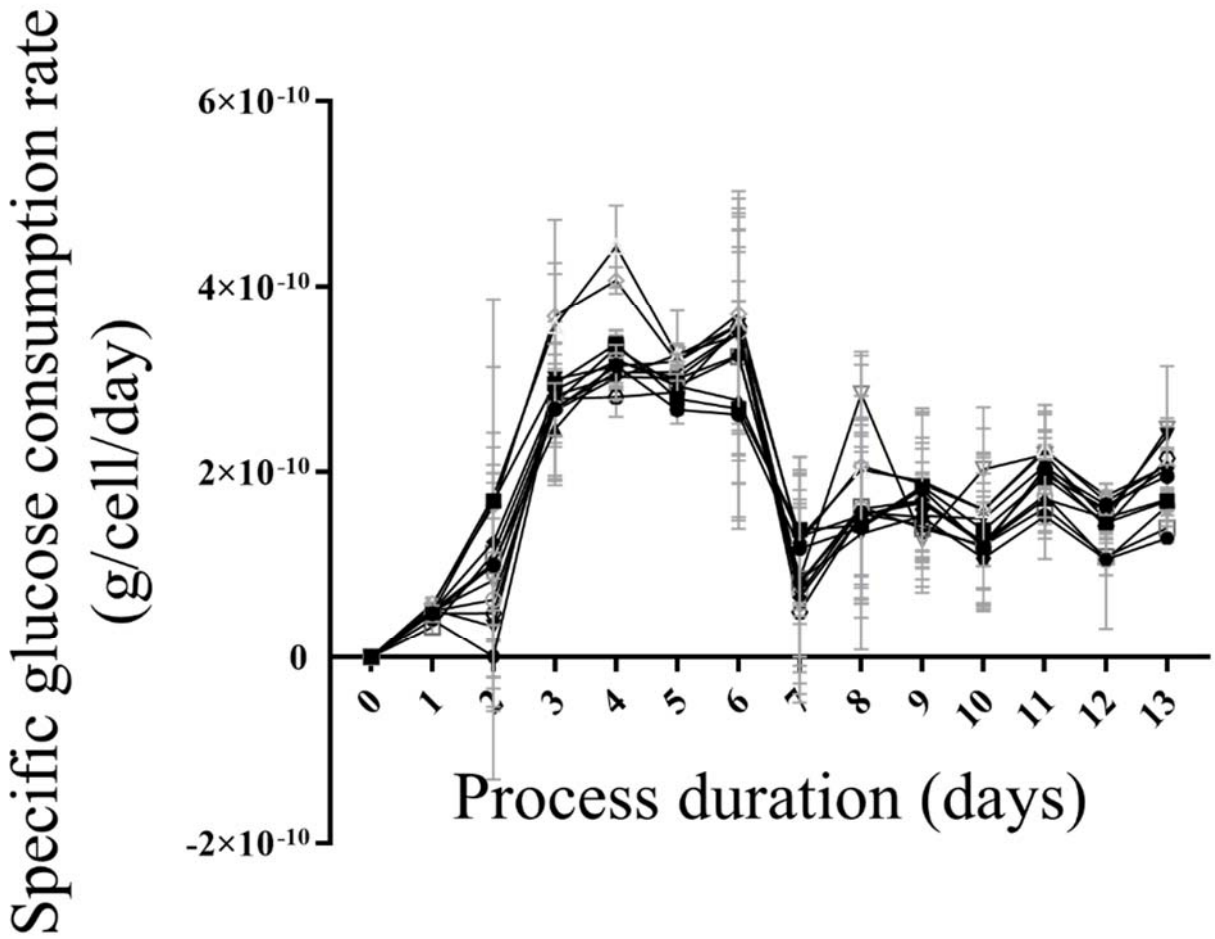

Figure 90 Specific glucose consumption rate (g/cell/day) of cultures within Experiment 5.2, plotted over duration (days)
Plotted conditions are, Vessel 1 - Control (●), Vessel 2 – pH up(■), Vessel 3 – pH down (▲), Vessel 4 – 30%DO (◆), Vessel 5 – Double Antifoam (⬣), Vessel 6 - 40% DO (○), Vessel 7 – Triple Antifoam (□), Vessel 8 – EM (Δ), Vessel 9 - EM (◊), Vessel 10 – 60%DO (◃), Vessel 11 (▼), Vessel 12 – 70% DO (▽)

The cell specific glucose consumption rate (g/cell/day) is displayed in Figure 90, above. The rate of glucose consumption rises during the first four days of culture, exceeding 3 $x10^{-10}$ g/cell/day for all cultures on day four, respectively. The increasing cell specific glucose consumption rate was observed to plateau on days five and six, averaging (3.0±0.3) and (3.3±0.3) $x10^{-10}$ g/cell/day, respectively. On day seven, a decline in the rate of glucose consumption was observed, (1.4±0.8), and (0.5±0.6) $x10^{-10}$ g/cell/day were calculated for the highest (Vessel 2) and lowest (Vessel 10) rates, respectively. Average rates were maintained below 2.0 $x10^{-10}$ g/cell/day for the remainder of the experiment.

Cultures inoculated from the DCB3 cell bank followed the trends outlined for glucose consumption rates (Figure 90). However, they displayed a significant increase in their rate of glucose consumption compared to control on days three and four, respectively (P-value < 0.05). The peak glucose consumption rate for all cultures was observed in vessels 8 and 9, at (4.4±0.4) and (4.1±0.1) $x10^{-10}$ g/cell/day on day four, respectively.

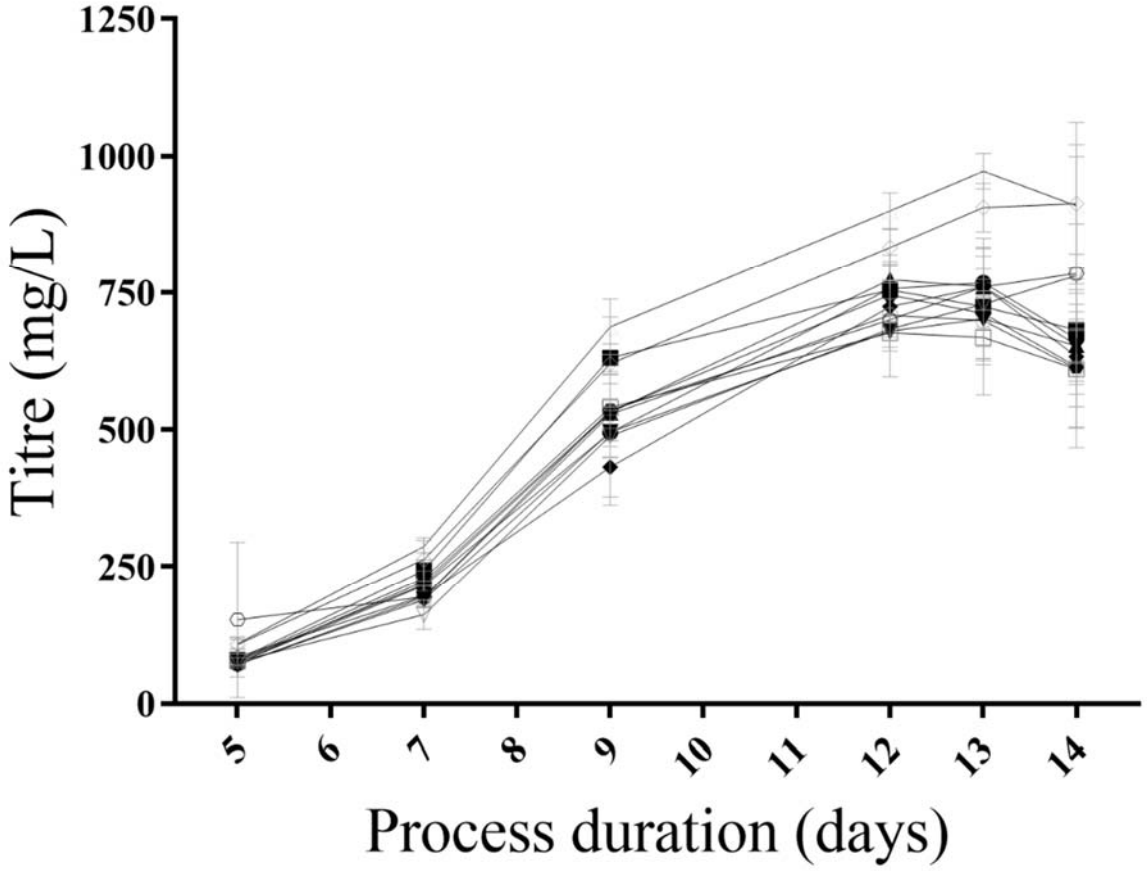

Figure 91 Titre (mg/L) of cultures within Experiment 5.2, plotted over duration (days)
Plotted conditions are, Vessel 1 - Control (●), Vessel 2 – pH up(■), Vessel 3 – pH down (▲), Vessel 4 – 30%DO (◆), Vessel 5 – Double Antifoam (⬣), Vessel 6 - 40% DO (○), Vessel 7 – Triple Antifoam (□), Vessel 8 – EM (Δ), Vessel 9 - EM (◊), Vessel 10 – 60%DO (◃), Vessel 11 - Control (▼), Vessel 12 – 70% DO (▽)

The profile of measured mAb titre (mg/L) was observed to increase for all cultures as the experiment progressed, the data is presented in Figure 91, above. The observed mAb titre increased rapidly between days seven and nine, respectively. During this period the control vessels 1 and 11 were observed to increase from (215±18) and (189±9) mg/L to (495±45) and (496±46) mg/L, respectively. On day 12, titre in control vessels had increased to (757±50) and (679±10) mg/L for vessels 1 and 11, respectively. Cultures inoculated with DCB3 cells (vessels 8 and 9) displayed significantly higher titre measurements from control, on days 12,

13, and 14, respectively. All other vessels displayed no significant difference to control on each of these days, respectively. The highest titre at harvest was observed in vessel 8, (910±89) mg/L.

The harvest samples from each condition were Protein A purified and analysed by size exclusion chromatography. The data generated by this analysis is present in Table 12, below.

Table 12 Product quality (percentage monomer and aggregates) present for Experiment 5.2 cultures, at harvest, post product capture purification.

Vessel - Condition	Monomer (%)	Aggregate (%)
Vessel 1 - Control	95.7±1.0	4.2±0.9
Vessel 2 – pH up	95.9±0.6	4.1±0.5
Vessel 3 – pH down	96.0±0.3	4.0±0.3
Vessel 4 – 30%DO	95.7±0.7	4.3±0.6
Vessel 5 – Double Antifoam	96.6±0.1	3.5±0.1
Vessel 6 - 40% DO	95.9±0.1	4.1±0.1
Vessel 7 – Triple Antifoam	96.3±0.6	3.6±0.5
Vessel 8 – DCB3	96.3±0.3	3.7±0.2
Vessel 9 – DCB3	96.4±0.4	3.6±0.4
Vessel 10 – 60%DO	95.8±0.5	4.2±0.5
Vessel 11 - Control	95.6±0.8	4.4±0.8
Vessel 12 – 70% DO	96.2±0.1	3.8±0.1

The monomer percentage from the conditions was observed to remain consistently high (> 95%) across all samples. These values are consistent with the SEC analysis performed on DCB1 and DCB3 cultures in Experiment 5.1a, where no hyperthermic temperature exposure was conducted on the final days of culture. This leads to a conclusion that the increase in temperature prior to harvest has no observable impact on the purity of the mAb. In addition, the consistency of the monomer percentage observed within the conditions of Experiment 5.2, supports the robustness of the cell line to process variation occurring post inoculation.

5.4 Discussion

The evaluation of cell line sensitivity presented within this chapter began with the generation of cell banks exposed to conditions common with continuous culturing. These were the high generation number of cells (DCB2) and exposure to an enriched nutrient environment (DCB3).

The cell banks DCB2 and DCB3 were generated from an expansion of DCB1. The fourth cell bank (DCB4) combined the exposure to an enriched nutrient environment followed by an accumulation of cell age.

Within Experiment 5.1a, the performance of the three conditioned cell banks (DCB2, DCB3, and DCB4) was evaluated in a fed-batch operation. This evaluation displayed significantly higher growth (P-value > 0.05) when compared to DCB1. The resulting peak VCDs for DCB2, DCB3, and DCB4 were each one-fold higher than those observed for DCB1, respectively.

The high VCD presented in higher generation number cultures (DCB2, DCB3, and DCB4) is beneficial in the operation of continuous cultures. In perfusion specifically, it provides a larger range for the cultures to be maintained within exponential growth, before reaching maximal cell density. However, the correlation of increase in VCD with cell generation number did not translate into an improved titre. The measured mAb produced at harvest was observed between (1079±23) and (1433±95) mg/L, for DCB4 and DCB3, the lowest and highest conditions, respectively.

The observed titre for the DCB1 cultures was (1152±19) mg/L, and these cultures maintained a higher cell specific productivity than DCB2, DCB3, and DCB4, respectively. The loss of cell specific productivity at higher generation numbers is a negative attribute specific to CHO cell lines (Ghorbaniaghdam, Chen, Henry, & Jolicoeur, 2014). This loss in productivity is not uncommon for transfected CHO cell lines and it impacts commercial manufacturing activities both in fed-batch and continuous cultures alike (Shukla & Thömmes, 2010).

The loss in cell specific productivity observed in DCB3 cultures was lower than for DCB2. The improved performance of DCB3 cultures appeared transiently, and further subculture of DCB3 cultures (the generation of DCB4), resulted in a reduction in titre. The lowest titre values reported in this chapter are occurring in DCB4 cultures. The exposure of cells to a high nutrient environment, as is observed in the generation of DCB3, can result in an improved production phenotype (F. Wurm, 2013).

These changes in specific productivity between DCB1 and the generated cell banks (DCB2, 3, and 4) display a genetic instability of the cell line. The instability in production and growth is not observed to impact the product quality attribute (aggregation of mAb). Analysis by SEC results in a high monomer percentage (> 96%) for all cultures.

In Chapters 3 and 4, observations were made of measured pH deviating by > 0.1 units from setpoint in perfusion vessels, without impacting CPPs (maximum VCD, cell specific production rates and product quality attributes, specifically). The pH of all cultures within Chapters 3 and 4 were tightly controlled to pH setpoint ± 0.1 during inoculation. The deviations of > 0.1 from setpoint occurred within microscale perfusion vessels after inoculation, during exponential growth, as sedimentation method was conducted. These observations led to challenging the cell line's sensitivity to pH deviations, at inoculation, and during exponential growth.

Within Experiment 5.1b, the sensitivity of Cell line 1 (DCB1) to deviations in pH was tested. This was conducted through the operation of conditions 'Basic', 'Neutral', and 'Acidic', characterised by pH setpoints of (7.2±0.1), (7.0±0.1), and (6.8±0.1), respectively. These cultures were inoculated at their respective setpoints and maintained through to harvest. The operation of the 'Drift' condition provided insight to cell line sensitivity to pH deviations of >0.1, following inoculation at the 'High' setpoint (7.2±0.1).

The growth characteristics of pH conditions that were kept consistent throughout the experiment ('Basic', 'Neutral', and 'Acidic') highlighted the cell line's sensitivity to pH. A correlation was observed between the magnitude of the pH setpoint change and the growth performance of the culture.

During exponential growth, the 'Basic' condition reached the highest cell density and was the most productive, generating a titre measurement at harvest of (1080±40) mg/L. The growth and productivity of the 'Neutral' and 'Acidic' conditions were significantly lower than those observed for the 'Basic' condition.

When compared to the fixed pH setpoints ('Basic', 'Neutral' and 'Acidic'), the 'Drift' condition ranked second overall, behind the 'Basic' condition, for growth and productivity measurements. During the first nine days, the pH correlated with the 'Basic' conditions. Following this, the pH was in the range of the 'Acidic' condition on day 10 of culture and in the 'Neutral' cultures from days 11 to 14, respectively. Whilst observations of performance are cell line specific, CHO cells have been well documented to possess an inherent sensitivity to pH (Brunner, Fricke, et al., 2017; F. Li et al., 2010) (Section 1.4.2 pH Control).

For continuous systems (specifically perfusion operation), the culture spends the majority of its time in exponential growth, and thus understanding the particular sensitivity during this

phase of the operation can allow operational ranges to be set to appropriately, with an understanding of the risk associated with the control of the CPPs.

Cell line sensitivity during exponential growth was also evaluated during Experiment 5.2. This experiment design expanded the pH evaluation of Experiment 5.1b, and sought CPP variation during exponential growth, after a successful inoculation at setpoint. The application of QbD principles will define sensitivity for CPPs at inoculation and deviation during operation would place the process at risk without explicitly understanding the situational impact that the deviation applies (Horvath, Mun, & Laird, 2010).

All conditions were inoculated at designated setpoint ranges for Cell line 1 (Detailed in Chapter 2). The majority of conditions of Experiment 5.2 (see Section 5.2.3) was conducted with DCB1, with the exception for vessels 8 and 9 on each culture station. These vessels (8 and 9, inoculated with DCB3) are important to consider for this experimental design as the sensitivity during the exponential expansion of continuous culture may be influenced by exposure of the culture to continuous operation (Cong, Chang, Deng, Xiao, & Su, 2001; Seth et al., 2013).

Differences were observed during Experiment 5.2 in these DCB3 conditioned cultures when compared with control vessels (DCB1). This difference was in the observed lactate concentrations of the cultures. Prolonged production of lactate within a pH controlled culture is thought to limit productivity through suppressed growth (Glacken, Fleischaker, & Sinskey, 1986; W. S. Hu, Dodge, Frame, & Himes, 1987).

High lactate producing cultures (Vessels 8 and 9 significantly higher than control) display comparable growth to control. Previous experience of the DCB3 cell bank (Section 5.3.1) indicates an expected improved growth characteristic compared to DCB1 is being suppressed by the lactate concentration within cultures.

Whilst no significant difference was observed in the VCD measurements of DCB3 cultures, the cultures were able to utilise excess glucose. This correlated with an observed increased mAb production. The increased mAb production aligns with the previously investigated CHO response phenomena to increased lactate accumulation, in both improved efficiency of metabolic processes (Zagari et al., 2013), and transcription signalling adjustments (M. Zhou et al., 2011).

In addition to the observation of DCB3 cultures in Experiment 5.2, the conditions aimed to evaluate the impact of deviations occurring during the exponential expansion of cultures.

Controlled conditions (pH, DO, antifoam addition) were simulated to experience probe failures and process operation errors. The resulting deviations displayed no significant difference to control in performance criteria for the pH and DO conditions. Increasing antifoam additions displayed a significant increase in peak viable cell density of cultures when compared to control. This may have been a result of the setpoint antifoam addition being sub-optimal for the cell line and increasing this provided improved control and culture performance.

The final condition for Experiment 5.2 was a temperature increase, conducted across all cultures on day 12. The temperature of all cultures was increased to 38°C on day 12 of culture. Analysis of data across the conditions displayed that no comparative impact in conditions against control. Whilst temperature deviations away from biological optimum are expected to limit growth and have a significant impact of process performance (Kaufmann et al., 1999), this variation occurs post peak viable cell density. Additionally, the deviation occurs in close proximity to the end of the fed-batch operation.

After exponential growth, culture process control is centred on delaying cell apoptosis, maintaining viability, and providing an environment for mAb secretion. Viability remains > 50% at the point of harvest, indicating that whilst declining the cellular membrane is intact for the majority of cells within the culture, and cellular waste products are not being released. Appropriate CHO cell survival at this mild temperature increase is supported by investigations into the heat shock response at incrementally increasing temperatures (Peksel et al., 2017) (Gerweck, Richards, & Michaels, 1982). Any decline in viability resulting may trigger the harvest criteria and thus the evaluation of the impact of this condition must be focused on the product quality attributes of the product.

A consistently high (>95%) monomer percentage was observed for all conditions. These values are consistent with the SEC analysis performed on DCB1 and DCB3 cultures in Experiment 5.1a, where no hyperthermic temperature exposure was conducted on the final days of culture. This leads to a conclusion that the increase in temperature before harvest has no observable impact on the purity of the mAb. In addition, the consistency of the monomer percentage observed within the conditions of Experiment 5.2, supports the robustness of the cell line to process variation occurring post inoculation.

Chapter 6 Overall Conclusions and Future Work

6.1 Overall Conclusions

The work contained within this thesis investigates the topic of continuous bioprocess development through a high-throughput microscale system. During the operation of continuous cultures at microscale, differences are observed in culture performance when compared to bench scale equivalent cultures. These differences highlight the potential and limitations of the system as a bioprocess development tool and indicate novel operation and control strategies for mammalian cultures that apply to both fed-batch and continuous modes of operation.

A key methodology utilised in continuous manufacturing is perfusion. In Chapter 3, a cell sedimentation method is applied to an existing automated microscale bioreactor system to enable it to operate perfusion. An early reference to the application of this methodology was contained in seminar presentations sponsored by the manufacturer of the system (Sartorius, 2016). The detailed design and evaluation of the technique was published for the first time from the work contained within Chapter 3 (Sewell et al., 2019).

The evaluation of the method indicates the microscale system's ability to operate in perfusion, achieving comparable maximal cell densities to bench scale operation. Variation was observed in the initial growth rates of cultures in the two scales. This manifested itself in a seven-day lag for the micro scale vessels to reach maximal density observed in bench scale. As the systems used for micro and bench scale had previously been presented as equivalent across many criteria (Lewis, 2010; Moses et al., 2012; Nienow et al., 2013; Rameez et al., 2014), differences in culture performance were accredited to the perfusion operations, namely the method of cell retention.

Inherent to the cell retention method was the need to stop gas sparging and agitation of the micro scale cultures. This allowed cells to settle and generate a ‘cell-free’ fraction for media exchange. The first potential cause for the lag in culture growth is identified in the pH and DO traces. Steep declines were observed in the measured values during the sedimentation that, if maintained for an extended period would be incompatible with high culture viability. This is confirmed by the decline in performance observed in the extension of the method from 30 minutes settling to 37 minutes. It is important to note that the location of the sensors within the vessels is on the bottom, facing upwards into the culture. During sedimentation, the local environment around these sensors will increase in cell density and present a biased measurement, not representative of the total culture.

This local heterogeneous environment is a known challenge of larger scale bioreactors whereby mixing may be sub-optimal and it has been shown to impact growth and productivity of cultures as poor DO and pH control will impact cellular physiology (Brunner, Braun, et al., 2017; Lara,

Galindo, Ramírez, & Palomares, 2006). The pH extremes at larger scales are the inverse of what is observed here, with pH spikes as opposed to drops, resulting in cellular stress (Jiang, Chen, & Xu, 2018; Ozturk, 1996). Within the microscale cultures, sustained increased lactate production was observed in the microscale cultures compared to bench scale that could be indicative of limited oxygen concentration during sedimentation through the Warburg effect (Warburg et al., 1927).

A compounding difference in the microscale cultures that could impact the growth profile was the efficiency of cell retention. In the bench scale cultures, 100% retention efficiency is assumed due to the hollow fibre filtration membrane used (Karst, Serra, Villiger, Soos, & Morbidelli, 2016). At micro scale, the efficiency was calculated to be between 95 and 99%, measured by counting cells present in the removed perfusate. The measured physical characteristics of these cells that were removed highlighted lower density, smaller size, and higher viability than the retained culture. The significantly smaller size (3 to 4µm difference in diameter), indicates that the calls are either very young, new cells or older cells in the stages of apoptosis resisting trypan blue ingress (Pan, Dalm, et al., 2017; Seewöster & Lehmann, 1997). Therefore, to comment further on the characteristics of the cells removed further cellular analysis techniques would be required, such as flow cytometry (Moore et al., 1995; Pekle et al., 2019).

Notwithstanding the differences to bench scale systems, the microscale perfusion method displayed functionality to support screening and ranking activities for cell lines in perfusion culture. Evaluating maximum growth potential, titre, and product quality attributes in a low resource, high throughput manner. Ultimately, the prevalence of the ambr® systems within industrial labs and the simple operation of the methodology will enable perfusion evaluations to be conducted without significant outlay in resource. Further development of the methodology is required to function as an efficient process development tool in defining operating ranges as the ambr® systems are used for fed-batch applications (Manahan et al., 2019).

As perfusion culture retains cells, holding them in a pseudo steady state of growth, the method has been utilised for expansion applications (culture inoculation expansion and cell therapy applications)(Levine, Miskin, Wonnacott, & Keir, 2017). Whilst Chapter 3 focused on the sedimentation method's impact on culture growth, productivity, and product quality,

In the absence of single-cell characterisation techniques, Chapter 4 highlights indicators of cellular health by progressing cells from micro and bench scale perfusion cultures, into fed-batch production. The performance of the production scale vessels was viewed as a surrogate characterisation tool, highlighting scale dependant differences in the perfusion methods. The

operating ranges of production vessels were varied to compound any differences, challenging the comparability of the scales further.

Operation of the microscale perfusion vessels displayed consistent performance in their respective production cultures, achieving performance ranking that aligned with the respective inoculation concentration. When the same perfusion, inoculation, and fed-batch parameters were tested on bench scale cultures, higher variation was observed, with a greater response to the increased nutrient feed concentrations applied. Proposed in the discussion was a sensitivity to fluctuating dilution rates inherent to the sedimentation method, thought to be removing culture heterogeneity (Stephens & Lyberatos, 1987). It is reasonable to also expect heterogenicity of the cultures to be impacted by the two differences highlighted above (frequent local pH &DO fluctuations and cell removal). The frequent media exchanges were tested in isolation to the other factors through a bench scale evaluation of dilution rate sensitivity and no significant difference in performance was observed.

On balance, as a tool for inoculum expansion for subsequent production cultures, it is not appropriate to utilise the microscale perfusion method as there is uncertainty in the impact of cellular sedimentation on the culture. However, the volumetric differences bench and microscale aligns well with the inoculum requirements if process development for n-1 perfusion was to be conducted with bench scale vessels, inoculating microscale production cultures. In the evaluation of microscale perfusion, the ambr® system displayed the ability to operate at very high cell densities and maintain control of critical process parameters.

Sensitivity to physiochemical conditions, defined within this thesis as poor growth and productivity, is generally thought to be cell line specific and management of the environment is bespoke for each cell line (Y. M. Huang et al., 2010). The performance of the cell line in perfusion culture through Chapters 3 and 4 highlighted a particular insensitivity to pH and DO concentrations that is misaligned with the understanding of pH and DO responses in fed batch cultures (F. Li et al., 2010).

In a fed-batch setting, pH sensitivity was investigated and in Experiment 5.1a, the pH setpoint was varied, at inoculation, but also during exponential growth and stationary phase. The testing indicated that cultures with pH tightly controlled at inoculation performed comparably regardless of the pH control applied through the remainder of the culture. Transversely, if pH was not controlled well during inoculation, the culture did not display high performance. The comparable performance of the culture with the ‘drift’ pH control could have been realised through the lower cellular stress experienced.

Altering key parameters, such as pH, at defined points in culture progression has previously been identified as an optimisation method for fed batch cultures (Trummer et al., 2006). This has application in continuous culture, however, the impact on culture longevity is an additional consideration over a terminally operated batch culture. For batch cultures, this is not widely performed as a dual setpoint process design is conflicting to current QbD directives and DoE techniques that use MVA of singular setpoints applied from inoculation through to harvest (Mandenius & Brundin, 2008; A. S. Rathore, 2009).

To apply multiple, progressive setpoints for a culture requires a profound understanding of the responses to the physiochemical environment. For continuous cultures, whereby there is a distinct bi-phase operation (inoculation and steady-state growth), this control strategy warrants further investigation as the culture will be maintained for the majority of its time away from inoculation. A phase-dependent pH control strategy could also provide benefits in commercial-scale fed-batch bioreactors whereby there are challenges with local extreme pH environments each time an adjustment is made (Brunner, Braun, et al., 2017).

During the operation of perfusion in Chapters 3 and 4, an insensitivity to pH is observed in this cell line and this was discretely investigated (Experiment 5.1b), focusing on the cell line's pH sensitivity during and after inoculation. It was found that cultures where pH was tightly controlled (pH 7.2±0.1) during inoculation performed well regardless of the level of control after inoculation. Cultures that had a varied setpoint (pH 7.0 or 6.8) at inoculation displayed significantly lower growth and productivity, in comparison. This finding aligns with pH control present in microscale perfusion, where the setpoint is tightly controlled at inoculation but can be seen to vary as cell sedimentation occurs, without a significant impact on culture performance.

The point of culture inoculation was identified as a critical control step. Further investigation within the chapter focused on expanding the understanding of culture phase-dependent sensitivity. Supporting Experiments 5.1a and 5.2, investigated pre inoculation and post inoculation control, respectively. In a highly regulated industry, such as bioprocess manufacturing, novel control measures around these process steps are not typically investigated, and as such their potential overlooked (Fisher et al., 2019).

The controlled expansion of a cell line from cell bank vial thaw to production vessel inoculation ensures consistent performance from batch to batch. Experiment 5.1a focused on disrupting the expansion step by introducing environments that would be observed during continuous culture expansion (as seeding cultures or as independent production vessels), such as high generation cell lines or exposure to nutrient-rich media environments. The cells displayed an

ability to adapt to pre-conditioning, aligning with an industry held perspective that culture heterogenicity is maintained beyond the point of clonality, due to the inherent stability of immortalised cell lines (Frye et al., 2016; Patel et al., 2018; Vcelar et al., 2018). This preconditioning is supported by studies investigating metabolomic and proteomic changes, and enhanced protein expression characteristics of cell lines exposed to high glucose environments (Z. Liu et al., 2015; Takuma, Hirashima, & Piret, 2007). Depending on the longevity of these effects, they have the potential to improve fitness and performance in production cultures if deployed at the correct stage in inoculum expansion (Cong et al., 2001; Seth et al., 2013). Whilst requirements to display phenotypic stability will dictate the maximum expansion period (manufacturing window), this may alleviate any loss in productivity observed at the end of that period. Ultimately, these findings for phenotypic stability loss over long term subculturing are expected for CHO cultures, and be caused by loss of gene copy number and assumably a malfunctioning splicing mechanism of the bicistronic mRNA (Beckmann et al., 2012).

Experiment 5.2 concluded the experimental work detailed within this thesis by testing a combination of pre and post inoculation control variations to determine the impact that they may pose on performance. An experimental design maintained tight parameter control (pH, seeding density, temperature, dissolved oxygen, etc) during inoculation and varied process control before, in inoculation expansion (as detailed in Experiment 5.1), or process control post inoculation. No significant difference in performance was observed in conditions whereby the process parameters were subject to variation post inoculation. These conditions ranged from pH and DO setpoint variation to increased antifoam additions. This data, in combination with that presented in previous chapters, leads to speculation that the window of inoculation for any culture is where the highest sensitivity is located, and thus should be controlled with increased attention. This assessment suggests that applying flexibility to parameter controls elsewhere in the process could present avenues for process improvement in optimisation and improved robustness.

In conclusion, this thesis has detailed the design, execution, and evaluation of a novel scale down perfusion methodology developed in an industrially relevant and commercially available system. Through highlighting the method's potential application, and ability to assist in screening in a perfusion setting, it is hoped that the benefits of continuous manufacturing can be realised to help meet future demand. Novel control strategies have been proposed that apply to both perfusion and fed-batch bioprocesses. These centre around culture phase sensitivity mapping and applying measured operational control limits appropriately, with the hope to reduce manufacturing risk in extremely high-value settings.

6.2 Future Work

6.2.1 Refinement and Characterisation of Microscale Perfusion Methodology

In the development, optimisation and characterisation of a microscale perfusion methodology, certain nuances of continuous operation have been observed. Further refinement and characterisation remains unexplored that may lead to increased robustness and inform scalability of the microscale perfusion methodology.

The methodology involves a period of time where the culture is uncontrolled. Method improvements are sought through the reduction of the time taken to operate the sedimentation/media exchange step.

The improvements to the exchange step could be made into two defined sections. The first section of this step is the sedimentation of the cells within the vessels, and investigations within this thesis details a minimum settling time of 30 minutes. To improve this settling time, some manipulation of the vessels must be made. The operation of continuous cultures details the use of centrifugation and incline settling as two processing improvements over gravity cell settling *in-situ* to be explored.

The media exchange section, post cell settling, is currently limited in the methodology due to the requirement of the system to utilise a 1ml pipette tip due to physical dimensional incompatibility of the 5 mL tip. This limitation triples the liquid handling operations per vessel, from what would be achieved with a 5mL tip.

Alternatively, the restriction to the 1 mL tip size could result in improvements. By limiting liquid handling interactions per sedimentation, the process operation results with more frequent smaller exchanges to achieve the same dilution rate.

A more frequent, lower volume sedimentation/media exchange protocol results in greater accuracy in the attainment of target dilution rate. A challenge in operating in this manner would be attaining sufficient process control for a process when it is frequently uncontrolled. If this is not feasible, media and feed optimisation for the addition in this bolus manner should be considered, specifically to mitigate the Warburg effect observed in Experiment 3.1.

The setup presented within Chapter 3 could utilise either the 48-vessel or the 24-vessel variants of the microscale system at 50% capacity with half of each culture station being utilised at a time. At a liquid exchange rate of 1 vessel volume per day, this setup allowed suitable maintenance downtime and a single operator intervention per day. This facilitates the

applicability of this setup in conducting multifactorial DoE to effectively evaluate perfusion process set points, medium optimisation or as a cell line screening tool. Any improvement or adjustment to the methodology must take these capacity requirements into account such that the method is able to support process development.

Ultimately, any application of a scale down system in an industrial setting and to be accepted by regulators would require extensive, multifactor characterisation of the system. As future work, this characterisation would need to present a detailed understanding of the scale dependent parameter interactions with multiple cell lines such that any scale-up activities could be performed within the QbD paradigm.

One aspect of this characterisation is the holistic impact that the sedimentation method is having on the culture. This assessment should include both cells within the culture that are exposed to the uncontrolled conditions, and the small percentage that are removed with each media exchange.

Due to the continuous nature of the cultures, there is opportunity to take many samples to conduct such characterisation without terminating or unbalancing the culture. Single cell analysis techniques, such as flow cytometry, provided they are conducted with suitable resolution allow the visualisation of culture heterogeneity for a number of factors. These include the growth and gene expression (Strovas, Sauter, Guo, & Lidstrom, 2007), proteomic and translation (Newman et al., 2006), and cell fate analysis (Colman-Lerner et al., 2005).

Combined with this single cell analysis, the detailed analysis of a product quality attribute that is heavily impacted by fluctuation in media nutrient levels(Y. Fan et al., 2015; Yang & Butler, 2000), culture conditions (Jiang et al., 2018) or cellular stress (Goldrick et al., 2017) is a good measure of comparability across scales.

Ultimately, to conclude the characterisation of the sedimentation perfusion methodology, operation with a variety of cell lines is required, with ranking of performance between micro and bench scale operations as a critical step in displaying suitability of the system for screening applications.

6.2.2 Culture Phase Focused Bioprocess Development

The design and observations from Experiment 5.1b represented an initial step in development of a novel control strategy for cultures, building on optimisations involving pH and temperature shifts in latter stages of fed-batch processes (Moore et al., 1997; Oguchi et al., 2006). Current

QbD application to process optimisation challenges the culture from inoculation to harvest with a single setpoint with upper and lower limits for each parameter. This method could not unveil the global optimum and will be restricted by the culture phase that displays the highest sensitivity to the parameter setpoints, assuming this sensitivity changes over time. Conclusions from Experiment 5.1b indicate that Cell line 1 has a high sensitivity to pH changes at inoculation, and a comparatively lower sensitivity during exponential growth.

To effectively and comprehensively evaluate culture sensitivity at inoculation and the subsequent process performance, an iterative strategy of process development is required. Firstly the optimal conditions for inoculation must be determined through screening of setpoints. Termination of these cultures after two days, and evaluation of the cell density, oxygen uptake rate and glucose utilisation will provide sufficient information to determine optimal conditions for inoculation.

A subsequent screening experiment is then required to evaluate conditions post inoculation. This will be initiated with the predetermined optimal conditions for inoculation and will continue to explore a design space for each parameter from day two onwards. Finally, progression with optimal inoculation and exponential growth setpoints may allow the final stationary and death phases to be interrogated in increasing detail to ensure culture success when operated at larger scale.

Such an investigation into culture phase focused sensitivities has examples of similar application, specifically in temperature and pH shifts during stationary operation to prolong culture longevity, increase productivity and manage the physiochemical environment (Kaufmann et al., 1999).

However, this description of process optimisation is envisaged to generate wider operating ranges as the culture sensitivity to setpoint deviation decreases as a function of time. Allowing wide operating ranges at commercial scales ultimately leads to robust, low risk manufacturing processes.

6.2.1 Production Improvements Through Preconditioning

Current inoculum expansion best practices are highly regulated and risk averse. They involve taking cell banks from vial thaw to inoculation through sub-culturing regimes that are centred around minimal process variation to ensure reproduceable production culture performance (Birch & Racher, 2006). However, it has been observed within this thesis that the action of preconditioning cultures a high nutrient environment generates some beneficial culture traits.

This is supported by literature investigating the metabolic and proteomic changes, and enhanced protein expression present when cultures are exposed to high glucose environments (Z. Liu et al., 2015; Takuma et al., 2007)

During Experiment 5.2, the preconditioned culture metabolism was observed to consume greater glucose quantities when compared cultures sub cultured in basal media for the inoculum expansion.

Future work could explore optimal conditions for priming cultures for production, prior to inoculation. As highlighted above this is likely to include high nutrient environments, but could also include a balance of the redox potential of the culture to mitigate against undesirable Warburg effects through media and pH adjustments (Zhang et al., 2015).

Whilst this would require extensive screening activities, including detailed analysis of the proteome and metabolome, findings are likely applicable to all CHO host systems. For an organisation that has multiple commercial processes deriving from the same host system, this outlay of resource could provide process improvements across the portfolio of products simultaneously.

Certainly, any commercial adoption would require extensive characterisation and need to stand up to regulatory interrogation, for an high value industry such as biologics the risk reward equation is balanced.

Appendix

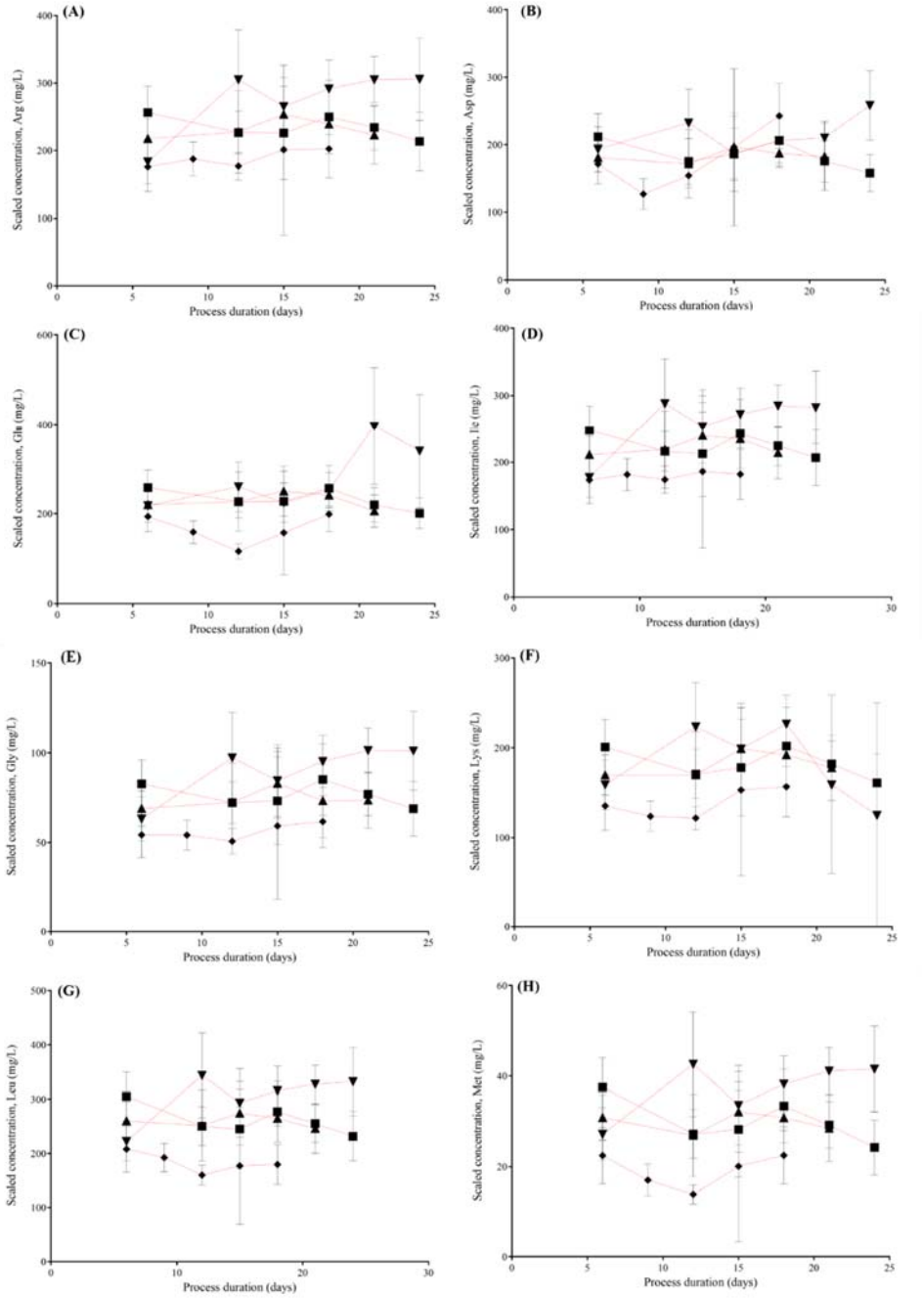

Appendix Figure I Perfusate amino acid profiles for microscale and bench scale experiments (Chapter 3)

Figure shows the Arginine, Aspartic acid, Glutamate, Isoleucine, Glycine, Lysine, Leucine and Methionine profiles, denoted by (A-H), respectively, starting from the 6th day post inoculation measured every three days. Concentrations were scaled randomly in the interest of protecting the IP of the proprietary medium and are reported as "Scaled concentrations (mg/L)". Microscale reactors: (▲) Experiment 3.1, n=6 (30 minutes settling); (▼) Experiment 3.2a, n=4 (33.5 minutes settling); (■) Experiment 3.2b, n=6 (37 minutes settling); (♦) Bench scale reactors: Experiment 3.1, n=2. Data shows mean ± SD

References

Adams, D., Korke, R., & Hu, W.-S. (2007). Application of Stoichiometric and Kinetic Analyses to Characterize Cell Growth and Product Formation. In R. Pörtner (Ed.), *Animal Cell Biotechnology: Methods and Protocols* (pp. 269-284). Totowa, NJ: Humana Press.

Ahn, W. S., & Antoniewicz, M. R. (2012). Towards dynamic metabolic flux analysis in CHO cell cultures. *Biotechnology Journal, 7*(1), 61-74. doi:doi:10.1002/biot.201100052

Al-Moslih, M. I., & Dubes, G. R. (1973). The Kinetics of DEAE-Dextran-induced Cell Sensitization to Transfection. *Journal of General Virology, 18*(2), 189-193. doi:doi:10.1099/0022-1317-18-2-189

Alkan, S. S. (2004). Monoclonal antibodies: the story of a discovery that revolutionized science and medicine. *Nature Reviews Immunology, 4*, 153. doi:10.1038/nri1265

Allen, R. C. (1987). Chapter 31 To Market, To Market - 1986. In D. M. Bailey (Ed.), *Annual Reports in Medicinal Chemistry* (Vol. 22, pp. 315-330): Academic Press.

Altamirano, C., Illanes, A., Becerra, S., Cairó, J. J., & Gòdia, F. (2006). Considerations on the lactate consumption by CHO cells in the presence of galactose. *Journal of Biotechnology, 125*(4), 547-556. doi:https://doi.org/10.1016/j.jbiotec.2006.03.023

Altamirano, C., Paredes, C., Illanes, A., Cairó, J. J., & Gòdia, F. (2004). Strategies for fed-batch cultivation of t-PA producing CHO cells: substitution of glucose and glutamine and rational design of culture medium. *Journal of Biotechnology, 110*(2), 171-179. doi:https://doi.org/10.1016/j.jbiotec.2004.02.004

Alves, C. S., & Dobrowsky, T. M. (2017). Strategies and considerations for improving expression of "difficult to express" proteins in CHO cells. In *Heterologous Protein Production in CHO Cells* (pp. 1-23): Springer.

Alvin, K., & Ye, J. (2014). Generation of cell lines for monoclonal antibody production. In *Monoclonal Antibodies* (pp. 263-271): Springer.

Amer, M., Feng, Y., & Ramsey, J. D. (2019). Using CFD simulations and statistical analysis to correlate oxygen mass transfer coefficient to both geometrical parameters and operating conditions in a stirred-tank bioreactor. *35*(3), e2785. doi:10.1002/btpr.2785

Amzel, L. M., & Poljak, R. J. (1979). Three-dimensional structure of immunoglobulins. *Annual review of biochemistry, 48*(1), 961-997.

Arpin, C., Dechanet, J., Van Kooten, C., Merville, P., Grouard, G., Briere, F., . . . Liu, Y. (1995). Generation of memory B cells and plasma cells in vitro. *Science, 268*(5211), 720-722. doi:10.1126/science.7537388

Avgerinos, G. C., Drapeau, D., Socolow, J. S., Mao, J.-i., Hsiao, K., & Broeze, R. J. (1990). Spin filter perfusion system for high density cell culture: production of recombinant urinary type plasminogen activator in CHO cells. *Nature Biotechnology, 8*(1), 54.

Bareither, R., & Pollard, D. (2011). A review of advanced small-scale parallel bioreactor technology for accelerated process development: Current state and future need. *Biotechnology Progress, 27*(1), 2-14. doi:10.1002/btpr.522

Barrett, T. A., Wu, A., Zhang, H., Levy, M. S., & Lye, G. J. (2010). Microwell engineering characterization for mammalian cell culture process development. *Biotechnol Bioeng, 105*(2), 260-275. doi:10.1002/bit.22531

Baruah, D. B., Dash, R. N., Chaudhari, M. R., & Kadam, S. S. (2006). Plasminogen activators: A comparison. *Vascular Pharmacology, 44*(1), 1-9. doi:https://doi.org/10.1016/j.vph.2005.09.003

Bastide, A., Peretti, D., Knight, J. R. P., Grosso, S., Spriggs, R. V., Pichon, X., . . . Willis, A. E. (2017). RTN3 Is a Novel Cold-Induced Protein and Mediates Neuroprotective Effects of RBM3. *Current Biology, 27*(5), 638-650. doi:10.1016/j.cub.2017.01.047

Beckmann, T. F., Krämer, O., Klausing, S., Heinrich, C., Thüte, T., Büntemeyer, H., . . . Noll, T. (2012). Effects of high passage cultivation on CHO cells: a global analysis. *Applied microbiology and biotechnology, 94*(3), 659-671. doi:10.1007/s00253-011-3806-1

Betts, J. I., & Baganz, F. (2006). Miniature bioreactors: current practices and future opportunities. *Microbial Cell Factories, 5*(1), 21. doi:10.1186/1475-2859-5-21

BioMarin Pharmaceutical, N., United States. (2017). *Automated High Throughput Cell Culture Methods for the Development and Investigation of Large Scale Perfusion Processes - Poster 142.* Paper presented at the The 25th Annual Meeting of the European Society of Animal Cell Technology, Lausanne.

Birch, J. R., & Racher, A. J. (2006). Antibody production. *Adv Drug Deliv Rev, 58*(5-6), 671-685. doi:10.1016/j.addr.2005.12.006

Blesken, C., Olfers, T., Grimm, A., & Frische, N. (2016). The microfluidic bioreactor for a new era of bioprocess development. *Engineering in Life Sciences, 16*(2), 190-193. doi:10.1002/elsc.201500026

Bloemkolk, J.-W., Gray, M. R., Merchant, F., & Mosmann, T. R. (1992). Effect of temperature on hybridoma cell cycle and MAb production. *Biotechnology and Bioengineering, 40*(3), 427-431. doi:doi:10.1002/bit.260400312

Bonham-Carter, J., & Shevitz, J. (2011). A brief history of perfusion biomanufacturing. *BioProcess Int, 9*(9), 24-30.

Boniello, C., Mayr, T., Bolivar, J. M., & Nidetzky, B. (2012). Dual-lifetime referencing (DLR): a powerful method for on-line measurement of internal pH in carrier-bound immobilized biocatalysts. *BMC Biotechnology, 12*(1), 11. doi:10.1186/1472-6750-12-11

Borth, N., Heider, R., Assadian, A., & Katinger, H. (1992). Growth and production kinetics of human × mouse and mouse hybridoma cells at reduced temperature and serum content. *Journal of Biotechnology, 25*(3), 319-331. doi:https://doi.org/10.1016/0168-1656(92)90164-5

Borth, N., Zeyda, M., & Katinger, H. (2000). Efficient selection of high-producing subclones during gene amplification of recombinant Chinese hamster ovary cells by flow cytometry and cell sorting. *Biotechnology and Bioengineering, 71*(4), 266-273. doi:doi:10.1002/1097-0290(2000)71:4<266::AID-BIT1016>3.0.CO;2-2

Bos, A. B., Luan, P., Duque, J. N., Reilly, D., Harms, P. D., & Wong, A. W. (2015). Optimization and automation of an end-to-end high throughput microscale transient protein production process. *Biotechnology and Bioengineering, 112*(9), 1832-1842. doi:doi:10.1002/bit.25601

Browne, S. M., & Al-Rubeai, M. (2007). Selection methods for high-producing mammalian cell lines. *Trends in biotechnology, 25*(9), 425-432. doi:https://doi.org/10.1016/j.tibtech.2007.07.002

Brunner, M., Braun, P., Doppler, P., Posch, C., Behrens, D., Herwig, C., & Fricke, J. (2017). The impact of pH inhomogeneities on CHO cell physiology and fed-batch process performance – two-compartment scale-down modelling and intracellular pH excursion. *12*(7), 1600633. doi:10.1002/biot.201600633

Brunner, M., Fricke, J., Kroll, P., & Herwig, C. (2017). Investigation of the interactions of critical scale-up parameters (pH, pO2 and pCO2) on CHO batch performance and critical quality attributes. *Bioprocess and Biosystems Engineering, 40*(2), 251-263. doi:10.1007/s00449-016-1693-7

Buchsteiner, M., Quek, L.-E., Gray, P., & Nielsen, L. K. (2018). Improving culture performance and antibody production in CHO cell culture processes by reducing the Warburg effect. *115*(9), 2315-2327. doi:10.1002/bit.26724

Butler, M., & Jenkins, H. (1989). Nutritional aspects of the growth of animal cells in culture. *Journal of Biotechnology, 12*(2), 97-110. doi:https://doi.org/10.1016/0168-1656(89)90009-6

Canelas, A. B., Harrison, N., Fazio, A., Zhang, J., Pitkänen, J.-P., van den Brink, J., . . . Nielsen, J. (2010). Integrated multilaboratory systems biology reveals differences in protein metabolism between two reference yeast strains. *Nature Communications, 1*, 145. doi:10.1038/ncomms1150

https://www.nature.com/articles/ncomms1150#supplementary-information

Chisti, Y. (2000). Animal-cell damage in sparged bioreactors. *Trends in biotechnology, 18*(10), 420-432.
Chong, W. P. K., Reddy, S. G., Yusufi, F. N. K., Lee, D.-Y., Wong, N. S. C., Heng, C. K., . . . Ho, Y. S. (2010). Metabolomics-driven approach for the improvement of Chinese hamster ovary cell growth: Overexpression of malate dehydrogenase II. *Journal of Biotechnology, 147*(2), 116-121. doi:https://doi.org/10.1016/j.jbiotec.2010.03.018
Choo, C.-Y., Tian, Y., Kim, W.-S., Blatter, E., Conary, J., & Brady, C. P. (2007). High-Level Production of a Monoclonal Antibody in Murine Myeloma Cells by Perfusion Culture Using a Gravity Settler. *Biotechnology Progress, 23*(1), 225-231. doi:doi:10.1021/bp060231v
Chu, L., & Robinson, D. K. (2001). Industrial choices for protein production by large-scale cell culture. *Current Opinion in Biotechnology, 12*(2), 180-187. doi:http://dx.doi.org/10.1016/S0958-1669(00)00197-X
Clark, J., Hirstenstein, H., & Gebb, C. (1980). Critical parameters in the microcarrier culture of animal cells. *Dev Biol Stand, 46*, 117-124.
Clincke, M. F., Molleryd, C., Zhang, Y., Lindskog, E., Walsh, K., & Chotteau, V. (2013). Very high density of CHO cells in perfusion by ATF or TFF in WAVE bioreactor. Part I. Effect of the cell density on the process. *Biotechnol Prog, 29*(3), 754-767. doi:10.1002/btpr.1704
Cohen, S. N., Chang, A. C. Y., Boyer, H. W., & Helling, R. B. (1973). Construction of Biologically Functional Bacterial Plasmids <em>In Vitro</em&gt. *Proceedings of the National Academy of Sciences, 70*(11), 3240. doi:10.1073/pnas.70.11.3240
Colman-Lerner, A., Gordon, A., Serra, E., Chin, T., Resnekov, O., Endy, D., . . . Brent, R. (2005). Regulated cell-to-cell variation in a cell-fate decision system. *Nature, 437*(7059), 699-706. doi:10.1038/nature03998
Cong, C., Chang, Y., Deng, J., Xiao, C., & Su, Z. (2001). A novel scale-up method for mammalian cell culture in packed-bed bioreactor. *Biotechnology Letters, 23*(11), 881-885. doi:10.1023/a:1010520009212
Costa, A. R., Withers, J., Rodrigues, M. E., McLoughlin, N., Henriques, M., Oliveira, R., . . . Azeredo, J. (2013). The impact of cell adaptation to serum-free conditions on the glycosylation profile of a monoclonal antibody produced by Chinese hamster ovary cells. *New Biotechnology, 30*(5), 563-572. doi:https://doi.org/10.1016/j.nbt.2012.12.002
Croughan, M. S., Hamel, J. F., & Wang, D. I. (2000). Hydrodynamic effects on animal cells grown in microcarrier cultures. *Biotechnology and Bioengineering, 67*(6), 841-852.
Davies, S. L., Lovelady, C. S., Grainger, R. K., Racher, A. J., Young, R. J., & James, D. C. (2013). Functional heterogeneity and heritability in CHO cell populations. *Biotechnology and Bioengineering, 110*(1), 260-274. doi:10.1002/bit.24621
De Jesus, M., & Wurm, F. M. (2011). Manufacturing recombinant proteins in kg-ton quantities using animal cells in bioreactors. *European Journal of Pharmaceutics and Biopharmaceutics, 78*(2), 184-188. doi:https://doi.org/10.1016/j.ejpb.2011.01.005
Delves, P. J., & Roitt, I. M. (2000). The Immune System. *New England Journal of Medicine, 343*(1), 37-49. doi:10.1056/nejm200007063430107
deZengotita, V. M., Schmelzer, A. E., & Miller, W. M. (2002). Characterization of hybridoma cell responses to elevated pCO2 and osmolality: Intracellular pH, cell size, apoptosis, and metabolism. *Biotechnology and Bioengineering, 77*(4), 369-380. doi:doi:10.1002/bit.10176
Dhara, V. G., Naik, H. M., Majewska, N. I., & Betenbaugh, M. J. (2018). Recombinant Antibody Production in CHO and NS0 Cells: Differences and Similarities. *BioDrugs, 32*(6), 571-584. doi:10.1007/s40259-018-0319-9
Dorai, H., Kyung, Y. S., Ellis, D., Kinney, C., Lin, C., Jan, D., . . . Betenbaugh, M. J. (2009). Expression of anti-apoptosis genes alters lactate metabolism of Chinese Hamster Ovary cells in culture. *Biotechnology and Bioengineering, 103*(3), 592-608. doi:10.1002/bit.22269
Dorka, P., Fischer, C., Budman, H., & Scharer, J. M. (2009). Metabolic flux-based modeling of mAb production during batch and fed-batch operations. *Bioprocess and Biosystems Engineering, 32*(2), 183-196.

Du, Z., Treiber, D., McCarter, J. D., Fomina-Yadlin, D., Saleem, R. A., McCoy, R. E., . . . Reddy, P. (2015). Use of a small molecule cell cycle inhibitor to control cell growth and improve specific productivity and product quality of recombinant proteins in CHO cell cultures. *Biotechnol Bioeng, 112*(1), 141-155. doi:10.1002/bit.25332

Dutton, R. L., Scharer, J., & Moo-Young, M. (2006). Cell cycle phase dependent productivity of a recombinant Chinese hamster ovary cell line. *Cytotechnology, 52*(1), 55-69. doi:10.1007/s10616-006-9041-4

Eibl, R., Löffelholz, C., & Eibl, D. (2014). Disposable Bioreactors for Inoculum Production and Protein Expression. In R. Pörtner (Ed.), *Animal Cell Biotechnology: Methods and Protocols* (pp. 265-284). Totowa, NJ: Humana Press.

Europa, A. F., Gambhir, A., Fu, P. C., & Hu, W. S. (2000). Multiple steady states with distinct cellular metabolism in continuous culture of mammalian cells. *Biotechnol Bioeng, 67*(1), 25-34.

Fan, L., Kadura, I., Krebs, L. E., Hatfield, C. C., Shaw, M. M., & Frye, C. C. (2012). Improving the efficiency of CHO cell line generation using glutamine synthetase gene knockout cells. *Biotechnology and Bioengineering, 109*(4), 1007-1015.

Fan, Y., Jimenez Del Val, I., Müller, C., Wagtberg Sen, J., Rasmussen, S. K., Kontoravdi, C., . . . Andersen, M. R. (2015). Amino acid and glucose metabolism in fed-batch CHO cell culture affects antibody production and glycosylation. *Biotechnology and Bioengineering, 112*(3), 521-535.

Fan, Y., Ley, D., & Andersen, M. R. (2018). Fed-Batch CHO Cell Culture for Lab-Scale Antibody Production. In V. Picanço-Castro & K. Swiech (Eds.), *Recombinant Glycoprotein Production: Methods and Protocols* (pp. 147-161). New York, NY: Springer New York.

Filpula, D. (2007). Antibody engineering and modification technologies. *Biomolecular Engineering, 24*(2), 201-215. doi:https://doi.org/10.1016/j.bioeng.2007.03.004

Fisher, A. C., Kamga, M.-H., Agarabi, C., Brorson, K., Lee, S. L., & Yoon, S. (2019). The Current Scientific and Regulatory Landscape in Advancing Integrated Continuous Biopharmaceutical Manufacturing. *Trends in biotechnology, 37*(3), 253-267. doi:https://doi.org/10.1016/j.tibtech.2018.08.008

Flegr, J. (1997). Two Distinct Types of Natural Selection in Turbidostat-like and Chemostat-like Ecosystems. *Journal of Theoretical Biology, 188*(1), 121-126. doi:https://doi.org/10.1006/jtbi.1997.0458

Fogolín, M. B., Wagner, R., Etcheverrigaray, M., & Kratje, R. (2004). Impact of temperature reduction and expression of yeast pyruvate carboxylase on hGM-CSF-producing CHO cells. *Journal of Biotechnology, 109*(1), 179-191. doi:https://doi.org/10.1016/j.jbiotec.2003.10.035

Follstad, B. D., Balcarcel, R. R., Stephanopoulos, G., & Wang, D. I. C. (1999). Metabolic flux analysis of hybridoma continuous culture steady state multiplicity. *Biotechnology and Bioengineering, 63*(6), 675-683. doi:10.1002/(sici)1097-0290(19990620)63:6<675::aid-bit5>3.0.co;2-r

Fomina-Yadlin, D., Mujacic, M., Maggiora, K., Quesnell, G., Saleem, R., & McGrew, J. T. (2015). Transcriptome analysis of a CHO cell line expressing a recombinant therapeutic protein treated with inducers of protein expression. *J Biotechnol, 212*, 106-115. doi:10.1016/j.jbiotec.2015.08.025

Frye, C., Deshpande, R., Estes, S., Francissen, K., Joly, J., Lubiniecki, A., . . . Anderson, K. (2016). Industry view on the relative importance of "clonality" of biopharmaceutical-producing cell lines. *Biologicals, 44*(2), 117-122.

Funke, M., Buchenauer, A., Schnakenberg, U., Mokwa, W., Diederichs, S., Mertens, A., . . . Büchs, J. (2010). Microfluidic biolector—microfluidic bioprocess control in microtiter plates. *Biotechnology and Bioengineering, 107*(3), 497-505. doi:doi:10.1002/bit.22825

Furukawa, K., & Ohsuye, K. (1998). Effect of culture temperature on a recombinant CHO cell line producing a C-terminal α-amidating enzyme. *Cytotechnology, 26*(2), 153-164. doi:10.1023/a:1007934216507

Gao, J., Gorenflo, V. M., Scharer, J. M., & Budman, H. M. (2007). Dynamic Metabolic Modeling for a MAB Bioprocess. *Biotechnology Progress, 23*(1), 168-181. doi:doi:10.1021/bp060089y

Gerweck, L. E., Richards, B., & Michaels, H. B. (1982). Influence of low pH on the development and decay of 42°C thermotolerance in cho cells. *International Journal of Radiation Oncology*Biology*Physics, 8*(11), 1935-1941. doi:https://doi.org/10.1016/0360-3016(82)90452-7

Ghorbaniaghdam, A., Chen, J., Henry, O., & Jolicoeur, M. (2014). Analyzing clonal variation of monoclonal antibody-producing CHO cell lines using an in silico metabolomic platform. *PLOS ONE, 9*(3), e90832-e90832. doi:10.1371/journal.pone.0090832

Girard, P., Meissner, P., Jordan, M., Tsao, M., & Wurm, F. M. (2002). Small Scale Bioreactor System for Process Development and Optimization. In A. Bernard, B. Griffiths, W. Noé, & F. Wurm (Eds.), *Animal Cell Technology: Products from Cells, Cells as Products: Proceedings of the 16th ESACT Meeting April 25–29, 1999, Lugano, Switzerland* (pp. 323-327). Dordrecht: Springer Netherlands.

Glacken, M. W., Fleischaker, R. J., & Sinskey, A. J. (1986). Reduction of waste product excretion via nutrient control: Possible strategies for maximizing product and cell yields on serum in cultures of mammalian cells. *Biotechnology and Bioengineering, 28*(9), 1376-1389. doi:10.1002/bit.260280912

Godoy-Silva, R., Chalmers, J. J., Casnocha, S. A., Bass, L. A., Ma, N. J. B., & bioengineering. (2009). Physiological responses of CHO cells to repetitive hydrodynamic stress. *103*(6), 1103-1117.

Godoy-Silva, R., Mollet, M., & Chalmers, J. J. (2009). Evaluation of the effect of chronic hydrodynamical stresses on cultures of suspensed CHO-6E6 cells. *Biotechnology and Bioengineering, 102*(4), 1119-1130.

Goh, J. B., & Ng, S. K. (2018). Impact of host cell line choice on glycan profile. *Critical Reviews in Biotechnology, 38*(6), 851-867. doi:10.1080/07388551.2017.1416577

Goldrick, S., Holmes, W., Bond, N. J., Lewis, G., Kuiper, M., Turner, R., & Farid, S. S. (2017). Advanced multivariate data analysis to determine the root cause of trisulfide bond formation in a novel antibody–peptide fusion. *Biotechnology and Bioengineering, 114*(10), 2222-2234. doi:doi:10.1002/bit.26339

Goletz, S., Stahn, R., & KREYE, S. (2016). Small scale cultivation method for suspension cells;. In (Vol. PCT/EP2016/061763): International Patent.

Gomez, N., Subramanian, J., Ouyang, J., Nguyen, M. D., Hutchinson, M., Sharma, V. K., . . . Yuk, I. H. (2012). Culture temperature modulates aggregation of recombinant antibody in cho cells. *Biotechnol Bioeng, 109*(1), 125-136. doi:10.1002/bit.23288

González-Leal, I. J., Carrillo-Cocom, L. M., Ramírez-Medrano, A., López-Pacheco, F., Bulnes-Abundis, D., Webb-Vargas, Y., & Alvarez, M. M. (2011). Use of a Plackett–Burman statistical design to determine the effect of selected amino acids on monoclonal antibody production in CHO cells. *Biotechnology Progress, 27*(6), 1709-1717. doi:doi:10.1002/btpr.674

Graham, F. L., & van der Eb, A. J. (1973). A new technique for the assay of infectivity of human adenovirus 5 DNA. *Virology, 52*(2), 456-467. doi:https://doi.org/10.1016/0042-6822(73)90341-3

Grilo, A. L., & Mantalaris, A. (2019). The Increasingly Human and Profitable Monoclonal Antibody Market. *Trends in biotechnology, 37*(1), 9-16. doi:https://doi.org/10.1016/j.tibtech.2018.05.014

Gronemeyer, P., Ditz, R., & Strube, J. (2014). Trends in upstream and downstream process development for antibody manufacturing. *Bioengineering, 1*(4), 188-212.

Grüning, N.-M., Lehrach, H., & Ralser, M. (2010). Regulatory crosstalk of the metabolic network. *Trends in biochemical sciences, 35*(4), 220-227.

Gstraunthaler, G. (2003). Alternatives to the use of fetal bovine serum: serum-free cell culture. *ALTEX-Alternatives to animal experimentation, 20*(4), 275-281.

Guideline, I. H. T. (2009). Pharmaceutical Development Q8 (R2). *Current step, 4*.

Hakemeyer, C., McKnight, N., St John, R., Meier, S., Trexler-Schmidt, M., Kelley, B., . . . Wurth, C. (2016). Process characterization and Design Space definition. *Biologicals, 44*(5), 306-318. doi:10.1016/j.biologicals.2016.06.004

Halestrap, A. P., & Wilson, M. C. J. I. l. (2012). The monocarboxylate transporter family—role and regulation. *64*(2), 109-119.

Handlogten, M. W., Zhu, M., & Ahuja, S. (2018). Intracellular response of CHO cells to oxidative stress and its influence on metabolism and antibody production. *Biochemical Engineering Journal, 133*, 12-20. doi:https://doi.org/10.1016/j.bej.2018.01.031

Hanson, M. A., Ge, X., Kostov, Y., Brorson, K. A., Moreira, A. R., & Rao, G. (2007). Comparisons of optical pH and dissolved oxygen sensors with traditional electrochemical probes during mammalian cell culture. *Biotechnology and Bioengineering, 97*(4), 833-841. doi:doi:10.1002/bit.21320

Hartley, F., Walker, T., Chung, V., & Morten, K. (2018). Mechanisms driving the lactate switch in Chinese hamster ovary cells. *115*(8), 1890-1903. doi:10.1002/bit.26603

Hayter, P. M., Curling, E. M., Baines, A. J., Jenkins, N., Salmon, I., Strange, P. G., . . . Bull, A. T. (1992). Glucose-limited chemostat culture of Chinese hamster ovary cells producing recombinant human interferon-γ. *Biotechnology and Bioengineering, 39*(3), 327-335.

Heidemann, R., Lütkemeyer, D., Büntemeyer, H., & Lehmann, J. (1998). Effects of dissolved oxygen levels and the role of extra- and intracellular amino acid concentrations upon the metabolism of mammalian cell lines during batch and continuous cultures. *Cytotechnology, 26*(3), 185-197. doi:10.1023/A:1007917409455

Hendrick, V., Winnepenninckx, P., Abdelkafi, C., Vandeputte, O., Cherlet, M., Marique, T., . . . Werenne, J. (2001). Increased productivity of recombinant tissular plasminogen activator (t-PA) by butyrate and shift of temperature: a cell cycle phases analysis. *Cytotechnology, 36*(1-3), 71-83.

Hogwood, C. E., Bracewell, D. G., & Smales, C. M. (2014). Measurement and control of host cell proteins (HCPs) in CHO cell bioprocesses. *Current Opinion in Biotechnology, 30*, 153-160.

Horvath, B., Mun, M., & Laird, M. W. (2010). Characterization of a Monoclonal Antibody Cell Culture Production Process Using a Quality by Design Approach. *Molecular Biotechnology, 45*(3), 203-206. doi:10.1007/s12033-010-9267-4

Hoskisson, P. A., & Hobbs, G. (2005). Continuous culture–making a comeback? *Microbiology, 151*(10), 3153-3159.

Hossler, P., Khattak, S. F., & Li, Z. J. (2009). Optimal and consistent protein glycosylation in mammalian cell culture. *Glycobiology, 19*(9), 936-949.

Hsu, W.-T., Aulakh, R. P. S., Traul, D. L., & Yuk, I. H. (2012). Advanced microscale bioreactor system: a representative scale-down model for bench-top bioreactors. *Cytotechnology, 64*(6), 667-678. doi:10.1007/s10616-012-9446-1

Hu, W., Berdugo, C., & Chalmers, J. J. (2011). The potential of hydrodynamic damage to animal cells of industrial relevance: current understanding. *Cytotechnology, 63*(5), 445. doi:10.1007/s10616-011-9368-3

Hu, W. S., Dodge, T. C., Frame, K. K., & Himes, V. B. (1987). Effect of glucose on the cultivation of mammalian cells. *Dev Biol Stand, 66*, 279-290.

Huang, C. J., Lin, H., & Yang, J. X. (2015). A robust method for increasing Fc glycan high mannose level of recombinant antibodies. *Biotechnol Bioeng, 112*(6), 1200-1209. doi:10.1002/bit.25534

Huang, Y. M., Hu, W., Rustandi, E., Chang, K., Yusuf-Makagiansar, H., & Ryll, T. (2010). Maximizing productivity of CHO cell-based fed-batch culture using chemically defined media conditions and typical manufacturing equipment. *Biotechnol Prog, 26*(5), 1400-1410. doi:10.1002/btpr.436

Hülscher, M., Scheibler, U., & Onken, U. (1992). Selective recycle of viable animal cells by coupling of airlift reactor and cell settler. *Biotechnology and Bioengineering, 39*(4), 442-446.

Janakiraman, V., Kwiatkowski, C., Kshirsagar, R., Ryll, T., & Huang, Y.-M. (2015). Application of high-throughput mini-bioreactor system for systematic scale-down modeling, process

characterization, and control strategy development. *Biotechnology Progress, 31*(6), 1623-1632. doi:doi:10.1002/btpr.2162

Jayapal, K. P., Wlaschin, K. F., Hu, W., & Yap, M. G. (2007). Recombinant protein therapeutics from CHO cells-20 years and counting. *Chemical Engineering Progress, 103*(10), 40.

Jiang, R., Chen, H., & Xu, S. (2018). pH excursions impact CHO cell culture performance and antibody N-linked glycosylation. *Bioprocess and Biosystems Engineering, 41*(12), 1731-1741. doi:10.1007/s00449-018-1996-y

Kallos, M. S., & Behie, L. A. (1999). Inoculation and growth conditions for high-cell-density expansion of mammalian neural stem cells in suspension bioreactors. *Biotechnology and Bioengineering, 63*(4), 473-483. doi:10.1002/(sici)1097-0290(19990520)63:4<473::aid-bit11>3.0.co;2-c

Karst, D. J., Serra, E., Villiger, T. K., Soos, M., & Morbidelli, M. J. B. E. J. (2016). Characterization and comparison of ATF and TFF in stirred bioreactors for continuous mammalian cell culture processes. *110*, 17-26.

Kaufman, R. J., & Sharp, P. A. (1982). Construction of a modular dihydrofolate reductase cDNA gene: analysis of signals utilized for efficient expression. *Molecular and cellular biology, 2*(11), 1304-1319.

Kaufmann, H., Mazur, X., Fussenegger, M., & Bailey, J. E. (1999). Influence of low temperature on productivity, proteome and protein phosphorylation of CHO cells. *Biotechnology and Bioengineering, 63*(5), 573-582. doi:10.1002/(SICI)1097-0290(19990605)63:5<573::AID-BIT7>3.0.CO;2-Y

Kelley, B. (2009). Industrialization of mAb production technology: the bioprocessing industry at a crossroads. *MAbs, 1*(5), 443-452.

Kelly, W., Scully, J., Zhang, D., Feng, G., Lavengood, M., Condon, J., . . . Bhatia, R. (2014). Understanding and modeling alternating tangential flow filtration for perfusion cell culture. *Biotechnol Prog, 30*(6), 1291-1300. doi:10.1002/btpr.1953

Kim, B. J., Diao, J., & Shuler, M. L. (2012). Mini-scale bioprocessing systems for highly parallel animal cell cultures. *Biotechnology Progress, 28*(3), 595-607. doi:doi:10.1002/btpr.1554

Kim, M.-S., Pinto, S. M., Getnet, D., Nirujogi, R. S., Manda, S. S., Chaerkady, R., . . . Pandey, A. (2014). A draft map of the human proteome. *Nature, 509*, 575. doi:10.1038/nature13302

https://www.nature.com/articles/nature13302#supplementary-information

Kim, T. K., & Eberwine, J. H. (2010). Mammalian cell transfection: the present and the future. *Analytical and bioanalytical chemistry, 397*(8), 3173-3178. doi:10.1007/s00216-010-3821-6

Kloth, C., Maclsaac, G., Ghebremariam, H., & Arunakumari, A. (2010). Inoculum Expansion Methods, Recombinant Mammalian Cell Lines. In *Encyclopedia of Industrial Biotechnology*.

Kregel, K. C. (2002). Invited review: heat shock proteins: modifying factors in physiological stress responses and acquired thermotolerance. *Journal of applied physiology, 92*(5), 2177-2186.

Kunert, R., & Reinhart, D. (2016). Advances in recombinant antibody manufacturing. *Applied microbiology and biotechnology, 100*(8), 3451-3461. doi:10.1007/s00253-016-7388-9

Kuwae, S., Ohda, T., Tamashima, H., Miki, H., & Kobayashi, K. (2005). Development of a fed-batch culture process for enhanced production of recombinant human antithrombin by Chinese hamster ovary cells. *Journal of Bioscience and Bioengineering, 100*(5), 502-510. doi:https://doi.org/10.1263/jbb.100.502

Labrijn, A. F., Janmaat, M. L., Reichert, J. M., & Parren, P. W. H. I. (2019). Bispecific antibodies: a mechanistic review of the pipeline. *Nature Reviews Drug Discovery, 18*(8), 585-608. doi:10.1038/s41573-019-0028-1

Lara, A. R., Galindo, E., Ramírez, O. T., & Palomares, L. A. (2006). Living with heterogeneities in bioreactors. *Molecular Biotechnology, 34*(3), 355-381. doi:10.1385/mb:34:3:355

Lee, S.-Y., Kim, Y.-H., Roh, Y.-S., Myoung, H.-J., Lee, K.-Y., & Kim, D.-I. (2004). Bioreactor operation for transgenic Nicotiana tabacum cell cultures and continuous production of recombinant human granulocyte-macrophage colony-stimulating factor by perfusion culture. *Enzyme and Microbial Technology, 35*(6), 663-671. doi:https://doi.org/10.1016/j.enzmictec.2004.08.019

Legmann, R., Schreyer, H. B., Combs, R. G., McCormick, E. L., Russo, A. P., & Rodgers, S. T. (2009). A predictive high-throughput scale-down model of monoclonal antibody production in CHO cells. *Biotechnol Bioeng, 104*(6), 1107-1120. doi:10.1002/bit.22474

Levine, B. L., Miskin, J., Wonnacott, K., & Keir, C. (2017). Global manufacturing of CAR T cell therapy. *4*, 92-101.

Lewis, G. L., R. Lee, K. Wales, R. (2010). Novel automated micro-scale bioreactor technology: A qualitative and quantitative mimic for early process development. *Bioprocessing Journal*(9), 22-25.

Li, F., Hashimura, Y., Pendleton, R., Harms, J., Collins, E., & Lee, B. (2006). A Systematic Approach for Scale-Down Model Development and Characterization of Commercial Cell Culture Processes. *Biotechnology Progress, 22*(3), 696-703. doi:10.1021/bp0504041

Li, F., Vijayasankaran, N., Shen, A., Kiss, R., & Amanullah, A. (2010). Cell culture processes for monoclonal antibody production. *MAbs, 2*(5), 466-479. doi:10.4161/mabs.2.5.12720

Li, J., Wong, C. L., Vijayasankaran, N., Hudson, T., & Amanullah, A. (2012). Feeding lactate for CHO cell culture processes: Impact on culture metabolism and performance. *Biotechnology and Bioengineering, 109*(5), 1173-1186. doi:doi:10.1002/bit.24389

Liu, H., Saxena, A., Sidhu, S. S., & Wu, D. (2017). Fc Engineering for Developing Therapeutic Bispecific Antibodies and Novel Scaffolds. *8*(38). doi:10.3389/fimmu.2017.00038

Liu, J. K. (2014). The history of monoclonal antibody development - Progress, remaining challenges and future innovations. *Ann Med Surg (Lond), 3*(4), 113-116. doi:10.1016/j.amsu.2014.09.001

Liu, Z., Dai, S., Bones, J., Ray, S., Cha, S., Karger, B. L., . . . Rossomando, A. (2015). A quantitative proteomic analysis of cellular responses to high glucose media in Chinese hamster ovary cells. *31*(4), 1026-1038. doi:10.1002/btpr.2090

Lloyd, D. R., Holmes, P., Jackson, L. P., Emery, A. N., & Al-Rubeai, M. (2000). Relationship between cell size, cell cycle and specific recombinant protein productivity. *Cytotechnology, 34*(1-2), 59-70. doi:10.1023/A:1008103730027

Longobardi, G. P. (1994). Fed-batch versus batch fermentation. *Bioprocess Engineering, 10*(5), 185-194. doi:10.1007/bf00369529

Looby, M., Ibarra, N., Pierce, J. J., Buckley, K., O'Donovan, E., Heenan, M., . . . Baganz, F. (2011). Application of quality by design principles to the development and technology transfer of a major process improvement for the manufacture of a recombinant protein. *Biotechnol Prog, 27*(6), 1718-1729. doi:10.1002/btpr.672

López-Meza, J., Araíz-Hernández, D., Carrillo-Cocom, L. M., López-Pacheco, F., Rocha-Pizaña, M. d. R., & Alvarez, M. M. (2016). Using simple models to describe the kinetics of growth, glucose consumption, and monoclonal antibody formation in naive and infliximab producer CHO cells. *Cytotechnology, 68*(4), 1287-1300. doi:10.1007/s10616-015-9889-2

Ma, N., Koelling, K. W., & Chalmers, J. J. (2002). Fabrication and use of a transient contractional flow device to quantify the sensitivity of mammalian and insect cells to hydrodynamic forces. *Biotechnology and Bioengineering, 80*(4), 428-437.

MacIntyre, F. (1972). Flow patterns in breaking bubbles. *Journal of Geophysical Research, 77*(27), 5211-5228.

Manahan, M., Nelson, M., Cacciatore, J. J., Weng, J., Xu, S., & Pollard, J. (2019). Scale-down model qualification of ambr® 250 high-throughput mini-bioreactor system for two commercial-scale mAb processes. *35*(6), e2870. doi:10.1002/btpr.2870

Mandenius, C.-F., & Brundin, A. (2008). Bioprocess optimization using design-of-experiments methodology. *24*(6), 1191-1203. doi:10.1002/btpr.67

Markert, S., & Joeris, K. (2017). Establishment of a fully automated microtiter plate-based system for suspension cell culture and its application for enhanced process optimization. *Biotechnology and Bioengineering, 114*(1), 113-121. doi:doi:10.1002/bit.26044

Marks, D. M. (2003). Equipment design considerations for large scale cell culture. *Cytotechnology, 42*(1), 21-33. doi:10.1023/a:1026103405618

Martinez, V. S., Dietmair, S., Quek, L. E., Hodson, M. P., Gray, P., & Nielsen, L. K. (2013). Flux balance analysis of CHO cells before and after a metabolic switch from lactate production to consumption. *Biotechnol Bioeng, 110*(2), 660-666. doi:10.1002/bit.24728

Matsunaga, N., Kano, K., Maki, Y., & Dobashi, T. (2009). Culture scale-up studies as seen from the viewpoint of oxygen supply and dissolved carbon dioxide stripping. *J Biosci Bioeng, 107*(4), 412-418. doi:10.1016/j.jbiosc.2008.12.016

MilliporeSigma, S. L., United States. (2017). *Perfusion Media Development Using Cell Settling in Automated Cell Culture System - Poster Presentation 054.* Paper presented at the The 25th Annual Meeting of the European Society for Animal Cell Technology, Lausanne.

Mollet, M., Godoy-Silva, R., Berdugo, C., & Chalmers, J. J. (2007). Acute hydrodynamic forces and apoptosis: a complex question. *Biotechnology and Bioengineering, 98*(4), 772-788.

Monod, J. (1949). THE GROWTH OF BACTERIAL CULTURES. *Annual Review of Microbiology, 3*(1), 371-394. doi:10.1146/annurev.mi.03.100149.002103

Monod, J. (1950). La technique de culture continue: theorie et applications.

Moore, A., Donahue, C. J., Hooley, J., Stocks, D. L., Bauer, K. D., & Mather, J. P. J. C. (1995). Apoptosis in CHO cell batch cultures: examination by flow cytometry. *17*(1), 1-11.

Moore, A., Mercer, J., Dutina, G., Donahue, C. J., Bauer, K. D., Mather, J. P., . . . Ryll, T. (1997). Effects of temperature shift on cell cycle, apoptosis and nucleotide pools in CHO cell batch cultues. *Cytotechnology, 23*(1-3), 47-54. doi:10.1023/A:1007919921991

Moses, S., Manahan, M., Ambrogelly, A., & Ling, W. L. W. (2012). Assessment of AMBR as a model for high-throughput cell culture process development strategy. *Advances in Bioscience and Biotechnology, 03*(07), 918-927. doi:10.4236/abb.2012.37113

Mostafa, S. S., & Gu, X. (2003). Strategies for improved dCO2 removal in large-scale fed-batch cultures. *Biotechnology Progress, 19*(1), 45-51.

Mozdzierz, N. J., Love, K. R., Lee, K. S., Lee, H. L., Shah, K. A., Ram, R. J., & Love, J. C. (2015). A perfusion-capable microfluidic bioreactor for assessing microbial heterologous protein production. *Lab Chip, 15*(14), 2918-2922. doi:10.1039/c5lc00443h

Nagashima, H., Watari, A., Shinoda, Y., Okamoto, H., & Takuma, S. (2013). Application of a quality by design approach to the cell culture process of monoclonal antibody production, resulting in the establishment of a design space. *J Pharm Sci, 102*(12), 4274-4283. doi:10.1002/jps.23744

Newman, J. R. S., Ghaemmaghami, S., Ihmels, J., Breslow, D. K., Noble, M., DeRisi, J. L., & Weissman, J. S. (2006). Single-cell proteomic analysis of S. cerevisiae reveals the architecture of biological noise. *Nature, 441*(7095), 840-846. doi:10.1038/nature04785

Nienow, A. W. (2006). Reactor Engineering in Large Scale Animal Cell Culture. *Cytotechnology, 50*(1), 9. doi:10.1007/s10616-006-9005-8

Nienow, A. W., Rielly, C. D., Brosnan, K., Bargh, N., Lee, K., Coopman, K., & Hewitt, C. J. (2013). The physical characterisation of a microscale parallel bioreactor platform with an industrial CHO cell line expressing an IgG4. *Biochemical Engineering Journal, 76*, 25-36. doi:10.1016/j.bej.2013.04.011

Nissom, P. M., Sanny, A., Kok, Y. J., Hiang, Y. T., Chuah, S. H., Shing, T. K., . . . Sim, M. Y. G. (2006). Transcriptome and proteome profiling to understanding the biology of high productivity CHO cells. *Molecular Biotechnology, 34*(2), 125-140.

Novick, A., & Szilard, L. (1950). Description of the chemostat. *Science, 112*(2920), 715-716.

Nyberg, G. B., Balcarcel, R. R., Follstad, B. D., Stephanopoulos, G., & Wang, D. I. (1999). Metabolic effects on recombinant interferon-γ glycosylation in continuous culture of Chinese hamster ovary cells. *Biotechnology and Bioengineering, 62*(3), 336-347.

Oguchi, S., Saito, H., Tsukahara, M., & Tsumura, H. (2006). pH Condition in temperature shift cultivation enhances cell longevity and specific hMab productivity in CHO culture. *Cytotechnology, 52*(3), 199-207. doi:10.1007/s10616-007-9059-2

Ozturk, S. S. (1996). Engineering challenges in high density cell culture systems. *Cytotechnology, 22*(1), 3-16. doi:10.1007/BF00353919

Pan, X., Dalm, C., Wijffels, R. H., & Martens, D. E. (2017). Metabolic characterization of a CHO cell size increase phase in fed-batch cultures. *Applied microbiology and biotechnology, 101*(22), 8101-8113. doi:10.1007/s00253-017-8531-y

Pan, X., Streefland, M., Dalm, C., Wijffels, R. H., & Martens, D. E. (2017). Selection of chemically defined media for CHO cell fed-batch culture processes. *Cytotechnology, 69*(1), 39-56. doi:10.1007/s10616-016-0036-5

Pappenreiter, M., Sissolak, B., Sommeregger, W., Striedner, G. J. F. i. b., & biotechnology. (2019). Oxygen Uptake Rate Soft-sensing via Dynamic kLa Computation: Cell Volume and Metabolic Transition Prediction in Mammalian Bioprocesses. *7*, 195.

Parag, H. A., Raboy, B., & Kulka, R. G. (1987). Effect of heat shock on protein degradation in mammalian cells: involvement of the ubiquitin system. *The EMBO journal, 6*(1), 55-61.

Park, J. H., Jin, J. H., Lim, M. S., An, H. J., Kim, J. W., & Lee, G. M. (2017). Proteomic Analysis of Host Cell Protein Dynamics in the Culture Supernatants of Antibody-Producing CHO Cells. *Scientific Reports, 7*, 44246. doi:10.1038/srep44246

https://www.nature.com/articles/srep44246#supplementary-information

Patel, N. A., Anderson, C. R., Terkildsen, S. E., Davis, R. C., Pack, L. D., Bhargava, S., & Clarke, H. R. G. (2018). Antibody expression stability in CHO clonally derived cell lines and their subclones: Role of methylation in phenotypic and epigenetic heterogeneity. *34*(3), 635-649. doi:10.1002/btpr.2655

Pavlou, A. K., & Belsey, M. J. (2005). The therapeutic antibodies market to 2008. *European Journal of Pharmaceutics and Biopharmaceutics, 59*(3), 389-396. doi:https://doi.org/10.1016/j.ejpb.2004.11.007

Pekle, E., Smith, A., Rosignoli, G., Sellick, C., Smales, C. M., & Pearce, C. J. B. j. (2019). Application of Imaging Flow Cytometry for the Characterization of Intracellular Attributes in Chinese Hamster Ovary Cell Lines at the Single-Cell Level. *14*(7), 1800675.

Peksel, B., Gombos, I., Péter, M., Vigh, L., Tiszlavicz, Á., Brameshuber, M., . . . Török, Z. (2017). Mild heat induces a distinct “eustress” response in Chinese Hamster Ovary cells but does not induce heat shock protein synthesis. *Scientific Reports, 7*(1), 15643. doi:10.1038/s41598-017-15821-8

Pirt, S. J. (1975). *Principles of microbe and cell cultivation*. Oxford, UK Blackwell Scientific Publications.

Pollock, J., Ho, S. V., & Farid, S. S. (2013). Fed-batch and perfusion culture processes: economic, environmental, and operational feasibility under uncertainty. *Biotechnol Bioeng, 110*(1), 206-219. doi:10.1002/bit.24608

Provost, A., & Bastin, G. (2004). Dynamic metabolic modelling under the balanced growth condition. *Journal of Process Control, 14*(7), 717-728.

Puck, T. T., & Marcus, P. I. (1955). A rapid method for viable cell titration and clone production with HeLa cells in tissue culture: the use of X-irradiated cells to supply conditioning factors. *Proceedings of the National Academy of Sciences, 41*(7), 432-437.

Quek, L.-E., Dietmair, S., Krömer, J. O., & Nielsen, L. K. (2010). Metabolic flux analysis in mammalian cell culture. *Metabolic Engineering, 12*(2), 161-171. doi:https://doi.org/10.1016/j.ymben.2009.09.002

Rameez, S., Mostafa, S. S., Miller, C., & Shukla, A. A. (2014). High-throughput miniaturized bioreactors for cell culture process development: reproducibility, scalability, and control. *Biotechnol Prog, 30*(3), 718-727. doi:10.1002/btpr.1874

Rathore, A. S. (2009). Roadmap for implementation of quality by design (QbD) for biotechnology products. *Trends Biotechnol, 27*(9), 546-553. doi:10.1016/j.tibtech.2009.06.006

Rathore, A. S., & Winkle, H. (2009). Quality by design for biopharmaceuticals. *Nat Biotech, 27*(1), 26-34.

Read, E. K., Shah, R. B., Riley, B. S., Park, J. T., Brorson, K. A., & Rathore, A. S. (2010). Process analytical technology (PAT) for biopharmaceutical products: Part II. Concepts and applications. *Biotechnol Bioeng, 105*(2), 285-295. doi:10.1002/bit.22529

Reinhart, D., Damjanovic, L., Kaisermayer, C., & Kunert, R. (2015). Benchmarking of commercially available CHO cell culture media for antibody production. *Applied microbiology and biotechnology, 99*(11), 4645-4657. doi:10.1007/s00253-015-6514-4

Restelli, V., Wang, M. D., Huzel, N., Ethier, M., Perreault, H., & Butler, M. (2006). The effect of dissolved oxygen on the production and the glycosylation profile of recombinant human erythropoietin produced from CHO cells. *Biotechnol Bioeng, 94*(3), 481-494. doi:10.1002/bit.20875

Reuveny, S., Velez, D., Macmillan, J., & Miller, L. (1986). Factors affecting cell growth and monoclonal antibody production in stirred reactors. *Journal of immunological methods, 86*(1), 53-59.

Ridgway, J. B. B., Presta, L. G., & Carter, P. (1996). 'Knobs-into-holes' engineering of antibody CH3 domains for heavy chain heterodimerization. *Protein Engineering, Design and Selection, 9*(7), 617-621. doi:10.1093/protein/9.7.617 %J Protein Engineering, Design and Selection

Rodrigues, M. E., Costa, A. R., Henriques, M., Azeredo, J., & Oliveira, R. (2012). Comparison of commercial serum-free media for CHO-K1 cell growth and monoclonal antibody production. *International Journal of Pharmaceutics, 437*(1), 303-305. doi:https://doi.org/10.1016/j.ijpharm.2012.08.002

Rodriguez, J., Spearman, M., Tharmalingam, T., Sunley, K., Lodewyks, C., Huzel, N., & Butler, M. (2010). High productivity of human recombinant beta-interferon from a low-temperature perfusion culture. *Journal of Biotechnology, 150*(4), 509-518. doi:https://doi.org/10.1016/j.jbiotec.2010.09.959

Rosano, G. L., & Ceccarelli, E. A. (2014). Recombinant protein expression in Escherichia coli: advances and challenges. *Frontiers in microbiology, 5*, 172-172. doi:10.3389/fmicb.2014.00172

Sandner, V., Pybus, L. P., McCreath, G., & Glassey, J. (2018). Scale-Down Model Development in ambr systems: An Industrial Perspective. *Biotechnology Journal, 0*(0), 1700766. doi:doi:10.1002/biot.201700766

Sartorius (Producer). (2016, 1st August 2016). ambr15 as a sedimentation-perfusion model for cultivation characteristics and product quality prediction. *Webinar*. Retrieved from http://www.tapbiosystems.com/ambr_webinar/ambrIrvine_WebinarPR.htm

Searles, J. A., Todd, P., & Kompala, D. S. (1994). Viable Cell Recycle with an Inclined Settler in the Perfusion Culture of Suspended Recombinant Chinese Hamster Ovary Cells. *Biotechnology Progress, 10*(2), 198-206. doi:10.1021/bp00026a600

Seewöster, T., & Lehmann, J. (1997). Cell size distribution as a parameter for the predetermination of exponential growth during repeated batch cultivation of CHO cells. *55*(5), 793-797. doi:10.1002/(sici)1097-0290(19970905)55:5<793::Aid-bit9>3.0.Co;2-6

Sellick, C. A., Croxford, A. S., Maqsood, A. R., Stephens, G., Westerhoff, H. V., Goodacre, R., & Dickson, A. J. (2011). Metabolite profiling of recombinant CHO cells: designing tailored feeding regimes that enhance recombinant antibody production. *Biotechnology and Bioengineering, 108*(12), 3025-3031.

Selvarasu, S., Ho, Y. S., Chong, W. P., Wong, N. S., Yusufi, F. N., Lee, Y. Y., . . . Lee, D. Y. (2012). Combined in silico modeling and metabolomics analysis to characterize fed-batch CHO cell culture. *Biotechnology and Bioengineering, 109*(6), 1415-1429.

Seth, G., Hamilton, R. W., Stapp, T. R., Zheng, L., Meier, A., Petty, K., . . . Chary, S. (2013). Development of a new bioprocess scheme using frozen seed train intermediates to initiate CHO cell culture manufacturing campaigns. *Biotechnology and Bioengineering, 110*(5), 1376-1385. doi:10.1002/bit.24808

Sewell, D. J., Turner, R., Field, R., Holmes, W., Pradhan, R., Spencer, C., . . . bioengineering. (2019). Enhancing the functionality of a microscale bioreactor system as an industrial process development tool for mammalian perfusion culture. *116*(6), 1315-1325.

Shukla, A. A., & Gottschalk, U. (2013). Single-use disposable technologies for biopharmaceutical manufacturing. *Trends in biotechnology, 31*(3), 147-154. doi:https://doi.org/10.1016/j.tibtech.2012.10.004

Shukla, A. A., & Thömmes, J. (2010). Recent advances in large-scale production of monoclonal antibodies and related proteins. *Trends in biotechnology, 28*(5), 253-261. doi:https://doi.org/10.1016/j.tibtech.2010.02.001

Sieblist, C., Hägeholz, O., Aehle, M., Jenzsch, M., Pohlscheidt, M., & Lübbert, A. (2011). Insights into large-scale cell-culture reactors: II. Gas-phase mixing and CO2 stripping. *Biotechnology Journal, 6*(12), 1547-1556. doi:doi:10.1002/biot.201100153

Sieblist, C., Jenzsch, M., & Pohlscheidt, M. (2016). Equipment characterization to mitigate risks during transfers of cell culture manufacturing processes. *Cytotechnology, 68*(4), 1381-1401. doi:10.1007/s10616-015-9899-0

Simpson, N. H., Singh, R. P., Perani, A., Goldenzon, C., & Al-Rubeai, M. (1998). In hybridoma cultures, deprivation of any single amino acid leads to apoptotic death, which is suppressed by the expression of the bcl-2 gene. *Biotechnology and Bioengineering, 59*(1), 90-98. doi:doi:10.1002/(SICI)1097-0290(19980705)59:1<90::AID-BIT12>3.0.CO;2-6

Singh, R. P., Al.-Rubeai, M., Gregory, C. D., & Emery, A. N. (1994). Cell death in bioreactors: A role for apoptosis. *Biotechnology and Bioengineering, 44*(6), 720-726. doi:doi:10.1002/bit.260440608

Spadiut, O., Capone, S., Krainer, F., Glieder, A., & Herwig, C. (2014). Microbials for the production of monoclonal antibodies and antibody fragments. *Trends in biotechnology, 32*(1), 54-60. doi:10.1016/j.tibtech.2013.10.002

Stephens, M. L., & Lyberatos, G. (1987). Effect of cycling on final mixed culture fate. *Biotechnology and Bioengineering, 29*(6), 672-678. doi:10.1002/bit.260290603

Strovas, T. J., Sauter, L. M., Guo, X., & Lidstrom, M. E. (2007). Cell-to-Cell Heterogeneity in Growth Rate and Gene Expression in Methylobacterium extorquens AM1. *189*(19), 7127-7133. doi:10.1128/JB.00746-07 %J Journal of Bacteriology

Sureshkumar, G., & Mutharasan, R. (1991). The influence of temperature on a mouse–mouse hybridoma growth and monoclonal antibody production. *Biotechnology and Bioengineering, 37*(3), 292-295.

Svoboda, J., Hložánek, I., Mach, O., Michlová, A., Říman, J., & Urbánková, M. (1973). Transfection of Chicken Fibroblasts with Single Exposure to DNA from Virogenic Mammalian Cells. *Journal of General Virology, 21*(1), 47-55. doi:doi:10.1099/0022-1317-21-1-47

Tait, A. S., Hogwood, C. E., Smales, C. M., & Bracewell, D. G. (2012). Host cell protein dynamics in the supernatant of a mAb producing CHO cell line. *Biotechnology and Bioengineering, 109*(4), 971-982.

Takuma, S., Hirashima, C., & Piret, J. M. (2007). Dependence on glucose limitation of the pCO2 influences on CHO cell growth, metabolism and IgG production. *97*(6), 1479-1488. doi:10.1002/bit.21376

Templeton, N., Dean, J., Reddy, P., & Young, J. D. (2013). Peak antibody production is associated with increased oxidative metabolism in an industrially relevant fed-batch CHO cell culture. *Biotechnology and Bioengineering, 110*(7), 2013-2024.

Tharmalingam, T., Ghebeh, H., Wuerz, T., & Butler, M. (2008). Pluronic enhances the robustness and reduces the cell attachment of mammalian cells. *Mol Biotechnol, 39*(2), 167-177. doi:10.1007/s12033-008-9045-8

Trummer, E., Fauland, K., Seidinger, S., Schriebl, K., Lattenmayer, C., Kunert, R., . . . Muller, D. (2006). Process parameter shifting: Part I. Effect of DOT, pH, and temperature on the performance of Epo-Fc expressing CHO cells cultivated in controlled batch bioreactors. *Biotechnol Bioeng, 94*(6), 1033-1044. doi:10.1002/bit.21013

Unkeless, J. C., Scigliano, E., & Freedman, V. H. (1988). Structure and function of human and murine receptors for IgG. *Annual review of immunology, 6*(1), 251-281.

Varma, A., & Palsson, B. O. (1994). Stoichiometric flux balance models quantitatively predict growth and metabolic by-product secretion in wild-type Escherichia coli W3110. *Applied and Environmental Microbiology, 60*(10), 3724-3731.

Vcelar, S., Melcher, M., Auer, N., Hrdina, A., Puklowski, A., Leisch, F., . . . Borth, N. (2018). Changes in Chromosome Counts and Patterns in CHO Cell Lines upon Generation of Recombinant Cell Lines and Subcloning. *13*(3), 1700495. doi:10.1002/biot.201700495

Venkat, R. V., Stock, L. R., & Chalmers, J. J. (1996). Study of hydrodynamics in microcarrier culture spinner vessels: a particle tracking velocimetry approach. *Biotechnology and Bioengineering, 49*(4), 456-466.

Venter, J. C., Adams, M. D., Myers, E. W., Li, P. W., Mural, R. J., Sutton, G. G., . . . Zhu, X. (2001). The Sequence of the Human Genome. *Science, 291*(5507), 1304-1351. doi:10.1126/science.1058040

Vidarsson, G., Dekkers, G., & Rispens, T. (2014). IgG subclasses and allotypes: from structure to effector functions. *Frontiers in immunology, 5*, 520.

Villiger-Oberbek, A., Yang, Y., Zhou, W., & Yang, J. (2015). Development and application of a high-throughput platform for perfusion-based cell culture processes. *Journal of Biotechnology, 212*, 21-29. doi:https://doi.org/10.1016/j.jbiotec.2015.06.428

Voisard, D., Meuwly, F., Ruffieux, P. A., Baer, G., & Kadouri, A. (2003). Potential of cell retention techniques for large-scale high-density perfusion culture of suspended mammalian cells. *Biotechnol Bioeng, 82*(7), 751-765. doi:10.1002/bit.10629

Walls, P. L., McRae, O., Natarajan, V., Johnson, C., Antoniou, C., & Bird, J. C. J. S. R. (2017). Quantifying the potential for bursting bubbles to damage suspended cells. *7*(1), 1-9.

Walsh, G. (2018). Biopharmaceutical benchmarks 2018. *Nature Biotechnology, 36*, 1136. doi:10.1038/nbt.4305

https://www.nature.com/articles/nbt.4305#supplementary-information

Walther, J., McLarty, J., & Johnson, T. The effects of alternating tangential flow (ATF) residence time, hydrodynamic stress and filtration flux on high-density perfusion cell culture. *Biotechnology and Bioengineering, 0*(ja). doi:doi:10.1002/bit.26811

Wang, S., Godfrey, S., Ravikrishnan, J., Lin, H., Vogel, J., & Coffman, J. (2017). Shear contributions to cell culture performance and product recovery in ATF and TFF perfusion systems. *Journal of Biotechnology, 246*, 52-60. doi:https://doi.org/10.1016/j.jbiotec.2017.01.020

Wang, Z., & Belovich, J. M. (2010). A simple apparatus for measuring cell settling velocity. *Biotechnol Prog, 26*(5), 1361-1366. doi:10.1002/btpr.432

Warburg, O., Wind, F., & Negelein, E. J. T. J. o. g. p. (1927). The metabolism of tumors in the body. *8*(6), 519.

Warr, S. R. C. (2014). Microbioreactors and Scale-Down Models: Growth of CHO Cells Using the Pall Micro24 MicroReactor System. In R. Pörtner (Ed.), *Animal Cell Biotechnology: Methods and Protocols* (pp. 149-165). Totowa, NJ: Humana Press.

Warr, S. R. C., Betts, J. P. J., Ahmad, S., Newell, K. V., & Finka, G. B. (2013). Streamlined process development using the Micro24 Bioreactor system. *BMC Proceedings, 7*(Suppl 6), P36-P36. doi:10.1186/1753-6561-7-S6-P36

Warr, S. R. C., Patel, J., Ho, R., & Newell, K. V. (2011). Use of Micro Bioreactor systems to streamline cell line evaluation and upstream process development for monoclonal antibody production. *BMC Proceedings, 5 Suppl 8*(Suppl 8), P14-P14. doi:10.1186/1753-6561-5-S8-P14

Warr, S. R. C., White, S. L., Chim, Y.-T., Patel, J., & Bosteels, H. (2011). Cell line selection using the Duetz Microflask system. *BMC Proceedings, 5*(8), P15. doi:10.1186/1753-6561-5-s8-p15

Watson, T. G. (1972). The present status and future prospects of the turbidostat.

Weidemann, R., Ludwig, A., & Kretzmer, G. (1994). Low temperature cultivation—a step towards process optimisation. *Cytotechnology, 15*(1-3), 111-116.

Wernersson, E. S., & Trägårdh, C. (1999). Scale-up of Rushton turbine-agitated tanks. *Chemical engineering science, 54*(19), 4245-4256.

Wewetzer, S. J., Kunze, M., Ladner, T., Luchterhand, B., Roth, S., Rahmen, N., . . . Büchs, J. (2015). Parallel use of shake flask and microtiter plate online measuring devices (RAMOS and

BioLector) reduces the number of experiments in laboratory-scale stirred tank bioreactors. *Journal of Biological Engineering, 9*(1), 9. doi:10.1186/s13036-015-0005-0

Woodside, S. M., Bowen, B. D., & Piret, J. M. (1998). Mammalian cell retention devices for stirred perfusion bioreactors. *Cytotechnology, 28*(1-3), 163-175. doi:10.1023/A:1008050202561

Wurm, F. (2013). CHO quasispecies—implications for manufacturing processes. *Processes, 1*(3), 296-311.

Wurm, F. M. (2004). Production of recombinant protein therapeutics in cultivated mammalian cells. *Nat Biotechnol, 22*(11), 1393-1398. doi:10.1038/nbt1026

Xing, Z., Kenty, B. M., Li, Z. J., & Lee, S. S. (2009). Scale-up analysis for a CHO cell culture process in large-scale bioreactors. *103*(4), 733-746. doi:10.1002/bit.22287

Xing, Z., Lewis, A. M., Borys, M. C., & Li, Z. J. (2017). A carbon dioxide stripping model for mammalian cell culture in manufacturing scale bioreactors. *Biotechnology and Bioengineering, 114*(6), 1184-1194. doi:doi:10.1002/bit.26232

Xing, Z., Li, Z., Chow, V., & Lee, S. S. (2008). Identifying Inhibitory Threshold Values of Repressing Metabolites in CHO Cell Culture Using Multivariate Analysis Methods. *Biotechnology Progress, 24*(3), 675-683. doi:doi:10.1021/bp070466m

Xu, J., Tang, P., Yongky, A., Drew, B., Borys, M. C., Liu, S., & Li, Z. J. (2019). *Systematic development of temperature shift strategies for Chinese hamster ovary cells based on short duration cultures and kinetic modeling.* Paper presented at the MAbs.

Yang, M., & Butler, M. (2000). Effects of ammonia on CHO cell growth, erythropoietin production, and glycosylation. *Biotechnol Bioeng, 68*(4), 370-380.

Ye, J., Alvin, K., Latif, H., Hsu, A., Parikh, V., Whitmer, T., . . . Salmon, P. (2010). Rapid protein production using CHO stable transfection pools. *Biotechnology Progress, 26*(5), 1431-1437.

Yim, M., & Shaw, D. J. B. p. (2018). Achieving greater efficiency and higher confidence in single-cell cloning by combining cell printing and plate imaging technologies. *34*(6), 1454-1459.

Zagari, F., Jordan, M., Stettler, M., Broly, H., & Wurm, F. M. (2013). Lactate metabolism shift in CHO cell culture: the role of mitochondrial oxidative activity. *New Biotechnology, 30*(2), 238-245. doi:https://doi.org/10.1016/j.nbt.2012.05.021

Zhang, S., Yang, C., Yang, Z., Zhang, D., Ma, X., Mills, G., & Liu, Z. (2015). Homeostasis of redox status derived from glucose metabolic pathway could be the key to understanding the Warburg effect. *American journal of cancer research, 5*(4), 1265-1280.

Zhou, G., & Kresta, S. M. (1996). Impact of tank geometry on the maximum turbulence energy dissipation rate for impellers. *AIChE Journal, 42*(9), 2476-2490. doi:doi:10.1002/aic.690420908

Zhou, M., Crawford, Y., Ng, D., Tung, J., Pynn, A. F., Meier, A., . . . Shen, A. (2011). Decreasing lactate level and increasing antibody production in Chinese Hamster Ovary cells (CHO) by reducing the expression of lactate dehydrogenase and pyruvate dehydrogenase kinases. *J Biotechnol, 153*(1-2), 27-34. doi:10.1016/j.jbiotec.2011.03.003

Zhou, Q., & Qiu, H. J. J. o. p. s. (2019). The mechanistic impact of N-glycosylation on stability, pharmacokinetics, and immunogenicity of therapeutic proteins. *108*(4), 1366-1377.

Zhu, M. M., Goyal, A., Rank, D. L., Gupta, S. K., Boom, T. V., & Lee, S. S. (2005). Effects of Elevated pCO2 and Osmolality on Growth of CHO Cells and Production of Antibody-Fusion Protein B1: A Case Study. *Biotechnology Progress, 21*(1), 70-77. doi:10.1021/bp049815s